THE ROLES OF SLOW ADSORPTION KINETICS AND BIOACTIVITY IN MODELLING OF ACTIVATED CARBON ADSORBERS

by

© RUSSELL G. PEEL, B.Eng., M. Eng. Sci.

A Thesis

Submitted to the School of Graduate Studies

in Partial Fulfilment of the Requirements

for the Degree

Doctor of Philosophy

McMaster University,

December, 1979

SLOW KINETICS AND BIOACTIVITY IN CARBON ADSORPTION COLUMNS

DOCTOR OF PHILOSOPHY (1979)
(Chemical Engineering)

McMASTER UNIVERSITY
Hamilton, Ontario

TITLE: The Roles of Slow Adsorption Kinetics and Bioactivity in Modelling of Activated Carbon Adsorbers.

AUTHOR: Russell G. Peel, B. Eng. (Monash University, Melbourne)
M. Eng. Sci. (Monash University, Melbourne).

SUPERVISOR: Dr. A. Benedek

NUMBER OF PAGES: (xxix), 323

ABSTRACT

Although adsorption of organic contaminants from the aqueous phase onto activated carbon is a widely used process, mechanistic models capable of describing the performance of adsorption beds are not presently available. Such models, if available, would allow an improved understanding of the behaviour of adsorption beds and could reduce the number of pilot plant studies which are presently required for system design. To develop a mechanistic model of activated carbon adsorption a two part study was undertaken.

In the first part, existing adsorption kinetic models were investigated and were found to be incapable of describing the adsorptive behaviour. Based on the structural properties of activated carbon, a branched pore kinetic model is presented which separates the carbon particle into two regions, a rapidly diffusing region which is associated with pores which are significantly larger than the adsorbing molecules, and a slowly diffusing region which is associated with pores which are of a comparable size to the diffusing molecules and in which diffusion is retarded. Equilibrium and batch kinetic experiments were conducted with pure phenolic compounds as adsorbates, and the model parameters were calculated from the data. The analysis shows that the slow diffusion region is important, and that some previously inconsistent results reported in the literature, such as premature breakthrough and tailing of the breakthrough curves, are due to the neglect of this factor.

When used in a model of an adsorption column, the kinetic parameters calculated from the batch experiments enabled the performance of experimental adsorption columns to be predicted with excellent accuracy over extended periods. The early breakthrough and characteristic tailing noted above are shown to be a result of uptake in the slow diffusion region.

The model as developed originally assumed a surface diffusion mechanism was responsible for transport in the rapidly diffusing region and as a result, solution of the model required extensive computation. The use of the quadratic driving force assumption was investigated to replace the surface diffusion mechanism and its use is shown to significantly reduce the solution complexity while giving an equally good interpretation of the data.

In the second part of the study the adsorptive behaviour of two feedstreams of environmental importance was studied. As in the first part, equilibrium and batch kinetic experiments were conducted and parameters for the quadratic driving force branched pore model were obtained by comparing the model to the data. Adsorption column experiments were conducted over extended periods and when the batch determined parameters are included in the adsorption bed model, the bulk of the breakthrough curve is shown to be well predicted. Because of the complexity of the feedstreams treated, the concentration can only be quantified in terms of a non-specific parameter such as Total Organic Carbon (TOC) and all the kinetic constants must be evaluated in terms of this parameter.

As with the pure solutes in the first part of the study, the slow diffusion region is very important in the adsorptive uptake of these complex organic contaminants. Removal by biological mechanisms is often suggested when adsorption columns continue to exhibit an uptake capacity after prolonged periods of operation, and the problems in differentiating between very slow adsorptive uptake and biological removal are discussed in detail. The present analysis shows that in many cases this removal may be due to continued slow adsorption rather than biological oxidation of the organics. The slow diffusion also has important consequences for the design of activated carbon contactors as contact times far in excess of current practice are indicated if maximum use is to be made of the adsorptive capacity.

ACKNOWLEDGEMENTS

The author wishes to thank all those who contributed to this work. He is particularly indebted to:

His supervisor Dr. A. Benedek for patient guidance, helpful suggestions, and financial support throughout the course of this work.

Dr. C.M. Crowe for help and direction with the mathematical aspects of the modelling and preparation of the thesis.

The members of the faculty and staff in the Chemical Engineering Department and in particular Messrs. R. Dunn, J. Newton, H. Behmann and J. Bancsi.

The many graduate students in the Wastewater Group who provided a social environment in which to work and in particular Eric Hall for providing some analyses and being a good listener.

Mrs. Peggy Johnstone for her patient and always accurate typing skills.

Finally, and most of all, to Debbie for the encouragement, reinforcement, and sacrifice which allowed me to complete this undertaking.

PREFACE

Due to the increasingly widespread use of activated carbon as a general purpose adsorbent for removal of organic contaminants from water, both at the source of pollution and also prior to human consumption, there is presently a need for improved design procedures in which the emphasis would be switched from purely experimental (pilot scale continuous studies) to a semi-theoretical approach. In the latter, batch experiments are combined with a mechanistic description of the adsorption process and thus the availability of such a mechanistic model would reduce or eliminate the need for pilot plant studies, and would enable the operation of existing activated carbon adsorbers to be better understood.

In actual application, the operating conditions of the majority of activated carbon adsorbers are far from ideal as feedstreams containing hundreds of different components of fluctuating concentrations are encountered. In many such cases the organic contaminants can only be quantified in terms of a gross measure of the system such as Total Organic Carbon (TOC), and a modelling strategy must be based on such a parameter. In addition, biological activity has been observed in many applications of activated carbon and it further complicates the process description.

Some attempts have been made recently to develop combined adsorption/biological models of activated carbon filters but these have concentrated on the application of relatively easily biodegradable substances to the columns. In reality, such feedstreams would be treated

in purely biological treatment systems because the adsorptive capacity of the carbon does not play a major role in the removal process. The applications where activated carbon appears to be best suited are those where the wastestreams are not amenable to biological treatment but may support some limited amount of biological activity within the carbon columns. The principal mode of removal is adsorptive but biological removal, if present, would supplement the adsorptive removal and may lead to extended operation of the carbon filter. It was the objective of the present study to develop a mechanistic model to describe the operation of such filters.

The report is presented in two separate and totally independent parts although it is assumed that the reader is familiar with the results of part I when reading part II.

In part I of the report an adsorption model is developed and rigorously tested against single solute adsorption data. Existing adsorption models developed under similarly ideal conditions were found to be inadequate as they could not describe the observed behaviour. The proposed model is based on the properties of the internal pore structure within the carbon particle, an aspect of carbon adsorption modelling which has previously been neglected, and is shown to give an excellent description of the adsorption process. The modelling study indicates that a fraction of the total capacity is utilized very slowly due to diffusional limitations, and that neglect of this capacity has been the cause of problems with some previous models. The inclusion of this slow diffusion capacity allows the performance of adsorption col-

umns operating on single solutes to be predicted solely on the basis of simple batch experiments to determine equilibrium and kinetic parameters.

Part II of the report concerns the application of activated carbon adsorption in environmentally important areas, and under actual operating conditions, including complex mixtures of feed components and potential biological activity. Following a review of the current theories regarding biological activity within activated carbon columns, two studies are presented in which the applicability of the adsorption model developed in part I is tested for use with complex substrates defined only in terms of the TOC. The model is shown to give a good description of the long term performance of the experimental columns, again using only parameters evaluated from batch experiments, and the slow diffusion capacity found previously with the pure solutes plays a very significant role in determining the breakthrough behaviour of the columns. The type of behaviour observed is very similar to that attributed to biological activity within carbon beds, and the possibility that slow adsorption rather than biological removal is responsible for the long term removal observed in some carbon filters is indicated.

PART ONE - FORMULATION AND VERIFICATION OF THE ADSORPTION MODEL.

TABLE OF CONTENTS

NOMENCLATURE

$\mathring{A}$	Angstrom
a	constant in isotherm equations (2.6) and (2.7)
a_p	specific external surface area of adsorbent, cm^2/cm^3
b	constant in isotherm, equations (2.6) and (2.7)
Bi_f	modified Biot number, $3\ k_f\ R/D_s$ or $3\ k_f/k_m$
Bi_p	modified Biot number, $k_b\ R^2/D_s$ or $k_b\ R/k_m$
c	liquid phase concentration, mg/l or g/cm^3
c_o	feed or initial liquid phase concentration, mg/l
C	liquid phase concentration, reduced units (c/c_o)
COD	chemical oxygen demand
d_p	adsorbent particle diameter, cm
D_{eff}	effective combined diffusion coefficient, cm^2/sec
D_α, D_s	diffusion coefficients in micropore-macroshell model, cm^2/sec
D_ℓ	free liquid diffusivity, cm^2/sec
D_o	surface diffusion coefficient at zero surface coverage, cm^2/sec
D_p	effective pore diffusion coefficient, cm^2/sec
D_s	effective surface diffusion coefficient, cm^2/sec
D_z	axial dispersion coefficient, cm^2/sec
$\mathcal{D}_{eff}$	liquid diffusion coefficient in pores, cm^2/sec
$\mathcal{D}_{\text{ }}$	liquid diffusion coefficient in diameter pore, cm^2/sec
f	fraction dividing adsorbent capacity between 'macropore' and 'micropore' regions
F	partitioning factor, $c_o/\ _c q_o$
H	vector in solution of solid phase equation
ΔH_{ad}	heat of adsorption

ΔH_o	heat of adsorption at zero surface coverage
ΔH_{sat}	heat of adsorption at saturation
k_b	pseudo mass transfer coefficient for transport from the 'macropore' to 'micropore' regions, sec^{-1}
k_f	external film transfer coefficient, cm/sec
k_m	'macropore' mass transfer coefficient in simplified model, cm/sec
k_p	pseudo mass transfer coefficient, cm/sec
K_f	forward reaction rate constant, equation (2.17)
K_r	reverse reaction rate constant, equation (2.17)
M	constant in isotherm equation
n	exponent in Freundlich isotherm, equation (2.5)
N	rotational speed of impeller, rpm
q	solid phase concentration, mg/g
q_o	solid phase concentration in equilibrium with c_o, mg/g
$\bar{q}$	mean solid phase concentration, mg/g
Q	solid phase concentration, reduced units (q/q_o)
r	radial variable, cm
R	radius of adsorbent particle, cm
R_b	rate of transfer from 'macropores' into 'micropores'
Re	Reynolds number, $\rho v_s \varepsilon d_p/\mu$
Sc	Schmidt number, $\mu/\rho D_\ell$
Sh	Sherwood number, $k_f d_p/D_\ell$
t	time, sec
T	absolute temperature
v_s	interstitial liquid phase velocity, cm/sec
V	volume of batch reactor, cm^3

W	mass of carbon in batch reactor, g
x	bed length variable, cm
X	tridiagonal matrix in solution of solid phase equation
Y	matrix in solution of solid phase equation
z	dimensionless bed depth variable, $D_s x/R^2 v_s$ or $k_m x/R v_s$

Greek symbols

α_i	constants
β_i	constants
ε	liquid volume fraction
ε_p	internal porosity of adsorbent particle
λ	ratio of solute radius to pore radius
η	transformed radial variable, $(r/R)^2$
θ	dimensionless time: batch model - $D_s t/R^2$ or $k_m t/R$

column model - $\frac{D_s}{R^2}(t - \frac{x}{v_s})$ or $\frac{k_m}{R}(t - \frac{x}{v_s})$

ρ	density of solvent, g/cm^3
ρ_c	apparent density of an adsorbent particle, g/cm^3
μ	viscosity of solvent, g/cm-sec
υ	adsorbent particle tortuosity
τ	time in Figure 2-2

subscripts

b	branch or 'micropore' value
e	equilibrium value
m	'macropore' value

s	surface value
sat	saturation value
$\underset{\sim}{}$	denotes vector, e.g., $\underset{\sim}{Q}$
$\underset{=}{}$	denotes matrix, e.g., $\underset{=}{Y}$
'	denotes monolayer value, e.g., $'Q'$

LIST OF FIGURES

LIST OF TABLES

PART TWO - STUDIES OF THE APPLICATION OF COMPLEX FEEDSTREAMS TO ACTIVATED CARBON COLUMNS CONTAINING BACTERIA.

TABLE OF CONTENTS

NOMENCLATURE

BOD	biochemical oxygen demand, mg/l
c	liquid phase concentration, mg/l
c_o	initial or feed liquid phase concentration, mg/l
c^+	liquid phase concentration of liquid/biofilm interface, mg/l
c_s	liquid phase concentration at liquid/solid interface, mg/l
CE	equilibrium liquid phase concentration (also c_e), mg/l
CNA	liquid phase concentration of non-adsorbable organics, mg/l
D_ℓ	free liquid diffusion coefficient, cm^2/sec
EBCT	empty bed contact time, min
f	fraction separating total adsorptive capacity between 'macro' and 'micro' pores (F on computer plots)
k_b	'micropore' mass transfer coefficient (KB on computer plots), sec^{-1}
k_f	external film mass transfer coefficient (KF on computer plots), cm/sec
k_m	'macropore' mass transfer coefficient (KM on computer plots), cm/sec
q_e	equilibrium solid phase concentration, mg/g
q_s	solid phase concentration in equilibrium with c_s, mg/g
$\bar{q}$	mean solid phase concentration, mg/g
TOC	Total Organic Carbon, mg/l

LIST OF FIGURES

LIST OF TABLES

PART I - FORMULATION AND VERIFICATION OF THE ADSORPTION MODEL

CHAPTER 1

INTRODUCTION

Design of adsorption systems is complicated by the unsteady state nature of their operation. Early mathematical models were restricted to relatively simple cases for which analytical solutions could be found. In recent years, with the advent of easy access to computational facilities, and the development of numerical solution techniques, it has become possible to solve virtually any chosen combinations of equilibrium and adsorption models. Solutions for almost all possible models based on existing adsorption mechanisms have been presented in the literature.

However, as discussed in the following chapter, some aspects of the observed behaviour of adsorption columns cannot be explained by the existing models. The mechanisms of adsorption on which these models are based are themselves as yet poorly understood, especially when activated carbon is the adsorbent. While the structure of some adsorbents such as ion exchange resins and molecular sieves can be defined with some certainty; the structure of activated carbon and the nature, location, and shape of the pores are not yet clearly defined even though considerable work has been devoted to the subject. It is possible that several different

mechanisms are simultaneously responsible for adsorption, and under particular conditions one or more may dominate. Thus researchers working on the same system under different conditions could reach different conclusions which are valid only for the particular case.

It is the aim of this study to review the properties of activated carbon to identify those characteristics which most strongly influence the adsorptive behaviour. Based on the proposed mechanisms a model is developed, and tested against batch kinetic data to measure the model parameters. The ability of the proposed model to explain results in the literature which have previously seemed to be inconsistent is also studied.

By incorporating the proposed mechanisms in a model of an adsorption column, comparison of the predictions of this model (using the parameters measured in batch kinetic experiments) against data obtained from experimental adsorption columns enables the kinetic model to be verified. At the same time, the usefulness of the proposed model as a predictive tool in adsorption column design is assessed. Having verified that the proposed mechanisms do indeed describe the observed performance, alternative mathematical expressions are assessed to obtain the simplest model form consistent with an accurate description of the data.

CHAPTER 2

LITERATURE REVIEW

2.1 Activated Carbon Properties

Even though activated carbon has become a widely used adsorbent in a multitude of applications, there is still much uncertainty regarding its structure and the effect of the structure on its adsorbent properties. In this section the manufacture and physical properties of activated carbon will be briefly outlined, and contradictory theories regarding the adsorption mechanism will be discussed in detail. For a comprehensive review of activated carbon properties the reader is referred to the detailed reviews of Dubinin (1966), Garten and Weiss (1957), Kipling (1956) and USEPA (1973) among many others.

2.1.1 Manufacture and Physical Properties

Activated carbons can be made from a variety of carbonaceous raw materials including coal, wood, coconut shell and bituminous substances. Those based on coal, either bituminous or lignite, are the most common forms presently in use. The material is first carbonized by heating to 400-700°C in the absence of oxidizing gases. During this process the raw material is dehydrated then oxygen and hydrogen containing groups such as CO, CO_2 and CH_3OH are driven off as decomposition products. Garten and Weiss (1957) noted that at the higher temperatures oxygen is eliminated from the carbon structure and an aromatization process pro-

ceeds. During this phase graphite-like microcrystallites are formed or enlarged. Chen (1970) described the microcrystallite structure as stacked planes of graphite in which the carbon atoms form an hexagonal structure. Each carbon atom within a plane forms three covalent bonds with adjacent carbon atoms and the fourth valence electron is free to resonate. The planes are held together by Van der Waal's forces and are 3.4Å apart. The diameters of these planes range from 10 to 60 Å and the height of stacking is also in the range of 20 to 50 Å (Snoeyink, 1968). It was further noted by Snoeyink (1968) that although the structure of the microcrystallites is similar to graphite, it differs in many ways including the inclusion of impurities, tetrahedrally bonded carbon atoms, and heterocyclic groups at the edges of the planes. These heterocyclic groups have free valence electrons which are presumed to be highly reactive. Furthermore, they may also promote the interconnection of adjacent carbon planes. Garten and Weiss (1957) have likened activated carbon to a giant organic polymer rather than an agglomeration of graphite like structures.

After carbonization the material consists of large numbers of microcrystallites in a randomly oriented structure. The spaces between the microcrystallites are largely filled with tarry or charred residues of the carbonization process. During the activation step in which steam or other oxidizing gases are contacted with the carbon at 750-950°C, the residues are preferentially burnt off thus opening up a vast pore structure within the carbon. Certain sites within the carbon structure are more susceptible to oxidation than others, and by controlling

the degree of severity of the oxidation step, the characteristics of the resultant activated carbon can be varied (Kipling, 1956).

The pore structure which develops consists of the irregularly shaped spaces between the microcrystallites as well as larger openings which are either the result of extensive burnout of vulnerable areas, or are a result of the filler or binder materials used in forming the raw material. The pore structure can be categorized in various ways including mercury porosimetry and nitrogen (B.E.T) and water isotherms, however it should be noted that the analyses which convert this experimental information into pore size distributions are based on assumptions which are not universally accepted (Chen, 1970; Dullien and Batra, 1970; Kipling, 1956; Rankin 1975).

The pores are generally divided into three categories, however, other classifications are used. According to the classification of Dubinin (1966) these are:

(i) Macropores - these are pores greater than 1000-2000 Å radius. The distribution of macropores is measured by mercury porosimetry as they are too large for capillary condensation to occur within them. The specific surface areas in the macropore region typically range from 0.5 to 2 m^2/g and the specific volumes from 0.2 to 0.8 cm^3/g. The macropores play a negligible role in physically adsorbing material because of the low surface area; however, they provide rapid access passages to the interior of the carbon particle.

(ii) Transitional pores - the linear dimensions of these pores,

commonly taken as 15 to 1500 Å, are much larger than those of the adsorbed molecules. Nevertheless, the surface curvature becomes a factor in their adsorptive properties. The pore measurement methods of mercury porosimetry and nitrogen adsorption overlap in this range. Mono and multilayer adsorption as well as volume filling by capillary condensation can take place in these pores. Commonly, the specific surface areas range from 20 to 70 m^2/g and the specific volumes from 0.02 to 0.10 cm^3/g, however, for some carbons such as those made of lignite, these figures may be as high as 450 m^2/g and 0.7 cm^3/g respectively.

(iii) Micropores - these are pores with radii less than 15 Å and are of a comparable size to many adsorbing molecules. The surface areas as calculated by the BET method show that the micropores often contribute as much as 90 to 95% of the total surface area within the carbon (Ying, 1978) and they have specific volumes of 0.20 to 0.60 cm^3/g.

2.1.2 The Nature of Adsorption

When considering planar surfaces, adsorption can be described thermo-dynamically by the Gibbs equation for surface excess. The driving force for surface adsorption is the reduction in surface tension when the adsorbing molecule enters the interface. Activated carbon is commonly believed to be an excellent general adsorbent because of its extremely high specific surface area and because it has a largely non-polar surface which has an affinity for non-polar organic molecules. There is however much discussion in the literature as to the validity of this assumption.

In short, the question becomes whether or not adsorption onto activated carbon would be the same if a planar carbon surface of equivalent surface area and surface properties could be formed. The standard Langmuir and Freundlich isotherms (see section 2.2.1) which assume either a linear or exponential distribution of adsorption energies do not explicitly take the effect of pore structure into account, however they receive very wide usage.

Dubinin (1966) presented a theory of volume filling of micropores, and claimed that the concept of surface adsorption within the micropores was meaningless because of the near molecular dimensions of the pores. In a similar vein, Chen (1970) gave examples from the literature which supported either one or the other of the two mechanisms, surface adsorption and pore volume filling. He proposed a theory of a surface curvature-concentration effect in which the concentration of adsorbate caused by the surface curvature in small pores was assumed to result in phase separation and subsequent pore filling with partly miscible adsorbents such as phenol. Totally miscible adsorbents such as acetic acid were assumed to adsorb conventionally on the pore surfaces. The two alternative descriptions of adsorption were also discussed by Dullien and Batra (1970) who concluded that because of the somewhat contradictory evidence, it was not possible to make definite conclusions as to the nature of the adsorption process taking place in micropores.

A theory of the adsorption process which places considerably more emphasis on the actual surface structure of the activated carbon, and the interaction of the surface with the adsorbate, has been summarized

recently by Weber and Van Vliet (1978). The results of many years of investigation indicate correlations between the numbers and types of surface oxide groups and the adsorptive capacity for various substrates. A detailed study of the surface properties has been given by Snoeyink et al. (1967,1968,1969) as well as by Mattson (1969), and the roles of the functional groups on the surface of activated carbons and their specific catalytic and exchange properties have been discussed by Garten and Weiss (1957).

While there is as yet no consensus as to the precise mechanisms of adsorption onto activated carbon, on some points there is agreement:

(i) It is generally acknowledged that, except in the case of extremely large molecules, the macropores play little part in adsorption except to act as transport passages from the exterior to the smaller pores.

(ii) The adsorptive capacities of most activated carbons are closely related to the micropore region. Although the mechanisms of adsorption in this region are uncertain, the adsorptive bonding energies in these pores are thought to be greater than on a planar surface because of multidimensional attractive forces (Chen, 1970; Calgon Corp., undated; Dubinin, 1966; USEPA, 1973).

(iii) The role of transitional pores is not well defined. The smaller pores can be assumed to be similar to the micropores and the larger to the macropores. In some instances (Calgon Corp, undated), only micro and macropores are considered. The upper limit of the micropore region in liquid phase adsorption should be determined by the size of the adsorbing molecule. The exis-

ting classifications were developed for gas phase adsorption where adsorbing molecules are generally small whereas in liquid phase adsorption, molecules of high molecular weight can be adsorbed.

2.2 Equilibrium Relationships in Adsorption Processes.

The equilibrium isotherm describes the relationship between the concentration of the adsorbate in the liquid phase and the concentration on the surface of the adsorbent. The term 'isotherm' arises because the equilibrium relationship is measured at constant temperature and it is generally given mathematical expression by fitting the experimental data to empirical or semi-empirical functions, some of which are discussed below. An isotherm can describe both the equilibrium relationship for a single adsorbate, and also for a complex substrate which can only be described by a gross measure of concentration such as Total Organic Carbon (TOC), Biochemical Oxygen Demand (BOD) or Chemical Oxygen Demand (COD). In the latter case no significance can be attached to the type of function fitting the data as the isotherm is purely an empirical description of the complex interactions between the many components in the feedstream. When the number of components in the adsorption mixture is small, multicomponent isotherms may be used to describe the equilibrium in some cases. The topics of bulk parameter and multicomponent modelling are discussed further in part II of this dissertation.

2.2.1 Single Solute Isotherm Expressions

In aqueous systems the most commonly used isotherms are (Figure 2-1)

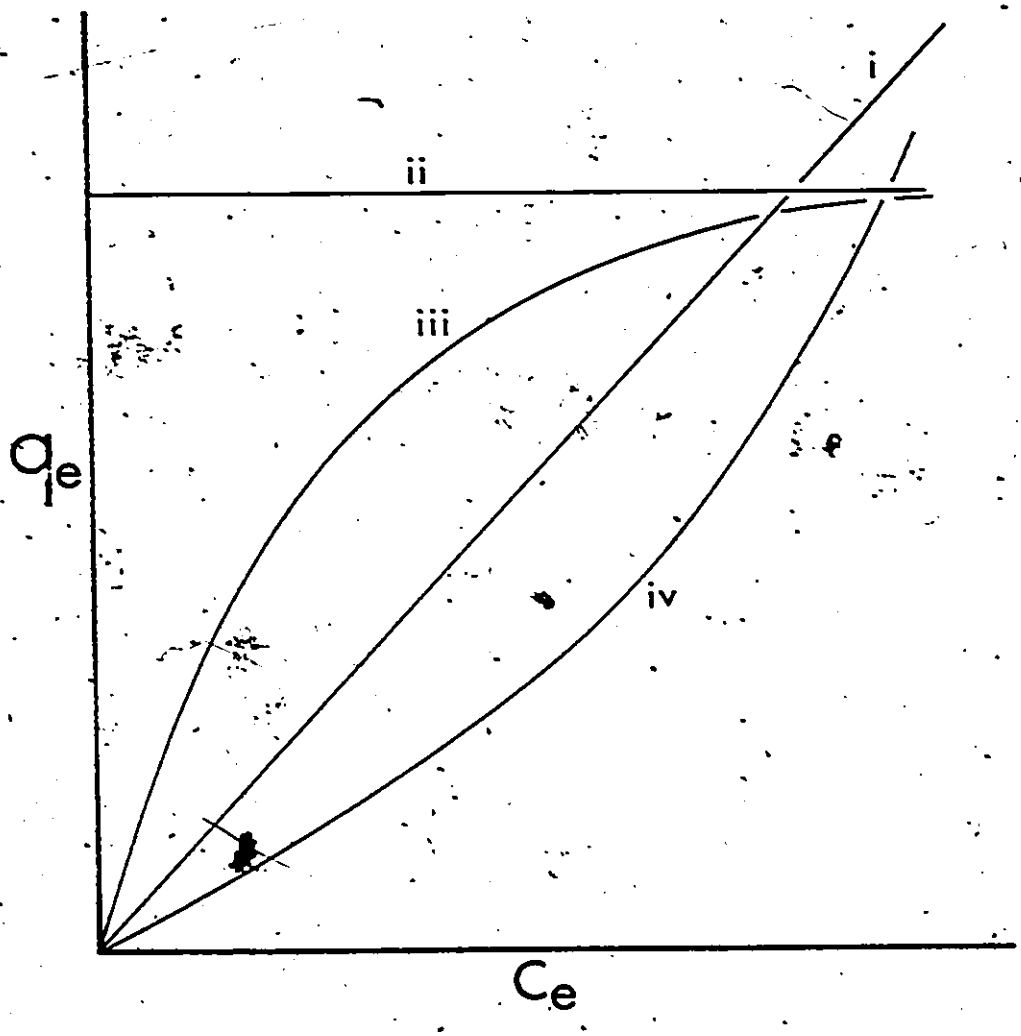

Figure 2-1. Common Types of Isotherms in Aqueous Systems.

(i)	linear	$q_e = M c_e$	(2.1)
(ii)	irreversible	$q_e = M$	(2.2)
(iii)	favourable	$q_e = f(c_e)$ $f' < 0$	(2.3)
(iv)	unfavourable	$q_e = f(c_e)$ $f' > 0$	(2.4)

in which q_e = equilibrium solid phase concentration, g/g of carbon; c_e = equilibrium liquid phase concentration, g/cm^3; M = a constant; and f is an arbitrary function.

The irreversible isotherm is a special case of the favourable isotherm, and the linear isotherm is the limit of both favourable and unfavourable isotherms as f' approaches zero. The terms favourable and unfavourable are based on the behaviour of the adsorption wave within an adsorbent bed, a favourable isotherm gives a constant pattern profile whereas an unfavourable isotherm gives a proportionate pattern which continues to lengthen as it travels through the bed and hence gives unfavourable breakthrough characteristics.

Fortunately, the majority of isotherms found in aqueous systems are of the favourable type and three common forms of description are:

(i)	Freundlich isotherm	$q_e = M c_e^n$	(2.5)
(ii)	Langmuir isotherm	$q_e = \frac{a.b.c_e}{b + c_e}$	(2.6)
(iii)	3-parameter isotherm	$q_e = \frac{a.c_e}{1 + b\, c_e^{\alpha}}$	(2.7)

The 3 parameter isotherm has been used by Mathews and Weber (1977), Crittenden (1976) and Ying (1978), and can yield both Langmuir and Freundlich isotherms as special cases.

The Langmuir isotherm can be derived theoretically both from kinetic and thermodynamic considerations based on the assumptions of constant adsorption site energy and no interaction between adsorbed molecules. It has been shown to fit some aqueous systems over limited concentration ranges as described by Singer and Yen (1978). Crittenden (1976) suggested that although activated carbons might be expected to have a heterogeneous distribution of adsorption site energies, over a limited concentration range the site energies might be almost constant and thus a Langmuir description may fit the data. The fact that a Langmuir isotherm describes the data does not imply that the adsorption sites have constant energy. As discussed by Weber and Van Vliet (1978) some systems which fit a Langmuir model have also been shown to fit the Freundlich model which is based on an exponential distribution of adsorption energies. Therefore, mechanistic significance should not be attached to the coefficients of the isotherms, and instead, they should be regarded essentially as empirical curve fitting procedures.

Since the activated carbon surface is heterogeneous it would appear to be most compatible with the Freundlich description and in fact the majority of liquid phase systems are found to be quite well described by the Freundlich isotherm. When dealing with extended concentration ranges, however, Mathews (1975) and Crittenden (1976) found that the 3-parameter model was necessary to describe the entire range. Ying (1978) worked with similar substrates and found that the 3-parameter model could generally be dropped in favour of the simpler Freundlich model over the concentration range studied.

2.3 Kinetic Factors in Adsorption Processes

The transfer of adsorbate from the bulk liquid to an adsorption site within the carbon particle controls the rate of attainment of equilibrium. This transfer process consists of 3 steps:

(i) Transfer across the external liquid film surrounding the particle..

(ii) Transfer from the liquid phase to the solid phase at a particular location (adsorption).

(iii) Intraparticle diffusion either in the liquid within the pores (pore diffusion), or in the adsorbed state along the walls of the pores (surface diffusion).

The order of steps (ii) and (iii) depends on which mechanism is assumed responsible for intraparticle diffusion. In the pore diffusion model a molecule is assumed to be immobile once adsorbed, and thus the adsorption step occurs at the site of final adsorption. In the surface diffusion model, adsorption occurs at the outer surface of the carbon particle and adsorbate diffuses to its final adsorption site along the pore walls. In pore diffusion the driving force for transport is the concentration gradient in the liquid phase whereas in surface diffusion it is the concentration gradient in the adsorbed phase. The surface diffusion model is analogous to the homogeneous diffusion model which was used in early adsorption studies (Vermeulen, 1958).

In the following sections the steps (i) to (iii) above are described in detail.

2.3.1 External Film Transfer

The complex microscopic behaviour in laminar or turbulent boundary layers can be simplified using boundary layer theories (Levich, 1962) through which integration of the local mass transfer resistances yields an overall resistance. This resistance is described by the Sherwood number which is related to the Reynolds and Schmidt numbers as shown in equation (2.8).

$$Sh = \alpha_1 + \alpha_2 Re^{\beta_1} Sc^{\beta_2} \qquad (2.8)$$

The parameters (α_i, β_i) can be calculated theoretically but are normally determined by correlating data collected over a range of Reynolds and Schmidt numbers. For mass transfer in packed beds, Crittenden (1976) reviewed a number of available correlations and chose that proposed by Williamson et al. (1963) as it most closely matched his experimental range. Westermark (1975) and Svedberg (1975) used a correlation for low Reynolds number flows developed by Wilson and Geankoplis (1966). The same correlation was used by Liapis and Rippin (1977) who compared it to a correlation of Mandelbaum and Böhm (1973) and found negligible difference.

In batch experiments, where the carbon is often in free suspension, Furusawa and Smith (1973) were able to correlate mass transfer coefficients with a Reynolds number based on Kolmogoroff's theory of isotropic turbulence. Their results were in accord with previously published results for related systems. However, since it is normally possible to directly measure the film transfer coefficient in batch experi-

ments, these correlations are not required to conduct a kinetic modelling study.

2.3.2 Intrinsic Rate of Adsorption

The rate of transfer of adsorbate from the liquid to adsorbed phase is generally assumed to be orders of magnitude faster than other diffusional processes and can therefore be neglected as a rate limiting step. As a consequence local equilibrium is assumed at the internal surfaces of the carbon particle as well as at the outer surface. Weber and Morris (1963) reasoned that this assumption could be made based on the extremely rapid rate of attainment of equilibrium when surfactant materials are added to planar systems and lower interfacial tensions. Crittenden (1976) argued quantitatively that adsorption is not rate limiting based on an analysis of the surface residence time of an adsorbed molecule.

2.3.3 Intraparticle Diffusion

The two possible mechanisms of intraparticle transport, pore diffusion and surface diffusion, can be described mathematically as follows. By making the following assumptions: (i) only dilute solutions are considered and therefore bulk flow terms can be neglected (Weber and Chakravorti, 1974), (ii) the effective diffusion coefficients are independent of concentration and radial position: the intraparticle diffusion equation can be written as

$$D_p \left\{ \frac{1}{r^2} \frac{\partial}{\partial r} \left(r^2 \frac{\partial c}{\partial r}\right)\right\} + D_s \left\{\frac{\rho_c}{r^2} \frac{\partial}{\partial r} \left(r^2 \frac{\partial q}{\partial r}\right)\right\} = \epsilon_p \frac{\partial c}{\partial t} + \rho_c \frac{\partial q}{\partial t} \quad (2.9)$$

in which D_p = effective pore diffusion coefficient, cm^2/sec; D_s = effec-

tive surface diffusion coefficient, cm^2/sec; r = radial variable, cm; c = liquid phase concentration in pores, g/cm^3; q = solid phase concentration, g/g adsorbent; ε_p = internal porosity of the adsorbent particle; ρ_c = apparent adsorbent particle density, g/cm^3.

The first term on the right hand side of equation (2.9) represents accumulation in the liquid filled pores and is generally considered to be negligible in comparison to the second term (Neretnieks 1976a) when dealing with adsorbents exhibiting strong partitioning behaviour.

As noted previously, the mechanisms of surface diffusion and homogeneous diffusion are mathematically identical. The homogeneous diffusion mechanism is the mass transfer analogue of heat transfer in a solid sphere, whereas the surface diffusion mechanism assumes that the adsorbent particle has an internal structure. The surface diffusion mechanism is discussed in detail by Komiyama and Smith (1974b).

The majority of early work dealing with adsorption modelling assumed either pore or homogeneous diffusion to be controlling. These works have been summarized in tabular form by Weber and Chakravorti (1974) who indicated that about equal use had been made of each mechanism. Weber and Chakravorti pointed out that care should be taken in the unsubstantiated use of a particular mechanism as their simulations indicated that breakthrough curves varied in shape depending upon the model chosen. Similar differences in shape were shown in the simulated curves of Fleck et al. (1973).

Since Brecher et al. (1967) and Dedrick and Beckmann (1967) pro-

posed a model in which both pore and surface diffusion mechanisms occurred simultaneously, many investigators have studied the combined model. Impetus for the inclusion of the surface diffusion mechanism came from the fact that in several studies assuming a pore diffusion mechanism (Dedrick and Beckmann, 1967; Di Giano and Weber, 1973; Furusawa and Smith, 1973 ; Westermark, 1975), pore diffusion coefficients were obtained which were higher than the corresponding free liquid diffusivities, and therefore tortuosity factors which were less than unity. The tortuosity factor (Wheeler, 1951) relates the actual path length travelled by an adsorbing molecule to the radial distance. The effective pore diffusivity can be defined as

$$D_p = \frac{\varepsilon_p D_\ell}{\nu} \qquad (2.10)$$

where ν is the tortuosity factor. Since there is no known mechanism for enhancing diffusion in the liquid phase, the high observed diffusion coefficients were attributed to the presence of simultaneous transport by surface diffusion.

In analyzing data of the adsorption of benzene from aqueous solution onto activated carbon, Furusawa and Smith (1973) found that after including surface diffusion in their model, the contribution of pore diffusion to the overall transport rate was negligible. An anticipated maximum pore diffusion coefficient was calculated based on the free liquid diffusivity and an assumed tortuosity.

A similar approach was taken by Fritz et al. (1978) who used a combined transport model to calculate diffusion coefficients from batch kinetic experiments. Since they could not measure the surface and pore

diffusion coefficients independently, they assumed a tortuosity of unity and calculated a maximum effective pore diffusivity. They then calculated effective surface diffusivities with and without the inclusion of pore diffusion, and found that in fitting binary systems the inclusion of pore diffusion generally gave a better fit to the data. For single solute systems the ability of the model to fit the data with and without pore diffusion was about equal.

Both pore and surface diffusion models were used by Liapis and Rippin (1977) to analyse batch kinetic experiments. By visual inspection of their data, the surface diffusion model appears to fit the data slightly better than the pore diffusion model, however, subsequent work on column modelling (Liapis and Rippin, 1978) used the pore diffusion mechanism alone. The measured pore diffusion coefficients were comparable to the free liquid diffusivities suggesting tortuosity factors of near unity, whereas Satterfield (1970) suggests that they should be in the range of 2 to 4. Even though the calculated model parameters do not appear to be mechanistically realistic, Liapis and Rippin (1978) were able to model breakthrough data in a two component system quite well. This suggests that the pore model gives a good empirical description of the system regardless of whether or not it is the actual mechanism of transport.

The question of which model to use in a particular system appears to depend on the properties of the system being studied. In fundamental studies of surface transport, Komiyama and Smith (1974a, 1974b) studied adsorption of benzaldehyde onto Amberlite particles from a meth-

anol/water solvent. By varying the percentage of methanol in the solvent they were able to vary the adsorptive characteristics of the benzaldehyde. They also investigated the effect of surface area by comparing adsorption rates on resins having the same surface properties but different total surface areas. Their results showed that the surface diffusion coefficient was relatively independent of surface area but that it was strongly dependent on the bonding energy of adsorption. As the bonding energy decreased, the surface diffusivity increased. They attributed significant surface diffusion on adsorbents exhibiting strong adsorptive characteristics as being due to the high surface concentration and consequently large concentration gradients. The effect of surface concentration was assumed to more than compensate for the relatively low surface diffusion coefficients found with such adsorbents. The analysis suggested that surface transport was favoured over pore transport at low concentration due to the concentration effect on the pore surfaces.

Thus if adsorption is strongly favoured and relatively dilute solutions are used, surface transport will normally be the dominant mechanism and in such instances, although pore transport occurs, its contribution to the total flux of adsorbate will be negligible and it can be ignored. In contrast, as shown by Komiyama and Smith (1974a), when the attraction between the adsorbent and adsorbate is relatively weak, or when liquid phase concentrations are high, pore diffusion will play a significant part in sorbate transport and should be incorporated in a kinetic model.

With regard to the liquid phase adsorption of organic molecules onto activated carbon, Weber and Van Vliet (1978) and Crittenden (1976) have suggested that pore diffusion can be neglected based on evidence concerning the temperature dependence of effective diffusion coefficients; the fact that measured pore diffusivities are many times greater than free liquid diffusivities; and on actual quantitative calculations of the contributions of the two mechanisms (Neretnieks, 1976c).

2.3.4 Concentration Dependence of the Diffusion Coefficient

In deriving equation (2.9) it was assumed that in addition to incorporating tortuosity , porosity, and constriction effects into the effective diffusion coefficients, that these coefficients were also independent of concentration. This assumption is not necessarily valid and if a concentration dependence exists, the diffusion coefficients must be included within the differential term (Neretnieks, 1976b). The literature concerning concentration dependent diffusion coefficients is reviewed below to provide a basis for either incorporating or neglecting this factor.

When dealing with dilute solutions which have activity coefficients close to unity, and in which it is assumed that there are no interactive effects with other species, there is no reason to assume that the liquid phase diffusion coefficient should be concentration dependent. There are,however,several theoretical reasons for hypothesizing a concentration dependence of the surface diffusion coefficient and experimental observations appear to substantiate some form of concentration dependence.

Komiyama and Smith (1974b) showed that the surface diffusion coefficient was a strong function of the adsorbate/adsorbent bonding energy. They presented a theory for surface transport based on the Eyring hole theory for molecular diffusion in liquids, and showed that their data were consistent with such a theory. If the rate of surface diffusion is related to the bonding energy, then it seems probable that some concentration dependence would be observed on an adsorbent such as activated carbon which has a broad spectrum of available bonding energies. If it is assumed that adsorbing molecules preferentially migrate to strongly adsorbing sites, then as surface coverage increases, more and more of the high energy sites may be occupied and the mean site bonding energies of the remaining open sites may continually decrease. Consequently, based on the data of Komiyama and Smith (1974b), the surface diffusion should increase with increasing surface concentration. A similar argument has recently been proposed by Fritz et al.(1978) to explain the observed concentration dependence of calculated surface diffusion coefficients.

A quantitative description of the surface diffusion coefficient's (D_S) concentration dependence was proposed by Neretnieks (1976b) for liquid adsorption systems. He based his analysis on the work of Gilliland et al.(1974) and Sladek et al.(1974), who had studied concentration dependencies in gas phase adsorption. Neretnieks reasoned that if the surface diffusion coefficient were a function of the heat of adsorption according to

$$D_S = \alpha_1 \exp\{ -\beta_1 \frac{\Delta H_{ad}}{RT} \} \qquad (2.11)$$

in which α_1, β_1 = constants; ΔH_{ad} = heat of adsorption; R = gas constant; and T = absolute temperature; and further that if the heat of adsorption was assumed to be linearly dependent on surface coverage, i.e.

$$\Delta H_{ad} = -\Delta H_o - (\Delta H_{sat} - \Delta H_o) \cdot Q \cdot \frac{q_o}{q_{sat}} \qquad (2.12)$$

in which ΔH_o = heat of adsorption at zero surface coverage; ΔH_{sat} = heat of adsorption at saturation; and Q = dimensionless surface concentration, q/q_o; then the surface diffusion coefficient could be written as

$$D_s = D_o \exp\{\alpha_2 Q\} \qquad (2.13)$$

Neretnieks solved equation (2.9) using equation (2.13) and presented a number of simulated curves for various values of the constant α_2.

In a subsequent paper, Neretnieks (1976c) rederived equation (2.13) commencing with the assumption of a modified Temkin isotherm. He analysed the data of several previous researchers using a simplified evaluation procedure based on a series of dimensionless plots. From the analysis he concluded that phenylacetic acid (PAA), phenol, and p-chlorophenol (PCP) showed a concentration dependence of D_s, whereas p-nitrophenol (PNP), and benzoic acid (BA) did not. No explanation was offered for the differences in behaviour of these compounds.

In a review of surface concentration dependence, Crittenden (1976) questioned the assumptions made by Neretnieks (1976b) on the basis that they were not consistent with the assumption of the Freundlich isotherm, an isotherm which is found to describe many liquid phase adsorption systems. As pointed out by Crittenden, a thermodynamic derivation

of the Freundlich equation suggests an exponential distribution of site bonding energies and a site entropy which is linearly proportional to the heat of adsorption. This is in contradiction to the assumption inherent in equation (2.12). He went on to tentatively propose a basis for a model of concentration dependence of D_S which would be compatible with the implications of a Freundlich isotherm. The model was to be based on the theory proposed by Komiyama and Smith (1974b) for surface migration. Crittenden did not develop the model as he concluded that the complications involved in including a concentration dependence for D_S were not justified until a sound phenomenological basis had been developed and experimentally verified. He also noted that his fixed bed model was not particularly sensitive to the magnitude of D_S, and further, since he was able to model the kinetic behaviour reasonably well over a limited concentration range, the inclusion of a concentration dependence of D_S did not appear to be necessary.

Two studies have been reported in the literature which specifically investigated the concentration dependence of D_S in liquid phase adsorption of organics onto activated carbon. In both studies, batch kinetic experiments commencing at different initial concentrations were used to gather experimental data. Sudo et al.(1978) obtained the D_S values by comparing the data to sets of curves generated by a surface diffusion model, whereas Fritz et al.(1978) calculated the D_S values by a direct regression analysis of the data using a surface diffusion model, with and without incorporation of pore diffusion. The D_S values calculated by Fritz et al. were shown to increase with increasing initial liquid phase concentration when studying phenol adsorption, and to either

increase or decrease slightly, depending upon whether or not pore diffusion was included, in studies with p-nitrophenol.

Sudo et al.(1978) studied several compounds and found that the D_s values always increased with increasing amounts of substrate adsorbed at equilibrium. They were able to fit their data to an equation of the type suggested by Neretnieks (1976b), however, they used this equation to describe the relationship between the equilibrium solid loading and a mean D_s value calculated from a model which assumed a constant D_s. In contrast, the equation of Neretnieks describes the relationship between the local D_s value and the local solid phase loading, and has a quite different meaning from that described by Sudo et al. Additionally, the range of D_s values reported by Sudo et al. may have been greater than actual. Fritz et al.(1978) have shown that the inclusion of pore diffusion reduces the apparent concentration dependence of D_s since pore diffusion plays an increasingly significant role at higher concentrations.

In summary, although an apparent concentration dependence of the diffusion coefficient has been noted in several studies, a functional form of this dependence has not been conclusively established. The data for a particular experiment appear to be well described by a model assuming a constant D_s, however, the measured coefficients appear to be a function of the initial concentration or final equilibrium loading in each experiment. In addition, anomalous behaviour has been observed as both Neretnieks (1976c), and Fritz et al.(1978), have indicated that whereas some compounds such as phenol exhibit an apparently strong con-

centration dependence, other related compounds such as p-nitrophenol exhibit little or no such dependence. This behaviour is not consistent with the proposed theories of concentration dependence.

Because of the uncertainties which exist with regard to a surface concentration dependence, a constant D_S is assumed in the present study. Batch kinetic experiments for parameter evaluation are normally conducted over the same concentration ranges that are used in the adsorption columns to be simulated, and therefore even if a concentration dependence of D_S were to occur, it would be taken into account by evaluating an average D_S and should not affect the modelling strategy. It was accepted, however, that if the experimental data were not compatible with the chosen model, reevaluation of this assumption might be necessary.

2.3.5 Additional Dependencies of the Diffusion Coefficient

Although there are several references in the literature to potential relationships between the diffusion parameters and the pore size distribution, models of activated carbon adsorption have not yet been developed to test this hypothesis.

In experiments of adsorption of pure solutes and complex mixtures onto fixed beds of activated carbon, Usinowicz (1972) measured asymmetric breakthrough curves. His data showed an extended tail on the breakthrough curve and he attributed this to the possibility of a slow reaction following an initial rapid one. He also cited three previous works which had shown similar behaviour, but did not elaborate on these observations.

Neretnieks (1976c) noted that activated carbon particles have a

polydisperse pore structure and that transport rates in pores of different sizes may not be equal. In very small pores of near molecular dimensions he suggested that transport rates would be very slow due to spatial hindrances, however, he did not include this possibility in developing his model. A similar concept was discussed by Crittenden (1976) in a preamble relating to pore diffusion mechanisms. He suggested that activated carbons have a bidisperse structure consisting of macropores and micropores and noted that it was possible to formulate an in series process such as macropore-micropore diffusion. Additionally, he noted that solutes may diffuse more or less rapidly depending upon the pore diameter. Eventually, however, he reasoned that the complex internal structure of activated carbon defies the quantitative description of this type of phenomenon and he chose to utilize a single effective diffusion coefficient model.

In studies with adsorbents or other materials having a well defined pore structure, the effect of steric hindrance in small pores has been proven. Beck and Schultz (1970) studied diffusion rates of a range of solutes through non-adsorbing membranes containing pores of known dimensions. They found large reductions in the effective pore diffusivity even at small particle diameter: pore diameter ratios, and were able to correlate their data quite well with the Renkin equation which includes the wall effects described by the Faxen equation as well as the exclusion effects based on geometrical considerations at the pore mouth. The Renkin equation is:

$$\frac{D_{eff}}{D_{\infty}} = (1 - \lambda)^2 (1 - 2.10\lambda + 2.09\lambda^3 - 0.95\lambda^5) \qquad (2.14)$$

in which λ = radius of solute/radius of pore; and D_∞ = diffusivity in free liquid.

Studies where the additional effect of adsorption was present were carried out by Satterfield et al.(1973). With non adsorbing solutes they found a simple relationship between the reduction in effective diffusivity and the solute diameter: pore diameter ratio. This finding did not agree with the results of Beck and Schultz (1970). Satterfield also found that adsorption further decreased the diffusivity below that for an equivalently sized non-adsorbing solute. They attributed this effect to the likelihood that intermolecular forces between the solute and the pore walls extend some distance into the fluid and do not just involve adsorbed molecules. These forces then exert a restraining effect on transport of solute molecules adjacent to the pore walls.

Additional work has recently been reported by Malone and Anderson (1978) which extends earlier work by Anderson and Quinn (1974). These authors generally confirmed the previous findings and introduced additional factors which were responsible for reducing the effective diffusion coefficient below that predicted by the Renkin equation alone.

The likelihood that this hindrance effect is present when pore diffusion occurs within an activated carbon particle has therefore been established. Nevertheless, as noted earlier, previous researchers have assumed that in spite of this potential effect adsorption can still be defined by a single effective diffusion coefficient.

Since the mechanisms of surface diffusion are still under investigation, subtleties such as the effect of pore size on the effective

diffusion coefficient have not been investigated. It might be assumed that the effect would be similar to the pore diffusion case but there is presently no mechanism available which might quantify such a phenomenon. It could be argued that since surface bonding energies are expected to be higher in small pores, and since it has been shown that surface diffusion coefficients decrease with increasing bonding energies (Komiyama and Smith, 1974b), that surface diffusion coefficients should be less in small pores. At the present stage of development of pore surface diffusion theory evidence does not yet exist to support this hypothesis.

2.3.6 Simplified Adsorption Rate Expressions.

Numerous simplified solutions of the pore and surface diffusion models based on the assumption of either linear or irreversible isotherms have been presented in the literature. These will not be discussed herein as they all relate to solution of equation (2.9), which has been discussed in detail. Since each of these solutions are restricted to a particular type of isotherm, their use in a general model is limited. There are, however, other ways of describing the adsorption rate phenomena.

The simplest of these methods is the replacement of the differential driving force expression of equation (2.9) by a driving force expression which gives the rate in terms of an average or bulk parameter rather than in terms of a continuous gradient. The earliest such approach was described by Glueckauf and Coates (1947) who introduced a linear driving force model to describe favourable and irreversible equi-

librium systems. Their equation was;

$$\frac{d\bar{q}}{dt} = k_p a_p (q_s - \bar{q}) \qquad (2.15)$$

in which $\bar{q}$ = mean solid phase concentration in the particle; k_p = pseudo mass transfer coefficient; and q_s = solid phase concentration at the particle's outer surface.

By comparing equation (2.15) to the exact solution of the homogeneous diffusion model for an irreversible isotherm, Vermeulen (1953) showed that it was a poor approximation in the initial stages of adsorption and he suggested a quadratic driving force which was simply an empirical fit to the exact solution. The form suggested was;

$$\frac{d\bar{q}}{dt} = k_p a_p \left(\frac{q_s^2 - \bar{q}^2}{2\bar{q}}\right) \qquad (2.16)$$

In a later paper Glueckauf (1955) compared equations (2.15) and (2.16), as well as two other more complex expressions, to the exact solution for homogeneous diffusion. He showed that for linear or near linear isotherms equation (2.15) was superior to equation (2.16) but that for non-linear isotherms the opposite was true. The criterion used by Glueckauf (1955) was the numerical value of $k_p a_p$ whereas Vermeulen (1953) had based his arguments on the actual shape of the adsorption rate curve. Although $k_p a_p$ can be predicted from a knowledge of the homogeneous diffusion coefficient (Vermeulen, 1973; Garg and Ruthven, 1975), for modelling purposes $k_p a_p$ is fitted to experimental data and therefore the shape of the adsorption curve, and not the numerical value, is the more important criteria.

Cooper (1965) compared the linear and quadratic driving force approximations to the exact solution obtained by assuming an irreversible isotherm. He found that the quadratic driving force very closely approximated the analytical solution even during the initial transient state and thus extended its applicability beyond the constant pattern period which had been investigated by Glueckauf (1955).

An alternative description of the adsorption rate was proposed by Thomas (1948). He assumed that the rate of adsorption could be described by a reaction kinetics approach which, if constant site bonding energies are assumed, can be written;

$$\frac{d\bar{q}}{dt} = \rho_c \{K_f (q' - \bar{q}) c - K_r \bar{q}\} \qquad (2.17)$$

in which K_f = forward reaction rate constant; K_r = reverse reaction rate constant; and q' = monolayer coverage concentration. At steady state equation (2.17) reduces to the familiar Langmuir equilibrium expression.

This equation is purely empirical since it does not describe the true diffusion limited situation, however, since it has an analytical solution, it has found application. Thomas (1948) gave analytical solutions for the fixed bed problem and Heister and Vermeulen (1952) described methods for determining the constant K_f from mass transfer information. The model was shown to be useful by Vermeulen and Huffman (1953) when modelling ion exchange data. It has also been used with some modification by Keinath and Weber (1968) and Usinowicz (1972) with limited success. Weber and Crittenden (1975) noted that the simple second order kinetic expression cannot be used unless a single rate controlling mecha-

nism is operative throughout the entire adsorption period. Since in many practical cases this situation does not arise, the use of this approach is limited.

2.4 Previous Column Modelling Studies

The possible mechanisms by which adsorption onto activated carbon can be modelled have been discussed in the previous section. When developing a model to describe the performance of an activated carbon adsorption bed, an additional mass balance in the fluid phase must be solved simultaneously with the equations describing adsorption onto the carbon. In the case of linear or irreversible isotherms, analytical solutions can normally be found. In addition, numerical solutions have been described for virtually all possible combinations of isotherm type and intraparticle transport mechanism. Weber and Chakravorti (1974) have tabulated most of these studies.

Aside from choosing the type of isotherm and the adsorptive mass transfer resistances, a decision must be made as to the inclusion or neglect of axial dispersion in the fluid phase equation. It is generally assumed that the radial gradient, and consequently radial dispersion, is negligible in packed adsorption beds.

2.4.1 Axial Dispersion

Axial or longitudinal dispersion is a measure of the spreading of an initially sharp wavefront as it moves through a packed bed. The components of dispersion are (Miyauchi and Kikuchi, 1975);

(i) Molecular diffusion,

(ii) Eddy dispersion due to convection.

An additional effect which is sometimes considered is the transfer of material between the flowing fluid and the stagnant boundary layer surrounding the packing (Babcock et al.,1966). Since the liquid boundary layer is usually modelled separately in adsorption column modelling, this effect need not be considered when k_f is evaluated independently.

If axial dispersion is assumed, the fluid phase equation obtained from a mass balance over a differential bed segment of length dz is:

$$\frac{\partial c}{\partial t} = D_z \frac{\partial^2 c}{\partial x^2} - v_s \frac{\partial c}{\partial x} - \left(\frac{1-\varepsilon}{\varepsilon}\right) \cdot \frac{3k_f}{R} (c - c_s) \qquad (2.18)$$

in which D_z = axial dispersion coefficient, cm^2/sec; x = bed length variable, cm; ε = liquid volume fraction; k_f = external film transfer coefficient, cm/sec; R = radius of adsorbent particle, cm; c_s = liquid phase concentration at the particle surface, g/cm^3; and v_s = interstitial liquid phase velocity, cm/sec.

Chakravorti (1973) compared experimental data in packed beds to models with and without axial dispersion. He concluded that axial dispersion was necessary to describe the observed behaviour, however his solution without axial dispersion is quite different from the solution with axial dispersion as $D_z \to 0$. Consequently, his conclusions may be incorrect.

In a comprehensive activated carbon adsorption model, Svedberg (1975) included the axial dispersion term and found for typical values of D_z, that the predicted model output was virtually identical to the

zero dispersion case. Axial dispersion was subsequently neglected. Svedberg concluded that since the column length : particle diameter ratio in adsorption columns is large, the lowest possible Peclet number based on column length would be about 500 and therefore D_z is small. A similar conclusion was reached by Crittenden (1976, 1978a) who calculated a Peclet number based on a correlation of Ebach. For bed length : particle diameter ratios of 200 to 1000, the Peclet number based on bed length was 100 to 500 and hence he concluded that axial dispersion could be neglected.

If, as indicated above, axial dispersion is negligible for most common situations of liquid phase adsorption, then its removal from equation (2.18) considerably simplifies the model solution. With the axial dispersion term, equation (2.18) is parabolic and its solution involves problems associated with defining the correct boundary conditions in axial flow reactors (Wehner and Wilhelm, 1956; Fan and Ahn, 1962; Ziegler, 1975). If the axial dispersion term can be neglected a priori the equation is hyperbolic, has a simple boundary condition, and its solution involves less computation.

2.4.2 Previous Experimental Column Modelling Studies.

Many theoretical models have been presented in the literature to describe the performance of activated carbon adsorption beds. In this section only those studies in which experimental column runs have been conducted to verify the proposed models will be discussed.

Mathematical models of adsorption beds differ principally in the choice of equations to describe the uptake rate onto the carbon. The

possible kinetic descriptions have been discussed in section 2.3. There are two ways of measuring the kinetic parameters of a proposed model, either in a batch kinetic experiment, or from the breakthrough behaviour of an adsorption bed. An adsorption kinetic model must be able to describe both phenomena using an identical set of parameters.

The parameters are most easily measured from a batch kinetic experiment. The parameters determined by batch experiment are then used in an adsorption bed model to predict the performance of experimental columns and comparison of the predicted and observed behaviour gives a means of verifying the kinetic model on an independent set of data. At the same time, the model's abilities as a predictive tool for design purposes can be assessed.

Keinath and Weber (1968) modelled the adsorption of an insecticide onto activated carbon in a fluidized bed. They used the reaction kinetics approach of Thomas (1948) and of Heister and Vermeulen (1952) with the inclusion of external film resistance, and they obtained the kinetic parameters by analysing a large amount of batch kinetic data. They were able to describe the breakthrough curves quite well except for the initial stages of uptake, and noted that film diffusion was the primary rate controlling mechanism for adsorption. Consequently, the results were relatively insensitive to the form used to describe the intraparticle kinetics.

The same model was used by Usinowicz (1972) in work which used a bulk parameter such as COD to describe the concentration of a multicomponent system. Even in the single pure solute part of the study, he

was unable to model the effluent concentration beyond 50% breakthrough. He found that whereas the model predicted a fairly symmetric 'S' shaped breakthrough curve, the experimental data were asymmetric, exhibiting strong tailing in the later stages. In a later study, Ying (1978) used the reaction kinetic model to analyse batch kinetic data and found that the predictions made by this model were not as good as those obtained using a surface diffusion model. He proposed that the reaction kinetics approach is suitable only when a fairly rapid but only approximate method is required.

Brauch and Schlünder (1975) presented a model based on combined film and pore diffusion control and assumed an irreversible isotherm. They obtained an analytical solution for the adsorption column model and measured the kinetic parameters for phenylacetic acid, phenol, and p-nitrophenol in batch kinetic experiments. In all cases quite good agreement between the predicted and experimental breakthrough curves was observed, however, the predicted curves consistently reached saturation quite rapidly whereas the experimental curves tailed off as saturation was approached. Typical sets of breakthrough curves reported by Brauch and Schlünder (1975) are shown in Figure 2-2.

In a study of multicomponent adsorption, Liapis and Rippin (1977, 1978) presented batch kinetic models for both pore and surface diffusion in series with an external film resistance, and developed a model to describe multicomponent adsorption column behaviour using a series film-resistance - pore diffusion model. Although the batch kinetic data appeared to be slightly better fitted by the surface diffusion model,

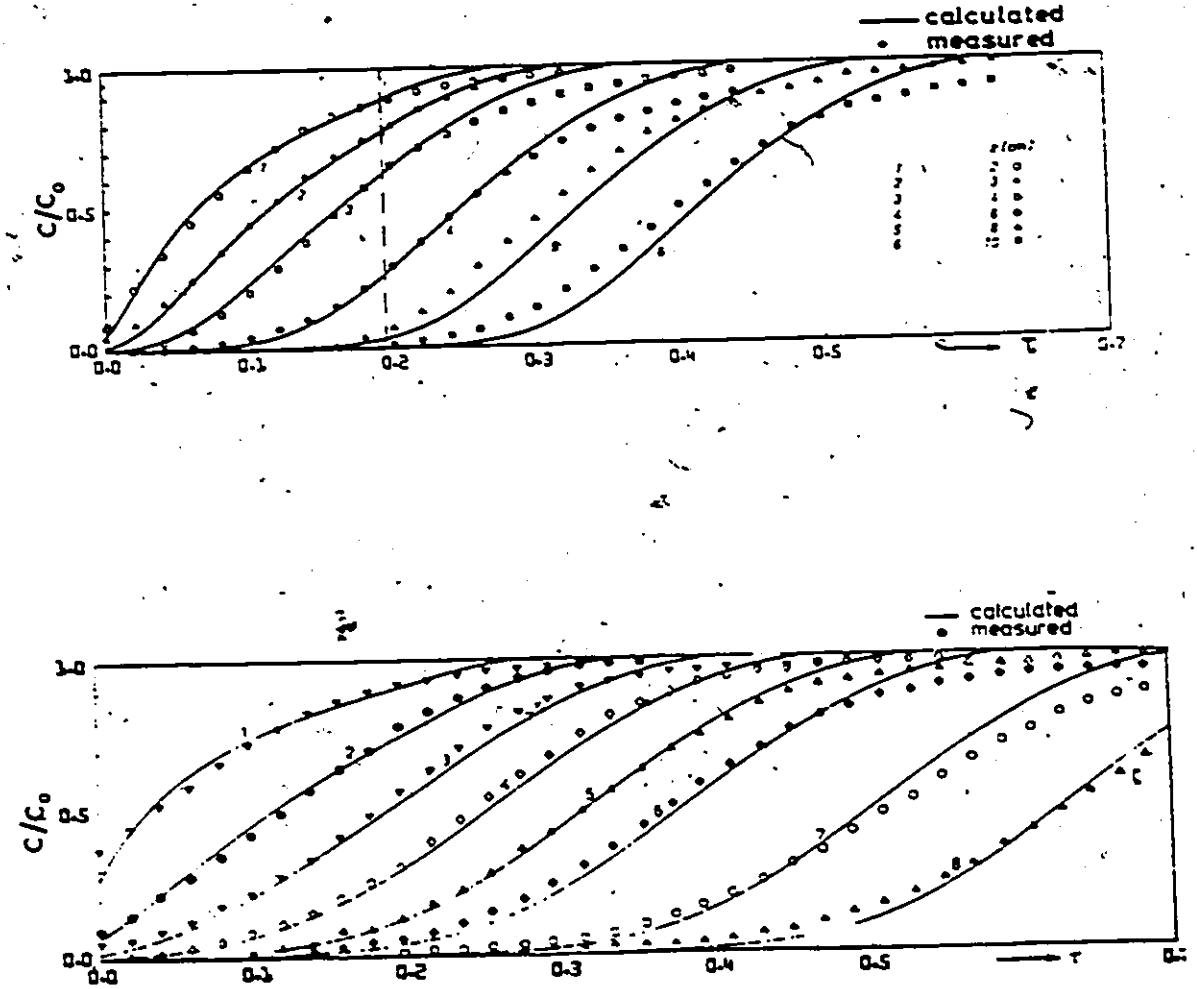

Figure 2-2. Experimental and Predicted Breakthrough Profiles for Phenylacetic Acid and Phenol. After Brauch and Schlünder (1975).

they chose to use the pore diffusion model in the column simulations without explanation. The measured pore diffusion coefficients appeared to be approximately equal to, or slightly higher than, the corresponding free liquid diffusivities suggesting that some surface diffusion was most probably occurring. Nevertheless, the column model predictions corresponded reasonably well to the experimental data with improved matches being obtained after adjustment of the kinetic parameters. In these experiments the breakthrough curves were obtained over relatively short periods on the order of 12 hours which, as explained in a later chapter, are more likely to result in a good prediction of performance than would runs over larger time periods.

Multicomponent adsorption modelling was also studied by Fritz et al. (1978) using both surface diffusion alone, and combined surface diffusion-pore diffusion models. The combined model was found to give a better prediction of the column performance than the surface diffusion alone model. The surface diffusion coefficients were obtained by fitting batch kinetic data and the pore diffusion coefficient was calculated from the free liquid diffusion coefficient assuming a tortuousity of unity. Because of the complications associated with multicomponent adsorption, disagreement between predicted and experimental curves can be attributed to both incorrect equilibrium description and incorrect kinetic description and therefore it is difficult to evaluate the correctness of the combined model. However, the predicted and experimental curves were in reasonably close agreement overall.

In a comprehensive study of the activated carbon system with

single and multicomponent adsorption, Weber and Crittenden (1975), Crittenden (1976), and Crittenden and Weber (1978a, 1978b) have presented a model based on external film resistance and surface diffusion. Equilibrium and kinetic parameters were measured separately by batch experiment and the resulting parameters were used in the column model for prediction and verification. In the initial work the experimental breakthrough data appeared much earlier than the column model predictions, and the authors introduced a revised isotherm based on the apparent column capacities and the end points of the batch kinetic experiments. Once adjusted for the different isotherm, the predicted and experimental profiles were quite similar except for some tailing of the experimental curves at long times such as those described in Figure 2-2. The tailing was observed with phenol and p-bromophenol but not with p-toluene sulphonate or dodecyl benzene sulphonate, both of which are larger molecules. The authors were not able to explain the differences between the experimental isotherms and the apparent capacities in the adsorption bed, and therefore were not able to predict column performance without first running a column experiment to calibrate the isotherm.

Ying (1978) used a similar kinetic approach to that of Crittenden in developing a model for a biologically active fluidized bed containing activated carbon. Before entering the biological phase of the study, he ran extensive isotherm and kinetic studies on a number of solutes to evaluate the adsorptive side of the model. Attempts to fit an external film resistance - surface diffusion model to batch kinetic data showed a systematic lack of fit of the model for the substrates potassium biphthalate, toluene sulphonate, sucrose and glucose. A reasonable fit was obtained with n-butanol. A typical example of the pronounced lack of fit is shown in Figure 2-3 which is reproduced from the data of Ying for potassium biphthalate. By inspection of the figure the least squares assumption of a random distribution of residuals is clearly violated, therefore the regressed coefficients have little or no meaning. In subsequent column verification experiments, Ying found that the regressed coefficients did not fit the experimental data and concluded that it was necessary to evaluate the surface diffusion coefficient from experimental column data. Returning to Figure 2-3 , it is apparent that there is an inconsistency between the apparent end point of the batch kinetic data, and the equilibrium implied by the fitted curves which is determined by the experimental isotherm. Thus, the results of Ying appeared to indicate the same problems of differences between the equilibrium isotherm and batch kinetic behaviour that had earlier been observed by Crittenden (1976). In both cases the final parameters used in the adsorption bed simulations had to be derived from previous column experiments.

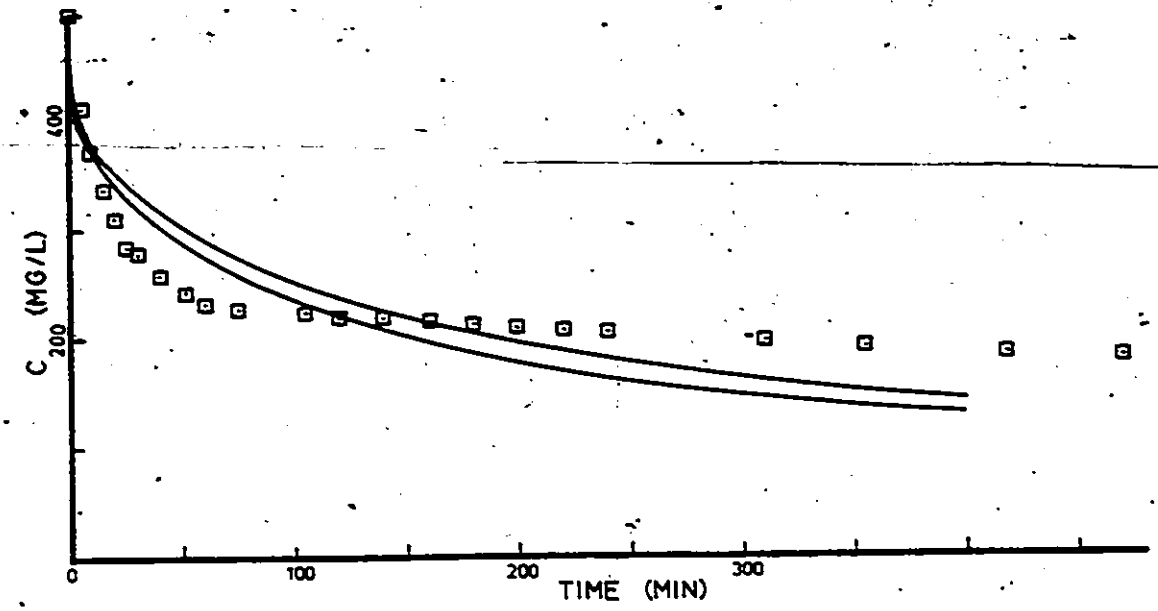

Figure 2-3. Batch Kinetic Data for Potassium Biphthalate with Solid Diffusion Model Fit. After Ying (1978).

In a recent study which ran parallel to the present work, Ramu-laro et al. (1978) developed a model which used the Glueckauf linear driving force approximation to describe the intraparticle kinetics. The authors further proposed that the carbon particle could be considered to consist of two separate regions, a micropore core surrounded by a macro-pore shell. They proposed that different rate parameters would be found in each section and proceeded to measure the kinetic rate parameters simultaneously in a batch kinetic experiment. When they applied the measured parameters to the column model a large adjustment of one of the kinetic parameters was required before the experimental data could be

matched. Consequently, the model was not fully predictive as a prior column run was required for parameter calibration.

In most of the studies reported above, there was a consistent failure to simultaneously explain the separate results of isotherm, batch kinetic, and column experiments. This lack of correspondence is tentatively attributed to inadequacies in the existing theories of the activated carbon adsorption mechanism and it was the aim of the study reported herein to develop a theory which would allow for consistent interpretation of the results of all three adsorption phenomena.

CHAPTER 3

EXPERIMENTAL MATERIALS AND METHODS

3.1 Adsorbates

The organic substrates chosen for this section of the work were phenol and o-chlorophenol (OCP). Phenol was obtained from the J.T. Baker Chemical Company (Baker Analysed Reagent, Specified Assay), and o-chlorophenol from BDH Chemicals Ltd. (Laboratory Reagent, min assay 99.5%). Phenol was selected as it has had wide usage in previous adsorption studies, thereby giving a sizeable data base for comparison with the results obtained in this work. It is also a common contaminant of industrial waste streams and water supply sources. o-Chlorophenol was selected as it adsorbs more strongly than phenol and has a highly non-linear isotherm and thus the two compounds covered the range from moderately adsorbable to strongly adsorbable. o-Chlorophenol is also difficult to degrade biologically and therefore its use minimized the possibility of biological removal of substrate during the experimental period. When chlorination is used for disinfection in either wastewater or drinking water treatment, and where phenolic compounds are present, chloro-substituted phenols result and according to Burttschell et al. (1959) o-chlorophenol is a likely first step in such substitutions. Also, Snoeyink et al. (1977) have suggested that chlorophenols may be a breakdown product of many pesticides in natural waters.

Water for the isotherm, kinetic, and column studies was obtained from a common source. Glass distillation was followed by deionization (Sybron-Barnstead, Ultrapure (mixed bed) cartridge, 5 ℓ/hr) and then by carbon adsorption by passing the stream through a large carbon filter containing 20 kg of activated carbon. The resulting TOC of the treated water was 100 µg/ℓ or less. No deterioration of the treated water quality as measured by either TOC or UV adsorbance (A_{254nm}^{10cm}) was observed during the study period.

Carbon filtered tap water was used in a preliminary series of column experiments but at pH 7, UV absorbance indicated that both the anionic and neutral species of o-chlorophenol were present even though the pKa of OCP is 8.49 (CRC,1966). Since the species have quite different UV absorption spectra and different adsorptive capacities, the experiments could not be conducted under these conditions. When the experiments were repeated at similar pH but using distilled water, only the neutral species of OCP was observed. The presence of the anionic form when dissolved in tap water at neutral pH could not be explained and all subsequent studies were carried out using only distilled water alone, or with a phosphate buffer.

Stock solutions of 10,000 mg/ℓ were made up of both substrates and stored at 4°C in the absence of light, dilution to the required concentration was made immediately prior to the start of an experiment. No attempt was made to control the pH except in two of the isotherm studies to be discussed later where a 0.002 M phosphate buffer at pH 7.0 was used. The pH was monitored in all experiments and did not vary out-

side of the range 6.8-7.2.

3.2 Adsorbent

The adsorbent used in all studies was Filtrasorb F400 (Calgon Corp., Pittsburgh, Pa.). The properties of the carbon as supplied by the manufacturer are given in Table 3-1. The carbon was obtained as 12 × 40 mesh and was subsequently sieved to 16 × 30 mesh to obtain a more uniform particle size (particle size based on average mesh dia. = 0.09 cm). A cumulative size distribution for this material is given in Figure 3-1 and was obtained using a Particle Size Analyser (Carl Zeiss - Model TGZ3). The distribution fits a log-normal probability function and therefore the geometric mean particle diameter is 0.094 cm (50th percentile). This diameter was used throughout the present work as the representative particle diameter.

The apparent particle density was calculated using the determined mean particle diameter and the calculation is described in Appendix A. The apparent density must be accurately known so that the external surface area of the granules can be calculated from the known mass of carbon.

The carbon was prepared by boiling in distilled deionized water then washing three times to remove fines and finally drying at 103°C to constant weight. The carbon was then stored in desiccators until used. Because the dried activated carbon is hygroscopic, care was taken when weighing out samples that the balance chamber was well dried otherwise rapid weight gain occurred on exposure to air.

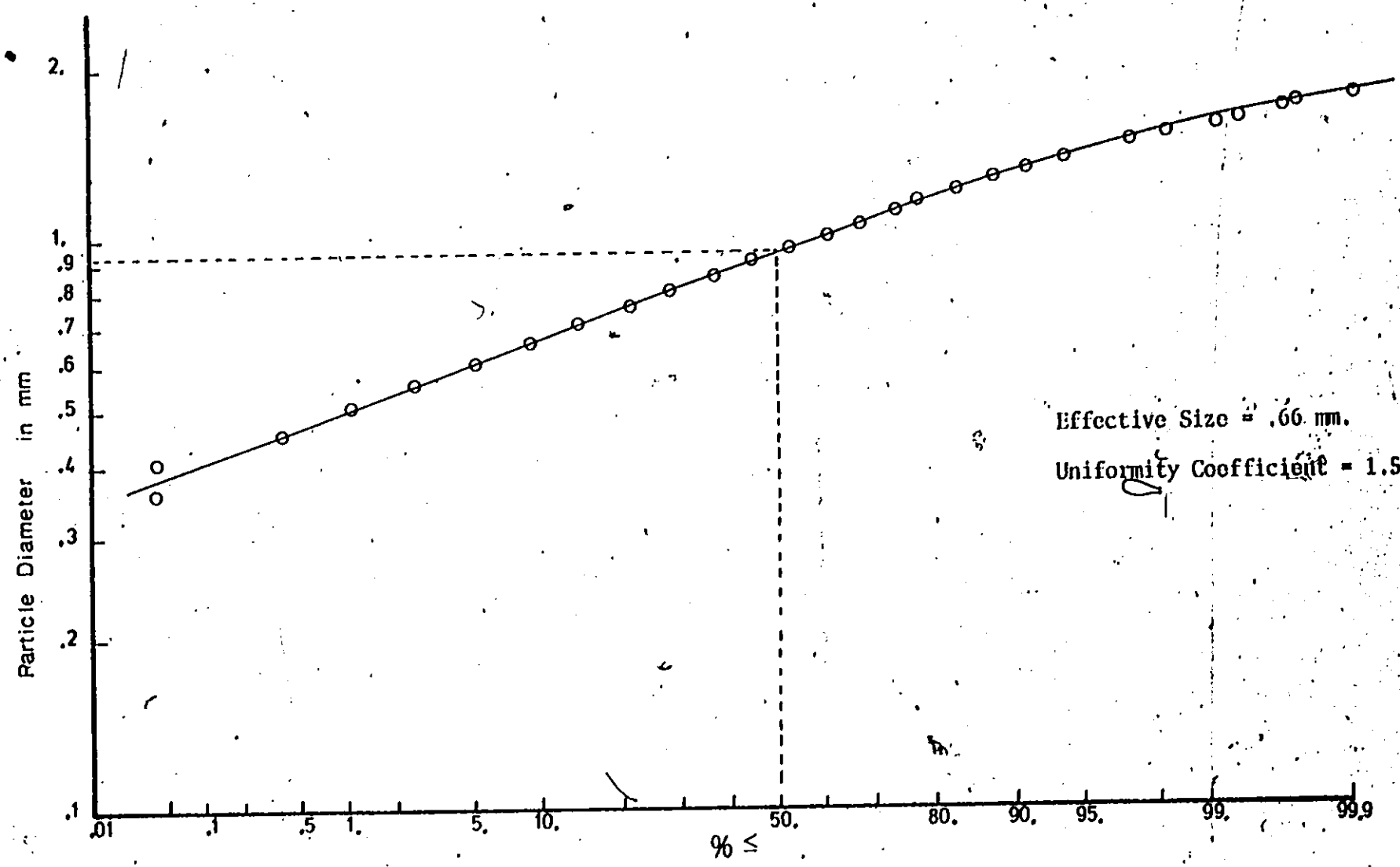

Figure 3-1. Cumulative Size Distribution - 16 × 30 mesh F400.

TABLE 3-1 : ADSORBENT PROPERTIES

	Manufacturer's * Specifications	This work
Total Surface Area (N_2, BET Method) m^2/g	1050-1200	
Bulk density, g/cm^3	0.401	0.416
Particle density, wetted in water, g/cm^3	1.3-1.4	
Apparent particle density, g/cm^3	0.75	0.75
Pore volume, cm^3/g	0.94	
Mesh size	12 × 40	16 × 30
Mean particle diameter, cm	0.09 - 0.11	0.094

* Chemviron (1970)

Powdered carbon for some of the isotherm studies was made by wet grinding a sample of the granular carbon in a mortar and pestle until the entire sample passed through a 200 mesh screen. The high purity water used was from the same source as described in the previous section thereby ensuring that the carbon was not contaminated by this procedure. After sieving the carbon was oven dried at 103°C and stored in a desiccator until used.

3.3 Analytical Techniques

Concentration analysis was principally performed by UV absorbance measurement. Both the substrates, phenol and OCP, have defined

UV absorption spectra with peaks at about 270 nm. A Beckman Model 25 UV Spectrophotometer was used for all measurements using a 1 cm path length cell.

An initial set of experiments indicated a linear relationship between concentration and absorbance over the 0.5 to 100 mg/ℓ range investigated, samples over 100 mg/ℓ were diluted to bring them into range. Because of the linearity of the absorbance measurement, the concentration scale on the instrument could be used and subsequent measurements were obtained by zeroing the instrument then calibrating the concentration scale using a known standard. Replicate measurements on several samples yielded a standard deviation of 0.065 mg/ℓ for both substrates. The result was highly reproducible with scatter principally caused by oscillation of the third significant figure within the machine.

The analyses on phenol were carried out at 270 nm and on OCP at 274 nm. Additionally, since the instrument could also be used for wavelength scans, periodic checks were made to ensure that only the neutral species of both substrates were present in measurable quantities. The spectra of the neutral and anionic forms are sufficiently different that anions could be detected if significant amounts were present.

As a check on the UV measurement, Total Organic Carbon analyses were made in some of the isotherm studies. A Beckman Model 915 TOC analyser was used for these measurements. In every case the TOC measurement corresponded very closely to the substrate specific UV measurement

and thus verified that no other species but the original substrate were present. This finding indicated that biological degradation of the substrate did not occur during the experiments.

3.4 Equilibrium Studies

The isotherms were measured by contacting a range of carbon masses with equal volumes of adsorbate solution of known initial concentration. The vessels used were 500 mℓ glass bottles with teflon liners inside the caps to provide an inert seal. Agitation was provided by rotating the bottles end over end at a rate sufficient to keep the carbon granules continuously in suspension. Both powdered and granular carbon isotherms were conducted; in the granular isotherms the bottles were completely filled with water while in the powdered carbon studies a 100 mℓ air space was left to aid agitation.

In each experiment accurately weighed quantities of activated carbon were added to all but one of the bottles, the last being a blank. The granular carbon samples were first boiled in distilled water to ensure that they were thoroughly wetted before being placed in the bottles, however, later studies indicated that this practice was not necessary. Furusawa & Smith (1973) had found a similar result in their adsorption studies. After carbon addition known volumes of the adsorbate solution were added and the bottles sealed and placed on the rotator. The concentrations within the bottles were monitored as functions of time so that equilibrium attainment could be verified. In the granular carbon experiments the agitation was stopped, 10 mℓ samples were withdrawn for UV analysis, the samples were replaced in the bottles, the bottles re-

sealed, and agitation recommenced. In the powdered carbon isotherms the withdrawn samples were not replaced as they were well mixed. The samples were filtered to remove the powdered carbon and analysed by UV absorbance. Previous tests verified that measurable adsorption of substrate onto the pre-washed 0.45 μm Gelman membrane filters did not occur. All isotherms were conducted in a constant temperature room maintained at 20 (± .5)°C.

3.5 Batch Kinetic Studies

The kinetic parameters describing a given adsorbate are estimated by statistically fitting an adsorption model to unsteady state batch adsorption data.

The data were obtained in a Carberry reactor (Carberry, 1964) which was originally developed to control external mass transfer resistances in gas phase catalytic reactions. In such apparatus the catalyst or adsorbent is contained in wire baskets which are rotated rapidly in the reacting or adsorbing fluid. For the present work a liquid phase Carberry reactor, as shown in Figure 3-2, was constructed. The body was built of aluminum and was painted with an epoxy coating to prevent oxidation. A cooling jacket enclosing the vessel walls was necessary to remove the heat generated by energy dissipation within the reactor. The jacket was part of a temperature control loop which maintained the internal reactor temperature at 20 ± 0.1°C.

Complete sealing of the system was achieved by using a floating lid made of perspex and o-ring seals on the shaft and on the outer rim.

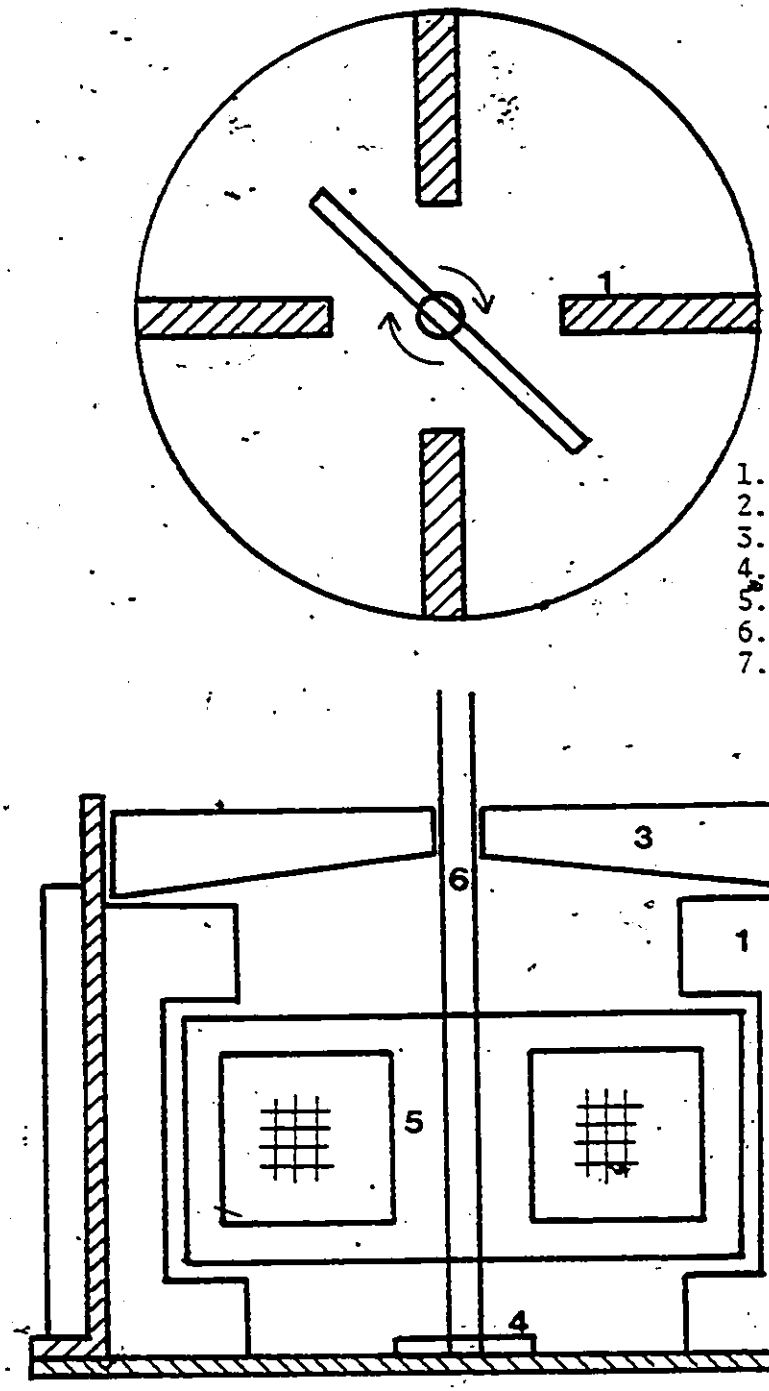

Figure 3-2. Liquid Phase Carberry Reactor.

As a result measurements could be carried out over extended periods without atmospheric exchange and with zero attrition as the carbon was fixed in place on a stainless steel screen. Initial tests showed that substrate concentrations were unchanged even after three days of operation in the absence of carbon.

All sampling was done through a septum on the side of the reactor and samples were reinjected after analysis to prevent cumulative errors due to sample loss. In each experiment an accurately weighed quantity of carbon was placed in the baskets and the apparatus assembled. The reactor was then filled with 2.5 ℓ of distilled, deionized water and allowed to run until at thermal equilibrium. At time zero a quantity of the concentrated stock solution of adsorbate was added and a sample taken immediately and at 30 second intervals thereafter for the first 3 or 4 minutes. This data was used to calculate the film transfer coefficient within the system. Subsequent concentration measurements were made at ever increasing intervals until the run was terminated.

The equipment could be operated at up to 600 rpm with the 3/4 H.P. motor available. At this speed the external film resistance was almost negligible however as the model could allow for external film resistance, and wear on the system at this speed was high, the majority of the runs were at significantly lower rotational speeds.

3.6 Column Studies

The pure solute column adsorption experiments were conducted in

a 5.08 cm I.D. perspex column which was thermally insulated with fibre-glass lagging. The column was charged with a known mass of activated carbon so that the packed density could be accurately measured and was operated in upflow mode at a typical hydraulic loading rate of 5.85 m/hr (2 igpm/ft^2). Sampling ports were placed 30 and 60 cm above the inlet and samples were collected in a fractionator prior to analysis.

Feed solutions were premixed daily and stored in 350 ℓ polyurethane tanks which were chilled and covered to minimize evaporation. The solution was circulated through a throttled loop using a centrifugal pump. A bleed off the high pressure side of the pump passed through a temperature control bath at 20°C, a flow regulating needle valve, and a rotameter, before entering the column. A schematic of the column system is shown in Figure 3-3.

According to Schwartz and Smith (1953) a column to particle diameter ratio in excess of 30 is necessary to ensure that wall effects are negligible; the ratio in the present case was 54 and was therefore sufficient. Eight experimental breakthrough profiles were measured with substrate, inlet concentration, and bed height as variables. The conditions for each experiment are given in Table 3-2.

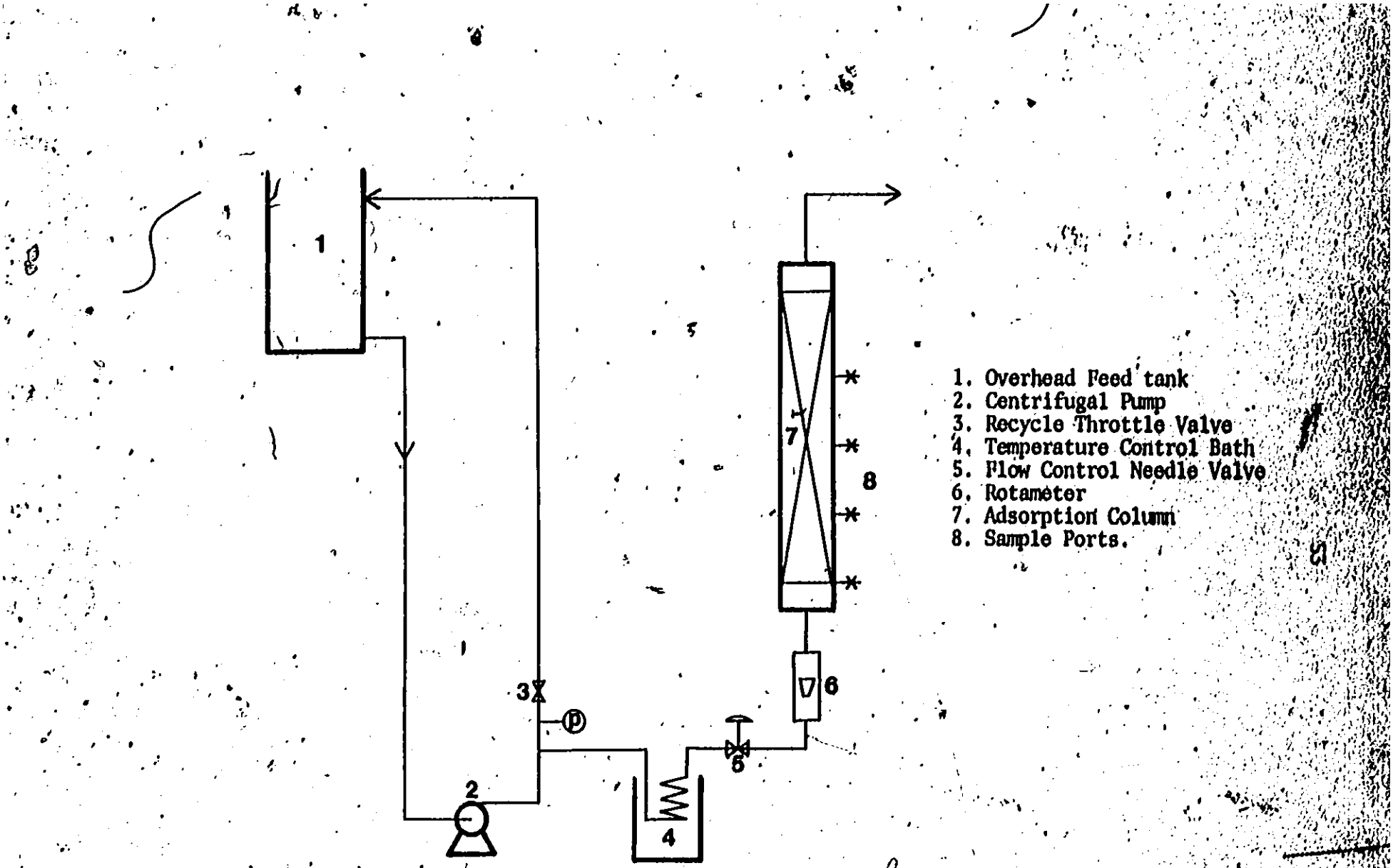

Figure 3-3. Experimental Column Flowchart.

Run No.	Substrate	Feed Conc. (mg/l)	Depth. (cm)
Ia	Phenol	50	30
Ib	"	50	60
IIa	"	100	30
IIb	"	100	60
IIIa	OCP	50	30
IIIb	"	50	60
IVa	"	100	30
IVb	"	100	60

Table 3-2. Experimental Conditions for Column Runs.

CHAPTER 4

ISOTHERM STUDIES

In any study involving activated carbon, an accurate isotherm is essential, whether for system design or research purposes. Without knowledge of the isotherm, bed life and location of the breakthrough curve cannot be predicted and kinetic data cannot be modelled meaningfully.

4.1 Preliminary Literature Study

A review of published isotherms for the adsorption of phenol onto activated carbon (Filtrasorb F400) yielded the information shown in Figure 4-1 and detailed in Table 4-1. All isotherm data have been converted to consistent units (mg/g, mg/l) and temperature, pH, duration of experiment and other relevant data have been noted. As discussed below, while some differences in equilibrium capacity could be expected due to variation in carbon properties and in environmental conditions, the observed differences are greater in magnitude than might reasonably be attributed to such causes. There is a substantial volume of evidence in the literature, as discussed below, showing that the effects of environmental conditions such as temperature, pH, and buffer strength are usually quite small.

The effect of temperature on isotherm capacity was investigated by Snoeyink et al. (1969) and was found to be slight. Over the narrow

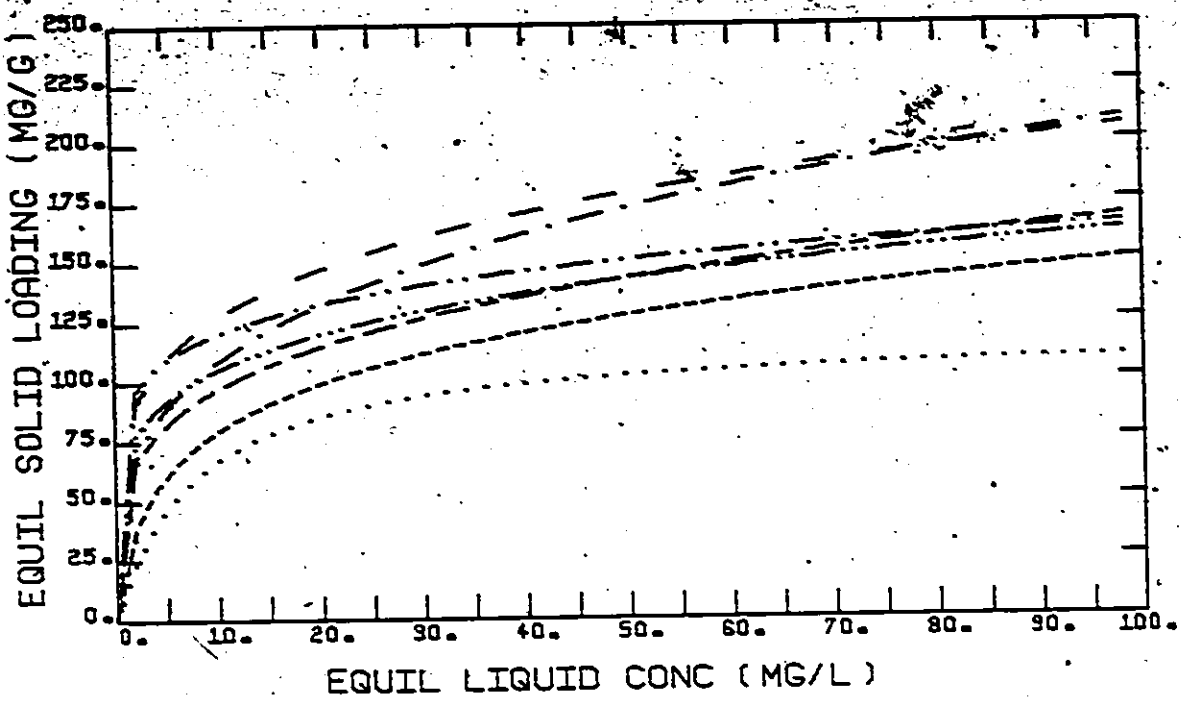

Figure 4-1. Published Isotherms for Phenol on F400
(Legend in Table 4-1)

Legend.	Reference.	Isotherm (mg/gC; mg/L)	pH	T
_ _ _	Present study	$Q_e = 78.1\ C_e^{.212}$	7.0	20°C
_ . _ . _	Ying (1978)	$Q_e = 56.\ C_e^{.288}$	10^{-2}M PO4	Room (T)
_ .. _ .. _	Crittenden (1976)	$Q_e = \frac{16160.\ C_e}{1 + 185.9\ C_e^{.8617}}$	7.0	Room (T)
_ ... _ ... _	Wadin (1976)	$Q_e = 68.\ C_e^{.19}$	-	25°C
_ . . _ . .	Huang (1977)	$Q_e = 56.\ C_e^{.24}$	-	Room (T)
. . . . .	Mathews (1975)	$Q_e = \frac{43.29\ C_e}{1 + .7138\ C_e^{.7942}}$	7.0	Room (T)
.....	Urinowicz (1972)	$Q_e = \frac{15.64\ C_e}{1 + .133\ C_e}$	-	Room (T)

Table 4-1. Published Phenol Isotherm Data.

range reported or assumed in Table 4-1, this influence can be regarded as insignificant in accounting for the observed variations.

Zogorski et al. (1976) studied the uptake rates from distilled water and phosphate buffer and found no discernible differences. Similarly, Ying (1978) found no difference between isotherms measured in tap water, distilled water, or weak phosphate buffers under otherwise identical conditions. Thus the effect of differing solvent conditions among the reported studies could not account for the observed variations.

The influence of pH is complex and potentially could have had a significant effect on the results of studies conducted in the vicinity of the pK_a. However, the phenol pK_a of 9.86 is well above the pH range reported in most of the studies in Table 4-1. At pH 7 phenol exists predominantly in the neutral form, and changes in capacity with pH appear to be largely due to competition with hydronium ions (Snoeyink et al. 1969). Myers and Zolandz(1978) found that in the pH range of 2 to 6 the adsorption of phenol was fairly constant, they showed significant changes to be due to a shift from the neutral to anionic species as the pH approached the pK_a of the adsorbate.

Therefore, on the basis of the wide variation among isotherms reported in the literature for the same system, it appeared possible that part if not all of the observed variation was due to problems in determining attainment of the true equilibrium. To test this hypothesis, isotherm studies in the present work were carried out according to the methods outlined in Chapter 3,,which allowed the approach to equili-

brium to be followed, and the attainment of equilibrium to be verified.

4.2 Experimental Results

Six isotherms were conducted, three for each of the substrates phenol and o-chlorophenol, according to the procedures given in Chapter 3. The conditions of each experiment are detailed in Table 4-2 which indicates that the initial concentration, ionic strength, and size of the carbon particles were varied between the experiments.

The time progression of the concentration relationship in isotherm No.1 (o-chlorophenol with granular activated carbon (GAC)) is shown in Figure 4-2. As the carbon loadings ceased to change after 33 days the true equilibrium had been reached at that time. Thus although 60% of the final capacity was obtained after only 4 hours of contact, the remaining capacity was utilized very slowly. This finding is in agreement with results previously reported by Snoeyink et al.(1969) and Zogorski et al (1976). It is interesting to note that after the first day, the capacity concentration relationships could all be fitted quite well by Freundlich isotherms with almost identical slopes but ever increasing capacities. In the remaining o-chlorophenol isotherms (Nos.2 and 3) excess time was allowed to ensure that equilibrium was obtained.

Similar studies were conducted with phenol as a substrate. In Figure 4-3 the data of isotherm No.4 at 14, 23 and 30 days are plotted. Equilibrium had almost been reached at 14 days, and the capacities were constant after 23 days, again ensuring that equilibrium has been attained. In comparison to the o-chlorophenol data, phenol appeared to reach equilibrium more quickly. This result was expected as phenol is smaller,

Isotherm Number	Adsorbate	Co (mg/L)	Gram/Flask	T°C	pH	Buffer	Time period (days)
1	OC-Phenol	100.7	G	20	~7	Distilled Water	33
2	OC-Phenol	203.5	G	20	7.0	.002 M PO4	40
3	OC-Phenol	101.8	P	20	7.0	.002 M PO4	14
4	Phenol	99.0	G	20	7.0	.002 M PO4	23
5	Phenol	104.5	P	20	7.0	.002 M PO4	4
6	Phenol	192.8	P	20	~7	Distilled Water.	7

Table 4-2. Experimental Conditions for Isotherms.

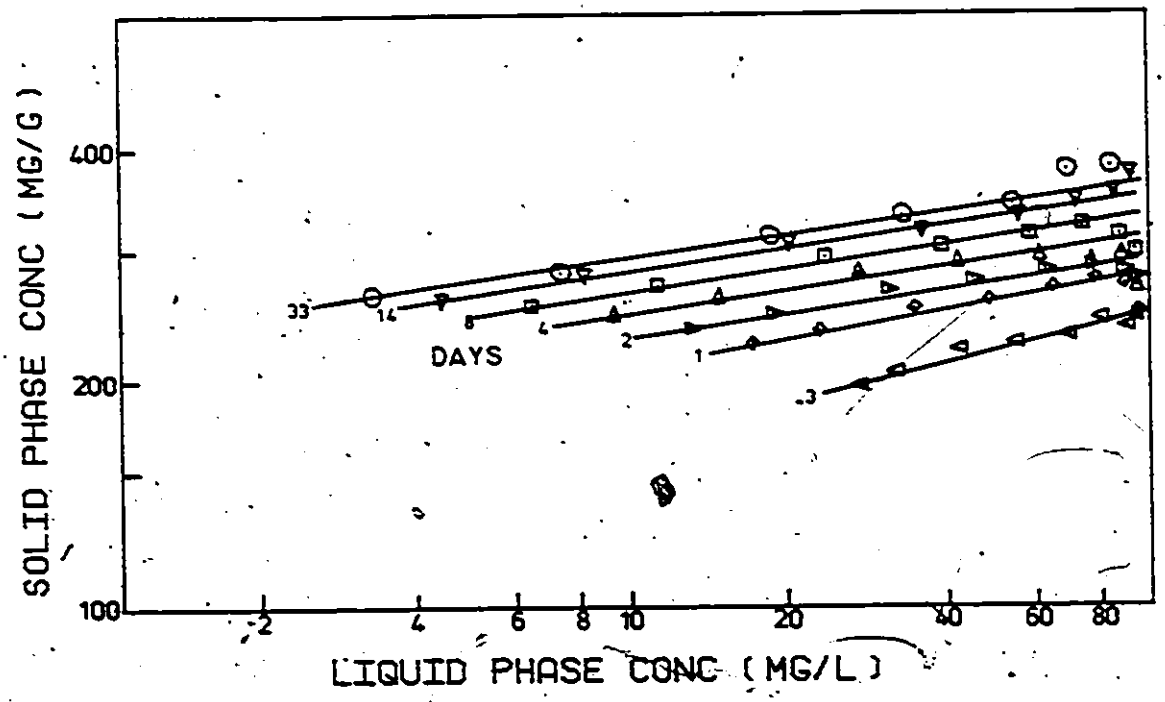

Figure 4-2. Apparent Loading as a Function of Time. (o-Chlorophenol Isotherm No. 1)

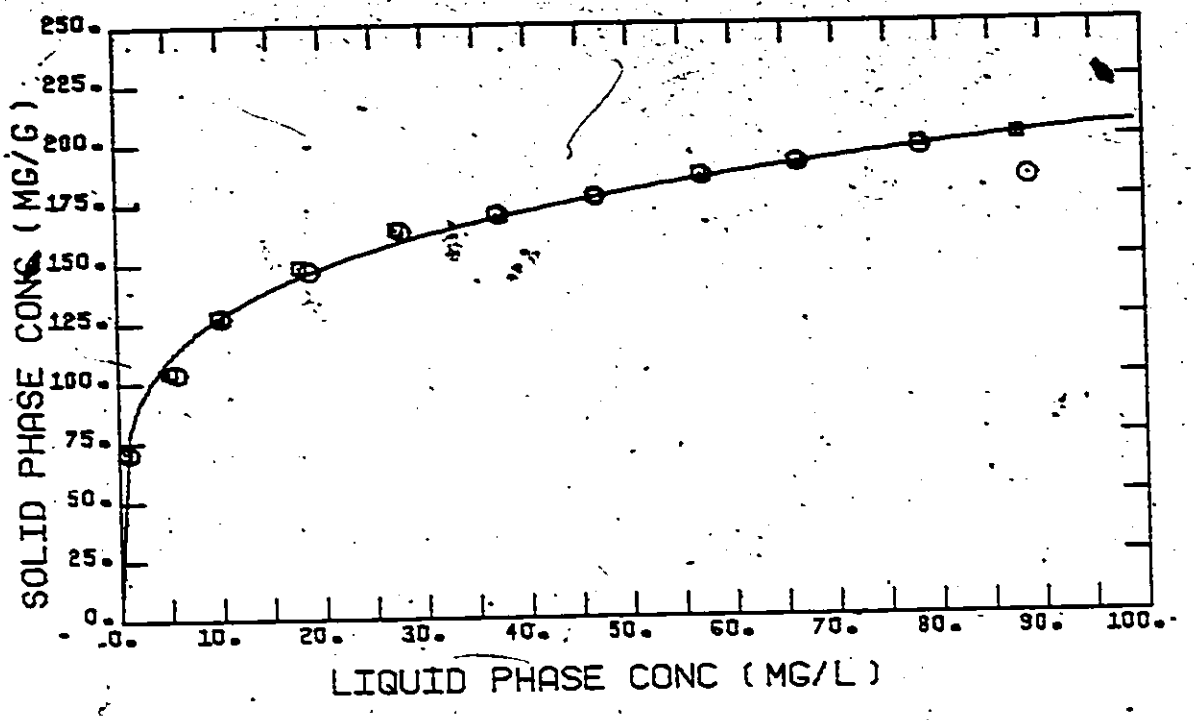

Figure 4-3. Granular Carbon Isotherm No.4.
(⊙ - I4 days, ⊡ - 23 and 30 days)

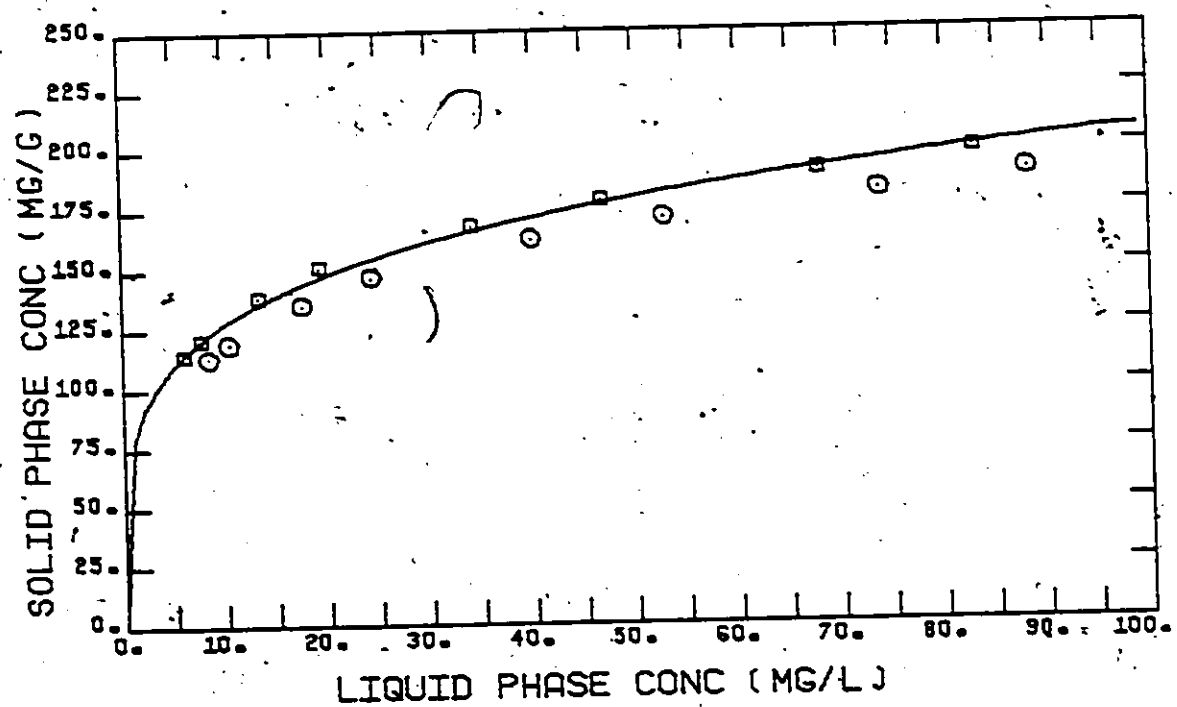

Figure 4-4. Powdered Carbon Isotherm No.6.
(⊙ - 2 days, ⊡-5 and 7 days)

and should therefore diffuse faster, and it also has a lower capacity.

Studies on the powdered carbon isotherms (Nos.5 and 6) indicated that equilibrium was achieved after 3 to 5 days. Data for isotherm No.6 are plotted in Figure 4-4 at 2,5 and 7 days. The figure shows that 2 days contacting was insufficient for powdered carbon isotherm studies with phenol.

The final equilibrium isotherms for experiments 1 to 6 are plotted in Figure 4-5. All the data for each adsorbate were regressed using a single Freundlich isotherm by a nonlinear least squares procedure. The parameters for the equation.

$$q_e = M c_e^n \qquad (4.1)$$

are given in Table 4-3 with the corresponding 95% confidence limits (based on a linear hypothesis).

For each substrate all data points were well fitted by a single line, no differences being observed between powdered and granular isotherms. On the basis of these results it is apparent that neither particle size, nor the presence or absence of weak buffer, has a significant effect on the equilibrium relationship. Additionally, changes in the initial concentration did not have an effect over the limited concentration range studied.

4.3 Implications of the Observed Slow Approach to Equilibrium

The occurrence of a slow approach to equilibrium following an initial rapid uptake period was established by the experimental results and had also been reported previously in the literature. The very slow approach to eventual equilibrium is a potential cause of incorrect isotherm evaluation as it can lead to the premature assumption of equilibrium att-

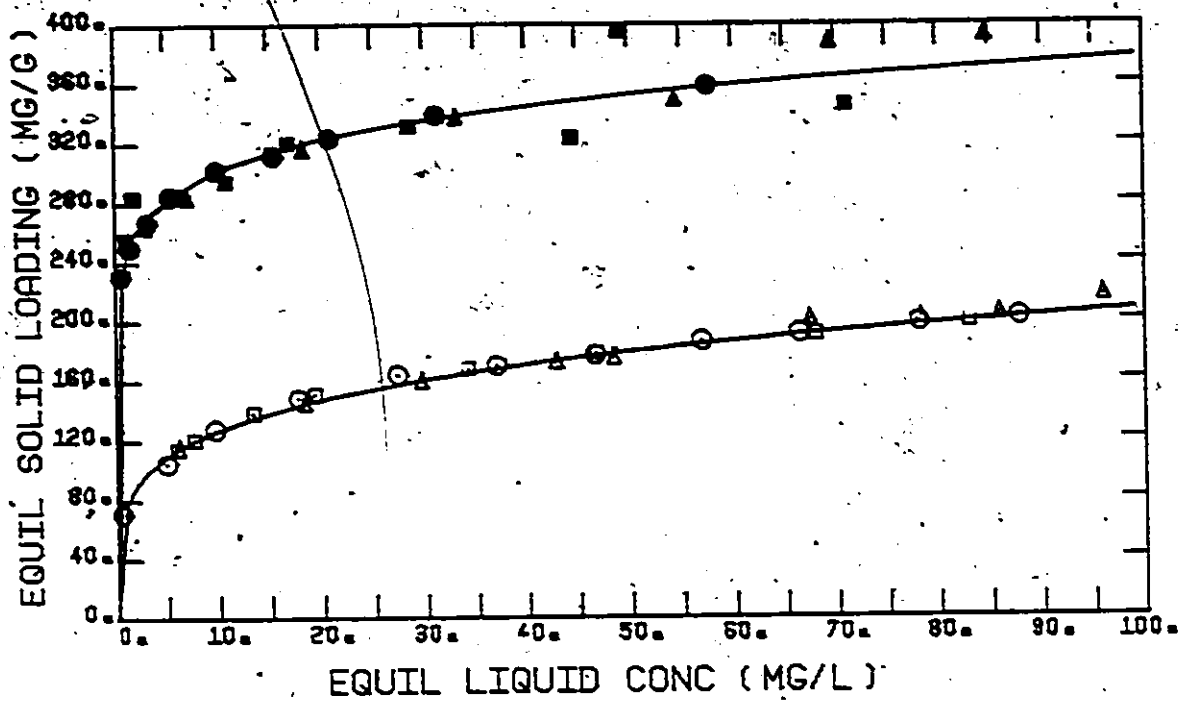

Figure 4-5. o-Chlorophenol and Phenol Isotherms.
(OCP; ▲ No.1, ● No.2, ■ No.3:
Phenol; ⊖ No.4, △ No.5, ⊡ No.6)

Substrate	M	n
Phenol	78.1 ± 3.3	.212 ± .011
o-Chlorophenol	240.2 ± 2.1	.098 ± .003

Table 4-3. Freundlich Isotherm Parameters
(incl. 95% confidence limits)

ainment. This possibility arises because even when the system is still a long way from equilibrium, the uptake rate falls to a level which may not be measurable if very accurate concentration measurements cannot be made. Additionally, even if very small uptake rates are observed, it may be assumed that the system is sufficiently close to equilibrium to neglect further uptake. The only way to ensure equilibrium is to make repeated accurate analyses at intervals on the order of several days at least, as was done in the present study. The inability to detect true equilibrium may be the cause of some previously unexplained results in the measurement of equilibrium isotherms.

The results of this study indicated that, at least over the range investigated, the initial concentration of sorbate had no effect on the resultant isotherm. This result is at variance with the findings of Crittenden and Weber (1978a) and Ying (1978) who observed a 'concentration dependence' when measuring isotherms of phenols and related compounds. These authors found that when two different initial liquid phase concentrations were used to evaluate equilibrium isotherms in the same range, the lower initial concentration gave higher observed capacities than the higher initial concentration. No explanation for this effect has yet been proposed, however, if the measured systems were kinetically limited, i.e. if true equilibrium was not achieved, the apparent concentration dependence could be explained. This possibility is discussed further in the following chapter. Although the present results indicate that isotherms are not a function of concentration, Crittenden and Weber (1978a) and Ying (1978) covered broader concentra-

tion ranges thus the occurrence of such a functional relationship cannot be precluded at higher concentrations on the basis of the present work.

Since the above results showed PAC and GAC isotherms to be identical, the use of PAC in the evaluation of the majority of isotherms seems justified. It has previously been shown (Rankin, 1975) that crushing carbon has a slight effect on the largest pore volume only, and a negligible effect on the surface area. Thus there is no logical reason for PAC and GAC isotherms to differ. By using PAC the experimental time required to measure an isotherm is considerably reduced, and the likelihood of premature assumption of equilibrium is also decreased.

On the basis of the reported results we can conclude that for both substrates there exists a unique equilibrium relationship between liquid and solid phase concentrations for a given sorbate/sorbent system. The relationship appears to be independent of the particle size of the carbon; the presence or absence of a weak buffer; and the initial liquid phase concentration. The potential misinterpretation of equilibrium attainment caused by the slow approach to equilibrium may well be the cause of much of the observed variation between isotherms reported in the literature for the system F400/phenol.

CHAPTER 5

PROPOSED KINETIC ADSORPTION MODEL AND BATCH KINETIC STUDIES

The isotherm study in the previous chapter demonstrated an apparent dual rate behaviour during the attainment of equilibrium. A rapid initial uptake of 60 - 80% of the final capacity was followed by a slow uptake stage during which the remaining capacity was utilized over a period of several weeks. Such behaviour does not appear to be compatible with a single intraparticle rate theory of adsorption in which rapid initial uptake must be followed by a rapid approach to equilibrium, or conversely, that a slow approach to equilibrium must be preceded by a slow initial uptake period.

In this chapter a model is proposed to describe the apparent dual rate behaviour during adsorption. After developing the model and obtaining a solution for the batch kinetic problem, experimental batch data is analyzed using the proposed model to evaluate system parameters.

5.1 Proposed Branched Pore Adsorption Model

In developing a model of activated carbon adsorption kinetics, consideration should be given to the physical structure of the activated carbon particle. As discussed in Chapter 2, activated carbons have a wide range of pore radii, and there is evidence showing that diffusion rates in small pores are a function of the ratio of pore radius : adsorbate radius. It should therefore be expected that a range of diffusion

rates exists within an adsorbing activated carbon particle. Those pores in which rapid diffusion occurs would become saturated in the early stages of adsorption and as time proceeds, only those pores in which slow diffusion occurs would continue to adsorb. A continual drop in the apparent diffusion coefficient would therefore be observed during the course of the experiment.

In the modelling of clearly bidisperse adsorbents such as molecular sieves and ion exchange resins, the dual rate nature of the adsorption process is widely accepted (Antonson and Dranoff, 1969b; Layton and Youngquist, 1969; Ruckenstein et al., 1971; Haynes, 1975; Shah and Ruthven, 1977). In such adsorbents two distinct regions can be recognized, a macroporous region which consists of spaces between the powder particles or zeolitic crystals, and a microporous region within the subunits (Ruckenstein et al, 1971). It is possible to quantitatively define the dimensions and locations of the microporous subunits and separate rates for the macropore and micropore regions can be introduced. Layton and Youngquist (1969) found two stages to occur in the adsorption of SO_2 by a polymeric macroreticular ion exchange resin, a rapid initial stage which was attributed to adsorption in the macropores followed by a very slow second stage in which adsorption occurred in the polymer matrix. This behaviour is very similar to that observed for activated carbon in Chapter 4, however, the physical description of the activated carbon particle is much more complex. Activated carbons are seldom bidisperse, they are instead polydisperse or have broad pore size distributions and it is not possible to define the dimensions of regular subunits as can be done with zeolites or macroreticular resins. Consequently, the

models developed for describing the adsorption kinetics of bidisperse adsorbents are not applicable to activated carbon, but they can give a general indication of a likely model form.

Recognizing the complexity and incomplete understanding of the internal structure of activated carbon, the proposed model form does not rely on a detailed knowledge of the carbon structure, but instead attempts to group sections of the carbon which exhibit similar behavioural characteristics. As a first approximation in differentiating between types of adsorption rates in activated carbon, the carbon particle pore structure has been divided into two distinct regions:

(i) Those pores in which the pore radii are several times greater than the radii of the diffusing species have been termed 'macropores'.

In these pores it is assumed that transport occurs by conventionally described diffusion mechanisms, either pore or surface, and that the presence of the pore walls has little or no effect on the diffusion rates. These larger pores are assumed to be homogeneously distributed throughout the particle and provide a complex network of interconnected access channels to the interior. It is further assumed that the rapid initial uptake of substrate which was discussed earlier takes place within this region. At the present state of knowledge of diffusion mechanisms in activated carbon pores, it is not possible to specify the lower size limit of these 'macropores'. The term should not, however, be confused with the conventional terminology of macropores as being those pores with radii greater than 1000Å. In this instance transitional

pores with radii as low as 50 Å or less may well be included in this category.

(ii) Those pores which have radii of comparable size to the diffusing species have been termed 'micropores' and this region encompasses all pores which are available for adsorption and are not included in the 'macropore' category.

Within these pores it is assumed that transport rates are strongly hindered, either by the proximity of the walls or by the restraining effect of the sorbate/sorbent interactive forces. The exact mechanisms both of transport and of adsorption within these small pores is as-yet unclear and may be due to surface adsorption and diffusion, to volume filling of the pores, or to a combination of these and perhaps other as yet undiscovered mechanisms. These pores are assumed to be homogeneously distributed throughout the particle but to be relatively short and therefore not to contribute significantly to radial transport. They are further assumed to branch off the macropore network which is the source of adsorbate diffusing into the micropores. It is in these small pores and fissures that the slow adsorption following the initial rapid uptake occurs.

A conceptual diagram of the proposed model is shown in Figure 5-1. Based on the definition given above of the macropore and micropore regions, it would be expected that the relative proportions of each would depend upon the size of the diffusing species.

The only other dual rate kinetic model for activated carbon adsorption is that proposed in a parallel study to the present work by

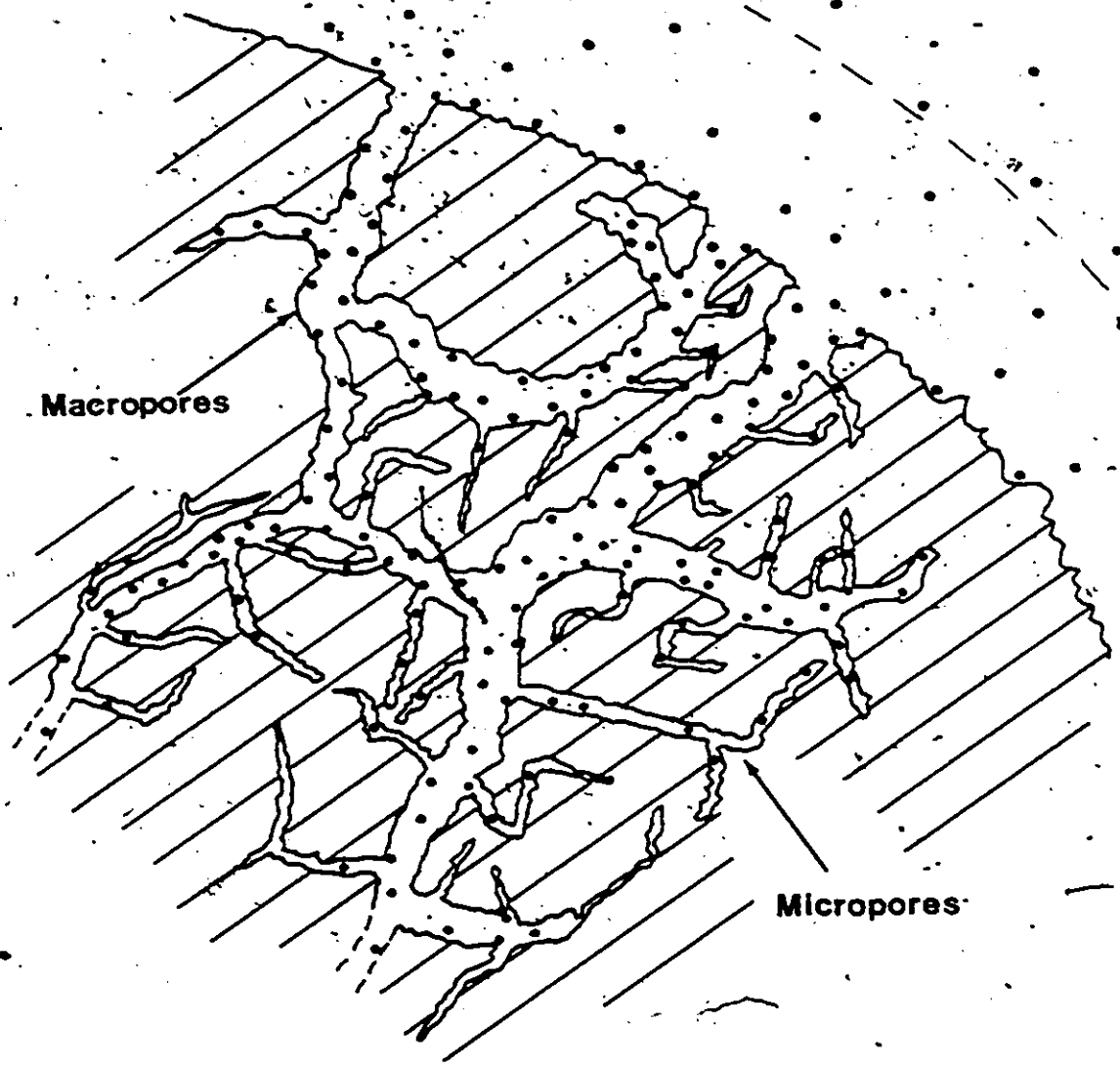

Figure 5-1. Idealized Activated Carbon Pore Structure.

Famularo et al.(1978). In that work a shell model was chosen to describe macropore/micropore adsorption, with a micropore core surrounded by a macropore shell. This model, which is shown schematically in Figure 5-2, was evaluated in the initial stages of the present work but was discarded as, in a fully discretized solution form, the uptake concentration profile undergoes a sharp change in slope as the wavefront passes from the outer region to the inner. Experimental data does not show such behaviour and additionally, the true physical description of the activated carbon particle does not suggest that the micropores are segregated at the centre of the particle.' Although Famularo et al. (1978) had reasonable success with this model, the kinetic parameters evaluated from batch experiments did not describe performance of experimental adsorption columns and one parameter had to be re-evaluated from a prior column experiment.

The branched pore adsorption model was chosen for the present work as it is consistent with the known physical structure of activated carbon. In the following section the mathematical formulation of the model is given and the solution technique for analysis of batch kinetic experiments is outlined.

5.2 Mathematical Formulation of Branched Pore Model

A conceptual diagram of the proposed mechanism controlling adsorption is shown in Figure 5-3. The assumptions made in developing the proposed model are:

(i) External film transfer controls the rate of diffusion of adsorbate across the liquid boundary layer surrounding the particle;

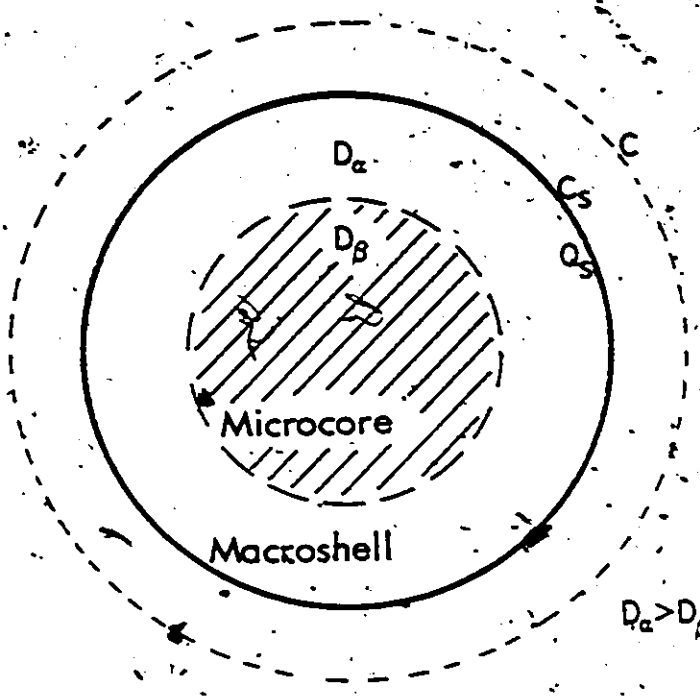

Figure 5-2. Conceptual Diagram of Microcore-Macroshell Model.

(ii) The carbon particles can be treated as equivalent spheres for modelling purposes (Antonson and Dranoff, 1969a);

(iii) Local equilibrium occurs at the solid-liquid interface;

(iv) Accumulation in the liquid phase within the pores of the adsorbent is negligible;

(v) The carbon particle can be divided into two homogeneously distributed regions, a fraction 'f', constituting the 'macropore' region, and a fraction '1-f' constituting the 'micropore' region. Consequently, if an equal density of adsorbent is assumed throughout the particle, this division corresponds to a fraction 'f' of the total adsorptive capacity occurring in the

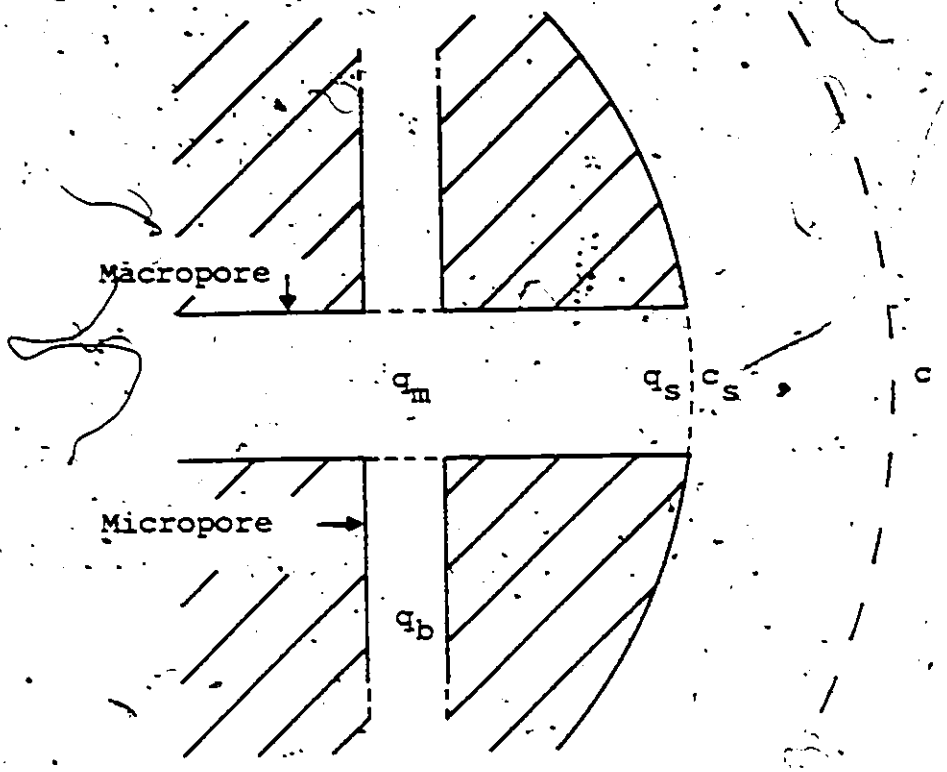

Figure 5-3. Conceptual Diagram of Proposed Branched Pore Model.

macropores, and a fraction '1-f' in the micropores;

(vi) The rate of transport in the macropore network can be described by a surface diffusion mechanism. As discussed in section 2.3.3, surface diffusion is usually the rate determining mechanism when dealing with molecules which adsorb strongly onto activated carbon. The surface diffusion coefficient is assumed to be constant;

(vii) The rate of transfer from the macropore to the micropore regions is described by a linear driving force equation between the local macro and micropore concentrations. Such an approach has been used previously (Goodknight et al., 1960; Friedman and Ramirez, 1977) in connection with models of flow through porous media with dead end pore volume. Such models are similar to the activated carbon model in that precise description of the internal structure of the media is not possible.

With reference to Figure 5-3 the following mass balances can be written.

Macropore Mass Balance

$$f \frac{\partial q_m}{\partial t} = \frac{f D_s}{r^2} \frac{\partial}{\partial r}\left(r^2 \frac{\partial q_m}{\partial r}\right) - R_b \qquad (5.1)$$

in which f = fraction of total capacity or particle volume in the macropore region; q_m = solid phase concentration in the macropores; and R_b = local rate of transfer from the macro to micropores.

Micropore Mass Balance

$$(1 - f) \frac{\partial q_b}{\partial t} = k_b (q_m - q_b) = R_b \qquad (5.2)$$

in which q_b = solid phase concentration in branch or micropores; and k_b

= pseudo mass transfer coefficient for transport from the macro to the micro or branch pores.

In addition, the following initial and boundary conditions apply:

$$q_m (r, o) = 0 \tag{5.3}$$

$$q_b (r, o) = 0 \tag{5.4}$$

$$q_m (R, t) = g\{c_s(t)\} \tag{5.5}$$

$$\frac{\partial q_m}{\partial r} (o, t) = 0 \tag{5.6}$$

Equation (5.5) denotes that the solid phase concentration on the external surface of the carbon particle is in equilibrium with the liquid phase concentration adjacent to the external surface. The functional form of $g\{c_s\}$ is determined by the isotherm experiments.

In addition to the equations describing uptake onto the adsorbent, solution of the batch kinetic problem requires a mass balance over the liquid phase in the batch reactor, giving:

$$\frac{dc}{dt} = - \frac{(1 - \varepsilon)}{\varepsilon} \cdot \frac{3k_f}{R} (c - c_s) \tag{5.7}$$

in which c = bulk liquid phase concentration; ε = liquid volume fraction in the batch vessel; k_f = external mass transfer coefficient; and R = adsorbent particle radius.

The choice of equation (5.7) is somewhat arbitrary as it can also be calculated from accumulation of sorbate in the solid phase. Comparison of the three alternative forms available was made in the preliminary work, and is reported in Appendix B. On the basis of the study, equation (5.7) was chosen as the most accurate and efficient

form.

To couple the liquid and solid phase equations a mass balance is written at the outer surface of the adsorbent particle by equating the surface fluxes to give:

$$f \cdot D_s \cdot \rho_c \left.\frac{\partial q_m}{\partial r}\right|_R = k_f (c - c_s) \qquad (5.8)$$

In equation (5.8) the fraction 'f' is included since it is assumed that only that fraction of the particle which constitutes the macropore region is available for radial transport.

The equations (5.1) to (5.8) are then reduced to dimensionless form using the substitutions:

$$\begin{aligned} C &= c/c_o \\ Q_m &= q_m/q_o \\ Q_b &= q_b/q_o \\ \theta &= D_s t/R^2 \\ \beta &= r/R \end{aligned} \qquad (5.9)$$

and in addition the change of variable

$$\eta = \beta^2 \qquad (5.10)$$

is introduced. This variable transformation was used by Svedberg (1975) and was shown to give a more accurate solution as it gives a finer spatial grid near the outer surface of the adsorbent particle where the gradients are steepest. From equation (5.10) it follows that

$$\frac{\partial}{\partial \beta} = 2\,\eta^{\frac{1}{2}} \frac{\partial}{\partial \eta} \qquad (5.11)$$

$$\frac{\partial^2}{\partial \beta^2} = 4\eta \frac{\partial^2}{\partial \eta^2} + 2\frac{\partial}{\partial \eta}$$

$$\frac{2}{\beta}\frac{\partial}{\partial \beta} = 4\frac{\partial}{\partial \eta}$$

Combining equations (5.1) to (5.11) yields the following set of equations to be solved.

$$\frac{dC}{d\theta} = -\frac{(1-\varepsilon)}{\varepsilon} B_{i_f} (C - C_s) \tag{5.12}$$

$$\frac{dQ_m}{\partial\theta} = 4\eta \frac{\partial^2 Q_m}{\partial \eta^2} + 6\frac{\partial Q_m}{\partial \eta} - \frac{B_{i_p}}{f}(Q_m - Q_b) \tag{5.13}$$

$$\frac{\partial Q_b}{\partial \theta} = \frac{B_{i_p}}{(1-f)}(Q_m - Q_b) \tag{5.14}$$

$$\left.\frac{\partial Q_m}{\partial \eta}\right|_{\eta=1} = \frac{B_{i_f}}{f}\cdot\frac{F}{6}(C - C_s) \tag{5.15}$$

in which $B_{i_f} = 3 k_f R/D_s$ (5.16)

$B_{i_p} = k_b R^2/D_s$ ... modified Biot numbers (5.17)

$F = c_o/\rho_c q_o$ ... a partitioning factor (5.18)

The initial and boundary conditions become:

$$\begin{aligned} C(o) &= 1 \\ Q_m(\eta,o) &= 0 \\ Q_b(\eta,o) &= 0 \\ Q_m(1,t) &= Q_s(t) = g(C_s) \end{aligned} \tag{5.19}$$

and the equation (5.6) is automatically satisfied by the change of variable (equation (5.10)).

5.2.1 Solution of the Batch Kinetic Model

The set of equations (5.12) to (5.19) were solved using Crank-

Nicholson finite difference analogues which have previously been shown by several authors to be excellent for solving the parabolic equations found in the present situation (Fleck et al.,1973; Garg and Ruthven, 1973; McGreavy et al.,1967; Svedberg, 1975; Weber and Crittenden, 1975).

The discretization of the equation set is described in detail in Appendix C at the end of part I. The final solution can be written in matrix form as

$$\underset{=}{X}\, \underset{\sim}{Q}_{j+1}^{(k+1)} = \underset{=}{Y}\, \underset{\sim}{Q}_j + \underset{\sim}{H}^{(k)} \left(C_j, C_{j+1}, C_{s.j}, C_{s.j+1}, \underset{\sim}{Q}_{b.j}, \underset{\sim}{Q}_{b.j+1}\right) \quad (5.20)$$

where the superscript on the vector H denotes that some values at the future time period (j+1) are incorporated within this vector. The solution is therefore iterative, initial guesses of the unknown values at (j+1) are inserted into $\underset{\sim}{H}^{(k)}$ and equation (5.20) is solved using the Thomas algorithm for tridiagonal matrices to obtain $\underset{\sim}{Q}_{j+1}^{(k+1)}$. The newly calculated (j+1) elements are then resubstituted into the vector H and the solution repeated until convergence is obtained. The solution algorithm is described in Appendix C following the solution description.

5.2.2 Solution Testing of the Batch Kinetic Model

McGreavy et al.(1967) have discussed the problem of showing that a finite difference scheme for a nonlinear problem will be stable and will converge to the solution of the differential equation. Since the techniques which can be used to prove convergence and stability in the linear case cannot be used in nonlinear situations, a common method of demonstrating convergence is by reducing the size of the time and

spatial increments to check that the solution eventually becomes constant. This method, while ensuring that the solution is convergent, does not prove that the solution obtained is necessarily the correct one. As has been shown by Parker and Crank (1964), and Keast and Mitchell (1966), the use of certain spatial derivatives in the boundary conditions of a parabolic equation can introduce persistent errors when Crank-Nicholson expansions of the derivatives are used.

In the present case the solution was tested by:

(i) Successively decreasing the time and spatial increments to prove convergence;

(ii) Allowing the solution to run to equilibrium and comparing the calculated equilibrium value to that predicted from the isotherm;

(iii) Comparing the solution in a restricted form against a previously published analytical solution.

The solution proved to be stable, and in the restricted form was correct. No change in the solution was observed for $\Delta n \leq 0.05$ and $\Delta\theta \leq 10^{-4}$, and the final equilibrium value under a particular set of conditions was accurate to within 0.0004% (See Appendix B). In addition, when the fraction 'f' was set equal to unity, which results in the standard surface diffusion or homogeneous diffusion model, the solution with a linear isotherm was identical to an analytical solution published by Paterson (1947) for the equivalent heat transfer case. The restricted model output and the data of Paterson (1947) are compared in Figure 5-4. Details of the comparison are given in Appendix C.2.

On the basis of the tests run on the model, it was concluded that

the model solution was stable, convergent and appeared to give the correct solution.

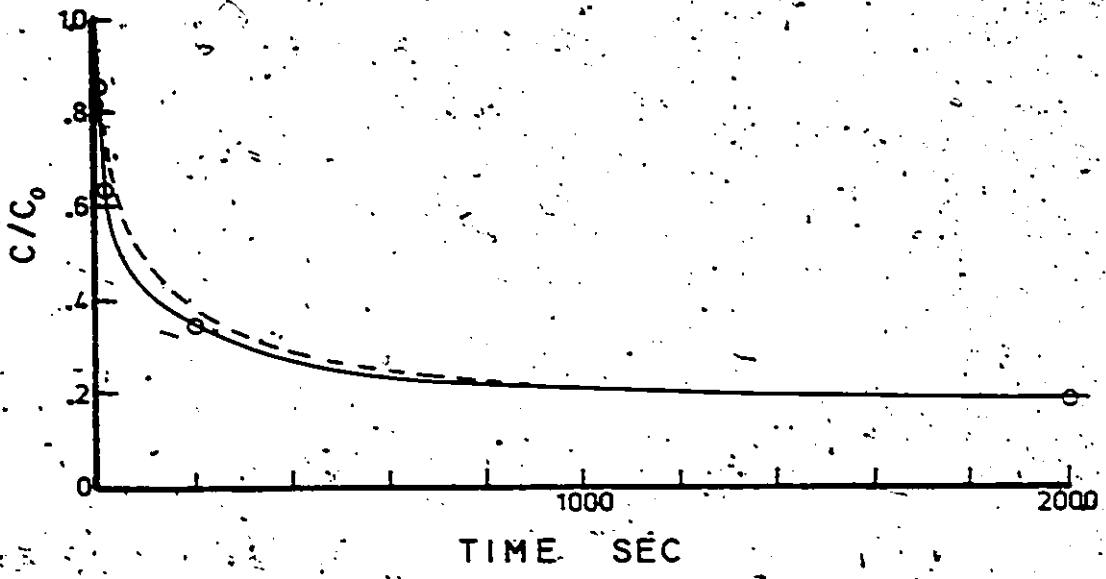

Figure 5-4. Comparison of Model Solution to Analytical Solution of Paterson (1947). (---$D_s = 10^{-7}$cm^2/sec, k_f = 0.1 cm/sec; —— $D_s = 10^{-7}$ cm^2/sec, $k_f = \infty$; ⊙- data of Paterson).

5.3 Batch Kinetic Studies

5.3.1 Measurement of the External Film Transfer Coefficient

In the very first stage of adsorption onto the carbon particles, the liquid phase concentration adjacent to the carbon surface is maintained at or very close to zero because adsorbate reaching the carbon surface is immediately adsorbed. As a consequence, the rate of uptake is controlled by the mass transfer resistance in the liquid film and the external mass transfer coefficient (k_f) can be measured directly from the initial data. If c_s is equal to zero, equation (5.7) becomes

$$\frac{dc}{dt} = -\frac{(1-\varepsilon)}{\varepsilon}\cdot\frac{3k_f}{R}\cdot c \qquad (5.21)$$

which is a first order process. The mass transfer coefficient can be measured directly from the slope of a plot of $\ln c$ against t. A typical plot of such data from one of the batch kinetic runs reported later in this chapter is shown in Figure 5-5. The coefficient k_f can be accurately measured in this manner as external film resistance is rate controlling for the first three minutes in this instance, with intraparticle diffusion becoming significant thereafter.

Measurement of the external film resistance in this manner is preferable to the approach of Mathews and Weber (1977) and Crittenden and Weber (1978a) who simultaneously fitted the external and intraparticle coefficients to the batch data. By separately measuring k_f in the region where it is the controlling resistance, better estimates of the intraparticle diffusion coefficient can be obtained, especially if there is some lack of fit between the data and the model.

To investigate the effect of rotational speed in the reactor on the external mass transfer coefficient, a series of three experiments was conducted using identical carbon masses and initial concentrations of o-chlorophenol, but different rotational speeds. The liquid concentration profiles measured in the three runs are shown in Figure 5-6 at 300, 450 and 600 r.p.m. As the data at 450 and 600 r.p.m. were virtually coincident, the external film resistance at and above 450 r.p.m. must be negligible for these experimental conditions. The measurement of the film transfer coefficient was difficult because at these high

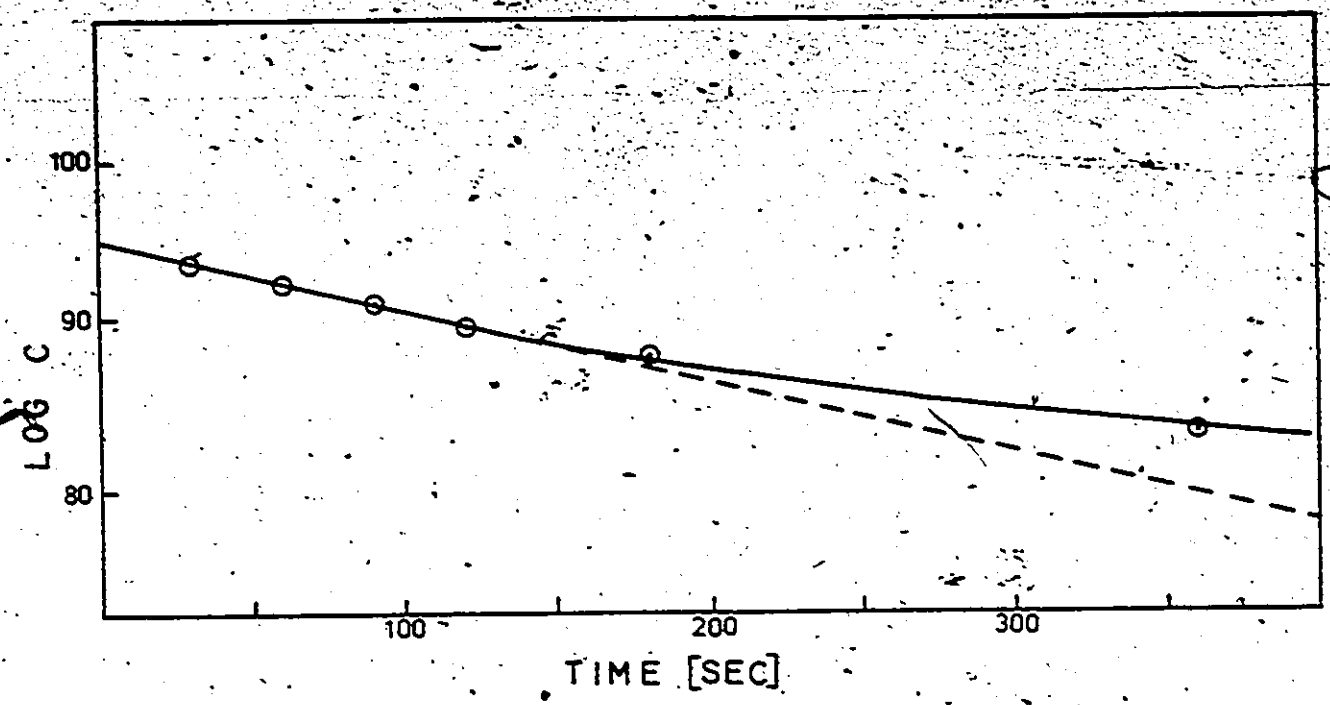

Figure 5-5. Initial Uptake Rate Data in Batch Reactor.

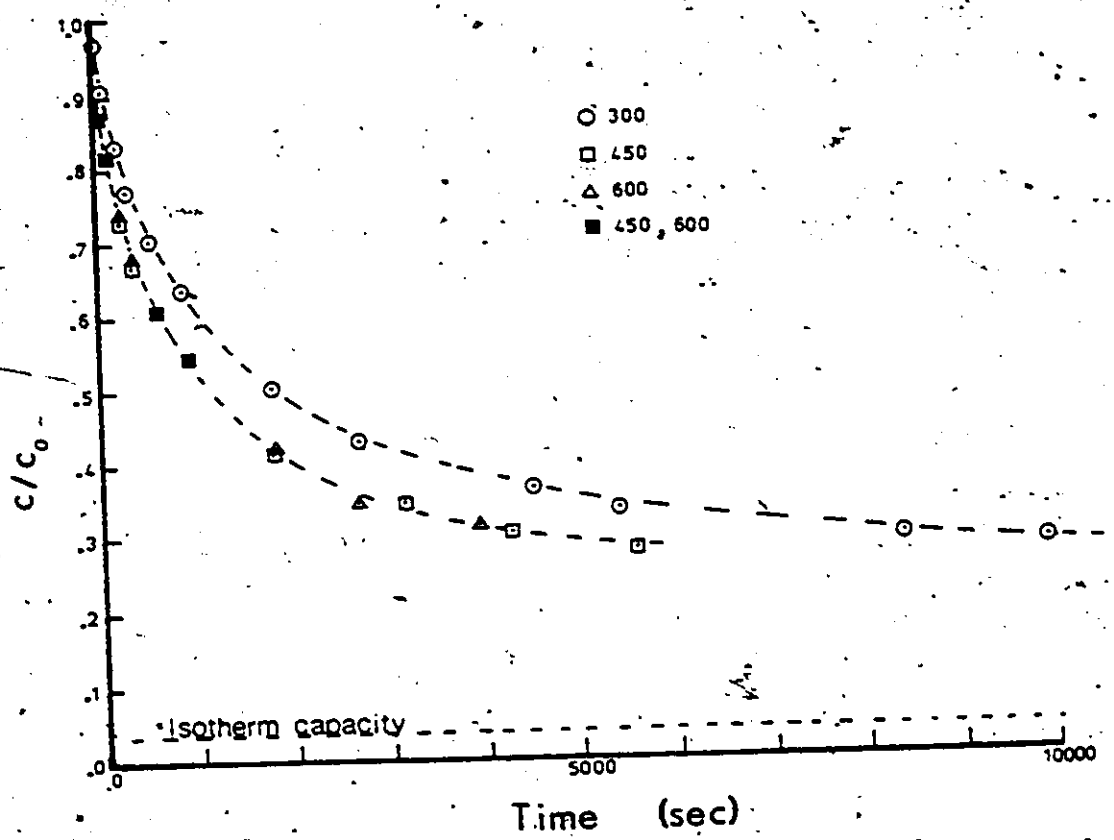

Figure 5-6. Variation of Rotational Speed in Batch Kinetic Experiments. (c_o = 100 mg/l OCP, w = 1.0 g)

speeds intraparticle resistance rapidly became significant within one minute's operation. The film transfer coefficients measured from the first minute's data were 0.025, 0.07 and 0.07 cm/sec at 300, 450 and 600 r.p.m. respectively. The reason for the same k_f being measured at 450 and 600 r.p.m. is attributed to the influence of intraparticle resistance even in the first minute. At these high rotational speeds it was not possible to accurately measure k_f. Consequently, subsequent experiments were run at lower rotational speeds both to allow accurate determination of k_f, and to reduce wear on the equipment. Since the model incorporated the effect of external liquid film resistance, the presence of significant resistance in the external film was not a problem in the data analysis as long as it did not become the rate controlling mechanism throughout the adsorption period.

5.3.2 Application of Existing Models to Batch Kinetic Data

Before investigating the use of the proposed model, analysis of some batch kinetic data with models previously reported in the literature was undertaken. If the fraction 'f' in the proposed model is set equal to unity, the model degenerates into the widely used external film resistance-surface diffusion mechanism model. The result of fitting this model to the experimental data reported in the previous section for the run at 300 r.p.m. is shown in Figure 5-7. The best fit surface diffusion coefficient was obtained using a multiparameter nonlinear least squares regression routine (UWHAUS - McMaster University Computing Centre). It is clear that there is a distinct lack of fit of the model, the behaviour being similar to that reported by Ying (1978) in related carbon

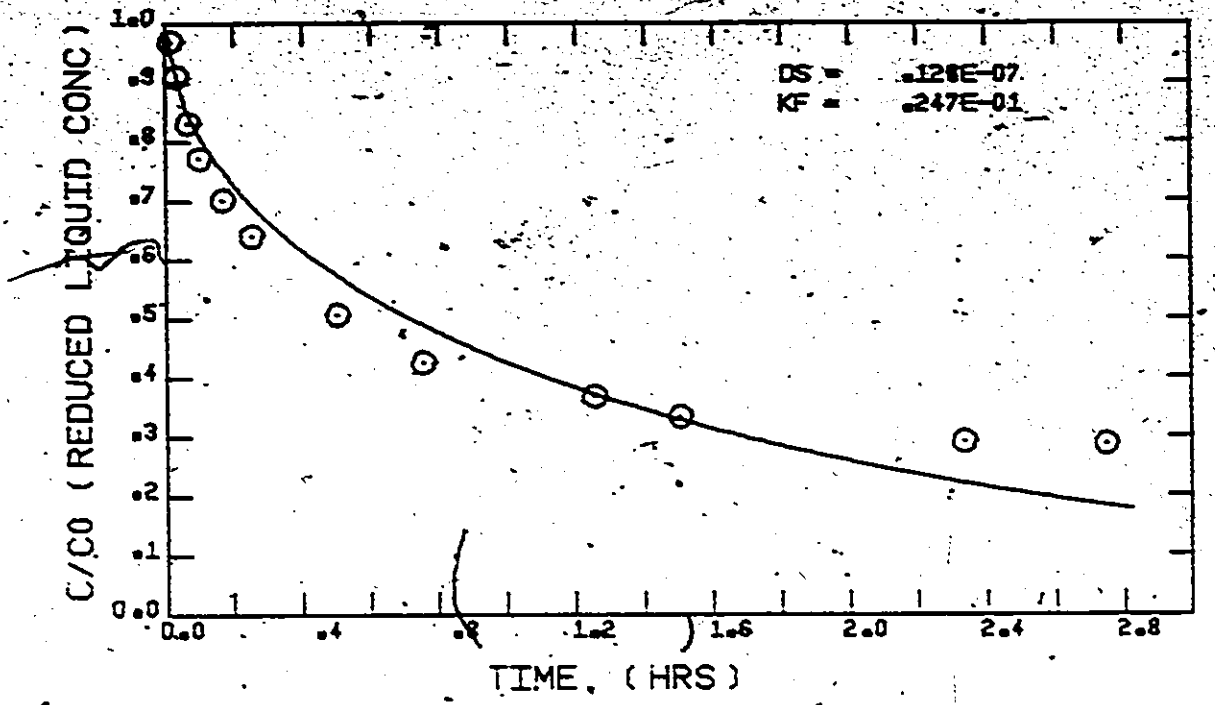

Figure 5-7. Single Parameter Model Fitted to Batch Kinetic Data.

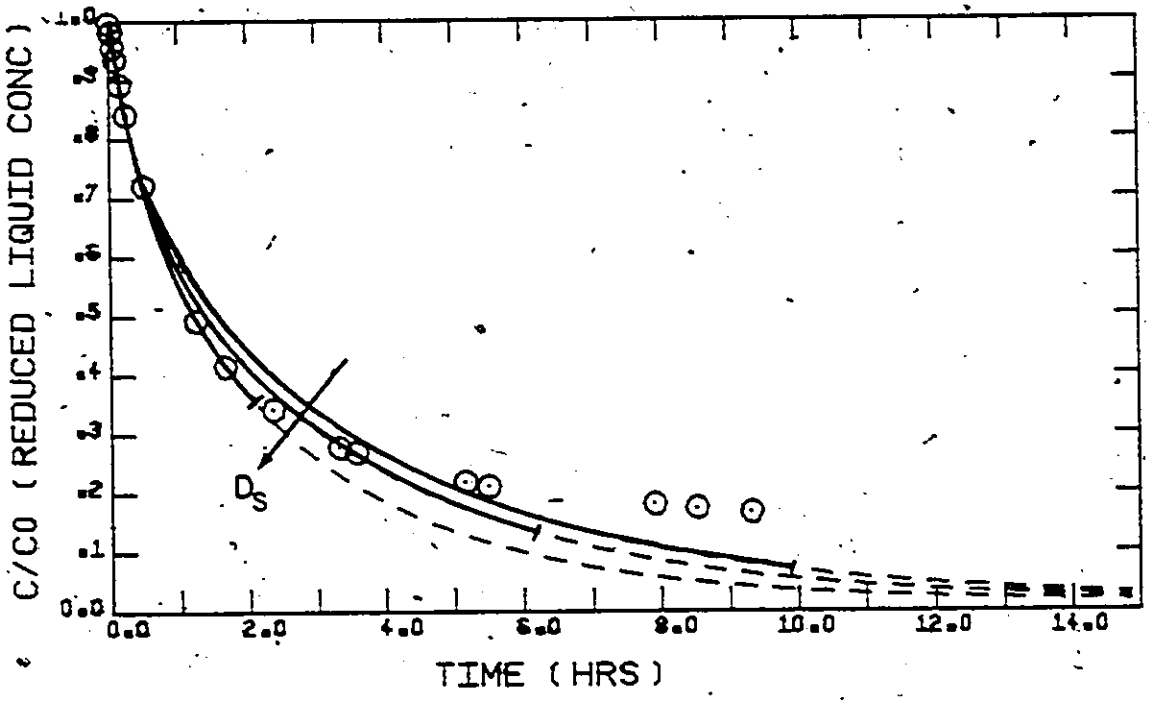

Figure 5-8. Single Parameter Model Fitted over Different Time Periods. (D_s = 6.67, 7.69, 10.0×10^{-8} cm^2/sec;—extent of fitted data)

adsorption studies. The lack of fit appears to be caused primarily by different end points, as the model prediction, which is constrained to approach the experimental isotherm reported in Chapter 4, indicates greater adsorption than is observed in the batch kinetic experiment. A kinetic analysis when the model shows distinct lack of fit is meaningless as is shown in Figure 5-8, in which the same set of batch kinetic data has been regressed three times using additional data each time. The measured surface diffusion coefficient is seen to be a function of the time span over which data is regressed. In addition to testing the single intraparticle surface diffusion coefficient model, alternative single rate models were developed and fitted to the data. A combined pore and surface diffusion model was solved using Crank-Nicholson difference analogues and a quasi-linearization scheme as suggested by Svedberg (1975). The solution was found to be reasonably efficient but required significantly more computation than the surface diffusion model alone. When fitted to the experimental data with either pore or surface diffusion alone, or pore and surface diffusion combined, the observed behaviour was similar to that reported above for the surface diffusion model. Although the pore/surface diffusion model has two parameters, the mechanisms are in parallel, and do not account for the large change in uptake rate between the early and later stages of adsorption. The combined transport equation within the carbon particle (equation 2.9) can be rewritten as

$$\rho_c \frac{\partial q}{\partial t} = \{D_p^{\,a} + \rho_c D_s \frac{\partial q}{\partial c}\} \frac{1}{r^2} \frac{\partial}{\partial r} \left(r^2 \frac{\partial c}{\partial r}\right) \qquad (5.22)$$

and an effective diffusion coefficient

$$D_{eff} = D_p + \rho_c D_s \frac{\partial q}{\partial c} \qquad (5.23)$$

can be defined. With a nonlinear isotherm, D_{eff} is a function of concentration because of the $\frac{\partial q}{\partial c}$ term. The permissible variation of D_{eff} does not, however, describe the experimental behaviour since the combined model was unable to fit the data.

The other model tested was the concentration dependent surface diffusion mechanism proposed by Neretnieks (1976b). Using the equations given by Neretnieks, the solution was again obtained using Crank-Nicholson finite difference analogues. In Neretnieks' notation

$$D_s = D_o e^{kQ} \qquad (2.13)$$

thus the surface diffusion coefficient increases exponentially with increasing surface concentration. It was anticipated that such a mechanism might explain the observed variation of the effective diffusion coefficient during the adsorption period as initially, when solid phase concentrations near the particle surface are high, the diffusion coefficient would also be large. As the solid phase concentrations fall as equilibrium is approached, the diffusion coefficient would also fall. When compared to the experimental data, however, various combinations of the parameters D_o and k were unable to explain the observed behaviour. In attempting to explain similar data, Famularo et al. (1978) also used Neretnieks' approach and found it to be unsatisfactory in explaining the experimental data.

Thus on the basis of the above studies, it was evident that

neither single intraparticle rate models, combined pore and surface diffusion models, or concentration dependent diffusion coefficient models could explain the initial rapid uptake followed by a slow approach to equilibrium.

5.3.3 Application of the Proposed Model and Parameter Estimation.

When fitting the experimental data with the branched pore kinetic model, three adjustable parameters are involved. These are the surface diffusion coefficient in the macropores (D_s), the pseudo mass transfer coefficient in the micropores (k_b), and the fraction separating the particle into macro and micropore regions (f).

The data for one set of runs using a constant initial concentration of phenol but varying masses of carbon are shown in Figure 5-9, along with the branch pore model predictions obtained by a nonlinear regression analysis routine (UWHAUS). The model is seen to give an excellent description of the data, and the fitted parameters and experimental conditions are given in Table 5-1, along with the 95% confidence limits on the parameters (on a linear hypothesis). The external film transfer coefficients were measured from the first few minutes data as described in section 5.3.1. The reason for the apparent dependence of k_f on the mass of carbon, as indicated in Table 5-1, is attributed to varying hydraulic flow patterns through the wire baskets when containing different amounts of carbon.

The calculated D_s and k_b values in Table 5-1 do not show a trend and are reasonably constant, however, the parameter f, which was estimated accurately as indicated by the approximate 95% confidence limits,

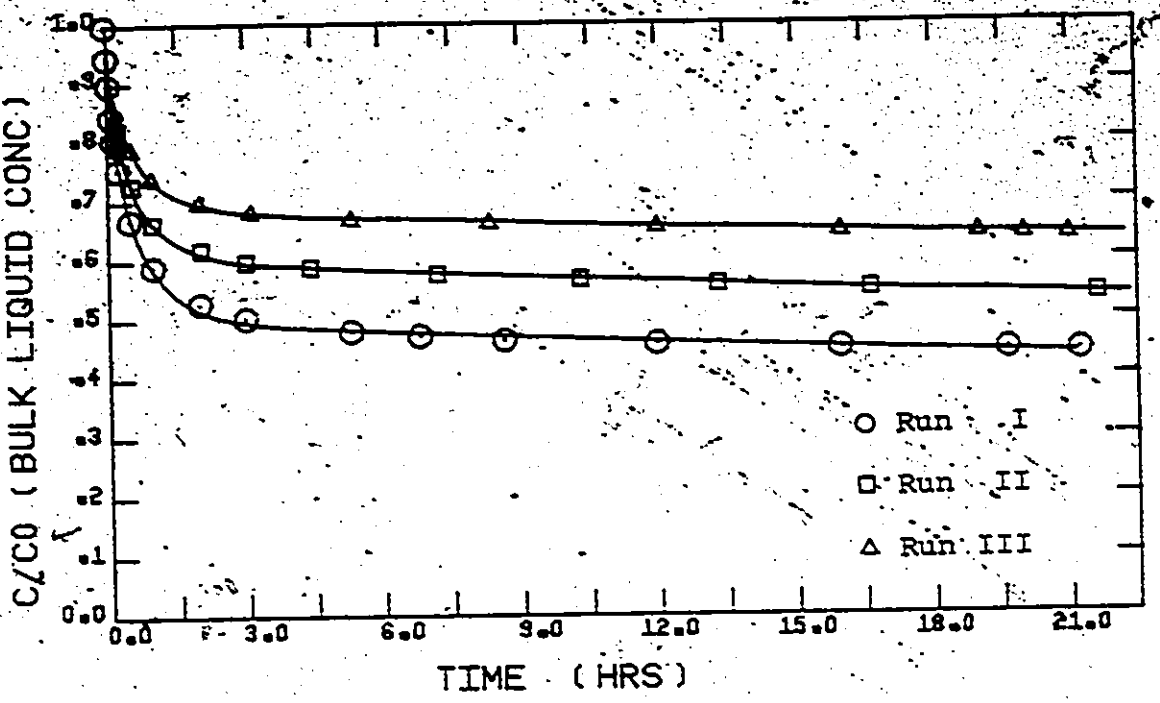

Figure 5-9. Batch Kinetic Experiments with Varying Carbon Mass. (c_o = 100 mg/l Phenol, N = 250 rpm).

Run No.	I	II	III
W (g)	0.9898	0.7216	0.5393
c_o (mg/l)	96.3	96.3	94.7
c_e/c_o	0.280	0.430	0.583
k_f (cm/sec x10^2)	1.33	1.82	2.01
D_s (cm^2/sec x10^8)	7.78 (± 10%)	9.01 (± 9%)	7.75 (± 7%)
k_b (sec^{-1} x10^6)	1.44 (± 27%)	1.87 (± 18%)	1.80 (± 16%)
f	0.63 (± 2%)	0.66 (± 2%)	0.68 (± 2%)

Table 5-1. Fitted Parameters and Experimental Conditions of Batch Runs in Figure 5-9. (incl. = 95% confidence limits).

appeared to increase with increasing liquid phase equilibrium concentration (c_e). The observation led to further investigation. In Figure 5-10 the results of the kinetic runs I to III have been plotted on the phenol isotherm. For each experiment the calculated capacity within the branch or micropore region (equal to $\{1-f\}q_e$) was determined and is shown on the figure. The capacities appeared to be virtually constant, independent of the equilibrium concentration. The extremely close agreement is probably fortuitous, but this result is consistent with the earlier proposal that micropore adsorption would involve multidirectional sorbate/sorbent interactions, and thus involve stronger bonding than in the macropores. The results shown in Figure 5-10 indicate that the micropore capacity is saturated over the experimental range investigated, whereas additional adsorption occurs in the macropore region with increasing liquid phase concentration. The fact that the micropore capacity is saturated at lower concentrations indicates that sorbates preferentially adsorb in this region because of the greater adsorption energies.

In adsorption-desorption studies of activated carbon using supercritical CO_2 as a regenerant fluid, Modell et al.(1978) found that only 70% of the initial adsorptive capacity could be recovered when adsorbing phenol on Filtrasorb F300. He attributed this lost capacity to irreversible adsorptive interactions with surface oxide groups. He also obtained higher regeneration recoveries when systems were regenerated after short adsorption periods, suggesting that much of the lost capacity was related to the slow adsorption mechanism.

Additionally, Snoeyink (1968) was able to desorb only about 50% of adsorbed phenol from a Columbia LC carbon even after 5 months of contact. The existence of an irreversibly or at least strongly bound fraction of the total capacity is thus established, and the results of the present study associate this fraction with the slow diffusing micropore region.

Having established typical parameter values for the branched pore model, as given in Table 5-1, a sensitivity analysis can be conducted with the model: The results of such a study are shown in Figures 5-11, 5-12 and 5-13. The almost sequential nature of macro and micropore diffusion can be seen in Figures 5-11 and 5-12 where the model is shown to be sensitive to D_s only during the initial rapid uptake period, and to k_b only during the long slow approach to equilibrium. In contrast, Figure 5-13 shows that the model is sensitive to the parameter 'f' throughout the adsorption period. This study indicates that adequate discrimination of the micropore transport rates requires accurate data over an extended period, a task for which the Carberry reactor used in these experiments is ideally suited.

To obtain kinetic parameters for use in the column simulations, batch kinetic runs for both substrates were carried out over 3 day periods. The data and the regressed model predictions are shown in Figures 5-14 and 5-15, and the experimental conditions and best fit parameters are presented in Table 5-2. Low rotational speeds were used in these experiments to minimize wear on the equipment during the extended period of operation.

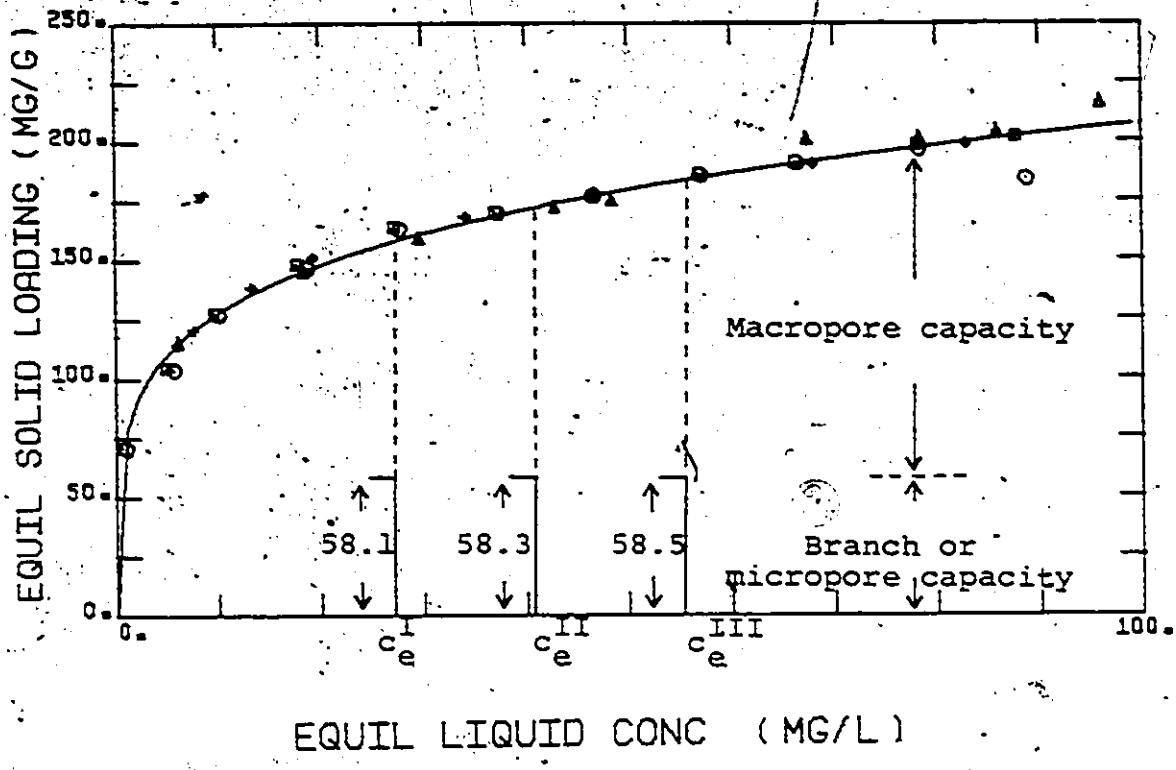

Figure 5-10. Distribution of Adsorptive Capacity Between Macropore and Micropore Regions.

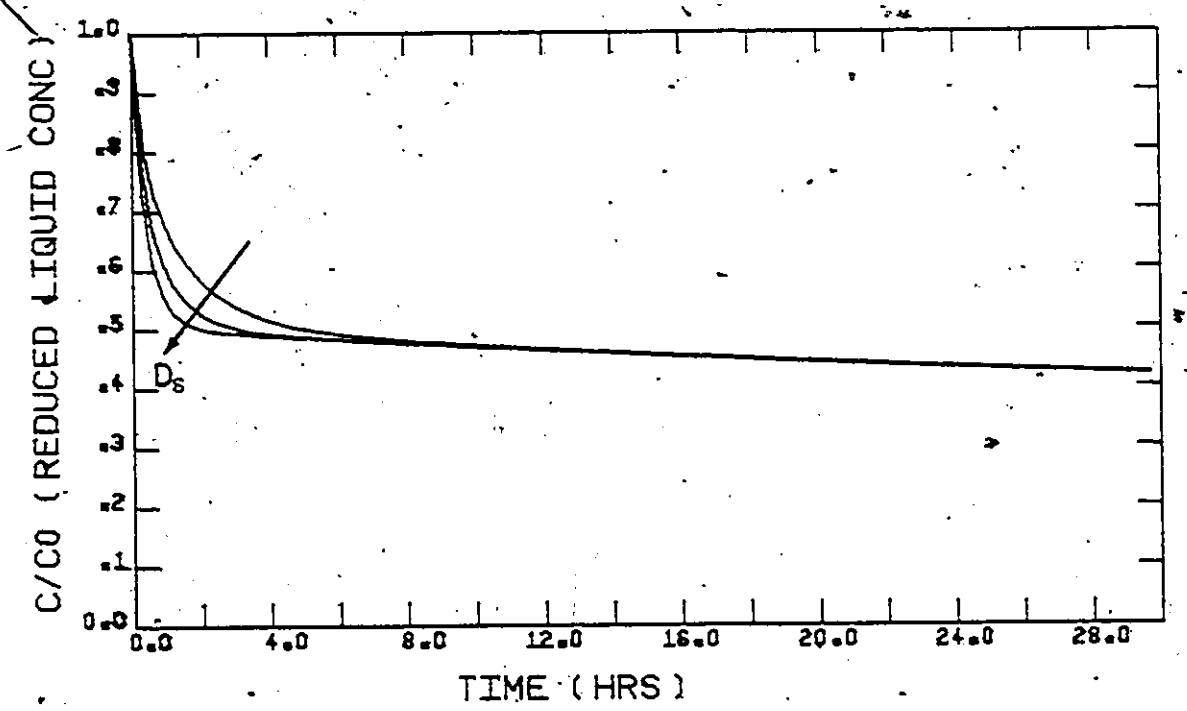

Figure 5-11. Sensitivity Analysis - D_S Parameter. (D_S = 3.75, 7.5, 15.0×10^{-8}cm^2/sec; k_b = 1.8×10^{-6}sec^{-1}; k_f = 0.01 cm/sec; f = 0.7).

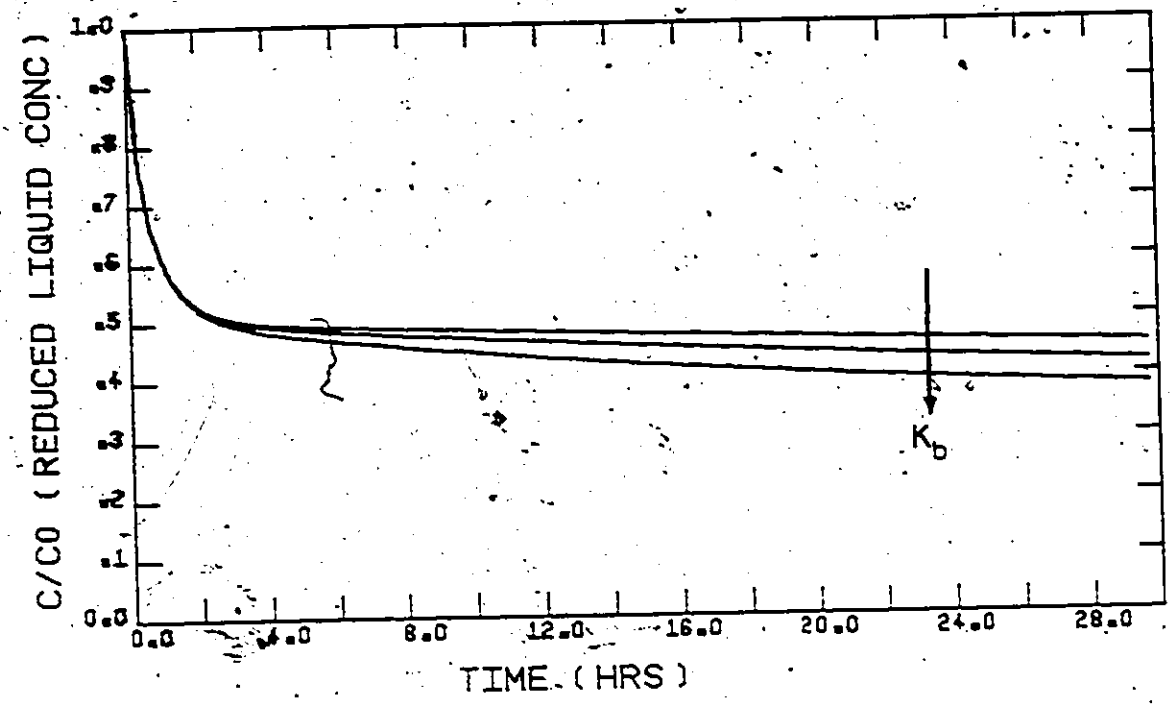

Figure 5-12. Sensitivity Analysis - k_b Parameter. (k_b = 0.9, 1.8, 3.6 × 10^{-6} sec^{-1}).

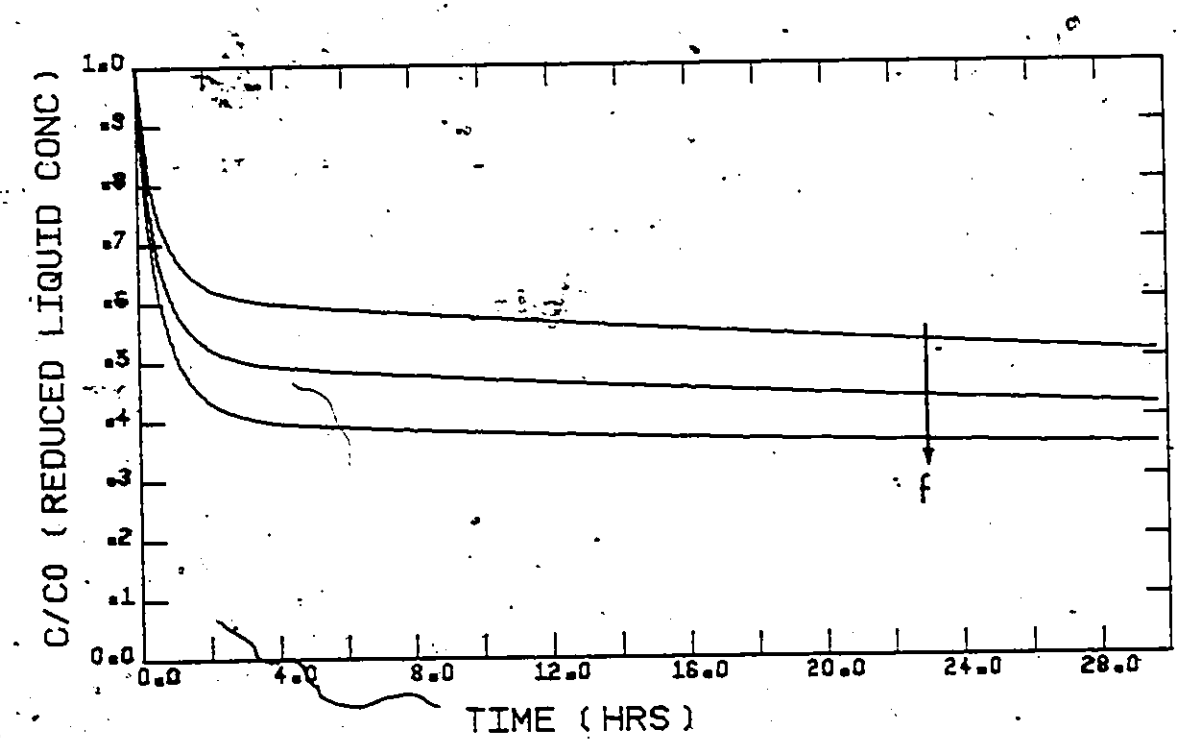

Figure 5-13. Sensitivity Analysis - f Parameter. (f = 0.525, 0.700, 0.875).

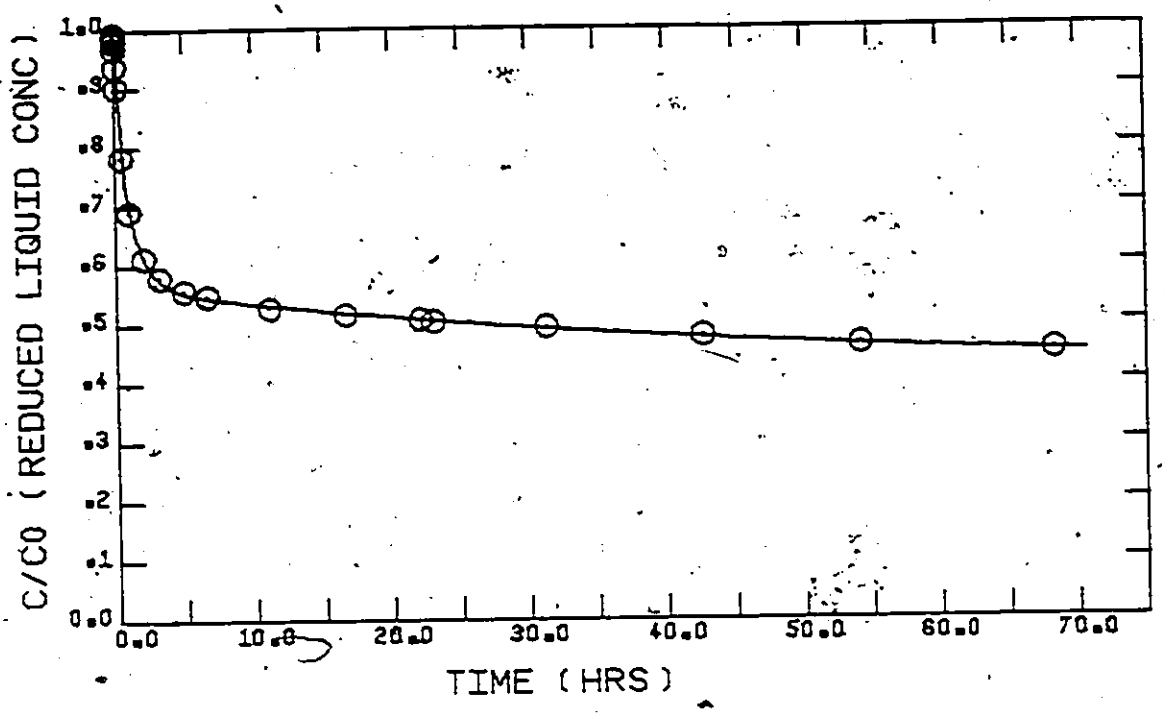

Figure 5-14. 3 Day Batch Kinetic Experiment - Phenol.

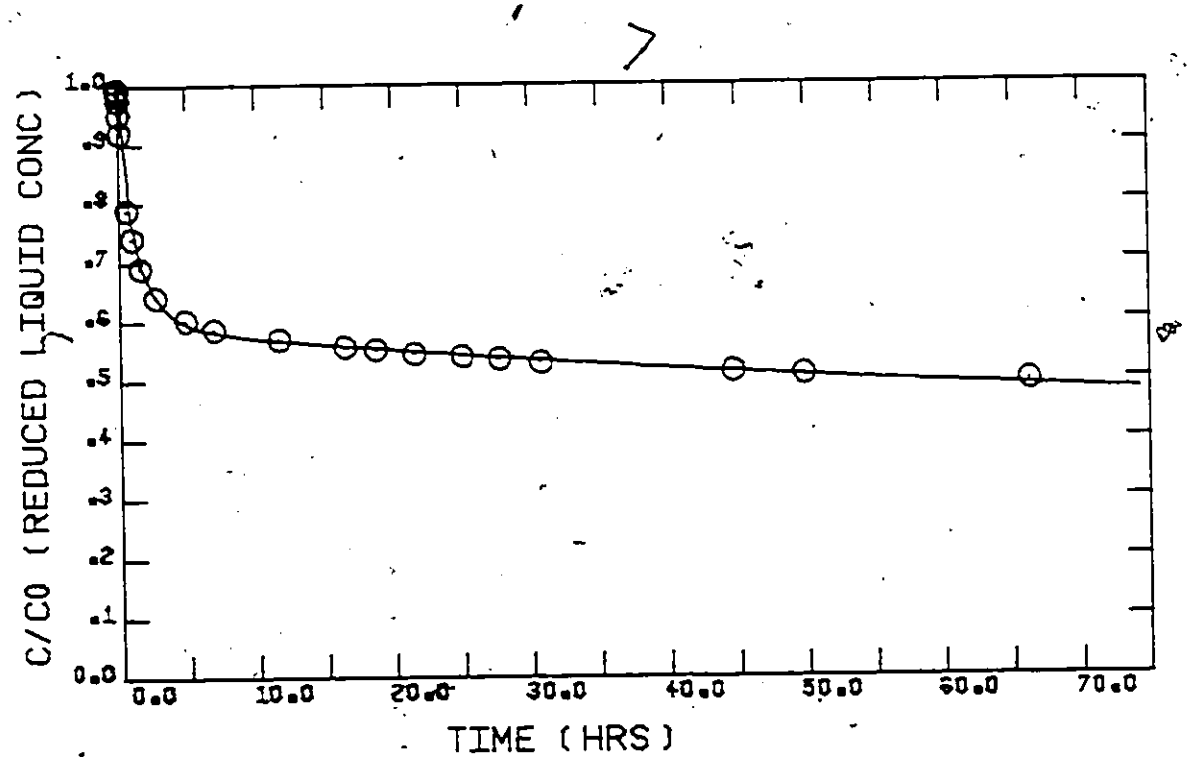

Figure 5-15. 3 Day Batch Kinetic Experiment - o-Chlorophenol.

The transport coefficients (D_s and k_b) in Table 5-2 are both larger for phenol than for o-chlorophenol as might be expected since phenol is both a smaller and less strongly adsorbing molecule than is o-chlorophenol. The result is in accord with that of Fritz et al.(1978), who measured larger surface diffusion coefficients for phenol than for p-nitrophenol.

The importance of obtaining sufficient data over an extended period can be seen by comparing the approximate 95% confidence intervals of the parameters in Tables 5-1 and 5-2. The data described in Table 5-1 were collected over 21 hour periods whereas the data described in Table 5-2 were collected over 75 hours. Only small decreases in the confidence limits on D_s and f were observed, however, the confidence limits on k_b decreased from 20% to about 9%. This indicated that the additional data gave improved estimates of the micropore rate coefficient since it is only in the long flat portion of the uptake curve that micropore transport is controlling.

Additional evidence of the effect of collecting data over an extended period is shown in Figure 5-16 in which the data of experiment No.V is plotted over 30 and 75 h. The data to 30 and 75 h have been regressed separately and the parameters are given on the figure. These show that although D_s changed by about 10% and f by about 3%, the value of k_b dropped by over 25%. This difference is attributed to the likelihood that the true rate in the micropores decreases with time as smaller and more inaccessible pores are penetrated. The fitted coefficient k_b is thus an average of a continuum of rates over the measurement period

Run No.	IV Phenol	V o-Chlorophenol
N (rpm)	43	57
W (g)	0.7588	0.3920
c_o (mg/l)	95.6	96.9
c_e (mg/l)	39.2	41.5
k_f (cm/sec x10^3)	6.78	9.69
D_s (cm^2/sec x10^8)	5.32 (± 6%)	3.81 (± 7%)
k_b (sec^{-1} x10^6)	1.59 (± 8%)	1.14 (± 9%)
f	0.708 (± 1%)	0.678 (± 1%)

Table 5-2. Model Parameters and Experimental Conditions for 3 Day Batch Experiments (incl. = 95% confidence limits).

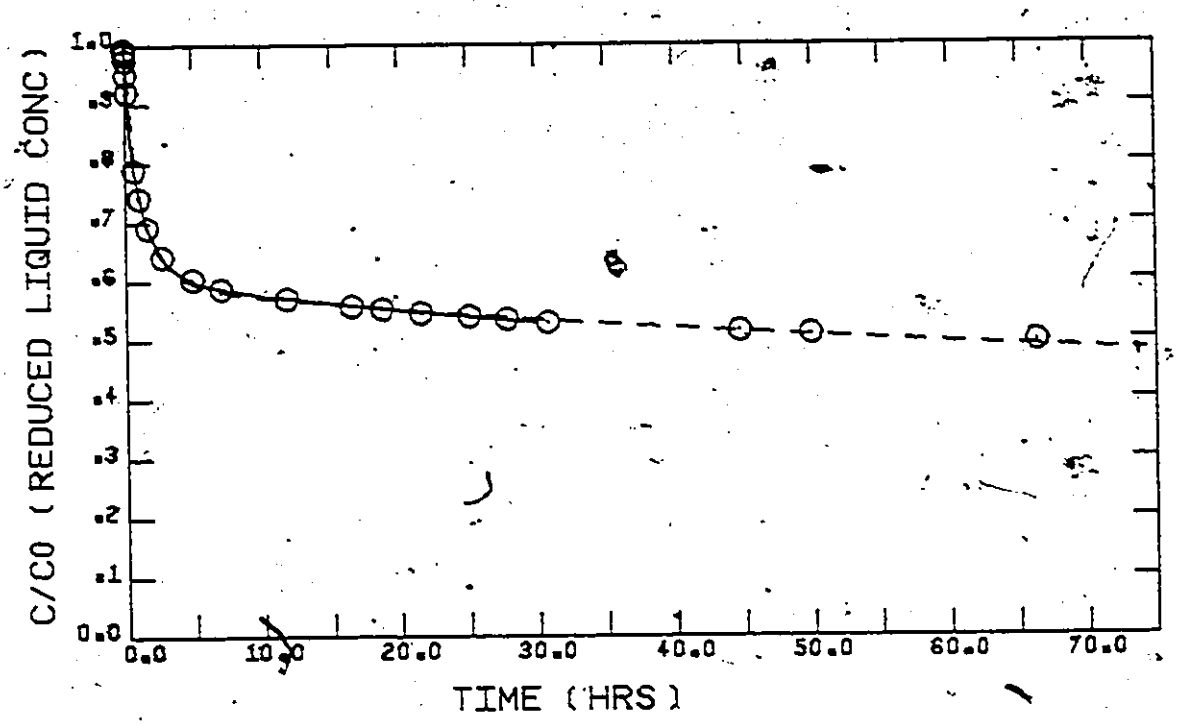

Figure 5-16. Batch Kinetic Experiment No.V, 0-30 and 0-75 h of Data Regressed. (0-30 h. D_s=4.18x10^{-8}, k_b=1.56x10^{-6}, f = 0.659
0-75 h. D_s=3.81x10^{-8}, k_b=1.14x10^{-6}, g = 0.678)
(D_s in cm^2/sec, k_b in sec^{-1})

and would therefore decrease as data was fitted over longer periods. The implications of this variation with respect to column modelling are discussed in the next chapter.

The same data plotted in Figure 5-17 clearly illustrates a point made in Chapter 4 concerning the difficulty in determining true equilibrium. In this figure the data from experiment No.V have again been plotted, on scales of 0 to 15 h and 0 to 15 days, along with the corresponding model predictions. The upper curve in this figure suggests that equilibrium has been reached at 15 h as the rate of uptake seems negligible in comparison to the initial rate. If the data are monitored over sufficiently long time periods, however, the system is seen to still be far from equilibrium at this time. The assumption of equilibrium at the plateau of the upper curve corresponds approximately to the capacity in the macropores, and would be analogous to the 'pseudo-equilibrium' introduced by Crittenden and Weber (1978a) to enable prediction of experimental column performance.

From the data in Figure 5-16, it was also noted that the macropore diffusion coefficient (D_s) decreased slightly as additional data was fitted. The same effect was observed in the phenol results reported in Table 5-1 and 5-2 where the coefficient D_s is less in the 75 h run than in the 21 h run. The reason for this difference is not known although some form of concentration dependence may be a possible explanation. Fortunately, as shown in the next chapter, the predicted breakthrough curves are relatively insensitive to D_s so the small variations in this parameter are not of particular importance with respect to pre-

diction of column performance. Nevertheless, it should be expected that batch kinetic parameters measured under similar conditions to the column operation would give the best description of column performance.

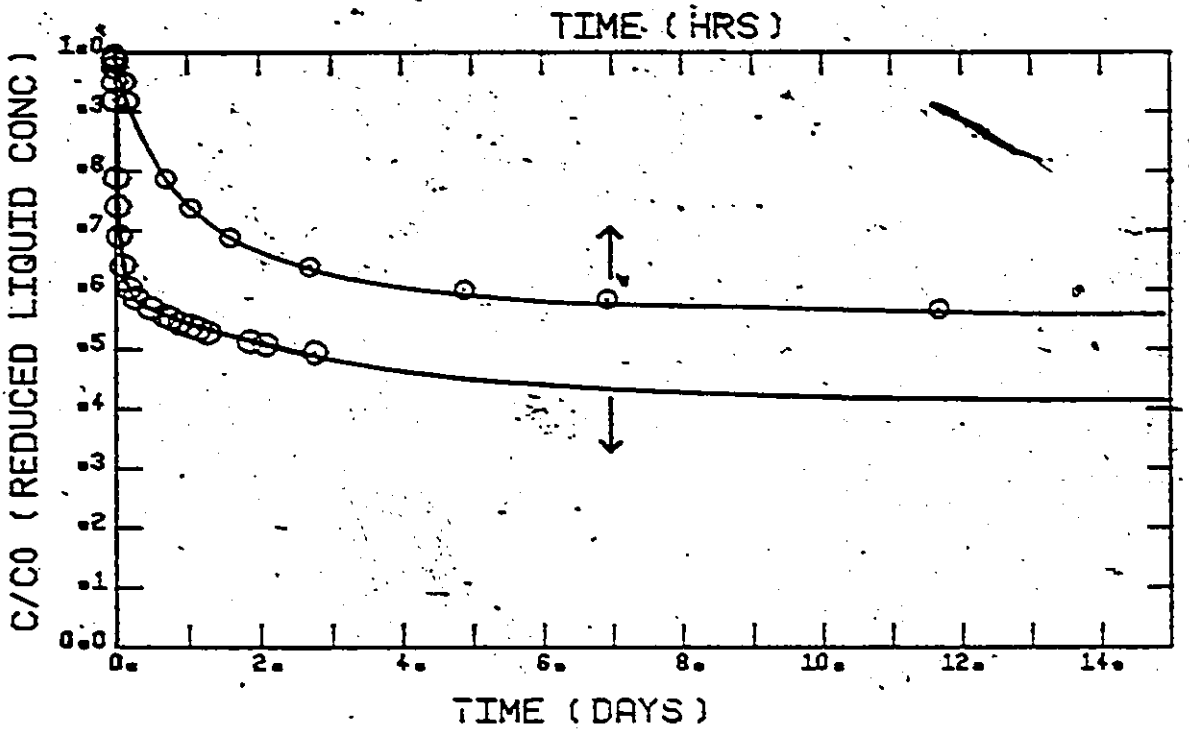

Figure 5-17. Batch Kinetic Data of Experiment No.V and Model Prediction over 15 h and 15 days.

CHAPTER 6

ADSORPTION COLUMN MODEL AND EXPERIMENTAL VERIFICATION STUDIES

6.1 Adsorption Column Model

In addition to the equations describing adsorption onto the carbon particle which are identical to those detailed in section 5-2, a model of an adsorption bed also requires an equation describing the liquid phase concentration.

A schematic diagram of an element of the adsorption bed of length dx is shown in Figure 6-1. From this figure, and based on the assumptions that:

(i) Axial dispersion is negligible;

(ii) Radial gradients do not exist in the liquid phase;

(iii) The adsorbent particles are stationary;

(iv) The adsorbent particles are small enough that the fluid surrounding a single particle has a uniform concentration;

the fluid phase mass balance can be written and gives the equation:

$$\frac{\partial c}{\partial t} = - v_s \frac{\partial c}{\partial x} - \frac{(1 - \varepsilon)}{\varepsilon} \cdot \frac{3k_f}{R} (c - c_s) \qquad (6.1)$$

Equation (6.1) is transformed to the Lagrangian coordinate system using the variable transformations

$$\theta = \frac{D_s}{R^2} (t - \frac{x}{v_s}) \qquad (6.2)$$

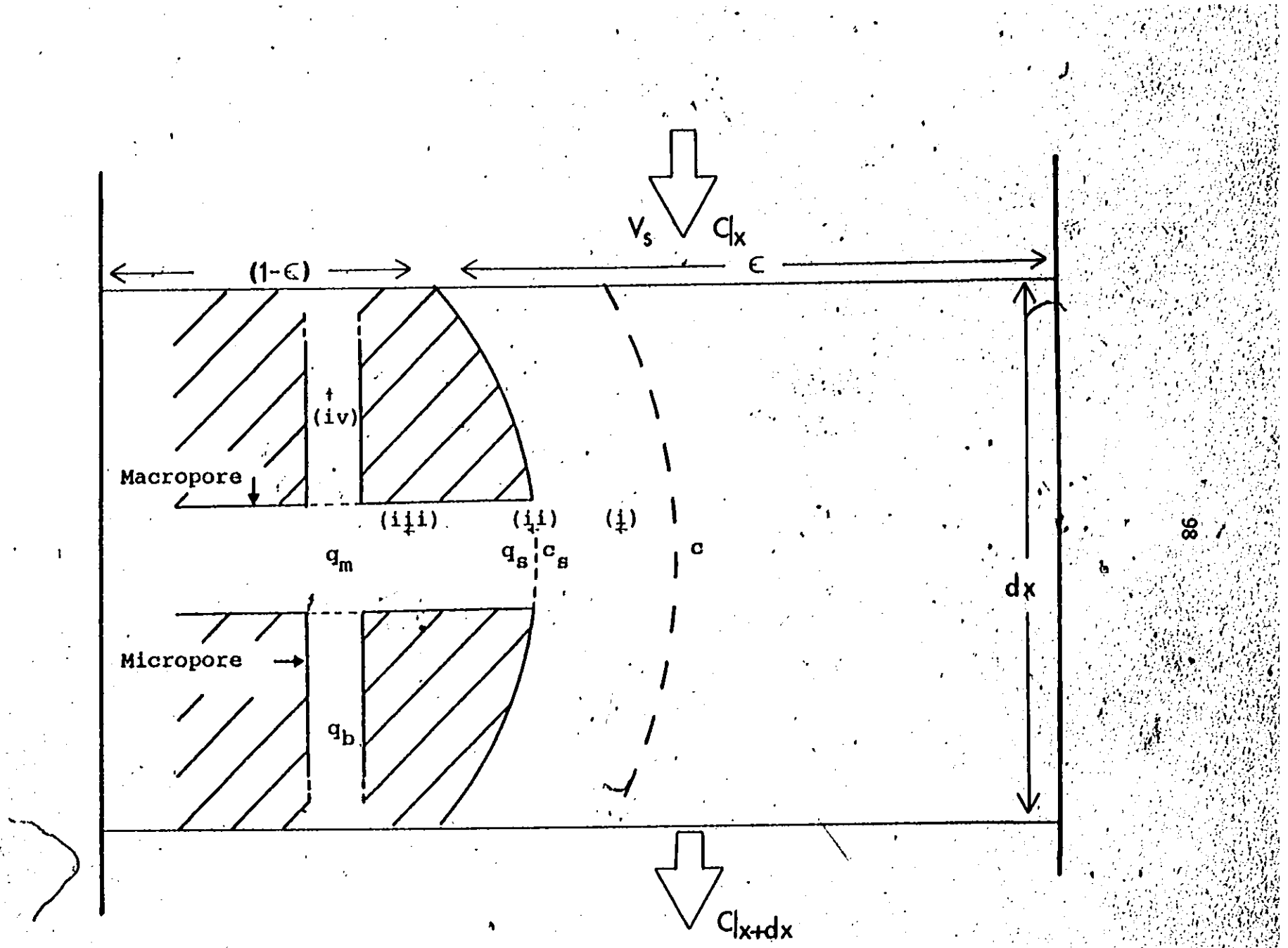

Figure 6-1. Differential Element of Adsorption Bed.

$$z = D_s x / R^2 v_s \tag{6.3}$$

in which v_s = interstitial liquid phase velocity; x = bed depth variable; ε = liquid volume fraction excluding internal pore volume; and θ, z = dimensionless Lagrangian coordinates.

Substitution of equations (6.2) and (6.3) into (6.1) results in

$$\frac{\partial C}{\partial z} = -\frac{(1-\varepsilon)}{\varepsilon} \cdot Bi_f (C - C_s) \tag{6.4}$$

subject to the initial and boundary conditions

$$C(z,o) = 0 \tag{6.5}$$

$$C(o,\theta) = 1 \tag{6.6}$$

In addition to solving equation (6.4), the equations

$$\frac{\partial Q_m}{\partial \theta} = 4\eta \frac{\partial^2 Q_m}{\partial \eta^2} + 6 \frac{\partial Q_m}{\partial \eta} - \frac{Bi_p}{f} (Q_m - Q_b) \tag{5.13}$$

$$\frac{\partial Q_b}{\partial \theta} = \frac{Bi_p}{(1-f)} (Q_m - Q_b) \tag{5.14}$$

$$\left.\frac{\partial Q_m}{\partial \eta}\right|_{\eta=1} = \frac{Bi_f}{f} \cdot \frac{F}{6} (C - C_s) \tag{5.15}$$

must also be solved at each point within the adsorption bed.

6.1.1 Mathematical Solution of the Column Model

Although the set of equations to be solved at each point within the bed was identical to the equations used to describe the batch kinetic problem, a different solution technique was used in which the liquid and solid phase concentrations are solved simultaneously. This approach was suggested by McGreavy et al. (1967) and the solution used in the pre-

sent work followed that of McGreavy but with some modification. The detailed solution of equations (6.4), (5.13), (5.14) and (5.15) is described in Appendix D and results in an equation to be solved at each bed increment of the form

$$\underline{\underline{X}}^{(k-1)} \underline{Q}^{m\,(k)}_{j+1} = \underline{\underline{Y}} \underline{Q}^{m}_{j} + \underline{H}^{(k-1)} \qquad (6.7)$$

where the liquid phase concentration is contained in the vector $\underline{Q}^m$. Because $\underline{\underline{X}}$ and $\underline{H}$ contain elements measured at the future time interval, these values must be guessed or predicted and the solution of equation (6.7) iterated until a converged solution is obtained. In practice the future values were first predicted by linear extrapolation of past data, and only two iterations were found to be necessary to achieve the desired accuracy.

6.1.2 Solution Testing of the Column Model

The lack of implied stability and convergence when using Crank-Nicholson or other numerical approximations in a nonlinear problem was discussed in section 5.2.2. One method of evaluating the accuracy of a new numerical solution is to compare the results to previously published solutions obtained by different solution techniques. If the results are in agreement, the solutions are in all probability correct.

This approach was taken in the present case with the solution being compared to the previously published results of Tien and Thodos (1959) and Fleck (1970). Both of these works used a model incorporating external film resistance, a surface diffusion mechanism, and a Freundlich isotherm. Tien and Thodos gave tabulated data while Fleck

published a series of curves from which points were obtained for comparison. The methods used to obtain the data for comparison are detailed in Appendix E. To enable comparison the present model was reduced to the surface diffusion model by setting f equal to unity and therefore eliminating the micropore capacity.

In both cases of comparison, as shown in Figures 6-2 and 6-3, good agreement was obtained between the present and previous models. The slight discrepancies observed could not be attributed to computational inaccuracies in the present model as decreasing time and spatial increments changed neither the shape nor position of the predicted breakthrough curve. The differences were therefore attributed in the case of Tien and Thodos (1959) to slight changes in their model caused by approximations used to obtain the solution, and in the case of Fleck (1970) to errors made in obtaining data from his plotted output. In any case, the agreement between the previously published solutions and the present model is sufficient for verifying the accuracy of the solution technique.

6.1.3 Model Parameters for Verification Studies

To be able to model the behaviour of adsorption beds, the equilibrium and kinetic parameters must be known. These have been determined in Chapters 4 and 5 are are given in Tables 4-3 and 5-2. These parameters can be used directly, without modification, for predicting the shapes and locations of the experimental breakthrough curves with one exception. As discussed previously, the parameter 'f' is a function of the final equilibrium concentration and since column experiments were run at influent concentrations of 50 and 100 mg/l, the relevant values

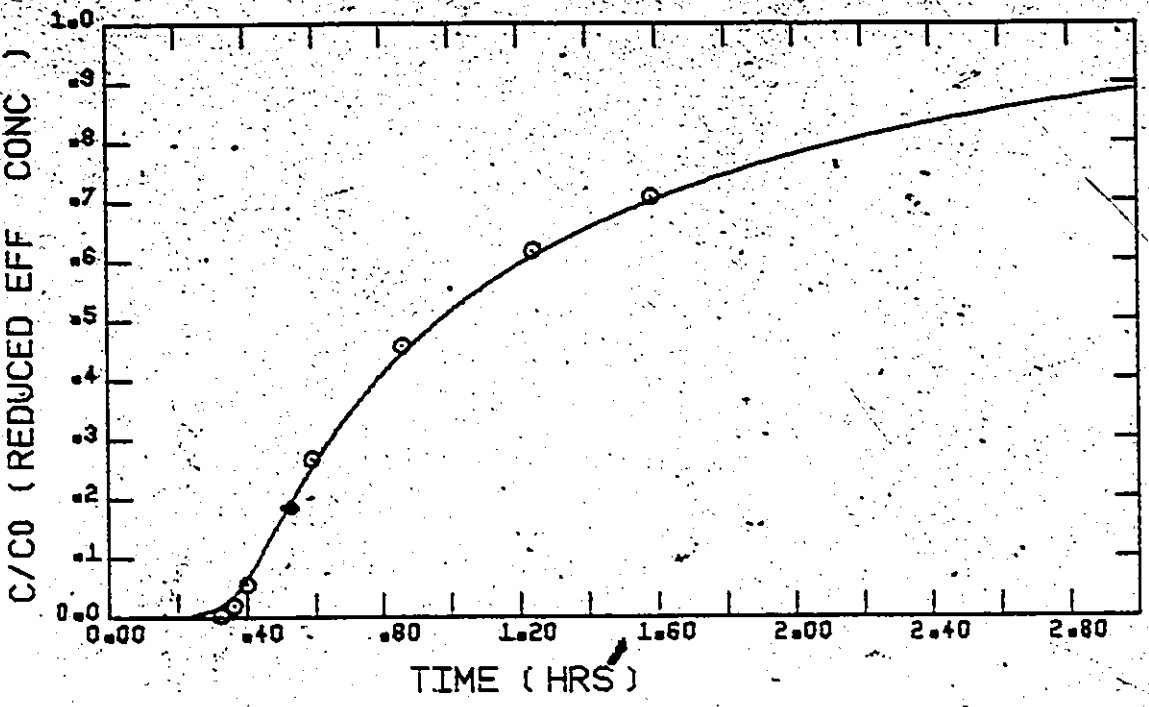

Figure 6-2. Comparison of Numerical Solution to that of Tien and Thodos (1959).

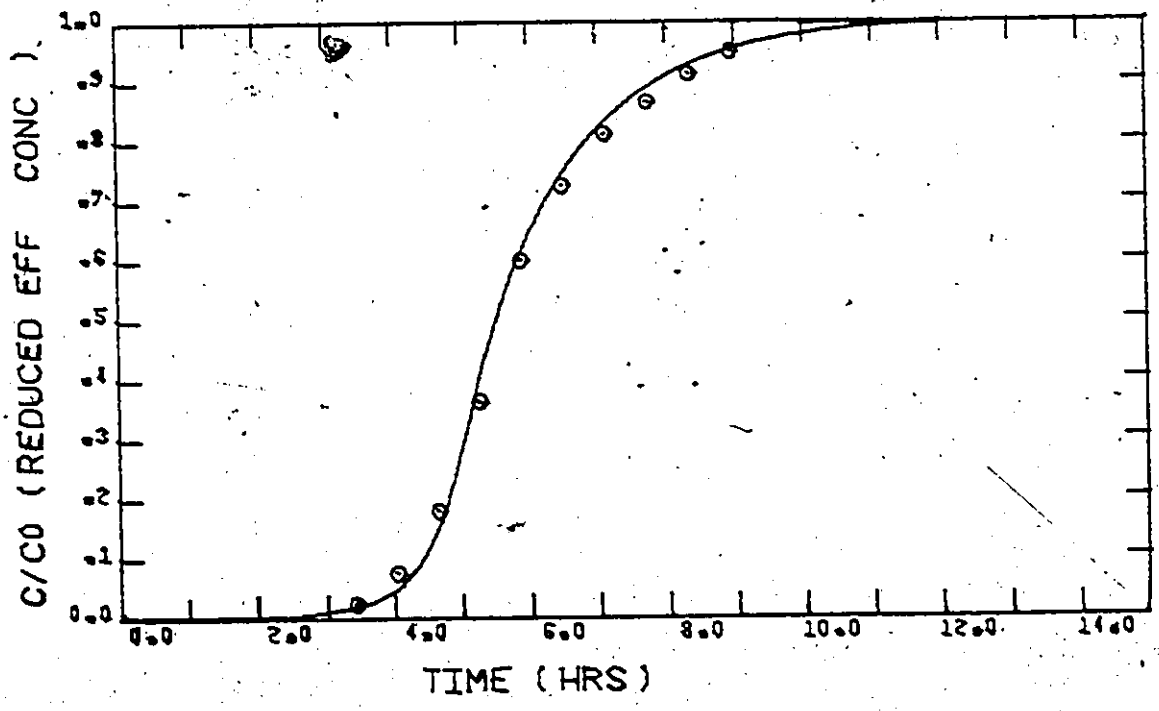

Figure 6-3. Comparison of Numerical Solution to that of Fleck (1970).

of 'f' at each concentration were required. In the batch kinetic experiments Nos.IV and V the equilibrium concentrations given in Table 5-2 were approximately 40 mg/l, and were considered close enough to 50 mg/l to be used directly for those simulations. For the 100 mg/l simulations the corresponding value of 'f' was calculated using the isotherm. Since the micropore capacity is almost constant,

$$q_{e,40}(1 - f_{40}) = q_{e,100}(1 - f_{100}) \qquad (6.8)$$

and as the $q_{e,i}$ are known from the isotherms and the f_{40} values are given in Table 5-2, the parameter f_{100} can be calculated to be:

$$\begin{aligned} &\text{Phenol} \quad f_{100} = 0.758 \\ &\text{o-Chlorophenol} \quad f_{100} = 0.704 \end{aligned} \qquad (6.9)$$

The only remaining information required to be able to simulate the column behaviour is the external mass transfer coefficient. As discussed in section 2.3.1 , a mass transfer correlation of Wilson and Geankoplis (1966) has been found to be suitable by several authors. The equation given by Wilson and Geankoplis for mass transfer in packed beds at low Reynolds numbers ($1.6 \times 10^{-3} < Re < 55$) is:

$$Sh = \frac{1.09}{\varepsilon} (Re\ Sc)^{1/3} \qquad (6.10)$$

in which Sh = Sherwood number, $k_f d_p/D_\ell$; Re = Reynolds number, $\rho v_s \varepsilon d_p/\mu$; Sc = Schmidt number, $\mu/\rho D_\ell$; d_p = particle diameter; and D_ℓ = free liquid diffusion coefficient of the adsorbate.

To calculate the Sherwood number the free liquid diffusion coefficients of phenol and o-chlorophenol are required. These were calcu-

lated at 20°C from a nomogram presented by Othmer and Thakar (1953) which was based on the molar volume calculated by the Schroeder method. The free liquid diffusion coefficients at 20°C were calculated to be

Phenol	9.0×10^{-6} cm^2/sec	(6.11)
o-Chlorophenol	8.0×10^{-6} cm^2/sec	

6.2 Experimental Model Verification Studies

The experimental data for the 8 breakthrough curves detailed in Table 5-2 are plotted in Figures 6-4 to 6-7 along with the model predictions using the parameters presented in the previous section. The curves are seen to have a characteristic tail in each case and the ability of the model to predict the column performance is clearly excellent, especially considering the time scale involved. The experimental conditions were deliberately chosen to give long bed service times so that the effects of slow diffusion could be easily observed.

In both the phenol and o-chlorophenol runs at 50 mg/l, the 60 cm breakthrough curves (Ib and IIIb) were distorted because of flow control problems either immediately prior to, or during the period when the curves passed the sample point. The location of breakthrough is well predicted even though the shapes of the experimental curves do not match the model predictions.

In most cases the model predicts a somewhat more rapid approach to equilibrium than is observed experimentally. This is attributed to the value of k_b being too large and therefore predicting saturation sooner than is actually achieved. The fact that batch kinetic experiments

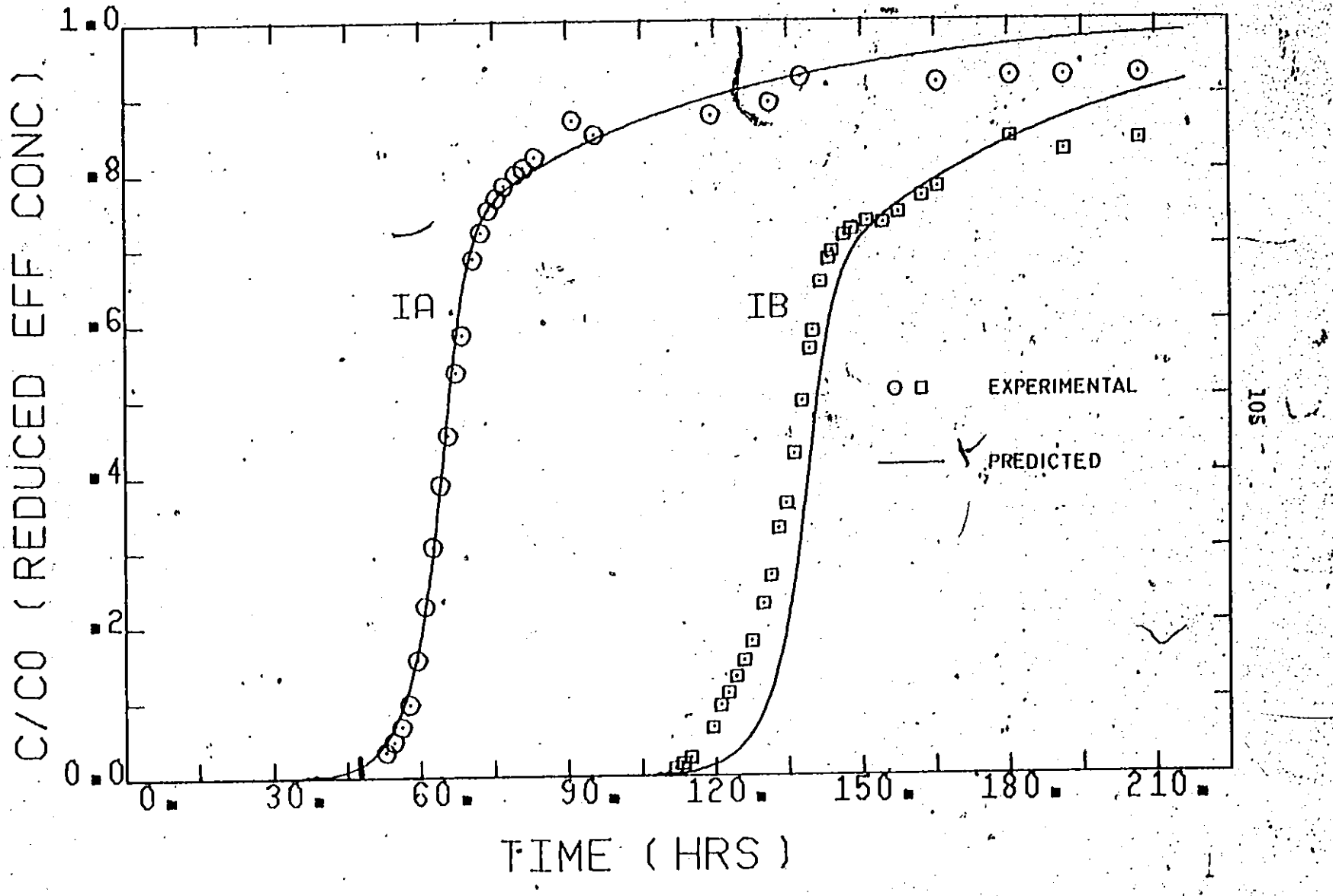

Figure 6-4. Experimental and Predicted Breakthrough Profiles - c_o = 50 mg/l Phenol (⊙-30 cm; ⊡-60 cm)

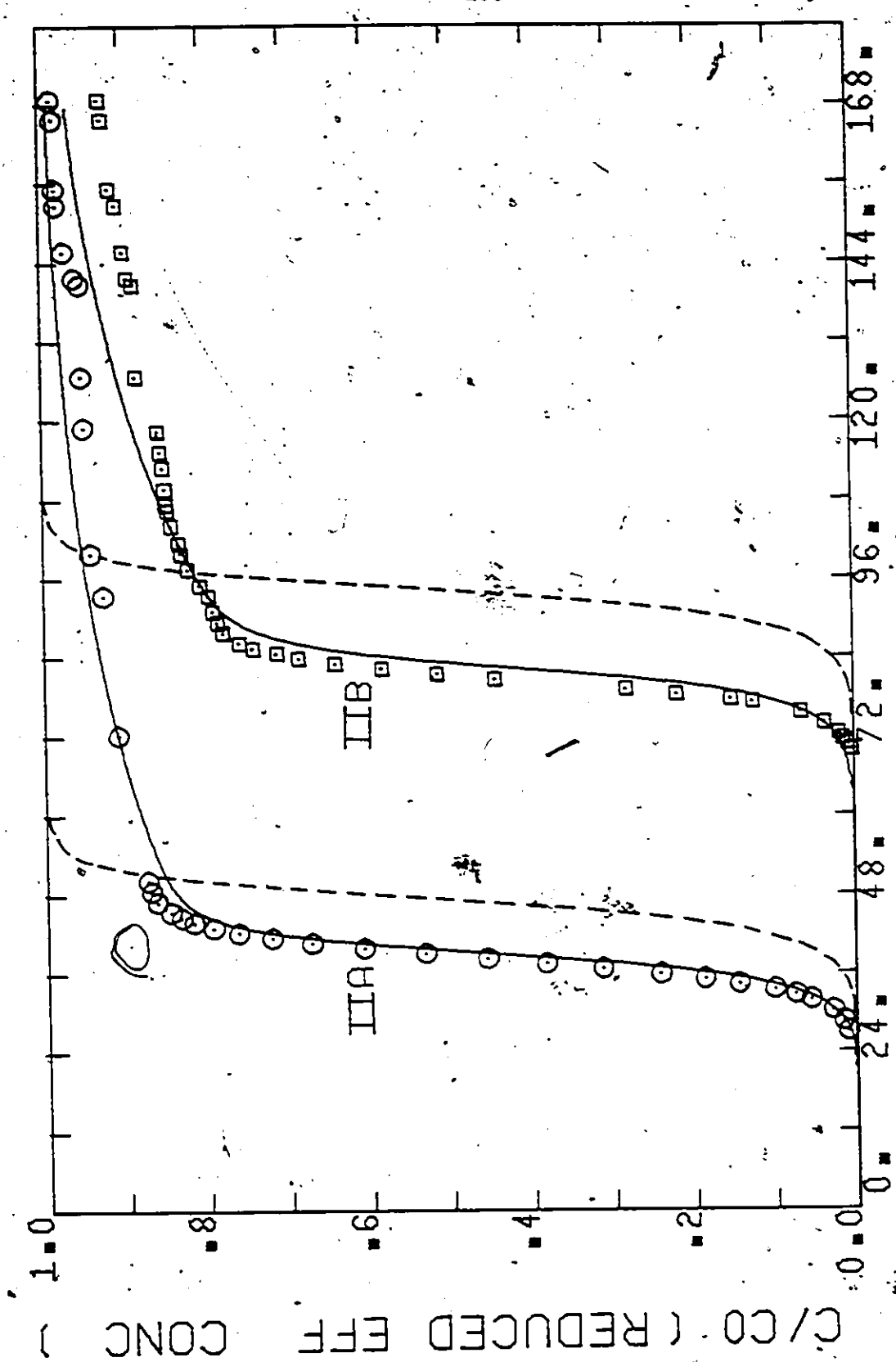

Figure 6-5. Experimental and Predicted Breakthrough Profiles - C_o =100 mg/l Phenol (⊙-30 cm, ⊡-60 cm)

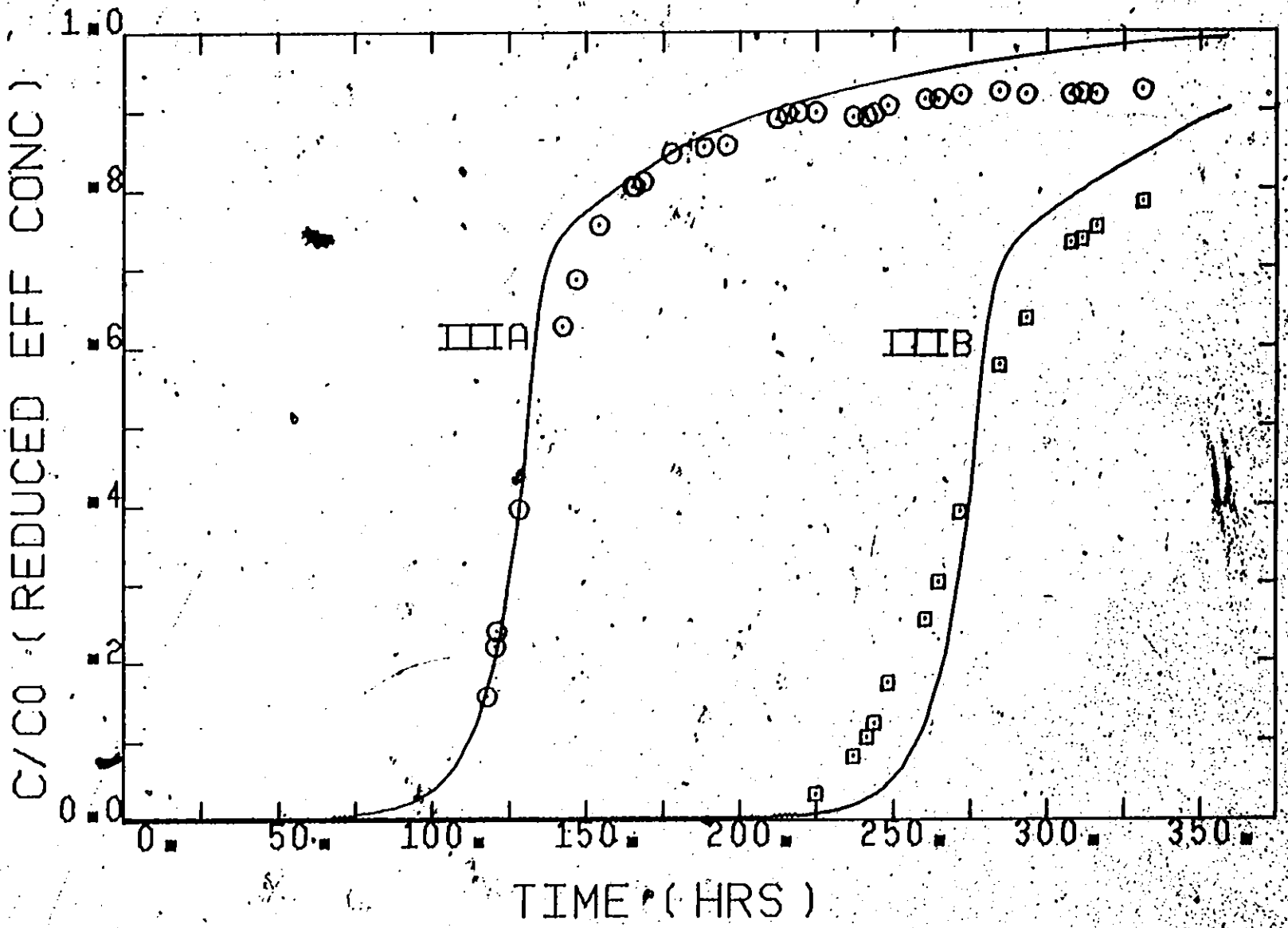

Figure 6-6. Experimental and Predicted Breakthrough Profiles-c_o=50 mg/l o-Chlorophenol

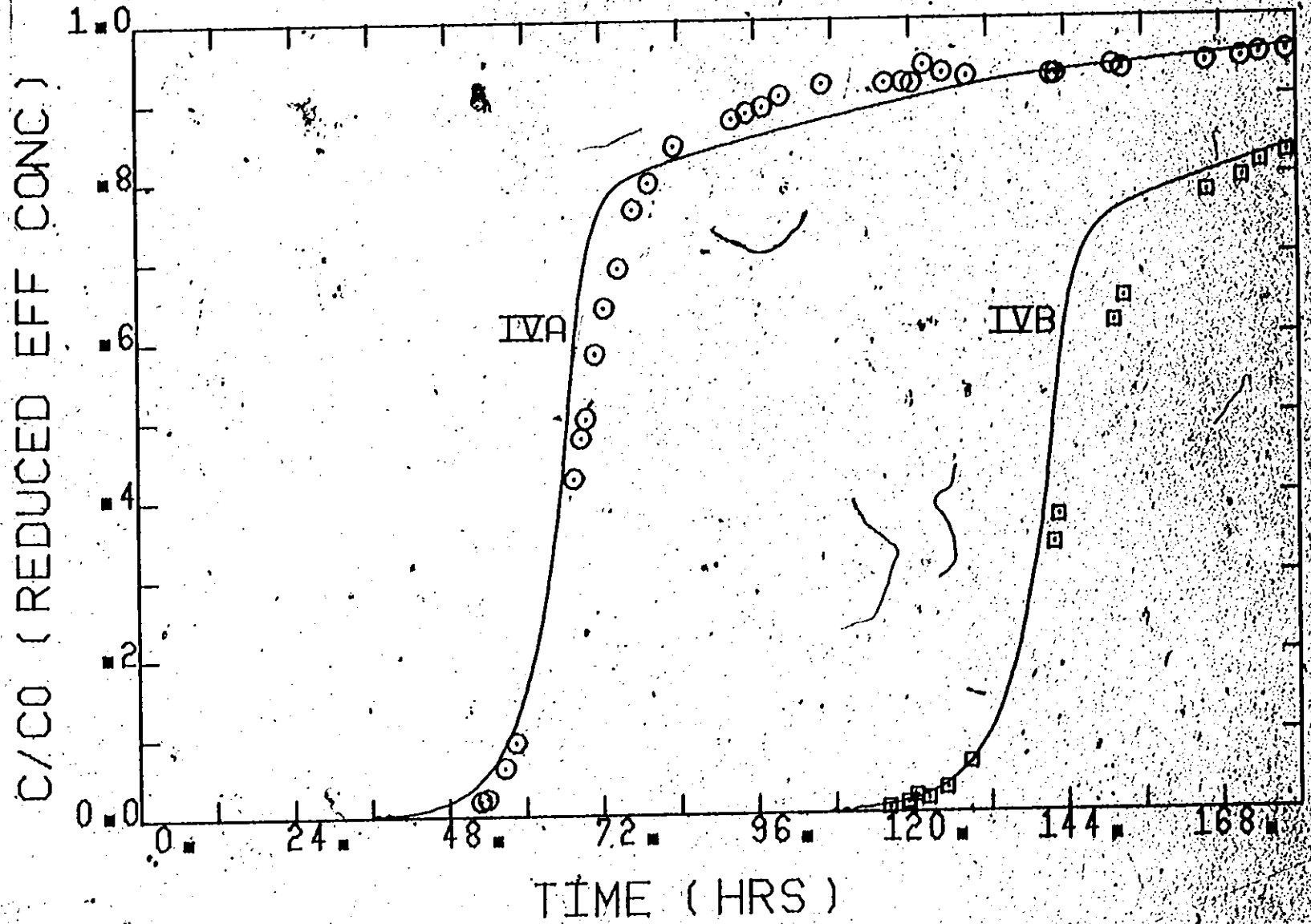

Figure 6-7. Experimental and Predicted Breakthrough Profiles-c_o=100 mg/l o-Chlorophenol

which are run over longer periods give lower values of k_b has been discussed previously, and it was suggested that the k_b value may actually decrease with time as smaller pores are penetrated. The results of the column simulations support this hypothesis. Obtaining a representative value of k_b by batch experiment thus becomes a compromise between measuring data over as long a period as possible, and still maintaining confidence in the accuracy of the results. Although the micropore transfer rate so obtained appears to be too large to predict the precise shape of the breakthrough curve, the predictions of the position of breakthrough are extremely accurate, and the compromise appears to be well justified. There is not enough information presently available regarding activated carbon internal structure or adsorption mechanisms to justify a more complex description of micropore adsorption than the linear driving force assumed in the present model.

The model predictions with $D_s = 5.32 \times 10^{-8}$ cm^2/sec and also 7.75×10^{-8} cm^2/sec were compared to the data for the phenol experiment with C_o = 100 mg/l. The predicted curves were virtually coincident and therefore the slight variation in D_s with batch kinetic experimental conditions (discussed in section 5.3.3) is not of significance in the predictive modelling of adsorption columns.

To further verify that the experimental isotherms were applicable to column operation, the effluent data profiles were integrated to calculate the overall uptake of sorbate by the carbon. The results are shown in Table 6-1 and indicate that the capacities measured in the columns and calculated from the isotherms differ by less than 5%. Some

uptake was still occurring at run termination, especially for the 60 cm depths, so that the measured column capacities should be slightly less than the predicted capacities as was observed. The agreement between the measured and calculated capacities in the columns further verified the experimental isotherms, and demonstrated the ability of the branched pore kinetic model to give a consistent interpretation of isotherm, batch kinetic, and column data.

6.3 Implications of the Slow Adsorption Phenomena

The specific effects of the slow adsorption phenomenon in isotherm and batch kinetic studies have been discussed in previous chapters. This slow phase of adsorption also has some significant effects on breakthrough behaviour of adsorption columns and the interpretation of that breakthrough behaviour.

The characteristic tailing of the breakthrough curves noted in the present study is evident in the results of many columnar adsorption studies but has only been specifically mentioned by Usinowicz (1972). Besides noting that the behaviour was indicative of a slow reaction following a rapid one, Usinowicz did not investigate the effect further. The reason that the tailing of the breakthrough curves has not received more attention is probably two-fold. Firstly, accurate control of feed concentration is normally only available in laboratory scale studies and without an accurate knowledge of the feed concentration, the small amount of removal in the tail of the breakthrough curve may well be within the measurement uncertainty. Laboratory studies, however, are generally conducted over relatively short periods when the amount of tailing

Run No.	Column Capacity* qms. adsorbate		Capacity Based on Isotherm	
	30 cm	60 cm	30 cm	60 cm
I	47.1	87.4	45.4	90.8
II	52.4	103.9	52.4	104.9
III	94.1	172.5	89.2	178.3
IV	91.6	178.6	95.3	190.7

* Saturation not obtained in all runs.

Table 6-1. Comparison of Isotherm and Measured Column Capacities.

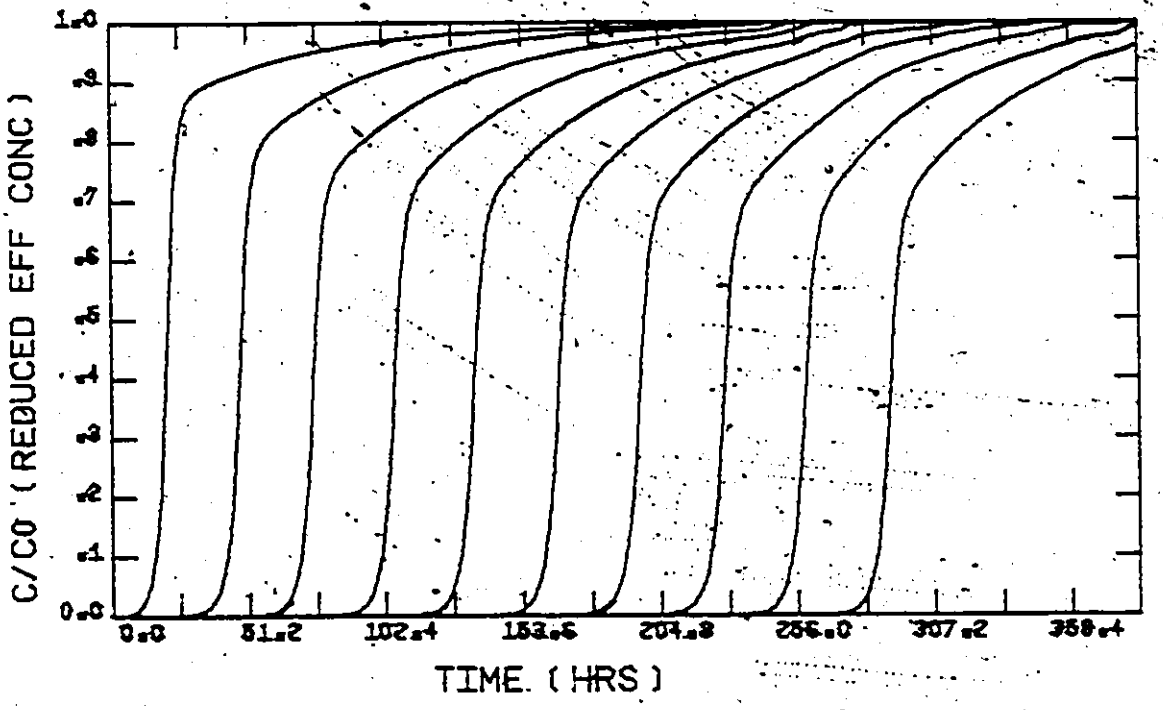

Figure 6-8. Developing Breakthrough Profiles, 20-200 cm depth. (c_o = 100 mg/l Phenol, v_s = 5.8 m/h).

is minimal. Secondly, the aim of most modelling work is to predict the location of breakthrough and consequently, little attention is generally paid to the latter sections of the breakthrough curve.

An example of the significance of the tail on the breakthrough curve is shown in Figure 6-5 where the dashed lines are the model predictions with f equal to unity, i.e. no micropore capacity. The model prediction in this case, when based on a properly evaluated isotherm, indicates that premature breakthrough of the columns is occurring and that the isotherm capacity is not being achieved. In fact the full capacity is obtained, but much of it lies in the long tail which the single parameter kinetic model cannot predict. The only way the single parameter kinetic model can be made to fit the data is to reduce the isotherm capacity by neglecting some or all of the micropore adsorptive capacity (Crittenden, 1976).

An additional consequence of the slow uptake phenomenon is that a constant pattern profile, which would be expected with the strongly favourable isotherms found in this study, takes a very long time to develop. In Figure 6-8 a series of breakthrough curves at 20 cm increments in a 200 cm deep bed are shown. The feed concentration was 100 mg/l phenol and the hydraulic loading was 5.83 m/h. Even at the full bed depth and after nearly two weeks' operation, the constant pattern is not fully developed. Thus in many practical cases, and in virtually all laboratory scale studies, the common simplifying assumption of constant pattern behaviour may not be valid when significant slow adsorption occurs.

CHAPTER 7

SIMPLIFIED DRIVING FORCE MODEL

The model developed in the previous chapters assumes that a surface diffusion mechanism is responsible for macropore transport. This in turn requires the calculation of both macro and micropore concentrations at each grid point in the numerical solution. Consequently, the amount of computation is considerable, especially in the column model where the solution involves the dimensions of radial position, axial position, and time. A typical solution time for the simulations reported in the previous chapter was of the order of 1000 sec on a CDC 6400.

To reduce the amount of computation required, and also to develop a simpler model form into which parallel removal mechanisms such as biological activity might be incorporated, the use of simplified driving force expressions was investigated to approximate the surface diffusion mechanism. The driving force approximations studied were the linear driving force of Glueckauf and Coates (1947),

$$\frac{d\bar{q}}{dt} = k_p a_p (q_s - \bar{q}) \qquad (2.15)$$

and the quadratic driving force (QDF) of Vermeulen (1953),

$$\frac{d\bar{q}}{dt} = k_p a_p \frac{(q_s^2 - \bar{q}^2)}{2\bar{q}} \qquad (2.16)$$

A study of the two alternatives is presented in Appendix F,

the study showed that use of the linear driving force expression can in many cases, including that reported by Famularo et al.(1978), introduce error into the kinetic analysis. On the other hand, the quadratic driving force was shown to be a good approximation to the exact solution and was the form chosen for the simplified model.

7.1 Batch Kinetic Studies

7.1.1 Solution of the Batch Model

The equations of section 5.2 are used to describe uptake in a batch reactor with the exception of the macropore mass balance. Instead of writing the internal mass balances over a differential spherical shell, they are written in terms of average particle concentrations.

Macropore Mass Balance

$$f.\ W.\ \frac{d\bar{q}_m}{dt} = k_m \rho_c \cdot \frac{3W}{R\rho_c} \left(\frac{q_s^2 - \bar{q}_m^2}{2\bar{q}_m} \right) - R_b \qquad (7.1)$$

in which $\bar{q}_m$ = average concentration in the macropores; k_m = mass transfer coefficient in QDF equation, cm/sec; and R_b = rate of transfer from the macropores to the micropores.

Micropore Mass Balance

$$(1-f)W \cdot \frac{d\bar{q}_b}{dt} = k_b W (\bar{q}_m - \bar{q}_b) = R_b \qquad (7.2)$$

in which $\bar{q}_b$ = average concentration in the micro or branch pores; and k_b = branched pore rate coefficient, sec^{-1}.

In addition, the solid and liquid phase solutions are coupled by equating the transport rates at the external surface of the particle to

give:

$$k_f (c - c_s) = k_m \rho_c \left[\frac{q_s^2 - \bar{q}_m^2}{2\bar{q}_m}\right] \tag{7.3}$$

and the liquid phase equation is as before:

$$\frac{dc}{dt} = -\frac{(1-\epsilon)}{\epsilon} \frac{3k_f}{R} (c - c_s) \tag{5.7}$$

By introducing the following variables and constants:

$$\begin{aligned} \theta &= k_m t/R \\ C &= c/c_o \\ Q_m &= \bar{q}_m/q_o \\ Q_b &= \bar{q}_b/q_o \\ Bi_f &= 3k_f/k_m \\ Bi_p &= R\, k_b/k_m \end{aligned} \tag{7.4}$$

the equations to be solved can be written:

$$\frac{dC}{d\theta} = -\frac{(1-\epsilon)}{\epsilon} Bi_f (C - C_s) \tag{7.5}$$

$$\frac{dQ_m}{d\theta} = \frac{3}{f}\left[\frac{Q_s^2 - Q_m^2}{2Q_m}\right] - \frac{Bi_p}{f}(Q_m - Q_b) \tag{7.6}$$

$$\frac{dQ_b}{d\theta} = \frac{Bi_p}{(1-f)} (Q_m - Q_b) \tag{7.7}$$

$$Bi_f (C - C_s) = \frac{3}{F}\left[\frac{Q_s^2 - Q_m^2}{2Q_m}\right] \tag{7.8}$$

The set of ordinary differential equations (7.5) to (7.7) was solved using a 4th order Runge-Kutta routine. No time step promotion was used so significant potential exists for further decreasing the solution time below that reported herein.

At any step, if C, Q_m and Q_b are known, equation (7.8) can be solved in conjunction with the isotherm to determine C_s and Q_s. In the present case Newton's method was used to obtain the roots of the nonlinear equation.

$$B_{if}(C - C_s) - \frac{3}{F}\left[\frac{C_s^{2n} - Q_m^2}{2Q_m}\right] = 0 \qquad (7.9)$$

in which the Freundlich isotherm

$$Q_s = C_s^n \qquad (7.10)$$

has been assumed.

To avoid recalculating C_s and Q_s at each internal step of the Runge-Kutta routine, the values of C_s and Q_s were predicted at the mid-time intervals by linear extrapolation. These predicted values were then assumed to be constant over the time interval. Once the values of C, Q_m and Q_b were calculated at the future time, Q_s and C_s were recalculated using equation (7.9) and new midpoint values were predicted. The use of the QDF model resulted in a 60% reduction in computation time over that required by the surface diffusion model when analysing the same data set at equal time step lengths. The decrease purely reflects the decreased amount of computation as little attempt was made to optimize the solution in either case.

7.1.2 Analysis of Batch Data

In Figures 7-1 and 7-2 the fit of the QDF model to the batch kinetic experiments Nos. IV and V (section 5.3.3) is shown. Comparison of Figures 7-1 and 7-2 with Figures 5-14 and 5-15 indicates that the QDF model gives as good a description of the data as the surface diffusion

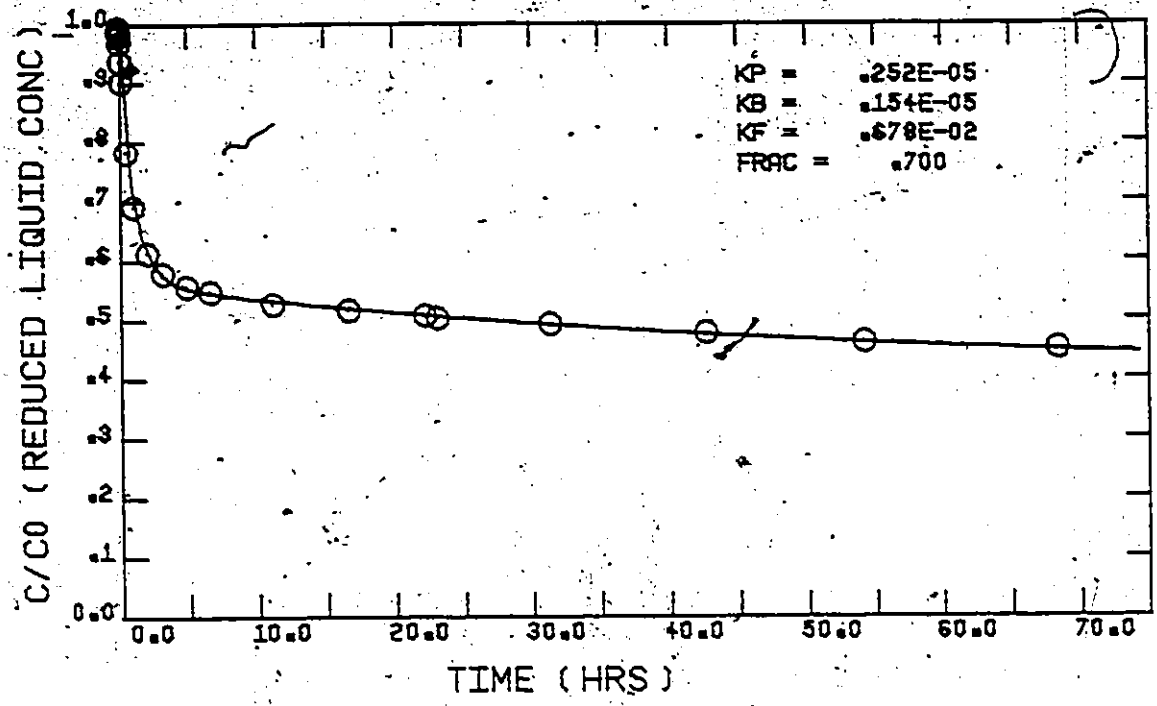

Figure 7-1. QDF Model Regression of Batch Kinetic Experiment IV.

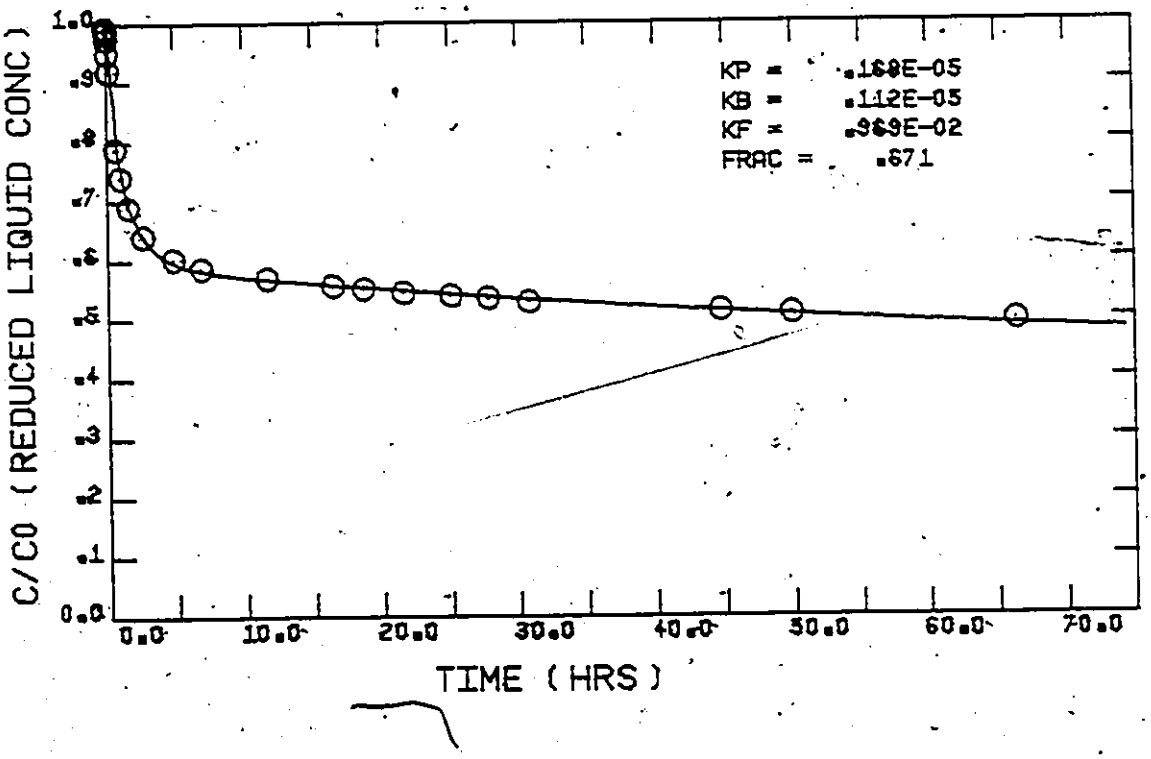

Figure 7-2. QDF Model Regression of Batch Kinetic Experiment V.

model. The QDF fitted parameters are given in Table 7-1 with the corresponding parameters from the surface diffusion model given in brackets. The differences in both k_b and f are slight indicating that the QDF model gives an excellent description of the macropore transport since the other parameters are almost unaffected by the change in the model.

7.2 Column Studies

7.2.1 Solution of the Column Model

The solid phase equations in the column model are identical to those given in section 7.1.1 for the batch kinetic model. The liquid phase mass balance:

$$\frac{\partial c}{\partial t} = - v_s \frac{\partial c}{\partial x} - \frac{(1 - \varepsilon)}{\varepsilon} \frac{3k_f}{R} (c - c_s) \qquad (6.1)$$

is transformed to the Lagrangian coordinate system using:

$$\theta = \frac{k_m}{R} (t - x/v_s) \qquad (7.11)$$

$$z = k_m x/R v_s \qquad (7.12)$$

The resulting equation is as previously:

$$\frac{\partial C}{\partial z} = - \frac{(1 - \varepsilon)}{\varepsilon} Bi_f (C - C_s) \qquad (6.4)$$

The equations (6.4), (7.6), (7.7) and (7.8), which together describe the adsorption bed model, were solved using an implicit finite difference solution, details of which are given in Appendix G.

7.2.2 Prediction of Experimental Column Data

The parameters given in Table 7-1 were used for the column simulation except that, as discussed in detail in section 6.1.3, the parameter 'f' was recalculated for the column experiments in which C_o = 100 mg/l. The values calculated from the isotherms and the data in Table 7-1 were:

Phenol	f_{100}	= 0.742
o-Chlorophenol	f_{100}	= 0.699

The experimental data and QDF model predictions are shown in Figures 7-3 to 7-6, for the experimental column runs detailed in Table 3-2. The ability of the simplified model to predict the observed column behaviour is excellent, and is quite comparable to the predictions obtained when using the full solution to the surface diffusion equation. The substitution of the QDF equation for the exact solution resulted in an 85% decrease in solution time when equal time increments were used.

7.2.3 Sensitivity Analysis of the Column Model.

Since the QDF model was shown to give very similar results to the surface diffusion model, it could be used to test the sensitivity of the branched pore column model to various parameters with considerably less computational requirement than would be required by the surface diffusion model.

The parameters varied were:

(i) k_m (or D_s) - the macropore diffusion coefficient. As shown in Figure 7-7, the breakthrough curve is relatively insensitive to this parameter at values near to or higher than those which are

σ	k_m cm/sec ($\times 10^6$)	k_b sec^{-1} ($\times 10^6$)	k_f cm/sec ($\times 10^3$)	f	f_{100}
Phenol	2.52	1.54 (1.59)	6.78 (6.78)	.700 (.708)	.742
OCP	1.68	1.119 (1.14)	9.69 (9.69)	.671 (.678)	.699

Table 7-1. Batch Kinetic Parameters of Figures 7-1 and 7-2. (Numbers in brackets are for exact solution from Table 5-2).

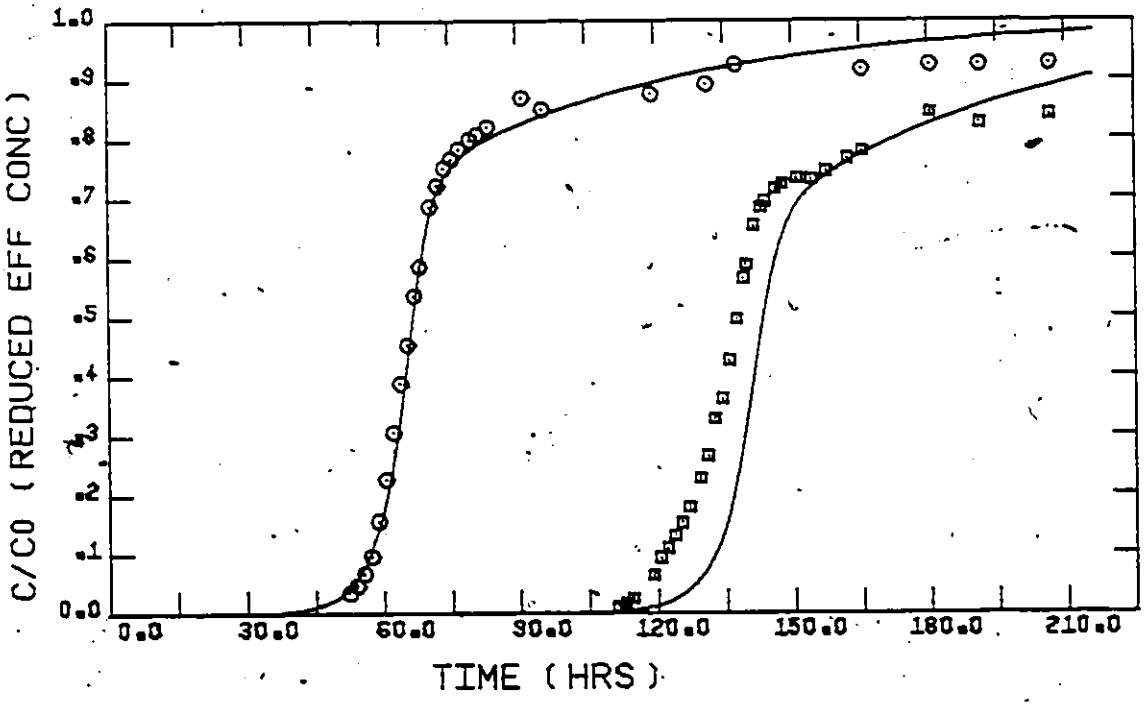

Figure 7-3. Experimental and Predicted Breakthrough Profiles - 50 mg/l Phenol - QDF Model.

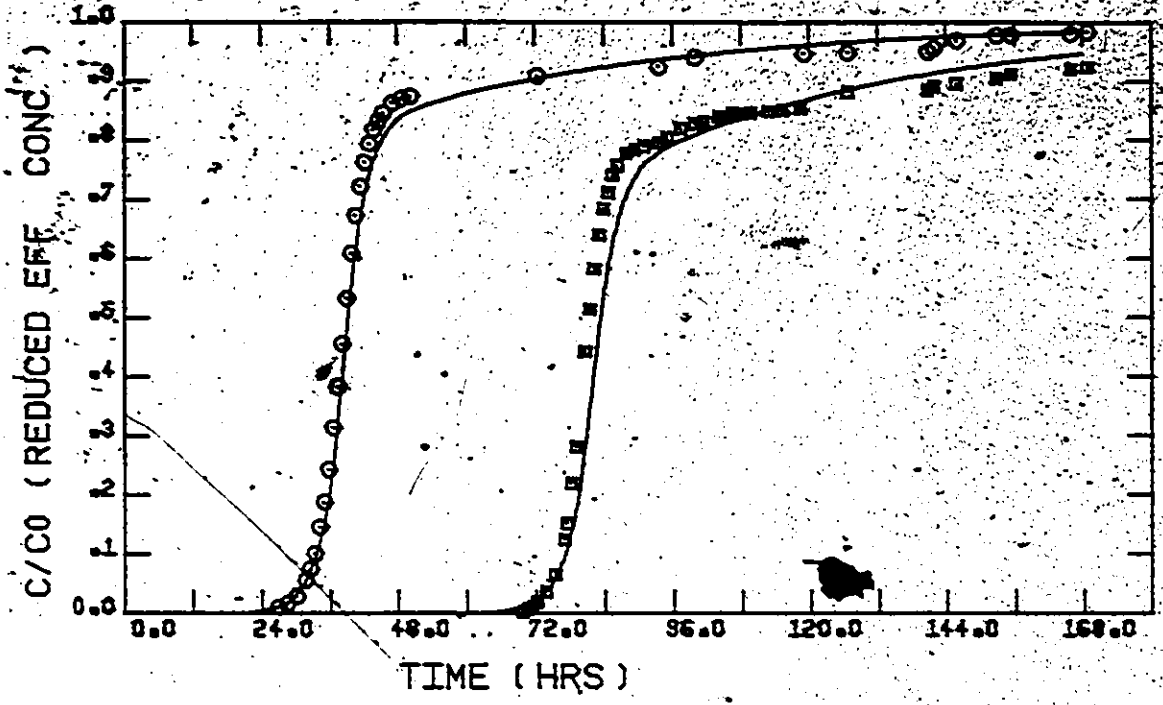

Figure 7-4. Experimental and Predicted Breakthrough Profiles -100 mg/l Phenol - QDF Model.

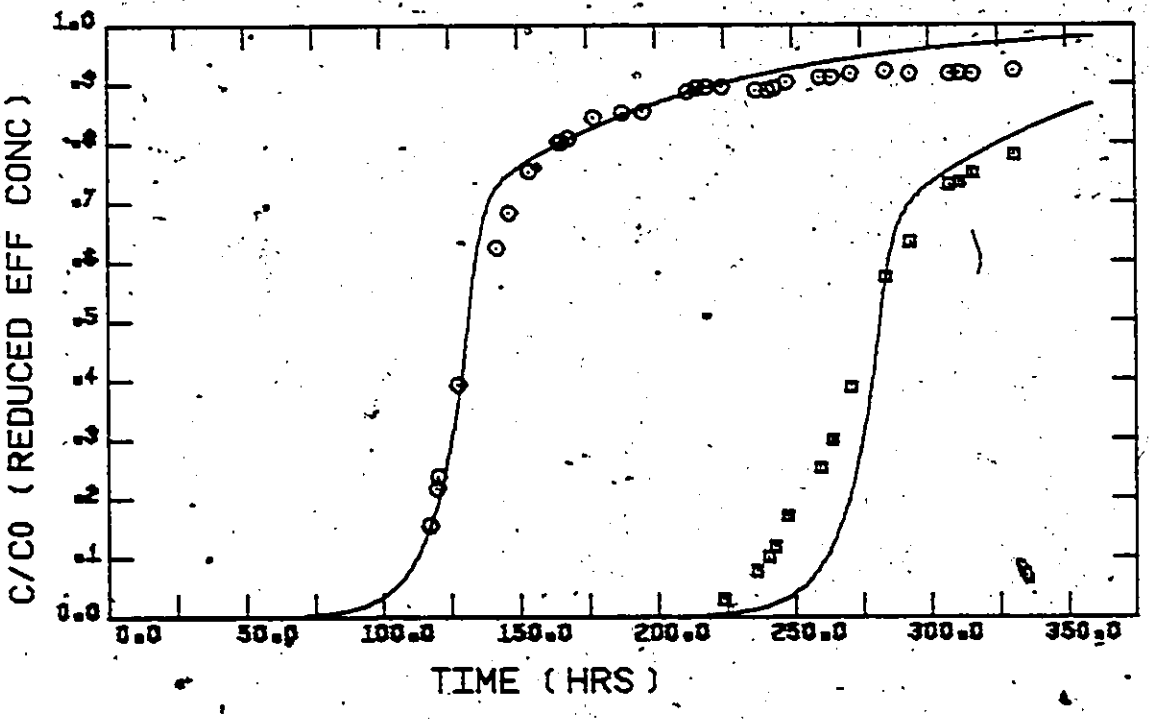

Figure 7-5. Experimental and Predicted Breakthrough Profiles - 50 mg/l o-Chlorophenol - QDF Model.

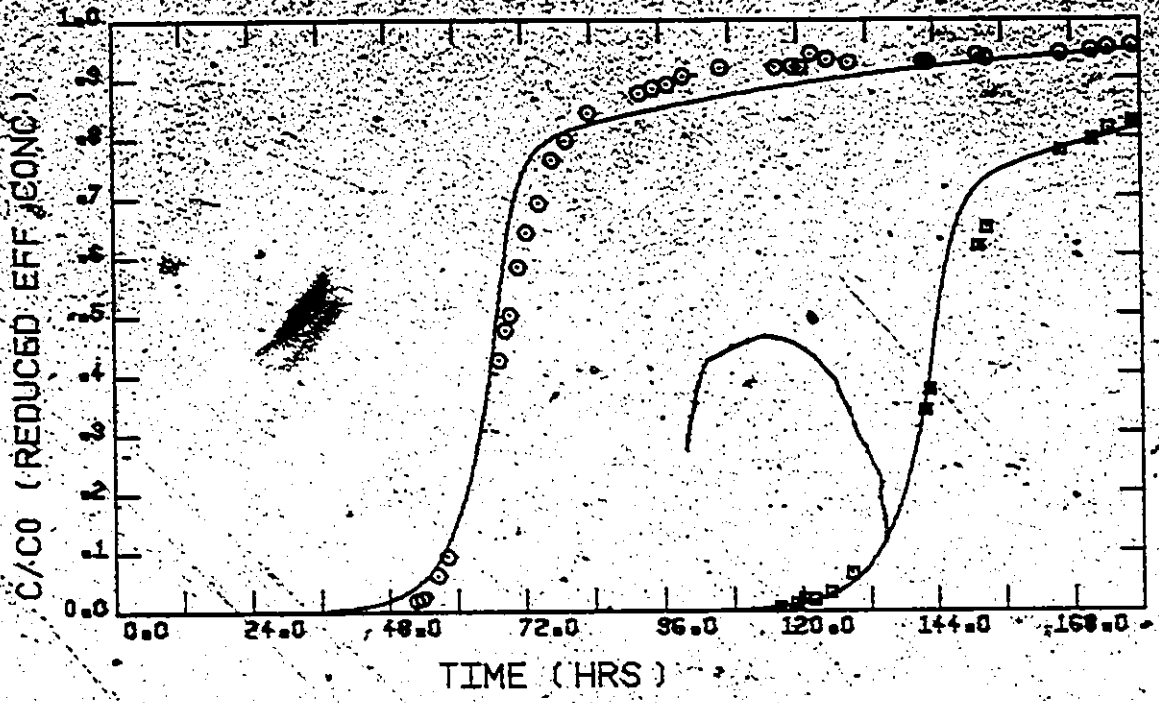

Figure 7-6. Experimental and Predicted Breakthrough Profiles -100 mg/l o-Chlorophenol -.QDF Model.

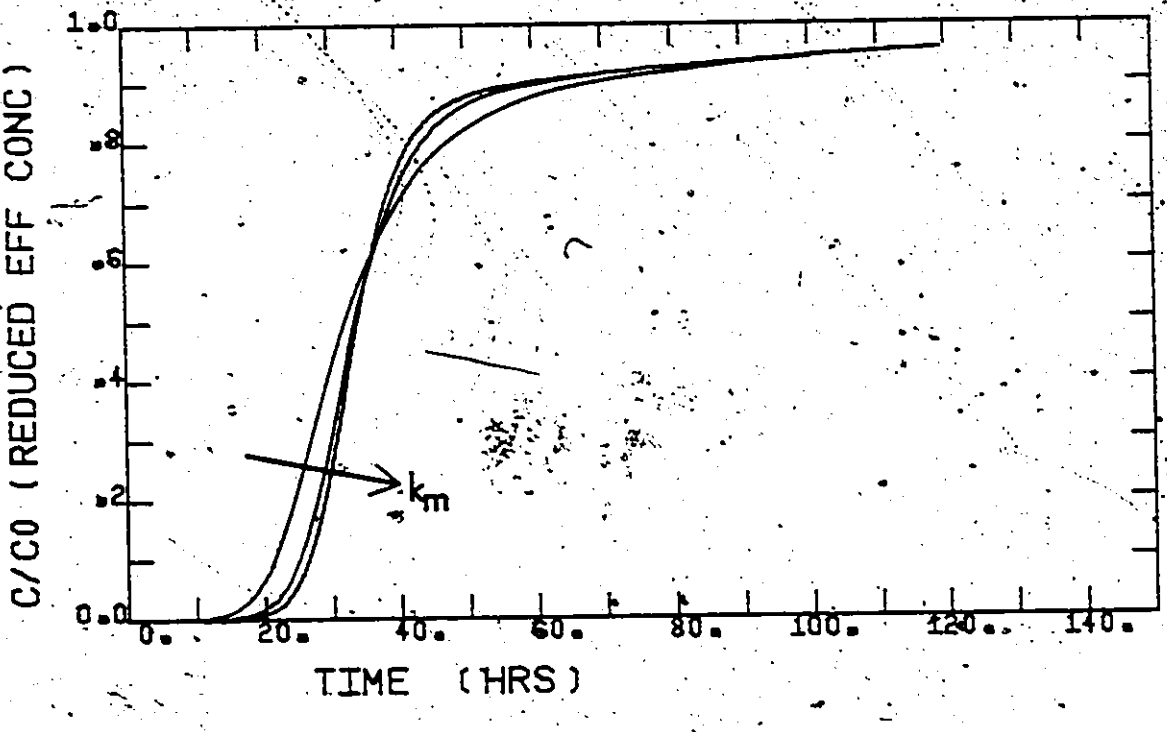

Figure 7-7. Column Model Sensitivity Analysis - k_m Parameter. (k_m = 0.8,2.0,4.0 × 10^{-6}cm/sec; k_b = 1.0 × 10^{-6}sec^{-1}; k_f = 3.0 × 10^{-3} cm/sec; f = 0.75;, n = 0.5).

typical of phenolic adsorption (2.0×10^{-6} cm/sec). At lower values of k_m (0.8×10^{-6} cm/sec) the macropore diffusional resistance becomes more significant relative to external film resistance, and the breakthrough curve becomes more sensitive to this parameter.

(ii) k_b - the micropore rate transfer coefficient. Figure 7-8 shows that changes in this parameter do not affect the position of breakthrough but as k_b increases, the rate of breakthrough decreases. An increase in k_b also results in a more rapid approach to saturation as the micropore capacity fills more quickly.

(iii) k_f - the external film transfer coefficient. A decrease in this parameter, as shown in Figure 7-9, results in earlier breakthrough and a less sharp breakthrough curve. The entire curve except for the micropore adsorption region in the tail of the breakthrough curve is sensitive to k_f. This fact, combined with the relative insensitivity of the breakthrough curve to the macropore diffusion coefficient, indicates that external film resistance is the primary rate controlling mechanism in adsorption columns operated under the conditions of this study which are typical of many adsorption systems. The importance of being able to accurately predict the external film transfer coefficient is emphasized by the sensitivity of the breakthrough curve to this parameter.

(iv) f - the fraction determining the relative proportions of macro and micropores. The results in Figure 7-10 show the typical S shaped breakthrough curve which results for f = 1 (the standard

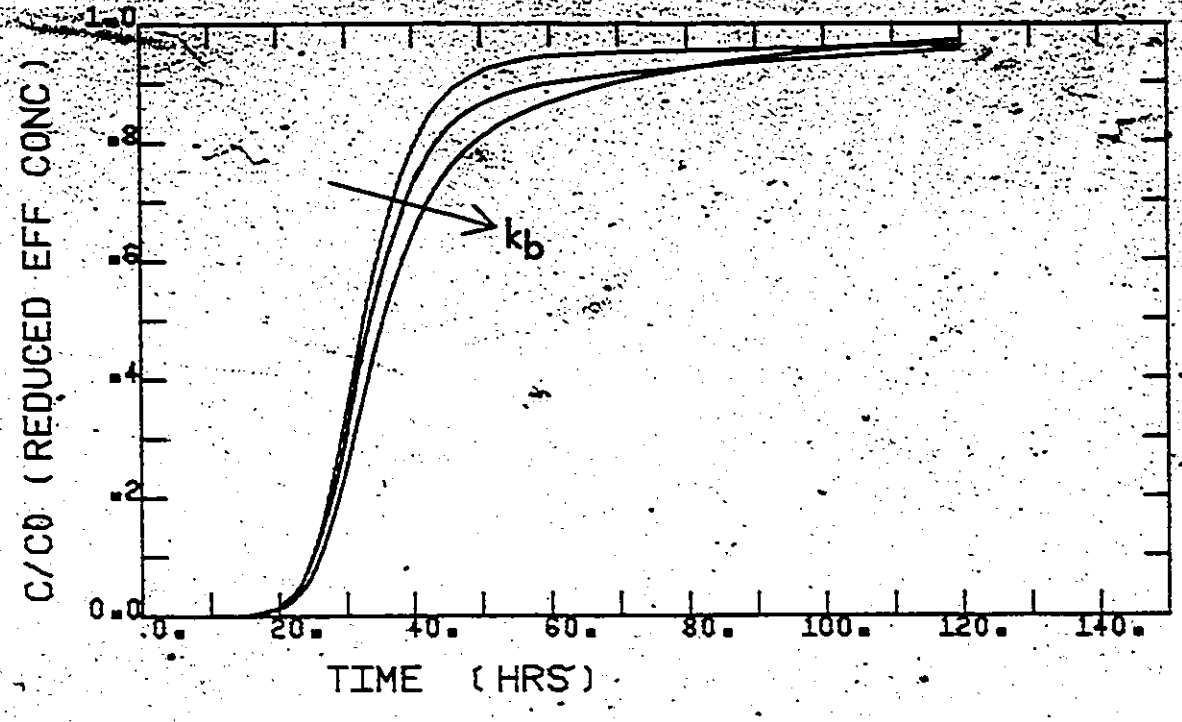

Figure 7-8. Column Model Sensitivity Analysis - k_b Parameter. (k_b = 0.4,1.0,2.0×10^{-6} sec^{-1})

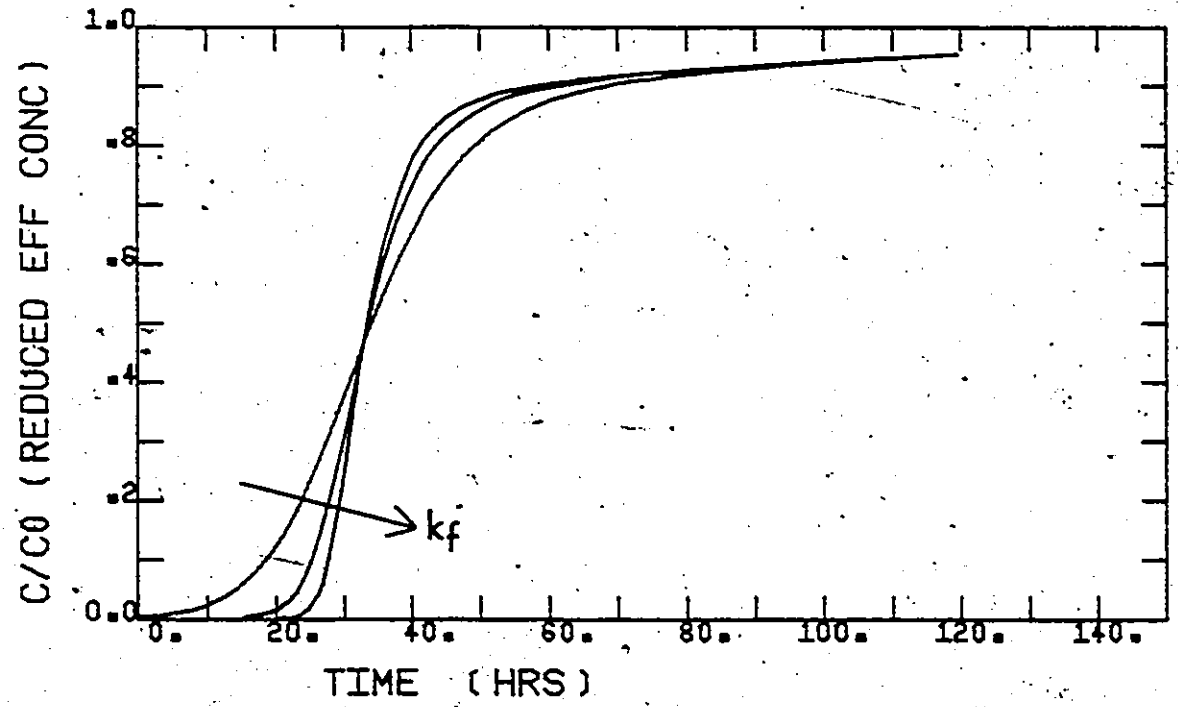

Figure 7-9. Column Model Sensitivity Analysis - k_f Parameter. (k_f = 1.0,3.0,9.0×10^{-3} cm/sec).

surface diffusion model). As 'f' decreases and micropore capacity becomes more important, earlier and earlier breakthrough is observed, and the tail on the breakthrough curve becomes more pronounced.

(v) n - the Freundlich exponent or measure of nonlinearity of the isotherm. Figure 7-11 shows that as the isotherm becomes increasingly nonlinear, the breakthrough curve becomes increasingly sharp. The relative inefficiency in adsorbing compounds which exhibit linear or near linear isotherms is seen by the increasingly earlier breakthrough as 'n' approaches unity. In the slow adsorption region of the breakthrough curve, the isotherm shape has relatively little effect on the column performance.

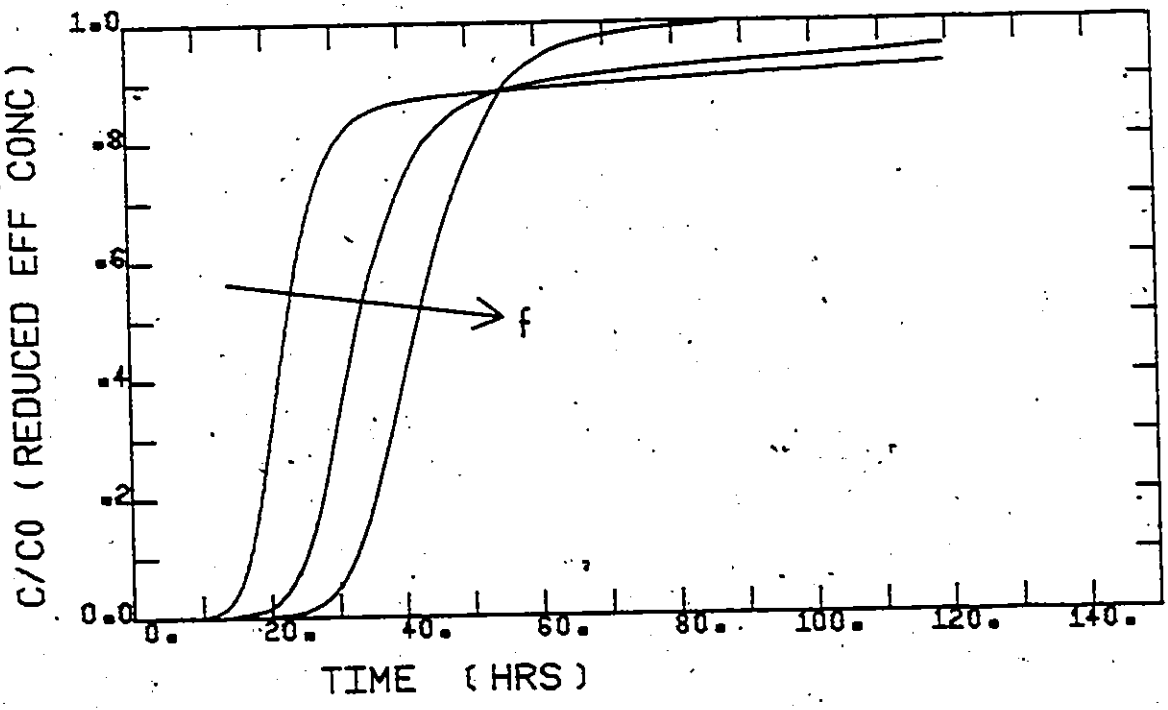

Figure 7-10. Column Model Sensitivity Analysis - f Parameter. (f = 0.5, 0.75, 1.0)

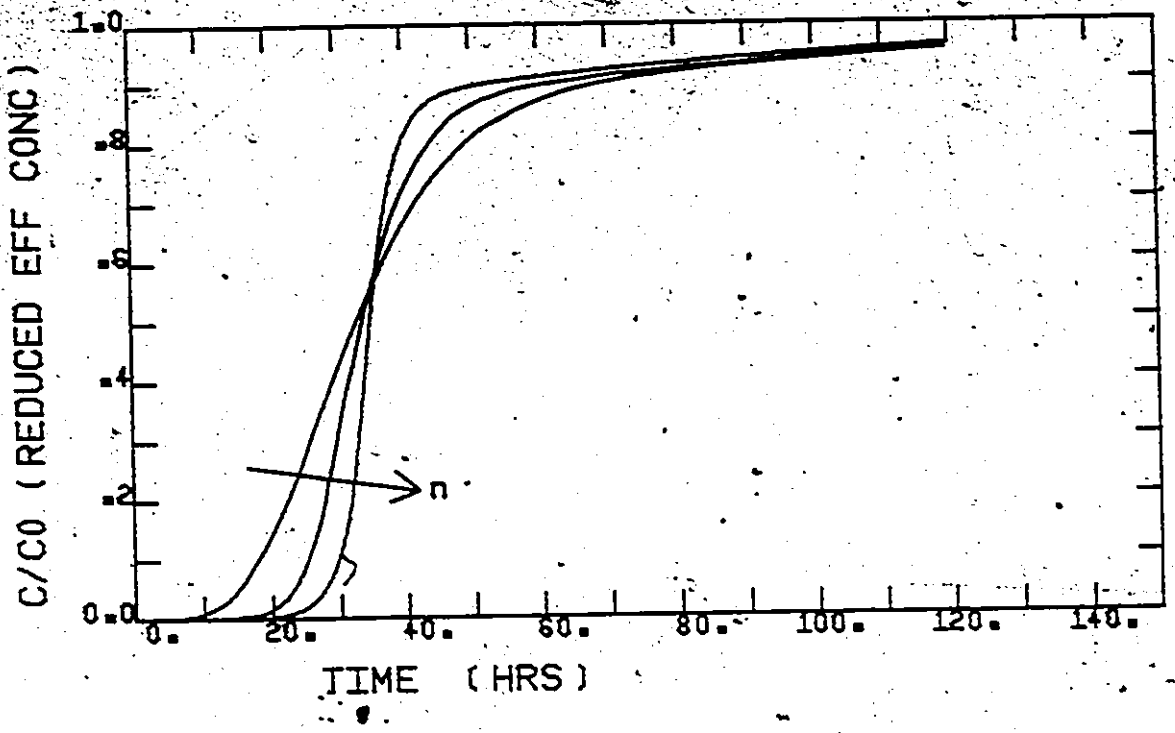

Figure 7-11. Column Model Sensitivity Analysis - Isotherm Exponent. (n = 0.2, 0.5, 0.8)

7.3 Summary

The use of the QDF approximation instead of the exact solution to the diffusion equation allows for a significant reduction in computational requirements. In addition, it does not in any way detract from the ability of the branched pore model to describe kinetic data and consequently there is little justification for using the more complex surface diffusion model when dealing with single solutes. Because of the local interactions between adsorbing species in multisolute adsorption, it cannot be concluded based on the present work that the QDF model can be used with more than one solute, however, the work of Famularo et al. (1978) suggests that this approach may be valid for the multisolute

case also.

The results of the sensitivity analysis indicate that the final shape of the breakthrough curve is determined by all five parameters investigated but is most strongly determined by the relative proportions of the macropore and micropore capacities.

CHAPTER 8

CONCLUSIONS AND RECOMMENDATIONS FOR FUTURE RESEARCH

8.1 Conclusions

1. Existing adsorption kinetic models, which assume that the interior of the carbon particle is homogeneous, are not capable of describing some aspects of adsorption behaviour that were observed experimentally, and have also been reported previously in the literature.

2. A proposed branched pore kinetic model which assumes that the carbon particle consists of two regions having different diffusion rates was shown to describe batch kinetic data well.

3. Analysis of the model parameters indicated that the magnitude of the diffusion coefficient in the rapidly diffusing or 'macropore' region was comparable to those reported in studies which had assumed a single intraparticle rate parameter model. About 70% of the total isotherm capacity occurred in the macropore region.

4. The remaining 30% of the total capacity was adsorbed at much lower rates and neglect of this capacity explained some previously inconsistent results reported in the literature. The capacity measured in the slowly diffusing region was virtually constant over the range of liquid phase equilibrium concentrations investigated. This capacity was associated with the 'micropore' region in which restricted diffusion and very strong or irreversible adsorption

can be anticipated.

5. Parameters measured in the batch kinetic experiments were able to predict the performance of experimental adsorption columns when used in a kinetic model of an adsorption bed. The proposed model was therefore verified on an independent data set.

6. The use of the quadratic driving force expression to replace the surface diffusion mechanism assumed in the original model gave equally good interpretation of batch kinetic experiments and prediction of experimental column performance. Computational requirements of the model solution were considerably reduced by the substitution of the driving force approximation.

7. An evaluation of the linear driving force expression showed that its use resulted in errors in the kinetic analysis, and that it was a poor approximation to the exact solution of the surface diffusion model.

8.2 Recommendations for Future Research

1. Extend the applicability of the proposed model to concentration ranges beyond those studied in the present work.

2. Investigate the slow adsorption phenomenon in activated carbons having varying pore sizes, and with adsorbates of different sizes. Such studies would give additional information on the mechanisms responsible for the slow diffusion and might eventually enable the model parameters to be correlated with physical properties of the system.

3. Conduct further experiments with regenerated rather than virgin

carbon to verify that the same effects occur. There is evidence to suggest that some micropore volume may be lost on regeneration and thus the importance of the slow adsorption phenomenon might be reduced.

4. Test the proposed kinetic model in a multicomponent system to determine the effect of micropore adsorption on the observed breakthrough behaviour.

BIBLIOGRAPHY

Anderson, J.L. and Quinn, J.A. "Restricted Transport in Small Pores: A Model for Steric Exclusion and Hindered Particle Motion," Biophys. Jl., 14 (2), 130-150 (1974).

Antonson, C.R. and Dranoff, J.S. "Nonlinear Equilibrium and Particle Shape Effects in Intraparticle Diffusion Controlled Adsorption", Chem. Eng. Prog. Symp. Series, 65, (No.96), 20 (1969a).

Antonson, C.R. and Dranoff, J.S. "Adsorption of Ethane on Type 4A and 5A Molecular Sieve Particles," Chem. Eng. Prog. Symp. Series, 65 (No.96), 27 (1969b).

Babcock, R.E., Green, D.W. and Perry, R.H. "Longitudinal Dispersion Mechanisms in Packed Beds," AIChE Jl,12, 922 (1966).

Beck, R.E. and Schultz, J.S. "Hindered Diffusion in Microporous Membranes with Known Pore Structure," Science, 170, 1302 (1970).

Brauch, V. and Schlünder, E.U. "The Scale-Up of Activated Carbon Columns for Water Purification Based on Results from Batch Tests - II," Chem. Eng. Sci., 30, 539-548 (1975).

Brecher, L.E., Kostecki, J.A. and Camp, D.T. "Combined Diffusion in Batch Adsorption Systems Displaying BET Isotherms, Part I," Chem. Eng. Prog. Symp. Series, 63 (74), 18 (1967).

Burttschell, R.H., Rosen, A.A., Middleton, F.M. and Ettinger, M.B. "Chlorine Derivatives of Phenol Causing Taste and Odour," Jl. Amer. Water Works Assoc., 51, 205(1959).

Calgon Corp., "Basic Concepts on Adsorption of Activated Carbon," Filtrasorb Department Report (undated).

Carberry, J.J., "Designing Laboratory Catalytic Reactors," Ind. & Eng. Chem., 56 (1), 39 (1964).

Chakravorti, R.K., Liquid Phase Adsorption in Batch and Fixed Bed Systems, Ph.D. Thesis, State University of N.Y. at Buffalo (1973).

Chemviron Product Bulletin, "Carbon Granule Type SGL," 1970/PP/SGL/12 700/F/1/IMP, (1970).

Chen, W., "The Effect of Surface Curvature on the Adsorption Capability of Porous Adsorbents," Ph.D. Thesis, University of South Carolina (1970).

Cooper, R.S., "Slow Particle Diffusion in Ion Exchange Problems," Ind. & Eng. Chem. Fund., 4, 308 (1965).

Crank, J., Mathematics of Diffusion, Oxford Univ.Press, London (1956).

CRC, Handbook of Chemistry and Physics, The Chemical Rubber Co., Cleveland, 47th Edition (1966).

Crittenden, J.C., Mathematical Modelling of Fixed Bed Adsorber Dynamics, Single Component and Multicomponent, Ph.D. Thesis, University of Michigan (1976).

Crittenden, J.C. and Weber, W.J., "Predictive Model for Design of Fixed Bed Adsorption: Parameter Estimation and Model Development," ASCE Jl. Envirn. Eng. Div., 104 (EE2) 185, (1978a).

Crittenden, J.C. and Weber, W.J. "Predictive Model for Design of Fixed Bed Adsorbers: Single Component Model Verification," ASCE Jl. Envrn. Eng. Div., 104, (EE3), 433 (1978b).

Dedrick, R.L. and Beckmann, R.B. "Kinetics of Adsorption by Activated Carbon from Dilute Aqueous Solution," Chem. Eng. Prog. Symp. Series, 63 (No.74), 68 (1967).

DiGiano, F.A. and Weber, W.J. "Sorption Kinetics in Infinite Bath Experiments," Jl. Water Poll. Contr. Fed., 45 (4), 713 (1973).

Dubinin, M.M. "Porous Structure and Adsorption Properties of Active Carbons," in Chemistry and Physics of Carbon, Vol.2, (Edited by P.L. Walker), Marcel-Dekker Inc., N.Y. (1966).

Dullien, F.A. and Batra, V.K. "Determination of the Structure of Porous Media," Ind. & Eng. Chem., 62 (10), 25 (1970).

Famularo, J., Pannu, A.S. and Mueller, J.A. "Prediction of Carbon Column Performance from Pure-Solute Data," Pres. 51st Annual Conf. of Water Poll. Contr. Fed., Anaheim, California (1978).

Fan, L.T. and Ahn, Y.K. "Critical Evaluation of Boundary Conditions for Tubular Flow Reactors," Ind. & Eng. Chem. Proc. Des. Devel., 1 (3), 190 (1962).

Fleck, R.D., Mixed Resistance Diffusion in Fixed Bed Adsorption Under Constant Pattern Conditions, M.Sci. Thesis, Univ. of Virginia (1970).

Fleck, R.D., Kirwan, D.J. and Hall, K.R. "Mixed-Resistance Diffusion Kinetics in Fixed-Bed Adsorption under Constant Pattern Conditions," Ind. & Eng. Chem. Fund., 12 (1) 95 (1973).

Friedman, F. and Ramirez, W.F., "A Single Phase Model of Mechanisms Effecting Miscible Surfactant Oil Recovery," Chem.Eng. Sci., 32, 687 (1977).

Fritz, W., Merk, W., Schlünder, E.U. and Sontheimer, H. "Competitive Adsorption of Dissolved Organics on Activated Carbon," Pres. Div. Environ. Chem., Amer. Chem. Soc., Miami, Florida (1978).

Furusawa, T. and Smith, J.M. "Diffusivities from Dynamic Data," AIChE Jl., 19 (2), 401 (1973).

Garg, D.R. and Ruthven, D.M. "Theoretical Prediction of Breakthrough Curves for Molecular Sieve Adsorption Columns-II - General Isothermal Solution for Micropore Diffusion Control," Chem. Eng. Sci., 28, 799 (1973).

Garg, D.R. and Ruthven, D.M. "Linear Driving Force Approximations for Diffusion Controlled Adsorption in Molecular Sieve Columns," AIChE Jl., 21(1), 200 (1975).

Garten, V.A. and Weiss, D.E. "The Ion and Exchange Properties of Activated Carbon in Relation to Its Behaviour as a Catalyst and Adsorbent," Reviews of Pure & Applied Chemistry, 7(3), 69 (1957).

Gilliland, E.R., Baddour, R.F., Perkinson, G.P. and Sladek, K. "Diffusion on Surfaces; Part I Effect of Concentration on the Diffusivity of Physically Adsorbed Gases," Ind. & Eng. Chem. Fund., 13 (2), 95 (1974).

Glueckauf, E. "Theory of Chromatography - Part 10 - Formulae for Diffusion into Spheres and Their Application to Chromatography," Trans. Faraday Soc., 51, 1540 (1955).

Glueckauf, E. and Coates, J. "Theory of Chromatography: Part IV, The Influence of Incomplete Equilibrium," Jl.Chem. Soc., 1315 (1947).

Goodknight, R.C., Klikoff, W.A. and Fatt, I. "Non Steady State Fluid Flow and Diffusion in Porous Media containing Dead End Pore Volume," Jl. Phys. Chem., 64, 1162 (1960).

Haynes, H.W., "The Determination of Effective Diffusivity by Gas Chromatography Time Domain Solutions," Chem. Eng. Sci., 30, 955 (1975).

Heister, N.K. and Vermeulen, T. "Saturation Performance of Ion Exchange and Adsorption Columns," Chem. Eng. Prog., 48, 505 (1952).

Huang, J. and Garrett, J.T. "Effects of Polyelectrolytes and Clay Colloids on Carbon Adsorption," Water & Sewage Works, 124 (3), 64 (1977).

Keinath, T.M. and Weber, W.J. "A Predictive Model for the Design of Fluid-Bed Adsorbers," Jl. Water Poll. Contr. Fed., 40,(5 Pt.I), 741 (1968).

Keast, P. and Mitchell, A.R. "On the Instability of the Crank-Nicholson Formula Under Derivative Boundary Conditions," Computer Jl., 9, 110 (1966).

Kipling, J.J. "The Properties and Nature of Adsorbent Carbons," Quarterly Reviews, 10, 1-26 (1956).

Komiyama, H. and Smith, J.M. "Intraparticle Mass Transport in Liquid Filled Pores," AIChE Jl., 20 (4), 728 (1974a).

Komiyama, H. and Smith, J.M. "Surface Diffusion in Liquid Filled Pores," AIChE Jl., 20 (6), 1110 (1974b).

Layton, L. and Younquist, G.R. "Sorption of Sulphur Dioxide by Ion Exchange Resins," Ind. & Eng. Chem. Proc. Des. Devel., 8 (3), 317 (1969).

Letterman, R.D., Quon, J.E. and Gemmel, R.S. "Film Transport Coefficients in Agitated Suspensions of Activated Carbon," Jl. Water Poll. Contr. Fed., 40, 2537 (1974).

Levich, V.G., Physiochemical Hydrodynamics, Prentice Hall (1962).

Liapis, A.I. and Rippin, D.W.T. "A General Model for the Simulation of Multi-Component Adsorption from a Finite Bath," Chem. Eng. Sci., 32, 619-627 (1977).

Liapis, A.I. and Rippin, D.W.T. "The Simulation of Binary Adsorption in Activated Carbon Columns Using Estimates of Diffusion Resistance Within the Carbon Particles Derived from Batch Experiments," Chem. Eng. Sci., 33, 593-600 (1978).

McGreavy, C., Nussey, C. and Cresswell, D.L. "Investigation of Numerical Methods for the Simulation of Fixed Bed Processes," I. Chem. E. Symp. Series, No.23, 111 (1967).

Malone, D.M. and Anderson, J.L. "Hindered Diffusion of Particles Through Small Pores," Chem. Eng. Sci., 33 (11), 1429 (1978).

Mandelbaum, J.A. and Böhm, U. "Mass Transfer in Packed Beds at Low Reynolds Numbers," Chem. Eng. Sci., 28. 569 (1973).

Mathews, A.P. Mathematical Modelling of Multicomponent Adsorption, Ph.D. Thesis, University of Michigan (1975).

Mathews, A.P. and Weber, W.J. "Effects of External Mass Transfer and Intraparticle Diffusion on Adsorption Rates in Slurry Reactors," AIChE Symp. Series, 73 (166), 91 (1977).

Mattson, J.S., Mark, H.B., Malbin, M.D., Weber, W.J. and Crittenden, J.C. "Surface Chemistry of Active Carbon: Specific Adsorption of

Phenols," Jl. Colloid & Interface Sci., 31(1), 116 (1969).

Miyauchi, T. and Kikuchi, T. "Axial Dispersion in Packed Beds", Chem. Eng. Sci., 30, 343 (1975).

Modell, M., De Fillippi, R.P. and Krukonis, V. "Regeneration of Activated Carbon with Supercritical CO_2," Pres. Div. Environ. Chem., Amer. Chem. Soc., Miami, Florida (1978).

Myers, A.L. and Zolandz, R.R. "Effect of pH upon Multicomponent Adsorption from Dilute Aqueous Solution," Pres. Div. Environ. Chem., Amer. Chem. Soc., Miami, Florida (1978).

Neretnieks, I. " Adsorption in Finite Bath and Countercurrent Flow with Systems Having a Nonlinear Isotherm," Chem. Eng. Sci., 31, 107-114 (1976a).

Neretnieks, I. "Adsorption in Finite Bath and Countercurrent Flow with Systems Having Concentration Dependent Coefficient of Diffusion," Chem. Eng. Sci., 31, 465-471 (1976b).

Neretnieks, I. "Analysis of Some Adsorption Experiments with Activated Carbon," Chem. Eng. Sci., 31,1029 (1976c).

Othmer , D.S. and Thakar, M.S. "Correlating Diffusion Coefficients in Liquids," Ind. & Eng. Chem., 45 (3), 589 (1953).

Parker, I.B. and Crank, J. "Persistent Discretization Errors in Partial Differential Equations of Parabolic Type," Computer Jl., 7, 163 (1964).

Paterson, S. "The Heating and Cooling of a Solid Sphere in a Well-Stirred Fluid," Proc. Phys. Soc.(London), 59, 50 (1947).

Rankin, P. An Appraisal of the Lignin/Activated Carbon Adsorption System, M. Eng. Thesis, McMaster University, Hamilton (1975).

Ruckenstein, E. Vaidyanathan, A.S. and Youngquist, G.R. "Sorption by Solids with Bidisperse Pore Structures," Chem. Eng. Sci., 26, 1305 (1971).

Satterfield, C.N. Mass Transfer in Heterogeneous Catalysis, M.I.T. Press, Cambridge, Mass. (1970).

Satterfield, C.N., Colton, C.K. and Pitcher, W.H. "Restricted Diffusion in Liquids Within Fine Pores," AIChE Jl.,19 (3), 628-(1973).

Schwartz, C.E. and Smith, J.M. "Flow Distribution in Packed Bed," Ind. & Eng. Chem., 45, 1209 (1953).

Shah, D.B. and Ruthven, D.M. "Measurement of Zeolitic Diffusivities and Equilibrium Isotherms by Chromatography," AIChE Jl., 23 (6), 804 (1977).

Singer, P.C. and Yen, C. "Adsorption of Alkyl Phenols by Activated Carbon," Pres. Div. Environ. Chem., Amer. Chem. Soc., Miami, Florida (1978).

Sladek, K.J., Gilliland, E.R. and Baddour, R.F. "Diffusion on Surfaces. II. Correlation of Diffusivities of Physically and Chemically Adsorbed Species," Ind. & Eng. Chem. Fund. 13, 100 (1974).

Snoeyink, V.L. Adsorption of Strong Acids, Phenol and 4-Nitrophenol From Aqueous Solution by Active Carbon in Agitated Non-Flow Systems, Ph.D. Thesis, University of Michigan (1968).

Snoeyink, V.L., McCreary, J.J. and Murin, C.J. "Activated Carbon Adsorption of Trace Organics," Environ. Prot. Technol. Series, EPA 600/2-77-223 (1977).

Snoeyink, V.L. and Weber, W.J. "The Surface Chemistry of Active Carbon: Discussion of Structure and Surface Functional Groups," Environ. Sci. & Technol., 1(5), 228 (1967).

Snoeyink, V.L., Weber, W.J. and Mark, H.B. "Sorption of Phenol and Nitrophenol by Activated Carbon," Environ. Sci. & Technol., 3, 918 (1969).

Sudo, Y., Misic, D.M. and Suzuki, M. "Concentration Dependence of Effective Surface Diffusion Coefficients in Aqueous Phase Adsorption on Activated Carbon," Chem. Eng. Sci., 33 (9-I), 1287-90 (1978).

Svedberg, G., Simulation of Sorption Processes, Ph.D. Thesis, Royal Institute of Technology, Stockholm (1975).

Thibault, J. and Hoffman, T.W. "Specification of the Correct Boundary Conditions," Int. Jl. Heat Mass Transfer, 21, 368 (1978).

Thomas, H.C. Solid Diffusion in Chromatography," Ann. N.Y. Acad. Sci., 49, 161 (1948).

Tien, C. and Thodos, G. "Ion Exchange Kinetics for Systems of Non-linear Equilibrium Relationships," AIChE Jl., 5, 373 (1959).

USEPA, "Process Design Manual for Carbon Adsorption," Technology Transfer Series, EPA 625/1-71-002a (1973).

Usinowicz, P. Mathematical Simulation and Prediction of Adsorber Performance for Complex Waste Mixtures, Ph.D. Thesis, University of

Michigan (1972).

Vermeulen, T. "Theory for Irreversible and Constant-Pattern Solid Diffusion," Ind. & Eng. Chem., 45, 1664 (1953).

Vermeulen, T. "Separation by Adsorption Methods," in Advances in Chem. Eng., Academy Press, N.Y., 2, 147 (1958).

Vermeulen, T., and Huffman, E.H. "Ion Exchange Column Performance," Ind. & Eng. Chem., 45, 1658 (1953).

Vermeulen, T., Klein, G. and Heister, N.K., "Adsorption and Ion Exchange" in Chemical Engineers Handbook, 5th Ed., (Editors Perry, R.H. and Chilton, C.H.), McGraw-Hill (1973).

Weber, T.W. and Chakravorti, R.K. "Pore and Solid Diffusion Models for Fixed Bed Adsorbers," AIChE Jl., 20 (2) 228 (1974).

Weber, W.J. and Crittenden, J.C. "MADAM I-A Numeric Method for Design of Adsorption Systems," Jl. Water Poll. Contr. Fed., 47 (5), 924 (1975).

Weber, W.J. and Morris, J.C. "Kinetics of Adsorption on Carbon from Solution," ASCE , Jl.San. Eng. Div., SA2, 31 (1963).

Weber, W.J. and Van Vliet, M.B. "Fundamental Concepts for Application of Activated Carbon in Water and Wastewater Treatment," Pres. Div. Environ. Chem., Amer. Chem. Soc., Miami, Florida (1978).

Wedin, J., Adsorption of Phenol on Activated Carbon in a Batch Reactor With a Basket Impeller, Masters Thesis, Royal Institute of Technology, Stockholm (1976).

Wehner, J.F. and Wilhelm, R.H. "Boundary Conditions of Flow Reactor," Chem. Eng. Sci., 6, 89 (1956).

Westermark, M. "Kinetics of Activated Carbon Adsorption," Jl. Water Poll. Contr. Fed., 47 (4), 704 (1975).

Wheeler, A. "Reaction Rates and Selectivity in Catalyst Pores," in Advances in Catalysis, vol.III, Academic Press (1951).

Williamson, J.E., Bazaire, K.E. and Geankoplis, C.J. "Liquid-Phase Mass Transfer at Low Reynolds Number," Ind. & Eng. Chem. Fund., 2, 126 (1963).

Wilson, E.J. and Geankoplis, C.J. "Liquid Mass Transfer at Very Low Reynolds Numbers in Packed Beds," Ind. & Eng. Chem. Fund., 5 (1) 9, (1966).

Ying, W. Investigation and Modeling of Bio-Physicochemical Processes in Activated Carbon Columns, Ph.D. Thesis, University of Michigan (1978).

Ziegler, E.N. "Note on Experiences in Simulating Axially Dispersed Tubular Reactors and Their Boundary Conditions," Chem. Eng. Comm., 2, 49 (1975).

Zogorski, J.S., Faust, S.D. and Haas, J.H. "The Kinetics of Adsorption of Phenols by Granular Activated Carbon," Jl. Colloid Interface Sci., 55 (2), 329 (1976).

APPENDIX A

Calculation of Apparent Particle Density

From the log-normal plot of the particle size distribution shown in Figure 3-1 in the text, the following properties can be determined.

Effective size (10th percentile)	0.066 cm
Uniformity coefficient (60th/10th percentile)	1.52
Geometric mean particle diameter (50th percentile)	0.094 cm
Number average particle diameter ($\sum n_i d_i / \sum n_i$)	0.0955 cm

The apparent density was determined by counting the total number of particles used in the size analysis. Since the total weight of the sample was known, the density was calculated according to

$$\rho_c = \frac{\text{number of particles}}{(\text{mass carbon}) \times (\frac{4}{3}\pi \frac{d_p^3}{8})}$$

$$= \frac{2429}{.7929 \times \frac{4}{3}\pi \frac{(.094)^3}{8}}$$

$$= 0.75 \text{ g/cm}^3.$$

Previously reported values are:

Crittenden (1976)	F400	0.74 g/cm^3
Chemviron (1970)	F300	0.75 g/cm^3

and consequently $\rho_c = 0.75$ g/cm^2 was assumed in the present study.

APPENDIX B

Calculation of the Liquid Concentration

During the development of the solution technique three alternatives for calculating the liquid phase concentration were investigated. These were:

$$V \frac{dc}{dt} = - W \frac{d\bar{q}}{dt} \qquad (B.1)$$

$$V \frac{dc}{dt} = - D_s A \left.\frac{\partial q}{\partial r}\right|_R \qquad (B.2)$$

$$V \frac{dc}{dt} = - k_f A (c - c_s) \qquad (B.3)$$

Equation (B.1) is based on a mass balance between the liquid and solid phases. The mean solid phase concentration ($\bar{q}$) is calculated by numerical integration of the solid phase concentration profile. This equation has been used by several authors (Chakravorti, 1973; Mathews and Weber, 1977; Weber and Crittenden, 1975). Equation (B.2) equates the rate of removal of adsorbate from solution to the rate of transfer through the carbon particle surface. It has been used previously by Brecher et al. (1967) who expressed the surface differential as a five point backward difference equation basing the surface gradient on the solid phase profile. Equation (B.3) is the simplest form and equates the rate of removal from solution to the rate of transfer across the external liquid film.

Since the equation used in the solution to couple the liquid and solid phases is obtained by equating eqns. (B.2) and (B.3) to give:

$$D_s \left.\frac{\partial q}{\partial r}\right|_R = k_f (c - c_s) \qquad (B.4)$$

an obvious choice for a consistent solution is to use either eqn.(B.2) or (B.3) to calculate the liquid phase concentration. In addition, external film diffusion is the controlling resistance at the start of the adsorption period when the intraparticle gradients are greatest. Because a discontinuity exists across the carbon particle surface at t = 0, the solution is initially stiff and errors occur in the finite difference representation of the solid phase concentration profile during this initial period. Since both eqns.(B.1) and (B.2) are based on the solid phase profile these errors could be expected to propogate into the liquid phase solution. The use of eqn.(B.3) should minimize this error as the solid phase concentration at the surface is low and hence c_s is close to zero and thus errors in the value of c_s should have little effect on the liquid phase solution during this period.

To investigate the relative behaviour of the three alternatives, computations were performed using Simpson's rule to integrate the profile in eqn.(B.1) and a seven point backward difference formula to calculate the differential in eqn. (B.2). The results of one set of computations as well as the system parameters used are presented in Table B-1.

With a fine grid spacing of $\Delta R = 0.01$ the three equations give similar profiles but only that based on eqn.(B.3) gives the correct initial slope shown in the column for film diffusion as the only resistance ($c_s \equiv 0$). As the grid spacing is increased to $\Delta R = 0.1$ the errors in the finite difference representation of the solid concentration profile

Time (sec)	Film Transfer Only - No Internal Resistance	Integrated Profile Eqn. (A.1)		Differential Profile Eqn. (A.2)		Film Transfer Eqn. (A.3)	
		ΔR = 0.1	ΔR = 0.01	ΔR = 0.1	ΔR = 0.01	ΔR = 0.1	ΔR = 0.01
0	1.000000	1.000000	1.000000	1.000000	1.000000	1.000000	1.000000
5	.999149	.999368	.999163	.999905	.999178	.999149	.999149
30	.994907	.995737	.995919	.997474	.994933	.994907	.994907
60	.989839	.990863	.989850	.992624	.989864	.989839	.989839
120	.979782	.980723	.979792	.981986	.979806	.979783	.979784
180	.969826	.970618	.969842	.971710	.969854	.969833	.969834
240	.959972	.9606	.959999	.961732	.960011	.959991	.959993
300	.950218	.950812	.950268	.951907	.950279	.950260	.950263
Relative Solution Time			1.54		1.04		1.00

$D_s = 5.0 \times 10^{-8}$ cm^2/sec. W = 1.0 g carbon A = 85.1 cm^2 $q_e = 78.1\, C_e^{.212}$

$k_f = 5.0 \times 10^{-3}$ cm.sec V = 2500 cm^3 C_o = 100 mg/l

Table B-1. Reduced Liquid Phase Concentrations as a Function of Solution Method - Initial Period.

increase and differences are observed in the liquid concentration profile for eqn.(B.1) and more so for eqn.(B.2). As expected the profile from eqn.(B.3) changes only slightly. Thus aside from being computationally faster, the solution based on eqn.(B.3) is also more accurate in this initial region, especially for widely spaced solution grids.

In Table B-2 the liquid concentrations to equilibrium are presented based on eqns.(B.1) and (B.3). The final equilibrium concentration calculated from the input parameters is given and is identical to the equilibrium reached by the solution based on film transfer. The solution based on the integrated profile with $R = 0.01$ is similar while $R = 0.1$ gives a less accurate result. Consequently the film transfer based solution while requiring less computation also appears to be more accurate throughout the entire solution and is preferable to the integrated and differential forms of calculation.

In the above calculations equal time steps were used for all three methods. Since the maximum time step size is normally determined by the intraparticle solution, speed of solution and accuracy are the determining parameters in choosing which equation is to be used for liquid phase calculation.

Time (sec)	Integrated Profile Eqn. (A.1)		Film Transfer Eqn. (A.3)
	ΔR = 0.1	ΔR = 0.01	ΔR = 0.1
0	1.000000	1.000000	1.000000
300	.950812	.950267	.950260
1200	.819195	.819306	.819318
3000	.642349	.642272	.642444
6000	.493601	.492774	.492928
9000	.421827	.420483	.420551
12000	.384477	.382874	.382892
15000	.364654	.362941	.362931
21000	.348440	.346678	.346640
30000	.342960	.341205	.341152
72000(equil)	.341976	.340230	.340173

Equilibrium based on input parameters = 0.340174

Table B-2. Reduced Liquid Phase Concentrations as a Function of Solution Method - Equilibrium.

APPENDIX C

C.1 Detailed Solution of Branched Pore Model Batch Kinetic Solution.

The equations to be solved are (see section 5.2):

$$\frac{dC}{d\theta} = -\frac{(1-\varepsilon)}{\varepsilon} \cdot Bi_f \{C - C_s\} \tag{5.12}$$

$$\frac{\partial Q_m}{\partial \theta} = 4\eta \frac{\partial^2 Q_m}{\partial \eta^2} + 6 \frac{\partial Q_m}{\partial \eta} - \frac{Bi_p}{f} (Q_m - Q_b) \tag{5.13}$$

$$\frac{\partial Q_b}{\partial \theta} = \frac{Bi_p}{(1-f)} (Q_m - Q_b) \tag{5.14}$$

$$\left.\frac{\partial Q_m}{\partial \eta}\right|_{\eta=1} = \frac{Bi_f}{f} \cdot \frac{F}{6} (C - C_s) \tag{5.15}$$

where the terms have the meanings given in the text.

Using Crank-Nicholson operators the following substitutions are made:

$$\frac{dC}{d\theta} = \frac{C_{j+1} - C_j}{\Delta\theta} \tag{C.1}$$

$$\frac{\partial Q_m}{\partial \theta} = \frac{Q^m_{i,j+1} - Q^m_{i,j}}{\Delta\theta} \tag{C.2}$$

$$\frac{\partial Q_b}{\partial \theta} = \frac{Q^b_{i,j+1} - Q^b_{i,j}}{\Delta\theta} \tag{C.3}$$

$$\frac{\partial^2 Q_m}{\partial \eta^2} = \frac{1}{2(\Delta\eta)^2} \{Q^m_{i-1,j+1} - 2Q^m_{i,j+1} + Q^m_{i+1,j+1} + Q^m_{i-1,j} - 2Q^m_{i,j} + Q^m_{i+1,j}\} \tag{C.4}$$

$$\frac{\partial Q_m}{\partial \eta} = \frac{1}{4\Delta\eta} \{Q^m_{i+1,j+1} - Q^m_{i-1,j+1} + Q^m_{i+1,j} - Q^m_{i-1,j}\} \tag{C.5}$$

In addition, the driving forces $(C - C_s)$ and $(Q_m - Q_b)$ are averaged over the time interval and written as:

$$(C - C_s) = \frac{1}{2}\{C_{j+1} + C_j - C_{s,j+1} - C_{s,j}\} \quad (C.6)$$

$$(Q_m - Q_b)_i = \{\frac{1}{2} Q^m_{i,j+1} + Q^m_{i,j} - Q^b_{i,j+1} - Q^b_{i,j}\} \quad (C.7)$$

When these substitutions are made, equation (5.12) becomes

$$C_{j+1} = \frac{1}{1 + \gamma_1} \{(1 - \gamma_1)C_j + \gamma_1(C_{s,j+1} + C_{s,j})\} \quad (C.8)$$

where $\gamma_1 = (1-\varepsilon)Bi_f \, \Delta\theta/2\varepsilon$

The expanded form of equation (5.14) is similar.

$$Q^b_{i,j+1} = \frac{1}{1 + \gamma_2} \{(1 - \gamma_2) Q^b_{i,j} + \gamma_2(Q^m_{i,j+1} + Q^m_{i,j})\} \quad (C.9)$$

where $\gamma_2 = Bi_p \, \Delta\theta/2(1-f)$

At a general point 'i' within the particle, the expansion of equation (5.13) results in:

$$x^i_3 Q^m_{i-1,j+1} + x^i_1 Q^m_{i,j+1} + x^i_2 Q^m_{i+1,j+1}$$
$$= y^i_3 Q^m_{i-1,j} + y^i_1 Q^m_{i,j} + y^i_2 Q^m_{i+1,j} + h^i \ldots\ldots \quad (C.10)$$

where the elements of the matrices $\underline{\underline{X}}$ and $\underline{\underline{Y}}$ and of vector $\underline{H}$ are detailed in Table C-1

At the centre of the particle, $n = 0$ so equation (5.13) can be written:

$$\frac{\partial Q^m}{\partial \theta} = .6 \frac{\partial Q^m}{\partial \eta} - \frac{Bi_p}{f}(Q_m - Q_b) \quad (C.11)$$

The concentration gradient is expressed as a forward difference averaged

$$x_1^o = 1 + 3\alpha + \beta \qquad y_1^o = 1 - 3\alpha - \beta$$

$$x_2^o = -3\alpha \qquad y_2^o = 3\alpha$$

$$x_1^i = 1 + 4i\alpha + \beta \qquad y_1^i = 1 - 4i\alpha - \beta$$

$$x_2^i = -2i\alpha - 1.5\alpha \qquad y_2^i = 2i\alpha + 1.5\alpha$$

$$x_3^i = -2i\alpha + 1.5\alpha \qquad y_3^i = 2i\alpha - 1.5\alpha$$

$$x_1^M = 1 + 4M\alpha + \beta \qquad y_1^M = 1 - 4M\alpha - \beta$$

$$x_3^M = -4M\alpha \qquad y_3^M = 4M\alpha$$

$$h^o = \beta(Q^b_{0,j+1} + Q^b_{0,j})$$

$$h^i = \beta(Q^b_{i,j+1} + Q^b_{i,j})$$

$$h^M = \beta(Q^b_{M,j+1} + Q^b_{M,j}) + \frac{B_{if}.F.\Delta\eta}{3f}(2M\alpha + 1.5)(C_{j+1} + C_j - C_{s,j+1} - C_{s,j})$$

$$\alpha = \Delta\theta/\Delta\eta$$

$$\beta = Bi_p\,\Delta\theta/2f$$

$$\underline{\underline{Z}} = \begin{bmatrix} Z_1^o & Z_2^o & 0 & \cdot & \cdot & \cdot & \cdot \\ Z_3^1 & Z_1^1 & Z_2^1 & 0 & \cdot & \cdot & \cdot \\ 0 & Z_3^2 & Z_1^2 & Z_2^2 & 0 & \cdot & \cdot \\ \cdot & \cdot & \cdot & \cdot & \cdot & \cdot & \cdot \\ \cdot & \cdot & \cdot & 0 & Z_3^{m-1} & Z_1^{m-1} & Z_2^{m-1} \\ \cdot & \cdot & \cdot & \cdot & 0 & Z_3^m & Z_1^m \end{bmatrix}$$

Table C-1. Elements of the Matrices and Vectors in the Solution

$$\underline{\underline{Y}}\,\underline{Q}^m_{j+1} = \underline{\underline{Y}}\,\underline{Q}^m_j + \underline{H}$$

over the time interval to give:

$$\frac{Q^m_{0,j+1} - Q^m_{0,j}}{\Delta\theta} = \frac{6}{2\Delta\eta}\{Q^m_{1,j+1} - Q^m_{0,j+1} + Q^m_{1,j} - Q^m_{0,j}\}$$

$$- \frac{B_{if}}{2f}(Q^m_{0,j+1} + Q^m_{0,j} - Q^b_{0,j} - Q^b_{0,j+1}) \qquad (C.12)$$

and equation (C.12) can be reduced to

$$x^o_1\ Q^m_{0,j+1} + x^o_2\ Q^m_{1,j+1} = y^o_1\ Q^m_{0,j} + y^o_2\ Q^m_{1,j} + h^o \qquad (C.13)$$

where the x, y and h elements are defined in Table C-1.

At the outer particle surface a method must be chosen for discretizing $\left.\frac{\partial Q^m}{\partial \eta}\right|_{\eta=1}$. McGreavy et al.(1967) noted that a central difference equation should be used as a first order difference representation results in a mismatch of truncation errors in $\Delta\eta$. Thibault and Hoffman (1978) compared the use of central and first order difference equations, and found that the first order approximation introduced errors into the solution. When $\left.\frac{\partial Q^m}{\partial \eta}\right|_{\eta=1}$ is expressed as a central difference equation, fictitious points $Q^m_{M+1,j(j+1)}$ are introduced which lie outside the outer boundary of the particle. By also expressing equation (C.10) at the outer boundary i = M, the fictitious points can be eliminated between the two equations as follows

Equation (5.15) is written as

$$\frac{1}{4\Delta\eta}\{Q^m_{M+1,j+1} - Q^m_{M-1,j+1} + Q^m_{M+1,j} - Q^m_{M-1,j}\}$$

$$= \frac{F.B_{if}}{6\ f}\left\{\frac{C_{j+1} + C_j}{2} - \frac{C_{s,j+1} + C_{s,j}}{2}\right\} \qquad (C.14)$$

and equation (C.10) becomes

$$x_3^M Q^m_{M-1,j+1} + x_1^M Q^m_{M,j+1} + x_2^M Q^m_{M+1,j+1}$$

$$= y_3^M Q^m_{M-1,j} + y_1^M Q^m_{M,j} + y_2^M Q^m_{M+1,j} + h^M \qquad (C.15)$$

By eliminating $Q^m_{M+1,j+1}$ and $Q^m_{M+1,j}$ from equations (C.14) and (C.15), the equation at the outer boundary is obtained.

$$x_3^M Q^m_{M-1,j+1} + x_1^M Q^m_{M,j+1} = y_3^M Q^m_{M-1,j} + y_1^M Q^m_{M,j} + h^M \qquad (C.16)$$

where again the x, y and h elements are defined in Table C-1.

The resulting set of equations (C.13), (C.16), (C.10) for i = 1, M-1, constitute a solution of the form

$$\underline{X}\, Q^m_{j+1} = \underline{Y}\, Q^m_j + \underline{H} \qquad (C.17)$$

which, in conjunction with equations (C.8) and (C.9), enables the batch kinetic problem to be solved. The solution algorithm is shown on the following page.

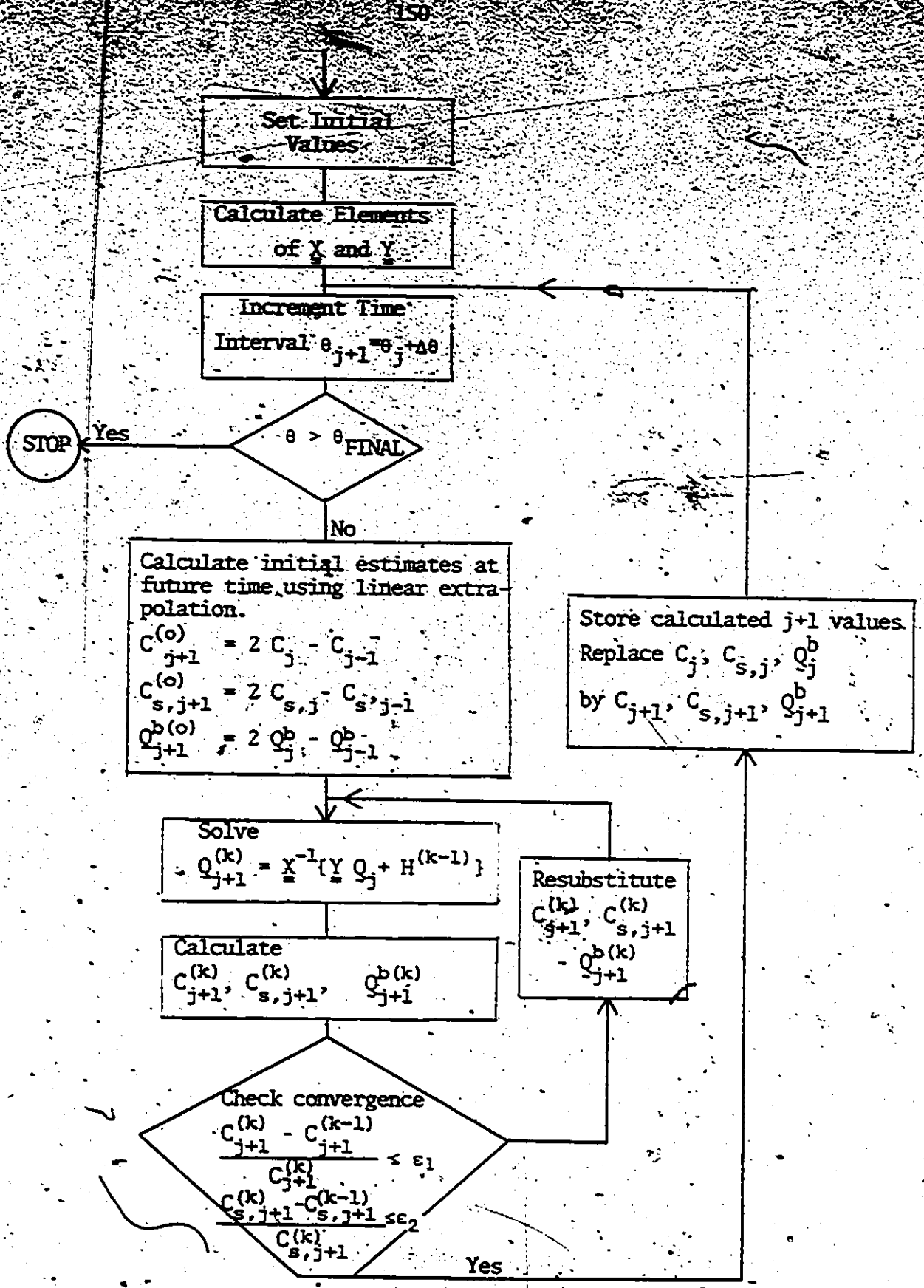
Set Initial Values
Calculate Elements of $\underline{X}$ and $\underline{Y}$
Increment Time Interval $\theta_{j+1} = \theta_j + \Delta\theta$
$\theta > \theta_{FINAL}$
Yes
STOP
No
Calculate initial estimates at future time using linear extrapolation.
$C^{(o)}_{j+1} = 2C_j - C_{j-1}$
$C^{(o)}_{s,j+1} = 2C_{s,j} - C_{s,j-1}$
$Q^{b(o)}_{j+1} = 2Q^b_j - Q^b_{j-1}$
Solve
$\underline{Q}^{(k)}_{j+1} = \underline{X}^{-1}\{\underline{Y}\,\underline{Q}_j + H^{(k-1)}\}$
Calculate
$C^{(k)}_{j+1}$, $C^{(k)}_{s,j+1}$, $Q^{b(k)}_{j+1}$
Resubstitute
$C^{(k)}_{j+1}$, $C^{(k)}_{s,j+1}$
$Q^{b(k)}_{j+1}$
Check convergence
$\frac{C^{(k)}_{j+1} - C^{(k-1)}_{j+1}}{C^{(k)}_{j+1}} \leq \varepsilon_1$
$\frac{C^{(k)}_{s,j+1} - C^{(k-1)}_{s,j+1}}{C^{(k)}_{s,j+1}} \leq \varepsilon_2$
Yes
Store calculated j+1 values
Replace C_j, $C_{s,j}$, Q^b_j
by C_{j+1}, $C_{s,j+1}$, Q^b_{j+1}

C.2 Comparison of the Branched Pore Model with an Analytical Solution

Analytical solutions for diffusion problems are only available for certain restricted cases. One such solution was reported by Paterson (1947) who tabulated data for the solution of heat flow in a solid sphere. If the fraction 'f' is set equal to unity in the branched pore model described in Chapter 5, the model degenerates to the standard surface or homogeneous diffusion model. With the additional assumptions of a linear isotherm and no external film resistance, the model solution can be directly compared to that of Paterson. The following similarities exist between Paterson's work and the present study.

This work		Patterson	
Diffusion Coefficient	D_s	Thermal Diffusivity	k
Concentration	Q	Temperature	T
Ratio of Mass Capacities	$\frac{1}{F} = \frac{w.q_o}{v.c_o}$	Ratio of Heat Capacities	$w = c_1/c_2$
Linear Isotherm	Q = C	Continuity of Temperature	$T_1 = T_2$

To eliminate external mass transfer resistance from the branched pore model, the program was modified slightly to allow for equilibrium between the bulk liquid and the external surface of the particle. In this solution the liquid phase calculation was based on the surface concentration gradient

$$\frac{dc}{dt} = -\frac{(1-\varepsilon)}{\varepsilon} \cdot \frac{3D_s \rho_c}{R} \left.\frac{\partial q}{\partial r}\right|_R \qquad (C2.1)$$

and the gradient was expanded as a seven point backward difference.

Shown in Figure 5-4 in Chapter 5 are predicted uptake curves for $D_s = 10^{-7}$ cm^2/sec using equation (C2.1) and also the predicted curve using the original model with a large film transfer coefficient ($D_s = 10^{-7}$ cm^2/sec, $k_f = 0.1$ cm/sec). As can be seen in the figure, the curve with a small external film resistance is asymptotic to the solution without an external film as would be expected. The data of Paterson which corresponds exactly to the solution of the model without film resistance, was obtained in the following manner.

Paterson gives a series of computed curves for the approach to equilibrium as a function of θ for different values of w. In the mass transfer case these are equivalent to curves of fractional approach to equilibrium, $(1-C)/(1-C_e)$, as a function of θ where $\theta = D_s t/R^2$ and $C_e = F/(1+F)$.

From one of the fractional uptake curves for w = 5, data points were extracted and tabulated below. Values of V, C_o, w and q_o, were calculated to give 1/F = 5 to enable comparison.

τ	$(1-T)/(1-T_e)$	t(sec)	$C(= c/c_o)$
10^{-5}	0.060	0.2045	0.950
10^{-4}	0.175	2.045	0.853
10^{-3}	0.440	20.45	0.630
10^{-2}	0.780	204.5	0.343
10^{-1}	0.975	2045.0	0.179

The values of C and t are plotted on Figure 5-4 in the text.

APPENDIX D

Detailed Solution of the Adsorption Bed Equations

The equations to be solved are (see section 6.1);

$$\frac{\partial C}{\partial z} = -\frac{(1-\varepsilon)}{\varepsilon} Bi_f (C - C_s) \qquad (6.4)$$

and at each bed position;

$$\frac{\partial Q_m}{\partial \theta} = 4\eta \frac{\partial^2 Q_m}{\partial \eta^2} + 6 \frac{\partial Q^m}{\partial \eta} - \frac{Bi_p}{f} (Q_m - Q_b) \qquad (5.13)$$

$$\frac{\partial Q_b}{\partial \theta} = \frac{Bi_p}{(1-f)} (Q_m - Q_b) \qquad (5.14)$$

$$\left.\frac{\partial Q_m}{\partial \eta}\right|_{\eta=1} = \frac{Bi_f F}{6f} (C - C_s) \qquad (5.15)$$

subject to the initial and boundary conditions

$$C(0, \theta) = 1$$

$$C(z, 0) = 0$$

$$Q_m(z, \eta, 0) = 0$$

$$Q_b(z, \eta, 0) = 0$$

$$Q_m(z, 1, \theta) = Q_s(z, \theta).$$

At any general bed position the solid phase concentrations within a particle are discretized using Crank-Nicholson expansions to give for i = 0, M-1;

$$x_3^i Q^m_{i-1,j+1} + x_1^i Q^m_{i,j+1} + x_2^i Q^m_{i+1,j+1} =$$

$$= y_3^i Q^m_{i-1,j} + y_1^i Q^m_{i,j} + y_2^i Q^m_{i+1,j} + \beta(Q^b_{i,j+1} + Q^b_{i,j}) \quad (D.1)$$

where the x_k^i, y_k^i are given in Appendix C and $\beta = B_{i_p} \Delta\theta/2f$.

At the external surface of the particle, eqn.(D.1) can be written for $i = M$,

$$x_3^M Q^m_{M-1,j+1} + x_1^M Q^m_{M,j+1} + x_2^M Q^m_{M+1,j+1}$$

$$= y_3^M Q^m_{M-1,j} + y_1^M Q^m_{M,j} + y_2^M Q^m_{M+1,j} + \beta(Q^b_{M,j+1} + Q^b_{m,j}) \quad (D.2)$$

and the coupling equation (5.15) can be expanded using central difference to give;

$$\frac{Q^m_{M+1,j+1} - Q^m_{M-1,j+1} + Q^m_{M+1,j} - Q^m_{M-1,j}}{4\Delta\eta}$$

$$= \frac{B_{i_f} F}{6f}\left(\frac{C_{\ell,j+1} + C_{\ell,j}}{2}\right) - \frac{C_{s,\ell,j+1} + C_{s,\ell,j}}{2} \quad (D.3)$$

where $C(z, \theta) = C(\ell\Delta z, j\Delta\theta) = C_{\ell,j}$.

Rearrangement of eqn.(D.3) gives

$$-Q^m_{M-1,j+1} + Q^m_{M+1,j+1} = Q^m_{M-1,j} - Q^m_{M+1,j} + \delta(C_{\ell,j+1} + C_{\ell,j} - C_{s,\ell,j+1} - C_{s,\ell,j}) \quad (D.4)$$

where $\delta = B_{i_f} F \Delta\eta/3f$

When equations (D.2) and (D.4) are solved simultaneously to eliminate the fictitious concentration at the (m+1)th position, the following equation is obtained;

$$- 4 M \alpha Q^m_{M-1,j+1} + (1 + 4 M \alpha + \beta) Q^m_{M,j+1}$$

$$= 4 M \alpha Q^m_{M-1,j} + (1 - 4 M \alpha - \beta) Q^m_{M,j} + \beta (Q^b_{M,j+1} + Q^b_{M,j})$$

$$+ (2 M \alpha + 1.5 \alpha) \delta (C_{\ell,j+1} + C_{\ell,j} - C_{s,\ell,j+1} - C_{s,\ell,j})$$

..... (D.5)

Now the $C_{s,\ell,j}$ are related to $Q^m_{M,j}$ through the isotherm, and for a Freundlich relationship

$$C_{s,\ell,j} = (Q^m_{M,j})^{1/n} = (Q^m_{M,j})^{(\frac{1}{n}-1)} Q^m_{M,j}$$

and consequently equation (D.5) can be rewritten as

$$x^M_3 Q^m_{M-1,j+1} + x^M_1 Q^m_{M,j+1} + x^M_2 C_{\ell,j+1}$$

$$= y^M_3 Q^m_{M-1,j} + y^M_1 Q^m_{M,j} + y^M_2 C_{\ell,j} + \beta (Q^b_{M,j} + Q^b_{M,j+1}) \quad (D.6)$$

where $x^M_3 = - 4 M \alpha$

$$x^M_1 = 1 + 4 M \alpha + \beta + (2 M \alpha + 1.5 \alpha) \delta Q^{m^{\frac{1}{n}-1}}_{M,j+1}$$

$$x^M_2 = - (2 M \alpha + 1.5 \alpha) \delta$$

$$y^M_3 = 4 M \alpha$$

$$y^M_1 = 1 - 4 M \alpha - \beta - (2M \alpha + 1.5 \alpha) \delta Q^{m^{\frac{1}{n}-1}}_{M,j}$$

$$y^M_2 = (2 M \alpha + 1.5 \alpha) \delta$$

The remaining equation to be discretized is the fluid phase equation (6.4). To make the driving forces across the liquid film in

equations (6.4) and (5.15) consistent, equation (6.4) was expanded about the mid time step using a backward difference to give:

$$x_3^{M+1} Q^m_{M,j+1} + x_1^{M+1} C_{\ell,j+1}$$

$$= y_3^{M+1} Q^m_{M,j} + y_1^{M+1} C_{\ell,j} + C_{\ell-1,j+1} + C_{\ell-1,j} \qquad (D.7)$$

where $x_1^{M+1} = (1 + \tau)$

$x_3^{M+1} = - \tau . Q^{m\,(\frac{1}{n}-1)}_{M,j+1}$

$y_1^{M+1} = - (1 + \tau)$

$y_3^{M-1} = \tau\, Q^{m\,(\frac{1}{n}-1)}_{M,j}$

and $\tau = (1 - \epsilon)\, B_{if}\, \Delta z/\epsilon$

The set of equations (D.1), (D.6) and (D.7) can be written in the matrix form

$$\underline{X}^{(k-1)}\, \underline{Q}^{m(k)}_{j+1} = \underline{Y}\, \underline{Q}^m_j + \underline{H}^{(k-1)} \qquad (D.8)$$

where $\underline{X}$ and $\underline{Y}$ are tridiagonal matrices having the elements given above and $\underline{H}$ is a vector containing the additional elements $Q^b_{i,j}$; $Q^b_{i,j+1}$; $C_{\ell-1,j}$; $C_{\ell-1,j+1}$. The superscripts (k-1) on $\underline{X}$ and $\underline{H}$ denote that some elements are functions of the concentrations at the future time interval (j+1) and therefore than an iterative solution is required. The vectors $\underline{Q}^m_j = \{Q^m_{0,j}, Q^m_{1,j} \ldots\ldots Q^m_{M,j}; C_{\ell,j}\}$.

The solution algorithm is as shown in Figure D-1, the solution being obtained by marching through the bed at each time interval solving equation (D.8) at each bed position. The solution grids used are as follows.

Intraparticle Equation (X = Centre of Computation)

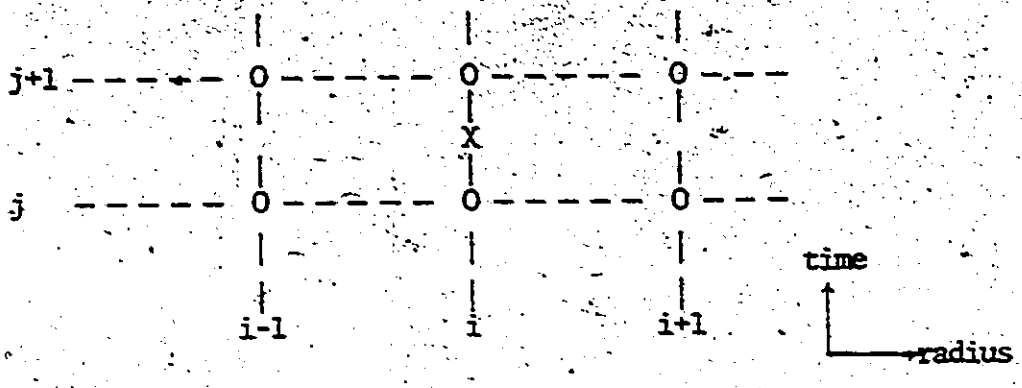

Liquid Phase Equation (X = Centre of Computation)

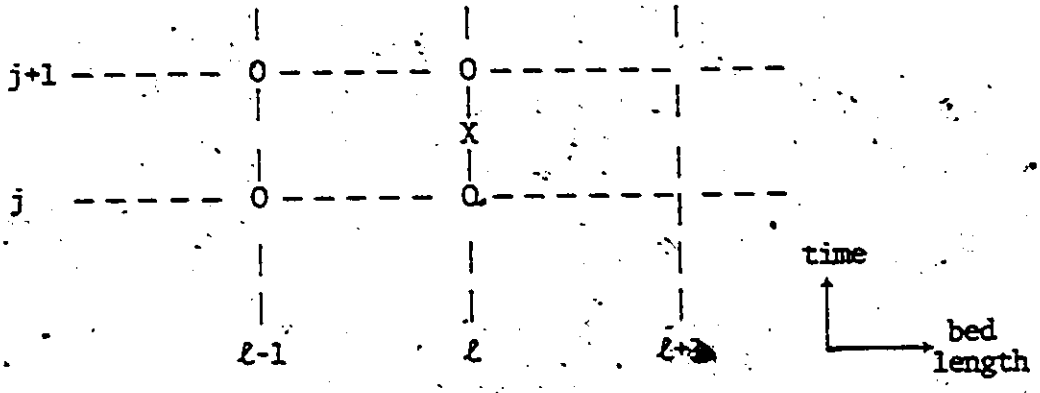

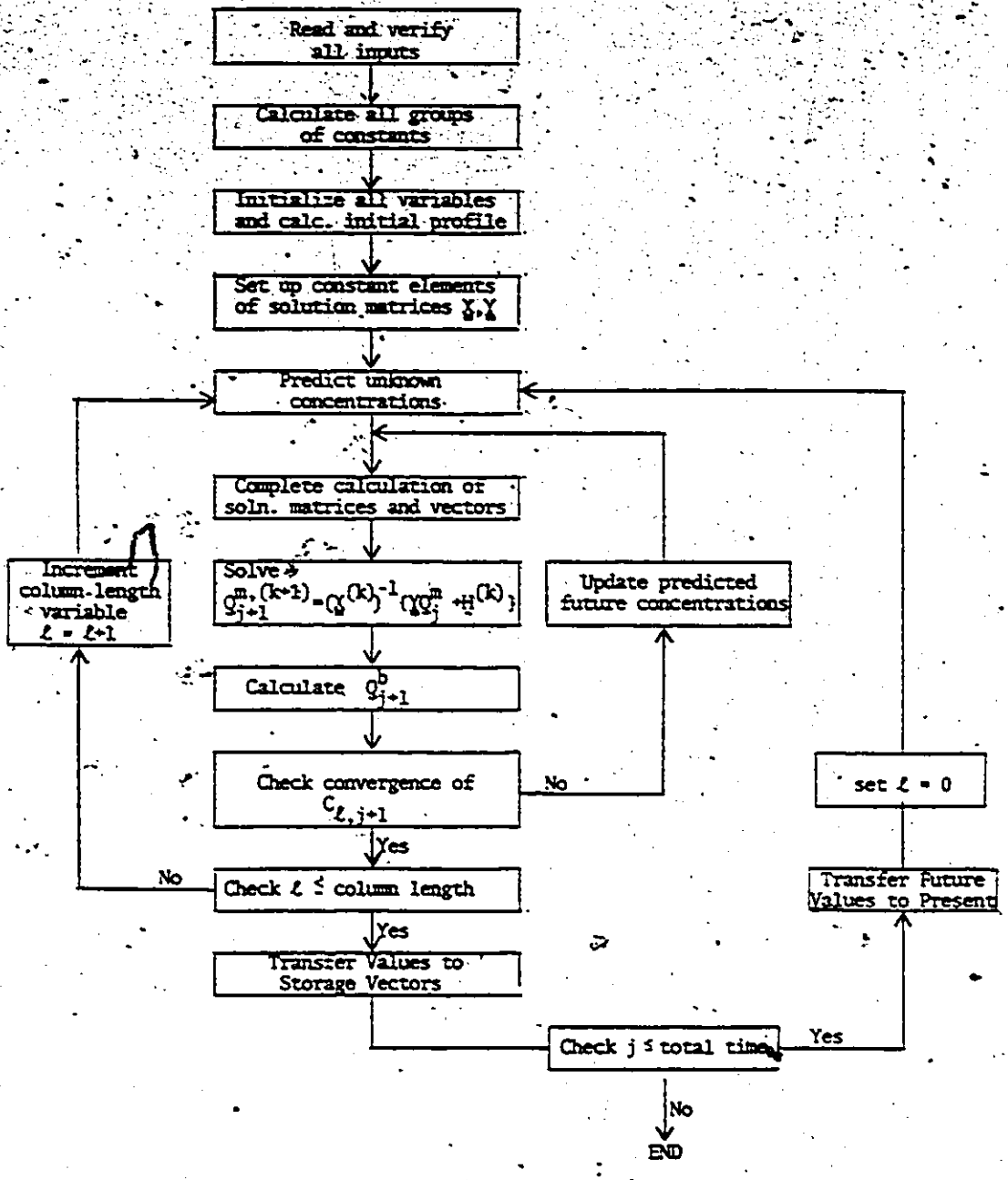

Figure D-1. Adsorption Column Solution Algorithm

APPENDIX E

Comparison of the Branch Pore Column Model with Previous Solutions

Since previously published comparable dual rate models were not available, the model could only be checked if 'f' were set equal to unity. For this case the model is identical to an in series external film resistance, surface diffusion model and numerical solutions for such models with Freundlich isotherms have previously been published by Tien and Thodos (1959) and Fleck (1970).

Tien and Thodos developed a numerical solution based on the approximation of an infinite series by a closed form expression. The infinite series arose as a result of their mathematical analysis. They used an explicit finite difference form of solution and published a table of concentration versus bed depth for the Freundlich exponent equal to 0.5. The values used for comparison were taken from Table 2 (p.377) of Tien and Thodos (1959) for the parameter x = 15.

The following set of parameters were chosen to give

$$\alpha_0 = \left| \frac{c_o R^2 \left[3k_f \right]}{4 \pi \left[\rho_c R \right] q_o D_s} \right|^{\frac{1}{1-0.5}} = 100$$

D_s	= 5×10^{-8}	cm^2/sec	(D)
k_f	= 3×10^{-3}	cm/sec	$(k_\ell R \rho_c / 3)$
R	= 0.047	cm	(b)
ρ_c	= 0.75	g/cm^3	

ρ_b = 0.416 g/cm^3 (ρ)

Q/A = 0.1644 cm/sec (u)

c_o = 10^{-4} g/cm^3 (c_o)

q_o = 8.976 × 10^{-3} g/gC (q_{max})

z = 23.22 cm ($x = \frac{3k_f \rho_b z}{R \rho_c u}$)

where the variables in brackets are the equivalent symbols used by Tien and Thodos.

From Table 2 of Tien and Thodos (1959),

$\nu \times 2^9$	c/c_o	t(hr)
161	.00200	.32455
181	.01854	.36272
201	.05496	.40086
301	.26564	.59158
441	.45686	.8586
641	.61635	1.2401
821	.70732	1.5834

where $\nu = \frac{4 \pi D_s}{R^2} (r - \frac{\varepsilon}{u} z)$ was used to calculate the equivalent real time of a tabulated value of ν. These values of c/c_o versus t were plotted against the branch pore model prediction in the text.

Fleck (1970) used the assumption of constant pattern behaviour to simplify the adsorption model and calculated a series of dimensionless curves for various resistances in series and parallel. In Figure 10 (p.73) of Fleck's thesis, a series of curves for combined external

and surface diffusion are given for the Freundlich exponent equal to 0.2. Data was read from this curve and used for comparison.

In the notation used in this report the variables used by Fleck are

$$N_s = \frac{15\, D_s\, \lambda\, v.}{r_s^2\, F} = \frac{15\, D_s\, \rho_b\, q_o\, z}{R^2 v_s\, \varepsilon\, c_o}$$

$$N_f = \frac{k_f\, A_p\, v\, \varepsilon}{F} = \frac{k_f\, 3(1-\varepsilon)\, z}{R\, v_s}$$

$$\alpha = \frac{N_s}{N_f} = \frac{5\, D_s\, \rho_b\, q_o}{\varepsilon(1-\varepsilon) c_o\, R\, k_f}$$

$$T = \frac{t - (v\,\varepsilon/F)}{(\Omega\, v/F)} = \frac{t - z/v_s}{(q_o\, \rho_b\, x/c_o\, v_s\, \varepsilon)}$$

Values for $\alpha = 0.5$ at increments of the ordinate $(T-1)/(1/N_f + 1/N_s)$ were read from Figure 10 of Fleck and are tabulated below

$(T-1)/(1/N_f + 1/N_s)$	c/c_o	t(hrs)
- 2	.021	5.466
- 1.5	.073	4.080
- 1.0	.178	4.693
- 0.5	.362	5.307
0.0	.600	5.921
+ 0.5	.725	6.534
+ 1.0	.812	7.148
+ 1.5	.865	7.762
+ 2.0	.912	8.375
+ 2.5	.950	8.989

The values in the above table were plotted against a predicted curve calculated by the branch pore column model with parameters arranged

to give $\alpha = 0.5$. The parameters used were:

$D_s = 5 \times 10^{-8}$ cm^2/sec

$k_f = 3 \times 10^{-3}$ cm/sec

$\rho_b = 0.416$ g/cm^3

$\rho_c = 0.75$ g/cm^3

$\varepsilon = 0.4453$

$R = 0.047$ cm

$c_o = 10^{-4}$ g/cm^3

$q_o = 0.01674$ g/gC

$n = 0.2$

APPENDIX F

A Comparative Study of the Linear and Quadratic Simplified Driving Force Expressions.

The linear driving force expression

$$\frac{d\bar{q}}{dt} = k_p a_p (q_s - \bar{q}) \qquad (2.15)$$

was chosen by Glueckauf and Coates (1947) to approximate the exact solution of the differential equation

$$\frac{\partial q}{\partial t} = \frac{D_s}{r^2} \cdot \frac{\partial}{\partial r} \left(r^2 \frac{\partial q}{\partial r}\right) \qquad (F.1)$$

which for the simple case of a constant external surface concentration (irreversible isotherm) has the solution (Crank, 1956);

$$\frac{q}{q_s} = 1 + \frac{2R}{\pi r} \sum_{1}^{\infty} \frac{(-1)^n}{n} \sin\left(\frac{n \pi r}{R}\right) \exp\left[\frac{-D_s n^2 \pi^2 t}{R^2}\right] \qquad (F.2)$$

By integrating equation (F.2), the mean particle concentration as a function of time can be obtained

$$\frac{\bar{q}}{q_s} = 1 - \frac{6}{\pi^2} \sum_{1}^{\infty} \frac{1}{n^2} \exp\left[\frac{-D_s n^2 \pi^2 t}{R^2}\right] \qquad (F.3)$$

From equation (F.1) the flux crossing the external surface of the particle at any time t is

$$\dot{n} = D_s \left.\frac{\partial q}{\partial r}\right|_R = k_p (q_s - \bar{q}) \qquad (F.4)$$

and therefore by differentiating equation (F.2) with respect to r,

$$k_p = \frac{2\pi^2 D_s}{\delta R} \sum_1^\infty \exp\{\frac{-D_s n^2 \pi^2 t}{R^2}\} \Big/ \sum_1^\infty \frac{1}{n^2} \exp\{\frac{-D_s n^2 \pi^2 t}{R^2}\} \quad \ldots\ldots \quad (F.5)$$

In the limit $t \to \infty$ it can be shown that

$$k_p \to 4\pi^2 D_s / 6 d_p \quad (F.6)$$

thus giving the familiar expression

$$k_p a_p = 4\pi^2 D_s / d_p^2 \quad (F.7)$$

However, in the limit $t \to 0$,

$$k_p \to \infty \quad (F.8)$$

and therefore the linear driving force model which assumes that k_p is a constant is a poor approximation to the exact solution for small 't'.

In contrast, Vermeulen (1953) showed that the quadratic driving force expression was a good approximation to the exact solution when an irreversible isotherm was assumed.

$$\frac{d\bar{q}}{dt} = k_p a_p (q_s^2 - \bar{q}^2)/2\bar{q} \quad (2.16)$$

In the present case the simplifications of irreversible or linear isotherms could not be made, and the numerical solution developed in Chapter 5 (with 'f' set equal to unity) was used to directly compare the two driving force expressions under nonlinear and nonconstant

conditions. The values of k_p in equations (2.15) and (2.16), which would at any time give identical uptake rates to the exact solution (equation F.1), were calculated for a range of different values of k_f, D_s and the Freundlich exponent 'n'. This was achieved by calculating the overall rate of uptake, the surface concentration (q_s), and the mean concentration ($\bar{q}$), and thus determining the necessary values of k_p. Under the conditions investigated, the external surface concentration undergoes complex changes representative of a real system, and therefore the applicability of the simplified forms could be tested under practical conditions.

In all cases studied the values of k_p for the linear driving force expression varied over two orders of magnitude in accordance with equations (F.6) and (F.8), whereas the k_p calculated for the quadratic driving force varied by less than 100%. A comparison of the calculated mass transfer coefficients for one set of conditions is shown in Figure F-1. The fact that k_p for the quadratic driving force model (QDF) was virtually constant over the entire adsorption period indicated that equation (2.16) was a good approximation to the exact solution of the surface diffusion model over the range of investigated conditions (typical of phenolic adsorption). In contrast, the approximation offered by the linear driving force was poor, and if used can lead to problems in the kinetic analysis as discussed below.

Because the assumption of constant k_p in the linear expression neglects the fact that $k_p \to \infty$ as $t \to 0$ if the equation is to approximate the exact solution, a model using the linear driving force will in many

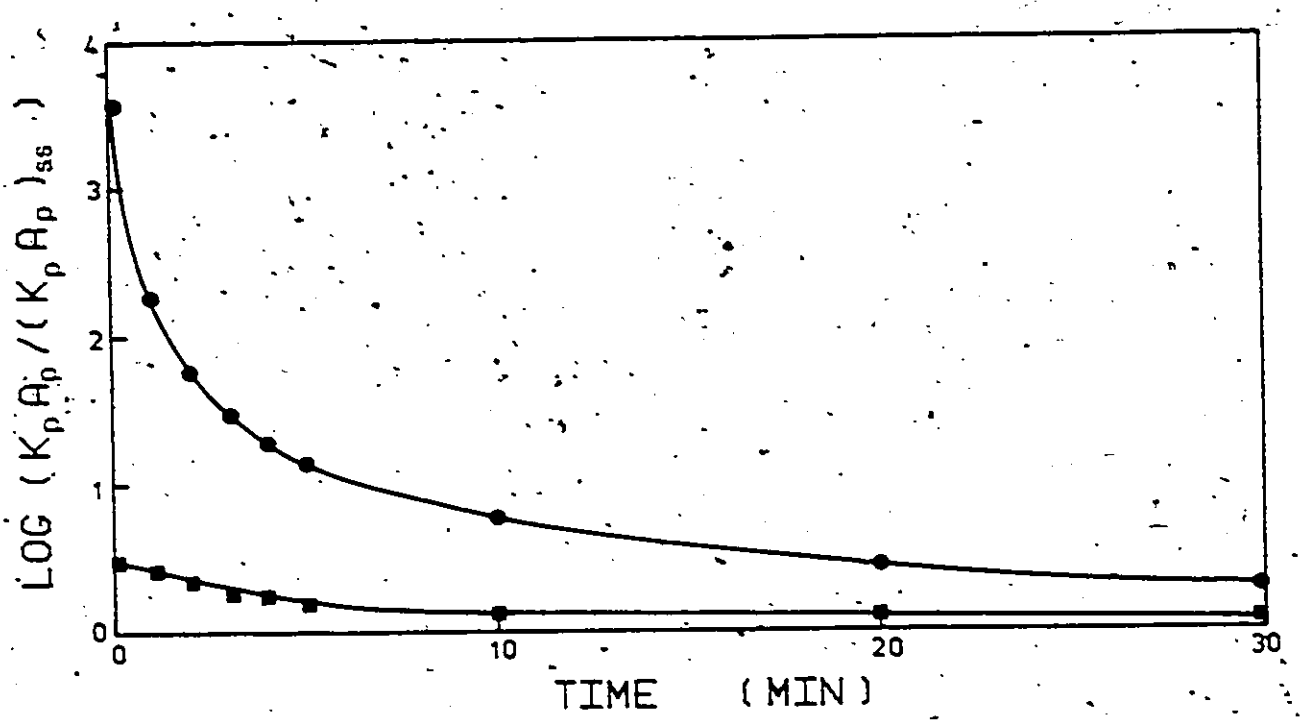

Figure F-1. Variation of Calculated Mass Transfer Coefficients with Time.
(■ - QDF equation; ● - Linear equation)

cases calculate a significant intraparticle resistance, and therefore a finite rate of uptake, even at t = 0. In fact the rate of uptake at t = 0, both observed in practice and predicted by equations (F.5) and (2.16), is infinite. Consequently, when using the linear driving force approximation, the calculated initial uptake rate is less than would be predicted if external film resistance alone were the controlling mechanism. The error in the kinetic analysis arises because the value of k_f is typically measured by analysing the initial uptake rate data after correctly assuming negligible intraparticle resistance. When this value of k_f is applied to the model, and the program begins to fit values of k_p to match the remaining data, the program also calculates an initial intraparticle resistance thus the predicted initial rate of uptake is less than that shown by the data. By adjusting k_p to account for the initially incorrect slope, biased estimates of the mass transfer parameter are obtained.

As an example of the problem discussed above, in the phenol adsorption experiment reported by Famularo et al.(1978), where the linear driving force approximation was used, the computed initial slope of the curve fitted to the batch kinetic data can be calculated to be only about one half of what was intended based on the measured external film transfer coefficient. A mass balance at the particle's outer surface gives

$$k_f(c - c_s) = k_p \rho_c (q_s - \bar{q}) \qquad \text{(F.9)}$$

and Famularo calculated $k_f = 1.02 \times 10^{-2}$ cm/sec (0.61 cm/min); $k_p = 1.17 \times 10^{-5}$ cm/sec (0.0007 cm/min); $c_o = 1.4 \times 10^{-3}$ m mole/cm^3 (1.4 m

mole/ℓ); and also $\rho_c = 0.75$ g/cm^3. At t = 0, no adsorbate has entered the carbon particle therefore $\dot{q} = 0$ thus,

$$1.02 \times 10^{-2}(1.4 \times 10^{-3} - c_s) = 1.17 \times 10^{-5} \times 0.75 \times q_s$$

or $$c_s = 10^{-3} (1.4 - 0.8603\ q_s) \qquad \text{(F.10)}$$

The values of c_s and q_s are also related through the equilibrium isotherm however and simultaneous solution of the isotherm and equation (F.10) gives

$$q_s = 0.84 \text{ m mole/g}$$

$$c_s = 0.686 \times 10^{-3} \text{ m mole/cm}^3$$

Thus although the assumed initial rate of uptake when calculating k_f was,

$$\dot{n}(o) = k_f (c - o)$$

the actual rate calculated by the model is

$$\dot{n}(o) = k_f (c - 0.686 \times 10^{-3})$$

and consequently, the initial slope predicted by the model is only about 50% of that required to fit the initial data.

The errors involved with the use of the linear driving force model do not arise with the QDF model and consequently it was the form chosen for use.

APPENDIX G

Quadratic Driving Force Column Model

The equations in dimensionless form which are to be solved are:

$$\frac{\partial C}{\partial z} = -\frac{(1-\varepsilon)}{\varepsilon} B_{i_f} (C - C_s) \qquad (6.4)$$

$$\frac{\partial Q_m}{\partial \theta} = \frac{3}{f}\left(\frac{Q_s^2 - Q_m^2}{2Q_m}\right) - \frac{B_{i_p}}{f}(Q_m - Q_b) \qquad (7.6)$$

$$\frac{\partial Q_b}{\partial \theta} = \frac{B_{i_p}}{(1-f)}(Q_m^2 - Q_b^2) \qquad (7.7)$$

$$Q_s = C_s^n \qquad (7.10)$$

These equations were solved using implicit finite difference and can be written in the following form.

$$\frac{C_{i,j+1} - C_{i-1,j+1}}{\Delta z} = -\frac{(1-\varepsilon)}{\varepsilon} B_{i_f} (C_{i,j+1} - C_{s,i,j+1}) \qquad (G.1)$$

$$\frac{Q^m_{i,j+1} - Q^m_{i,j}}{\Delta\theta} = \frac{3}{f}\left(\frac{Q^2_{s,i,j+1} - Q^{m^2}_{i,j+1}}{2Q^m_{i,j+1}}\right) - \frac{B_{i_p}}{f}(Q^m_{i,j+1} - Q^b_{i,j+1}) \qquad (G.2)$$

$$\frac{Q^b_{i,j+1} - Q^b_{i,j}}{\Delta\theta} = \frac{B_{i_p}}{(1-f)}(Q^m_{i,j+1} - Q^b_{i,j+1}) \qquad (G.3)$$

where $z = i\,\Delta z$, $\theta = j\,\Delta\theta$

If $FK1 = \frac{(1-\varepsilon)}{\varepsilon} B_{i_f}\,\Delta z$

$FK2 = \frac{3\,\Delta\theta}{f}$

$$FK2P = \frac{B_{i_p}\,\Delta\theta}{f}$$

$$FK3 = \frac{B_{i_p}\,\Delta\theta}{(1-f)}$$

the equations (G.1) to (G.3) can be written after some manipulation

$$C_{i,j+1} = \frac{1}{1+FK1}\,(C_{i-1,j+1} + FK1\,C_{s,i,j+1}) \qquad (G.4)$$

$$Q^{m^2}_{i,j+1}\,[\,2 + FK2 + 2FK2P\,(1 - \frac{FK3}{1+FK3})\,]$$

$$+ Q^{m}_{i,j+1}\,[\,-2\,Q^{m}_{i,j} - \frac{2FK2P}{1+FK3}\,Q^{b}_{i,j}\,]$$

$$- FK2\,Q^{2}_{s,i,j+1} = 0 \qquad (G.5)$$

$$Q^{b}_{i,j+1} = \frac{1}{1+FK3}\,(FK3\,Q^{m}_{i,j+1} + Q^{b}_{i,j}) \qquad (G.6)$$

and equations (7.8) and (7.10) can be combined to give:

$$B_{i_f}\,(C_{i,j} - C_{s,i,j}) = \frac{5}{F}\,(C^{2n}_{s,i,j} - Q^{m^2}_{i,j})/2\,Q^{m}_{i,j} \qquad (G.7)$$

The solution was obtained in the following manner. At any time interval j, the predicted future values of $C_{s,i,j+1}$ and $Q_{s,i,j+1}$ were calculated by linearly extrapolating the data at (j-1) and j using;

$$C^{(o)}_{s,i,j+1} = 2\,C_{s,i,j} - C_{s,i,j-1}$$

these values were then used in equations (G.4) to (G.6) to solve for C, Q_m and Q_b at (i,j+1) and equation (G.7) was then solved using Newton's method for the roots of a non-linear equation to obtain $C^{(1)}_{s,i,j+1}$. These improved estimates of C_s, Q_s were then resubstituted into equations (G.4) to (G.6) and the calculation repeated until convergence was obtained to a specified accuracy.

APPENDIX.H

COMPUTER PROGRAMS

H.1 DISCRETE MODEL BATCH KINETIC PROGRAM.

```
      PROGRAM BRANCH(INPUT,OUTPUT,TAPE5=INPUT,TAPE6=OUTPUT)
C-----------------------------------------------------------------------
C
C     PROGRAM BRANCH CALCULATES CONCENTRATION PROFILES ASSUMING
C     SOLID DIFFUSION IN MACRO PORES AND LINEARIZED DRIVING FORCE
C     INTO MICROSIZED PORES. PARTICLE IS DIVIDED INTO TWO DISTINCT
C     REGIONS BY PARAMETER FRAC. THE SOLUTION ALGORITHM IS .....
C
C     (A)   GUESS INITIAL VALUES
C
C     (B)   USE EXPANSION OF DZ/DF2=0 TO PREDICT FUTURE VALUES
C
C     (C)   SOLVE C-N EQUATIONS FOR FUTURE VALUES
C
C     (D)   SUBSTITUTE CORRECTED FUTURE VALUESAND RETURN TO (C)
C
C     (E)   UPDATE TIME STEP AND RETURN TO (B)
C
C     THE RADIUS IS TRANSFORMED BY INTRODUCING THE VARIABLE R=(RADIUS)**2
C     WHICH GIVES A GREATER CONCENTRATION OF GRID POINTS NEAR THE SURFACE
C-----------------------------------------------------------------------
      DIMENSION TH(3),SIGNS(3),DIFF(3),SCRFY(200)
      COMMON /A/ NPROB,NOB,NP,XC(100)
      COMMON /BC/ TT,DT,V,W,C0,F,G0,AF,DS,BK,KF,PHOC,POR
      COMMON /DZ/Z0(3),FRAC,NCYC,DP
      COMMON PT(100)
      EXTERNAL MODIL
      REAL KF
C-----------------------------------------------------------------------C
C
C     SET UP PARAMETERS FOR NON-LINEAR LEAST SQUARES REGRESSION
C     ROUTINE (UNHAUS - MACMASTER UNIVERSITY COMPUTING CENTRE)
C
      DATA SIGNS(1),SIGNS(2),SIGNS(3) /1.,1.,1./
      DATA DIFF(1),DIFF(2),DIFF(3) / .01,.01,.01 /
      DATA EPS1,EPS2,MIT,FLAM,FNU /5.E-4,1.E-2,20,0.1,10. /
C-----------------------------------------------------------------------C
C
      CALL READIN
      TH(1)=DS
      TH(2)=BK
      TH(3)=FRAC
      CALL DATAPLT(NPROB,TH,XC,NOB,NP)
      STOP
      END
```

```
      SUBROUTINE READIN
C*****************************************************************C
C
C     ALL INPUT VARIABLES IN C.G.S. UNITS EXCEPT FOR RT IN MINUTES
C
C     NPROB          ARBITRARY PROBLEM NO.
C     NOB            NO. OF DATA PAIRS
C     NP             NO. OF PARAMETERS REGRESSED
C     NR             NO. OF RADIAL INCREMENTS
C     TT             TOTAL LENGTH OF EXPERIMENT IN SEC
C     DT             TIME STEP LENGTH ,SEC
C     DS             INITIAL GUESS OF SURFACE DIFFN. COEFF.,CM**2/SEC
C     BK             INITIAL GUESS OF MICROPORE TRANSPORT COEFF.,SEC-1
C     KF             EXTERNAL FILM COEFF.,CM/SEC
C     V              REACTOR VOLUME,CM**3
C     W              MASS OF CARBON IN REACTOR,G
C     C0             INITIAL LIQUID PHASE CONC.,G/CM**3
C     R              RADIUS OF ADSORBENT PARTICLE
C     EQ(I)          EQUILIBRIUM PARAMETERS, Q=EQ(1)*CE**EQ(2)
C     RHOC           APPARENT ADSORBENT PARTICLE DENSITY, G/CM**3
C     FRAC           PARAMETER DIVIDING MACRO AND MICROPORE CAPACITIES
C     NCYC           LIMIT ON ITERATION LOOP, NORMALLY 4
C     XC             LIQUID PHASE CONC. DATA IN REDUCED UNITS
C     RT             TIME OF DATA POINT COLLECTION, MIN.
C*****************************************************************C
      COMMON /A/ NPROB,NOB,NP,XC(100)
      COMMON /BC/ TT,DT,V,W,C0,R,DD,NR,DS,BK,KF,RHOC,POR
      COMMON /D/EQ(3),FRAC,NCYC,DF
      COMMON RT(100)
      REAL KF
      READ(5,*) NPROB,NOB,NP,NR
      READ(5,*)  TT,DT,DS,BK,KF
      READ(5,*) V,W,C0,R
      READ(5,*) EQ(1),EQ(2),EQ(3),RHOC
      READ(5,*)FRAC,NCYC
      READ(5,*)  (XC(I),I=1,NOB)
      READ(5,*)  (RT(I),I=1,NOB)
      DO 10 I=1,NOB
 10   RT(I)=RT(I)*60.
      DD=EQ(1)*C0**EQ(2)
      WRITE(6,1)
 1      FORMAT(1H1,////)
      PRINT*,' PROGRAM BRANCH OUTPUT '
      PRINT*,NPROB,NOB,NR,NP,TT,DT,DS,BK,KF,V,W,C0,DD,R,EQ,RHOC
      PRINT*, NPROB,NOB,NR,NP,TT,DT,DS,BK,KF,V,W,C0,DD,R,EQ,RHOC
      PRINT*,FFRAC,NCYC   ,FRAC,NCYC
      WRITE(6,*)(XC(I),RT(I),I=1,NOB)
1000  FORMAT(5F10.5)
1001  FORMAT(5I10)
      RETURN
      END


      SUBROUTINE MODEL(NPROB,TH,X,NOB,NZ)
C*****************************************************************C
C
C     MODEL SOLVES BRANCHED PORE EQUATIONS USING CRANK-NICHOLSON
C     FINITE DIFFERENCE ANALOGS. PROGRAM HAS FACILITY FOR ALTERING
C     TIME STEP LENGTH DURING EXECUTION VIA DTO.
C
C*****************************************************************C
      COMMON /BC/ TT,DT,V,W,C0,R,DD,NR,DS,BK,KF,RHOC,POR
      COMMON /D/EQ(3),FRAC,NCYC,DF
      COMMON /GG/ Y1(101),Y2(101),Y3(101),QB(101),QBF(101),Q(101)
      COMMON RT(100)
      DIMENSION X(100),TH(NZ)
      DIMENSION DF(101),G(101),X1(101),X2(101),X3(101)
      REAL KF
      LOGICAL FLAG
      FUNC(A1,A2,A3,A4)=((1.-A1)*A2+A1*(A3+A4))/(1.+A1)
```

```
      DS=TH(1)
      BK=TH(2)
      FRAC=TH(3)
      IF(FRAC.EQ.1.) BK=0.
      DRIVF=2.
      GAM=999.
      KC=1
      NIT=INT(TT/DT)
      PRINT*,'NIT = ',NIT
      T=0.
      DTO=DT
      FLAG=.T.
      DR=1./FLOAT(NR)
      NRP1=NR+1
      RNP1=FLOAT(NRP1)
      RNR=FLOAT(NR)
      DO 10 J=1,NRP1
        C(J)=0.
        DR(J)=0.
        DBF(J)=0.
10    CONTINUE
      XB=1.
      XF=XB
      XS=0.
      XSF=XS
C
C*****************************************************************C
C
C     XB IS BULK LIQUID CONCENTRATION IN DIMLESS. UNITS. A PREDICTOR
C     EQUATION IS TO BE USED TO EVALUATE THE INITIAL GUESSES AT EACH NEW
C     ITERATION.  THE FORM TO BE USED IS AN EXPANSION OF D2C/DR2 = 0
C     I. E.    Z(I+1)=Z(I)*2 - Z(I-1) OR Z(I+1) = Z(I) + DELC
C
C     CALCULATE THE SYSTEM CONSTANTS
C
C*****************************************************************C
C
102   SHN=KF*CB*R/RHOC/DS/DB/FRAC
      A=2.*DS*DTO/F/R/DR
      B=BK*DTO/2./FRAC
      AREA=1.5*KF*K*DTO/V/F/RHOC
      HMULT=    (PHI+.75)*A*CF*SHN
      IF(FRAC.NE.1.) GAM=FRAC*B/(1.-FRAC)
      PRINT*,'SHN,A,B,AREA,HMULT,GAM'
      PRINT*, SHN,A,B,AREA,HMULT,GAM
C
C*****************************************************************C
C
C     CALCULATE X, Y MATRICES WHERE X*CF = Y*C+B*(DB+DBF)+H.
C     AT EACH ITERATION DBF AND H ARE PREDICTED AND ITERATION
C     CONTINUES UNTIL CONVERGED RESULT IS OBTAINED
C
C*****************************************************************C
C
      DO 20 J=2,NR
        RJ=FLOAT(J-1)
        X1(J)=1.+2.*A*RJ+B
        X2(J)=-(RJ+.75)*A
        X3(J)=(RJ+.75)*A
        Y1(J)=2.-X1(J)
        Y2(J)=-X2(J)
        Y3(J)=-X3(J)
20    CONTINUE
      X1(1)=1.+1.5*A+B
      X2(1)=-1.5*A
      Y1(1)=2.-X1(1)
      Y2(1)=-X2(1)
      X1(NRP1)=1.+2.*RNP*A+B
      X3(NRP1)=-2.*RNP*A
      Y1(NRP1)=2.-X1(NRP1)
      Y3(NRP1)=-X3(NRP1)
100   CONTINUE
      T=T+DTO
```

```
      DO 40 I=1,NCYC
        HTERM=HFUNCT(DIVF
        CALL GMAKE(HTERM,B,NRP1,G)
        CALL TRIDIAG(OF,G,X1,X2,X3,NRP1)
        IF(FRAC.EQ.1.) GO TO 55
        DO 50 K=1,NRP1
          OBF(K)=FUNC(GAM,OB(K),OF(K),Q(K))
   50   CONTINUE
   55   CONTINUE
        XSF=OF(NRP1)**(1./EQ(2))
        XF=FUNC(AREA,XB,XSF,XS)
        DELXF=XB-XS*XF-XSF
   40 CONTINUE
      IF(T.GE.PT(KC)) GO TO 60
      GO TO 61
   60 X(KC)=XB+(T-PT(KC))*(XB-XF)/DTO
      KC=KC+1
      IF(KC.GT.NOB) GO TO 65
   61 CONTINUE
C*****************************************************************C
C
C     CALCULATES PREDICTED VALUES AT NEXT TIME AND TRANSFERS NEWLY
C     CALCULATED VALUES INTO PRESENT TIME
C*****************************************************************C
C
        DELX=XF-XB
      XB=XF
      XF=XB+DELX
        DELXS=XSF-XS
        XS=XSF
        XSF=XS+DELXS
        DO 62 J=1,IPP1
          Q(J)=OF(J)
          IF(OBF(J).LE.0.) GO TO 63
          DELOB   =OBF(J)-OB(J)
          OB(J)=OBF(J)


          OBF(J)=OB(J)+DELOB
          GO TO 62
   63     OBF(J)=0.
   62     CONTINUE
      IF(FLAG) GO TO 30
      IF(T.GE.80000.) GO TO 101
   30 CONTINUE
      GO TO 100
  101 DTO=60.
      FLAG=.
      GO TO 102
   65 WRITE(6,1000)(X(I),PT(I),I=1,NOB)
 1000  FORMAT(10X,F12.6,10X,F12.6)
      RETURN
      END



      SUBROUTINE GMAKE(HTERM,B,LIM,G)
C*****************************************************************C
C
C     GENERATES VECTOR 'G' FOR SUBROUTINE TRIDIAG
C*****************************************************************C
C
      COMMON /GG/ Y1(101),Y2(101),Y3(101),OB(101),OBF(101),Q(101)
      DIMENSION G(101)
      LM1=LIM-1
      G(1)=Y1(1)*Q(1)+Y2(1)*Q(2)+B*(OB(1)+OBF(1))
      DO 10 J=2,LM1
        G(J)=Y1(J)*Q(J)+Y2(J)*Q(J+1)+Y3(J)*Q(J-1)+B*(OB(J)+OBF(J))
   10 CONTINUE
      G(LIM)=Y1(LIM)*Q(LIM)+Y3(LIM)*Q(LM1)+B*(OB(LIM)+OBF(LIM))+HTERM
      RETURN
      END
```

```
      SUBROUTINE TRIDIAG(VF,G,A1,A2,A3,NRP1)
C*****************************************************************C
C     THE EQUATION A*VF=G IS SOLVED USING THE THOMAS ALGORITHM FOR TRIDIAGONAL
C     MATRICES TO GIVE THE FUTURE CONCENTRATION VECTOR VF
C*****************************************************************C
      DIMENSION VF(NPP1),G(NRP1),A1(NRP1),A2(NPP1),A3(NRP1)
      DIMENSION U(101),Y(101),Z(101)
      U(1)=A1(1)
      DO 90 K=2,NPP1
      Y(K-1)=A2(K-1)/U(K-1)
   90 U(K)=A1(K)-A3(K)*Y(K-1)
      Z(1)=G(1)/U(1)
      DO 40 K=2,NPP1
   40 Z(K)=(G(K)-A3(K)*Z(K-1))/U(K)
      VF(NPP1)=Z(NPP1)
      DO 50 K=2,NPP1
      II=NPP1+1-K
   50 VF(II)=Z(II)-Y(II)*VF(II+1)
      RETURN
      END
```

H.2 DISCRETE MODEL COLUMN PROGRAM

```
      PROGRAM COLSOL(INPUT,OUTPUT,TAPE5=INPUT,TAPE6=OUTPUT,TAPE1,TAPE2)
C*****************************************************************
C     THIS PROGRAM SOLVES AXIAL FLOW EQUATIONS IN A FIXED BED ADSORBER.
C     EXTERNAL FILM RESISTANCE AND INTRAPARTICLE DIFFUSION AS DESCRIBED
C     BY A BRANCHED PORE MODEL ARE USED.  THE MODEL SOLUTION HAS THE FORM
C     X(N)*OF(N+1)=G(N) WHERE THE SOLUTION IS OBTAINED ITERATIVELY AND
C     X AND G ARE UPDATED ON EACH SUCCESSIVE ITERATION.  OF(N+1) IS SOLVED
C     FOR USING THE THOMAS ALGORITHM.  OF=(OF(1),.....OF(M),C).
C     CRANK-NICHOLSON EXPANSION FORMULA ARE USED TO DISCRETIZE THE PARTICLE
C     DIFFUSION EQUATION AND IMPLICIT BACKWARD FINITE DIFFERENCE IS USED
C     IN THE FLUID PHASE SOLUTION.
C
C     THE SOLUTION ASSUMES THE FOLLOWING.....
C        (A)    AXIAL DISPERSION IS NEGLIGIBLE
C        (B)    RADIAL GRADIENTS ARE NONEXISTENT IN FLUID PHASE
C        (C)    CARBON PARTICLES ARE UNIFORM AND SPHERICAL
C        (D)    EQUILIBRIUM IS DESCRIBED BY A FREUNDLICH ISOTHERM
C
C      PARAMETERS ARE AS DEFINED IN OUTPUT OF SUBROUTINE READIN
C*****************************************************************
      COMMON CL,NZ,R,NR,RHOB,RHOC,CF,EQ(2),NCYC,DS,BK,FRAC,CB,V,KF
      COMMON CO,NIT,DR,DZ,NRP1,NRP2,NZP1,SHN,A,B,A1,B1,EXR,RNP,RNR,GTERM
      COMMON VEL,QQ(101,22),QBF(101,22),Q(101,22),QF(101,22),C(101)
      COMMON CF(101),X1(22),X2(22),X3(22),Y1(22),Y2(22),Y3(22),G(22)
      COMMON TT,DT,XSA,EPS,CTHETA,GAM ,TPRINT,QFR(22)
      REAL KF
      DIMENSION CSTORE(400,3)
      FUNC(F1,F2,F3,F4)=((1.-F1)*F2+F1*(F3+F4))/(1.+F1)
```

```
      ERR=1.0E-10
      TMIN=0.
      N=18
      IPLOT=0
      CALL READIN
      CALL CONSTS
      CALL SETINIT
      CALL VTSET
      MULT=NIT/300 +1
      IMNZ=NZ/2 + 1
      IZZ=TT*1440./10.
      WRITE(1) IZZ
      IPROF=IFIX(TT*1440./TPRINT) + 1
C     WRITE(2)IPROF,NZP1
      PMUL=10./DT
      NMULT=IFIX(PMULT)
C*****************************************************************
C     COMMENCE ITERATIONS IN TIME
C*****************************************************************
C
      DO 100 ITIME=1,NIT
      IF((ITIME/PMULT)*MULT.NE.ITIME) GO TO 99
      IPLOT=IPLOT+1
      CSTORE(IPLOT,1)=Q(NZP1,NRP2)
      CSTORE(IPLOT,2)=TMIN
      CSTORE(IPLOT,3)=Q(IMNZ,NRP2)
 99   CONTINUE
      TMIN=TMIN+DT
C*****************************************************************
C
C
C     COMMENCE ITERATIONS ALONG THE BED
C*****************************************************************
C
      IZ=2
      IF(Q(2,NRP2).GT..9999) GO TO 204
        CALL VBSET(IZ)
        CALL GMAKE(IZ)
      DO 205 J=1,NRP2
 205  GPR(J)=G(J)+B*QBF(IZ,J)
      DO 201 ICYC=1,NCYC
      OST=QF(IZ,NRP1)
        CALL TRIDIAG(IZ)
        QF(1,NRP1)=QF(2,NRP1)
      IF(ABS(OST-QF(IZ,NRP1)).LT.ERR) GO TO 204
      Z=QF(IZ,NRP1)**EXP
      X1(NRP1)=1.+2.*A*RNR+B+GTERM*Z
      X2(NRP2)=-B1*Z
        IF(FRAC.EQ.1.) GO TO 203
          DO 202 II=1,NRP1
          QBF(IZ,II)=FUNC(GAM,QB(IZ,II),QF(IZ,II),Q(IZ,II))
      GPR(II)=G(II)+B*QBF(IZ,II)
 202      CONTINUE
 203    CONTINUE
 201  CONTINUE
 204  CONTINUE
      DO 700 IZ=3,NZP1
      IF(Q(IZ,NRP2).GT..9999) GO TO 208
        CALL VBSET(IZ)
        CALL GMAKE(IZ)
      DO 340 J=1,NRP2
 340  GPR(J)=G(J)+B*QBF(IZ,J)
      DO 300 ICYC=1,NCYC
      OST=QF(IZ,NRP1)
        CALL TRIDIAG(IZ)
      IF(ABS(OST-QF(IZ,NRP1)).LT.ERR) GO TO 301
      Z=QF(IZ,NRP1)**EXP
      X1(NRP1)=1.+2.*A*RNR+B+GTERM*Z
      X2(NRP2)=-B1*Z
        IF(FRAC.EQ.1.) GO TO 310
          DO 320 II=1,NRP1
          QBF(IZ,II)=FUNC(GAM,QB(IZ,II),QF(IZ,II),Q(IZ,II))
      GPR(II)=G(II)+B*QBF(IZ,II)
 320      CONTINUE
 310    CONTINUE
```

```
C*****************************************************************
C
C     CHECK FOR CONVERGENCE AND LEAVE LOOP IF OBTAINED
C
C*****************************************************************
C
  300  CONTINUE
  301  CONTINUE
       IF(DF(I7,NRP2).LT..005) GO TO 330
  200  CONTINUE
  330  CONTINUE
C*****************************************************************
C
C     PREDICT FUTURE VALUES OF DF AND DBF TO BEGIN NEXT ITERATION LOOP.
C
C*****************************************************************
C
       IF(FRAC.EQ.1.) GO TO 420

       DO 400 I=1,NZP1
          DD=DF(I,NRP1)-D(I,NRP1)
          DO 410 J=1,NRP2
          DELDB=DBF(I,J)-DB(I,J)
          DB(I,J)=DBF(I,J)
          DBF(I,J)=DB(I,J)+DELDB
  410     D(I,J)=DF(I,J)
  400  DF(I,NRP1)=D(I,NRP1)+DD
       GO TO 430
  420  DO 440 I=1,NZP1
          DD=DF(I,NRP1)-D(I,NRP1)
          DO 450 J=1,NRP2
          D(I,J)=DF(I,J)
  450  DF(I,NRP1)=D(I,NRP1)+DD
  430  CONTINUE
       IF((ITIME/NMULT)*NMULT.NE.ITIME) GO TO 98
       WRITE(1) D(IHRZ,NRP2),D(NZP1,NRP2),TMIN
   98  CONTINUE
       IF(ITIME.EQ.1) GO TO 501
       IF(IFIX(TMIN/TPRINT)*TPRINT.NE.TMIN) GO TO 100
  501  PRINT*,' TIME IN MINUTES = ',TMIN
       PRINT*,(D(I,NRP2),I=1,NZP1)
       N=N+1
       DO 500 JJ=1,NZP1
       XXX=FLOAT(JJ)
       YYY=D(JJ,NRP2)
C      WRITE(2)  XXX,YYY,TMIN
       IF(YYY.GT.1.0)  YYY=1.0
  500  CALL PLOTPT((XXX,YYY,N)
  100   CONTINUE
       CALL OUTPLT
       DO 600 I=1,IPLOT
       IF(CSTORE(I,1).GT.1.0) CSTORE(I,1)=1.0
  600  CALL PLOTPT((STORE(I,2),CSTORE(I,1),1)
       CALL OUTPLT
       DO 700 I=1,IPLOT
       IF(CSTORE(I,3).GT.1.0) CSTORE(I,3)=1.0
  700  CALL PLOTPT((CSTORE(I,2),CSTORE(I,3),1)
       CALL OUTPLT
       END FILE 1
       END FILE 2
       STOP
       END
```

```
      SUBROUTINE READIN
C*****************************************************************
C
C     ALL INPUT PARAMETERS ARE READ UNDER FREE FORMAT SPECIFICATION
C
C*****************************************************************
      COMMON CL,NZ,R,NR,RHOB,RHOC,CR,EQ(2),NCYC,DS,BK,FRAC,CO,V,KF
      COMMON QQ,NIT,DR,DZ,NRP1,NRP2,NZP1,SHN,A,B,A1,B1,EXR,RNP,RNR,STEPM
      COMMON VEL,QB(101,22),CRF(101,22),Q(101,22),QF(101,22),C(101)
      COMMON CF(101),X1(22),X2(22),X3(22),Y1(22),Y2(22),Y3(22),G(22)
      COMMON TT,DT,XSA,EPS,CTHETA,GAM ,TPRINT,GFR(22)
      COMMON /R/ DFREE
      REAL KF
      READ(5,*)     CL,NZ
      READ(5,*)     R,NR
      READ(5,*)     V,CF
      READ(5,*)     RHOB,RHOC
      READ(5,*)     DS,BK,FRAC
      READ(5,*) DFREE
      READ(5,*)     CO
      READ(5,*)     (EQ(I),I=1,2)
      READ(5,*)     NCYC
      READ(5,*)     TT,DT
      READ(5,*) TPRINT
C     PRINT OUT VALUES WITH LABELS TO VERIFY INPUT DATA AND UNITS
      WRITE(6,1000)
      PRINT*,'CL    =',CL,' CMS COLUMN LENGTH'
      PRINT*,'NZ    =',NZ,' AXIAL INCREMENTS'
      PRINT*,'NR    =',NR,' RADIAL INCREMENTS'
      PRINT*,'R     =',R,' CMS PARTICLE RADIUS'
      PRINT*,'V     =',V,' CM**3/SEC VOLUMETRIC FLOWRATE'
      PRINT*,'CR    =',CR,' CMS COLUMN RADIUS'
      PRINT*,'RHOB  =',RHOB,' GM/CM**3 PACKED BED DENSITY'
      PRINT*,'RHOC  =',RHOC,' GM/CM**3 APPARENT PERTICLE DENSITY'
      PRINT*,'DS    =',DS,' CM**2/SEC PARTICLE DIFFUSIVITY'
      PRINT*,'BK    =',BK,' SEC**(-1) BRANCH PORE M. T. RATE'
      PRINT*,'FRAC  =',FRAC,' PARTICLE PARTITIONING FRACTION'
      PRINT*,'CO    =',CO,' GM/CM**3 FEED CONCENTRATION'
      PRINT*,'EQ(I)=',EQ(1),EQ(2),' EQUIL. COEFFS. Q=EQ(1)*C**EQ(2)'
      PRINT*,'NCYC  =',NCYC,' MAX. NO. ITERATIONS PER STEP'
      PRINT*,'DFREE=',DFREE,' FREE LIQUID DIFFUSIVITY  CM**2/SEC'
      PRINT*,'TT,DT =',TT,DT,' RUN TIME IN DAYS, STEP TIME IN MIN.'
      PRINT*,'TPRINT =',TPRINT,' MINUTES BETWEEN EACH PLOTTED PROFILE'
 1000  FORMAT(1H1,///,32H INPUT PARAMETERS ARE AS FOLLOWS ,//)
      RETURN
      END


      SUBROUTINE CONSTS
C*****************************************************************
C
C     CALCULATES ALL PARAMETER GROUP CONSTANTS
C     FILM TRANSFER COEFF. IS BASED ON CORRELATION OF WILSON AND
C     GEANKOPOLIS FOR LOW REYNOLDS NUMBER FLOW. WATER WITH DENSITY
C     1. GM/C**3 AND VISCOSITY 0.01 POISE IS ASSUMED. FREE LIQUID
C     DIFFUSIVITY IS AN INPUT VARIABLE.
C
C*****************************************************************
      COMMON CL,NZ,R,NR,RHOB,RHOC,CR,EQ(2),NCYC,DS,BK,FRAC,CO,V,KF
      COMMON QQ,NIT,DR,DZ,NRP1,NRP2,NZP1,SHN,A,B,A1,B1,EXR,RNP,RNR,STEPM
      COMMON VEL,QB(101,22),CRF(101,22),Q(101,22),QF(101,22),C(101)
      COMMON CF(101),X1(22),X2(22),X3(22),Y1(22),Y2(22),Y3(22),G(22)
      COMMON TT,DT,XSA,EPS,CTHETA,GAM ,TPRINT,GFR(22)
      COMMON /R/ DFREE
      REAL KF
      QQ=EQ(1)*CO**EQ(2)
      NIT=INT(TT*24.*60./DT)
      XSA=3.142*CR*CR
      EPS=1.-RHOB/RHOC
      VEL=V/XSA/EPS
      RE=VEL*EPS*2.*R/0.01
      SC=0.01/DFREE
      SH=1.00*(RE*SC)**0.3333/EPS
      KF=SH*DFREE/2./R
```

```
      DTHETA=DT*60.*CS/R/R
      DR=1./FLOAT(NR)
      DZ=CS*CL/VEL/F/R/FLOAT(NZ)
      NRP1=NR+1
      NRP2=NR+2
      NZP1=NZ+1
      SHN=KF*CO*R/RHOCC/CS/CO/FRAC
      A=2.*DTHETA/DP
      IF(FRAC.EQ.1.) BK=0.0
      B=BK*DTHETA*CS*F/2./FRAC/CS
      A1=3.*KF*RHOE*R/EPS/RHOCC/CS
C     B1=A1*C7/2.
      B1=A1*DZ
      EXP=1./E0(2)-1.
      RNP=FLOAT(NRP1)
      RNR=FLOAT(NR)
      GTERM=(RNR+0.75)*A*DP*SHN
      GAM=999.
      IF(FRAC.NE.1.) GAM=FRAC*B/(1.-FRAC)
      PRINT*,'KF   =',KF,' CM/SEC  FILM TRANSFER COEFF.='
      PRINT*,'DO,NIT,DR,DZ,NRP1,NRP2,NZP1,SHN,A,B,A1,B1='
      PRINT*, DO,NIT,DR,DZ,NRP1,NRP2,NZP1,SHN,A,B,A1,B1
      PRINT*,'EXR,RNP,RNR,GTERM,GAM,VEL,XSA,EPS='
      PRINT*, EXR,RNP,RNR,GTERM,GAM,VEL,XSA,EPS
      RETURN
      END


      SUBROUTINE SETINIT
C*****************************************************************
C
C     SET ALL INITIAL VALUES
C
C*****************************************************************
      COMMON CL,NZ,P,NR,RHOP,FHOC,CP,E0(2),NCYC,DS,BK,FRAC,CO,V,KF
      COMMON DO,NIT,DR,DZ,NRP1,NRP2,NZP1,SHN,A,B,A1,B1,EXP,RNP,RNR,GTERM
      COMMON VEL,D(101,22),CBF(101,22),O(101,22),OF(101,22),C(101)
      COMMON CF(101),X1(22),X2(22),X3(22),Y1(22),Y2(22),Y3(22),G(22)
      COMMON TT,CT,XSA,EPS,DTHETA,GAM ,TPRINT,GFR(22)
      DO 10 J=1,NZP1
         DO 20 I=1,NRP2
         OB(J,I)=0.0
         OBF(J,I)=0.0
         O(J,I)=0.0
20       OF(J,I)=0.0
10    CONTINUE
      O(1,NRP2)=1.
      OF(1,NRP2)=1.
      DO 30 J=2,NZP1
      O(J,NRP2)=O(J-1,NRP2)/(1.+B1)
30    OF(J,NRP2)=O(J,NRP2)
      RETURN
      END
```

```
      SUBROUTINE VTSET
C*****************************************************************C
C
C     THIS SUBROUTINE SETS UP THE TRIDIAGONAL MATRIX ELEMENTS WHICH ARE
C     NOT RECALCULATED AT EACH ITERATIVE STEP.
C
C*****************************************************************C
C
      COMMON CL,NZ,R,NR,RHOB,FMCC,CR,EO(2),NCYC,DS,BK,FRAC,CO,V,KF
      COMMON CO,NIT,DR,DZ,NRP1,NRP2,NZP1,SMN,A,E,A1,B1,EXR,RNP,RNR,GTERM
      COMMON VEL,OB(101,22),OBF(101,22),O(101,22),OF(101,22),C(101)
      COMMON CF(101),X1(22),X2(22),X3(22),Y1(22),Y2(22),Y3(22),G(22)
      COMMON TT,DT,XSA,EPS,CTHETA,GAM ,TPRINT,GPR(22)
      DO 20 J=2,NR
      RJ=FLOAT(J-1)
      X1(J)=1.+2.*A*RJ+B
      X2(J)=-(RJ+0.75)*A
      X3(J)=(-RJ+0.75)*A
      Y1(J)=2.-X1(J)
      Y2(J)=-X2(J)
      Y3(J)=-X3(J)
 20   CONTINUE
      X1(1)=1.+1.5*A+B
      X2(1)=-1.5*A
      Y1(1)=2.-X1(1)
      Y2(1)=-X2(1)
      X2(NRP1)=-GTERM
      X3(NRP1)=-2.*A*RNR
      Y2(NRP1)=-X2(NRP1)
      Y3(NRP1)=-X3(NRP1)
      X1(NRP2)=1.+B1
      Y1(NRP2)=-X1(NRP2)
C     Y1(NRP2)=1.-E1
      RETURN
      END
```

```
      SUBROUTINE GRAKE(I)
C*****************************************************************C
C
C     SUBROUTINE SETS UP VECTOR G TO BE USED IN SUBROUTINE TRIDIAG
C
C*****************************************************************C
C
      COMMON CL,NZ,R,NR,RHOB,FMCC,CR,EO(2),NCYC,DS,BK,FRAC,CO,V,KF
      COMMON CO,NIT,DR,DZ,NRP1,NRP2,NZP1,SMN,A,E,A1,B1,EXR,RNR,RNR,GTERM
      COMMON VEL,OB(101,22),OBF(101,22),O(101,22),OF(101,22),C(101)
      COMMON CF(101),X1(22),X2(22),X3(22),Y1(22),Y2(22),Y3(22),G(22)
      COMMON T,DT,XSA,EPS,CTHETA,GAM ,TPRINT,GPR(22)
      G(1)=Y1(1)*O(I,1)+Y2(1)*O(I,2)+B*(OB(I,1)
C     G(1)=Y1(1)*O(I,1)+Y2(1)*O(I,2)+B*(OB(I,1)+OBF(I,1))
      DO 10 K=2,NR
      G(K)=Y1(K)*O(I,K)+Y2(K)*O(I,K+1)+Y3(K)*O(I,K-1)+B*(OB(I,K))
C     G(K)=Y1(K)*O(I,K)+Y2(K)*O(I,K+1)+Y3(K)*O(I,K-1)+B*(OB(I,K)+
C    1   OBF(I,K))
 10   CONTINUE
      G(NRP1)=Y3(NRP1)*O(I,NR)+Y1(NRP1)*O(I,NRP1)+Y2(NRP1)*O(I,NRP2)
     1   +B*(OB(I,NRP1))
C     1   +B*(OB(I,NRP1)+OBF(I,NRP1))
      G(NRP2)=Y3(NRP2)*O(I,NRP1)+Y1(NRP2)*O(I,NRP2)+O(I-1,NRP2)
     1+OF(I-1,NRP2)
C     G(NRP2)=Y3(NRP2)*OF(I-1,NRP1)+Y1(NRP2)*OF(I-1,NRP2)
C     PRINT*,*G*,I,(G(J),J=1,NRP2)
      RETURN
      END
```

```
      SUBROUTINE TRIDIAG(I)
C*****************************************************************C
C
C     THE EQUATION X*VF=G IS SOLVED USING THE THOMAS ALGORITHM
C     FOR TRIDIAGONAL MATRICES.
C
C*****************************************************************C
      COMMON CL,NZ,R,NR,RHO9,PHCC,CF,EO(2),NCYC,DS,BK,FRAC,CB,V,KF
      COMMON OO,NIT,DR,DZ,NPP1,NPP2,NZP1,SHN,A,E,A1,B1,EXR,RNP,RNR,GTERM
      COMMON VEL,OF(101,22),OBF(101,22),O(101,22),OF(101,22),C(101)
      COMMON CF(101),X1(22),X2(22),X3(22),Y1(22),Y2(22),Y3(22),G(22)
      COMMON TT,DT,XSA,EPS,CTHETA,GAM ,TPRINT,GFR(22)
      DIMENSION  U(22),Y(22),Z(22),VF(22)
      U(1)=X1(1)
      DO 90 K=2,NPP2
      Y(K-1)=X2(K-1)/U(K-1)
   90 U(K)=X1(K)-X3(K)*Y(K-1)
      Z(1)=GFR(1)/U(1)
      Z(1)=G(1)/U(1)
C
      DO 60 K=2,NPP2
C     Z(K)=(GFR(K)-X3(K)*Z(K-1))/U(K)
   60 Z(K)=(G(K)-X3(K)*Z(K-1))/U(K)
      VF(NPP2)=Z(NPP2)
      DO 50 K=2,NPP2
      II=NPP2+1-K
   50 VF(II)=Z(II)-Y(II)*VF(II+1)
      DO 60 J=1,NPP2
   60 OF(I,J)=VF(J)
C     PRINT*,'VFF',I,(VF(J),J=1,NPP2)
      RETURN
      END
```

```
      SUBROUTINE VSET(I)
C*****************************************************************C
C
C     CALCULATES MATRIX DIAGONAL ELEMENTS WHICH ARE RECALCULATED ON
C     EACH ITERATIVE STEP.
C
C*****************************************************************C
      COMMON CL,NZ,R,NR,RHO9,PHCC,CF,EO(2),NCYC,DS,BK,FRAC,CB,V,KF
      COMMON OO,NIT,DR,DZ,NPP1,NPP2,NZP1,SHN,A,E,A1,B1,EXR,RNP,RNR,GTERM
      COMMON VEL,OF(101,22),OBF(101,22),O(101,22),OF(101,22),C(101)
      COMMON CF(101),X1(22),X2(22),X3(22),Y1(22),Y2(22),Y3(22),G(22)
      COMMON TT,DT,XSA,EPS,CTHETA,GAM ,TPRINT,GFR(22)
      Z=OF(I,NPP1)**EXR
      Z1=O(I,NPP1)**EXR
      X1(NPP1)=1.+2.*A*RNP+E+GTERM*Z
      Y1(NPP1)=1.-2.*A*RNP-E-GTERM*Z1
      X2(NPP2)=-B1*Z
      Y3(NPP2)=B1*Z1
      RETURN
      END
```

H.3 QUADRATIC DRIVING FORCE BATCH PROGRAM

```
      PROGRAM QDFSOL(INPUT,OUTPUT,TAPE5=INPUT,TAPE6=OUTPUT)
      DIMENSION TH(3),SIGNS(3),DIFF(3),SCRAT(200)
      COMMON /A/ NPROB,NOB,NF,XO(100)
      COMMON /B/TT,DT,V,W,QQ,CO,R,NP,KP,KB,KF,RHOC
      COMMON /C/ EQ(3),FRAC,ALPHA,BETA
      COMMON CT(100)
      EXTERNAL MODEL
      REAL KP,KB,KF,K1,K2,K3
C*****************************************************************C
C
C     SET UP PARAMETERS FOR NON-LINEAR LEAST SQUARES ROUTINE (UNHAUS -
C     MCMASTER UNIVERSITY COMPUTING CENTRE)
C*****************************************************************C
C
      DATA SIGNS(1),SIGNS(2),SIGNS(3) /1.,1.,1./
      DATA DIFF(1),DIFF(2),DIFF(3) / .01,.01,.01 /
      DATA EPS1,EPS2,MIT,FLAM,FNU /1.E-6,1.E-2,20,0.1,10. /
      CALL READIN
      TH(1)=KP
      TH(2)=KB
      TH(3)=FRAC
      CALL UNHAUS (NPROB,MODEL,NOB,XO,NP,TH,DIFF,SIGNS,EPS1,EPS2,MIT,
     1FLAM,FNU,SCRAT)
      CALL DATAPL (NPROB,TH,XO,NOB,NP)
      STOP
      END
C
C
C
      SUBROUTINE READIN
      COMMON /A/ NPROB,NOB,NF,XO(100)
      COMMON /B/TT,DT,V,W,QQ,CO,R,NP,KP,KB,KF,RHOC
      COMMON /C/ EQ(3),FRAC,ALPHA,BETA
      COMMON CT(100)
      REAL KP,KB,KF,K1,K2,K3
C*****************************************************************C
C
C     ALL PARAMETERS READ IN UNDER FREE FORMAT - C.G.S. UNITS
C*****************************************************************C
C
      READ(5,*) NPROB,NOB,NF
      READ(5,*) TT,DT,KP,KB,KF
      READ(5,*) V,W,CO,R
      READ(5,*) EQ(1),EQ(2),EQ(3),RHOC
      READ(5,*) FRAC
      IF(FRAC.EQ.1.) KB=0.0
      READ(5,*)  (XO(I),I=1,NOB)
      READ(5,*)  (CT(I),I=1,NOB)
      QQ=EQ(1)*CO**EQ(2)
      DO 10 I=1,NOB
   10   CT(I)=60.*CT(I)
      WRITE(6,1000)
 1000   FORMAT(1H1//* PROGRAM QDFSOL OUTPUT*///)
      PRINT*, NPROB,NOB,NP,TT,DT,KP,KB,KF,V,W,QQ,CO,R,EQ,RHOC,FRAC*
      PRINT*, NPROB,NOB,NF,TT,DT,KP,KB,KF,V,W,QQ,CO,R,EQ,RHOC,FRAC
        PRINT*,(XO(I),CT(I),I=1,NOB)
      RETURN
      END
```

```
      SUBROUTINE MODEL(NPROB,TH,X,NOB,NP)
      COMMON /B/TT,DT,V,W,DO,CO,P,RE,KP,KB,KF,PHOC
      COMMON /C/ EO(3),FRAC,ALPHA,BETA
      COMMON PT(100)
      REAL KP,KB,KF,K1,K2,K3
      DIMENSION X(100),TH(3) ,K1(4),K2(4),K3(4)
C*****************************************************************C
C
C     BRANCHED PORE MODEL SOLUTION USING QUADRATIC DRIVING FORCE APP-
C     ROXIMATION TO DESCRIBE MACROPORE TRANSPORT.  4TH ORDER RUNGE-KUTTA
C     USED TO SOLVE O.D.E.S AND NEWTON'S METHOD TO INVERT NON-LINEAR
C     EQUATION IN XSU.
C
C
      KC=1
      KP=TH(1)
      IF(NP.EQ.1) GO TO 11
      KB=TH(2)
      FRAC=TH(3)
   11  CONTINUE
      T=0.
      S=0.
      DS=KP*DT/D
      IF(ABS(FRAC-1.).LE.0.0001) KB=0.0
      BIF=W*KF/V/PHOC/KP
      BIP=KB*D/KP
      FAV=CO/W/DO
      BI=1./BIF/F
      PRINT*,*BIF,BIP,BI,F    *,BIF,BIP,BI,F
      OMP=1.0E-10    $      QBP=0.    $      XP=1.     $      XSP=1.0E-5
      LOOP=1
   20 FX=BI*XSP**(2.*EO(2)) + 2.*OMP*(XSP-XP) - BI*OMP**2
      FPX=2.*EO(2)*BI*XSP**(2.*EO(2)-1.) + 2.*OMP
      XN=XSP-FX/FPX
      IF(XN.LE.0.0) XN=XSP/10.
      IF(XN.GE.1.0) XN=(1.+XSP)/2.
      XSP=XN
      IF(ABS(FX/FPX/XN).LT.0.01) GO TO 23
      LOOP=LOOP+1
      IF(LOOP.GT.10) PRINT*,*LOOP GT 10*
      GO TO 20
   23  CONTINUE
      XSF=XSP
      PRINT*,*YSF,LOOP =*,XSF,LOOP
      FK1=3.*BIF
      FK2=3.*KPE/KF/FRAC
      FK2P=BIP/FRAC
      FK3=0.
      IF(FRAC.LT.1.)  FK3=BIF/(1.-FRAC)
  500 T=T+DT
      S=S+DS
      XU=XP    $      OMU=OMP    $      QBU=QBP    $      XSU=XSF
      DO 5 J=1,4
      K1(J)=FK1*(XSU-XU)
      K2(J)=FK2*(XSU**(2.*EC(2)) - OMU**2)/2./OMU - FK2P*(OMU-QBU)
      K3(J)=FK3*(OMU-QBU)
      GO TO (1,1,2,3),J
    1 XU=XP+DS*K1(J)/2.
      OMU=OMP+DS*K2(J)/2.
      QBU=QBP+DS*K3(J)/2.
      GO TO 6
    2  XU=XP+DS*K1(J)
      OMU=OMP+DS*K2(J)


      QBU=QBP+DS*K3(J)
      GO TO 6
    3  XU=XP+DS*(K1(1)+2.*K1(2)+2.*K1(3)+K1(4))/6.
      OMU=OMP+DS*(K2(1)+2.*K2(2)+2.*K2(3)+K2(4))/6.
      QBU=QBP+DS*(K3(1)+2.*K3(2)+2.*K3(3)+K3(4))/6.
    6  CONTINUE
    5 CONTINUE
      IF(EO(2).EQ.1.) GO TO 30
   12 FXSU=BI*XSU**(2.*EO(2)) + 2.*OMU*(XSU-XU) - BI*OMU**2
      FPXSU=2.*EO(2)*BI*XSU**(2.*EO(2)-1.) + 2.*OMU
      XSU=XSU-FXSU/FPXSU
```

```
      IF(XSU.LT.0.) XSU=1.0E-10
      IF(ABS(FXSU/FPXSU/XSU).GT.0.01) GO TO 12
      GO TO 31
   38  XSU=(-QMU+SQRT(QMU**2+BI*(2.*QMU*XU+BI*QMU**2)))/BI
   31  CONTINUE
   12 XF=XU
      QMF=QMU
      QBF=QBU
C     CALCULATE XSF OVER NEXT TIME INTERVAL BASED ON LINEAR EXTRAPOLATION
C     OF SLOPE OVER PREVIOUS INTERVAL.
      XSF=1.5*XSU-0.5*XSP
      XSP=XSU
      IF(T.GE.RT(KC)) GO TO 7
      GO TO 8
   7  X(KC)=XF+(T-RT(KC))*(XF-XF)/DT
      IF(KC.GE.NOB) GO TO 101
      KC=KC+1
   8  XP=XF
      QMP=QMF
      QBP=QBF
      GO TO 538
  101 WRITE(6,2000)(X(I),RT(I),I=1,NOB)
 2000   FORMAT(10X,F9.6,10X,F12.2)
      RETURN
      END
```

H.4 QUADRATIC DRIVING FORCE COLUMN PROGRAM

```
      PROGRAM QDFCOL(INPUT,OUTPUT,TAPE5=INPUT,TAPE6=OUTPUT,TAPE1,TAPE2)
C*****************************************************************
C
C     THIS PROGRAM SOLVES AXIAL FLOW EQUATIONS IN A FIXED BED ADSORBER.
C     EXTERNAL FILM RESISTANCE AND INTRAPARTICLE DIFFUSION AS DESCRIBED
C     BY A BRANCHED PORE MODEL ARE USED.  THE MODEL SOLUTION HAS THE FORM
C     RATE=CONSTANT*(SURFACE CONC.**2 - AVERAGE PARTICLE CONC**2)/(2*
C     AVERAGE PARTICLE CONC) FOR TRANSPORT
C     TO THE MACROPORES AND RATE=CONSTANT*(MACROPORE CONC - MICROPORE CONC)
C     FOR TRANSPORT INTO THE MICROPORES. THE SURFACE CONCENTRATION AT THE
C     MID INTERVAL IS PREDICTED BY LINEAR EXTRAPOLATION OF THE GRADIENT
C     OVER THE PREVIOUS INTERVAL AND IS ASSUMED CONSTANT OVER A GIVEN TIME
C     INTERVAL. THIS ELIMINATES THE NEED TO SOLVE THE SUFACE EQUATION ITERIVELY
C     BECAUSE OF THE NON-LINEAR NATURE OF THE EQUATION.
C
C     THE SOLUTION ASSUMES THE FOLLOWING.....
C        (A)   AXIAL DISPERSION IS NEGLIGIBLE
C        (B)   RADIAL GRADIENTS ARE NONEXISTENT IN FLUID PHASE
C        (C)   CARBON PARTICLES ARE UNIFORM AND SPHERICAL
C        (D)   EQUILIBRIUM IS DESCRIBED BY A FREUNDLICH ISOTHERM
C
C      PARAMETERS ARE AS DEFINED IN OUTPUT OF SUBROUTINE READIN
C*****************************************************************
      COMMON CL,NZ,R,RHOB,RHOC,CP,EQ(2),KM,K9,KF,FRAC,CO,V
      COMMON QO,NIT,DZ,DTHETA,NZP1,VEL,IT,DT,XSA,EPS,IPRINT,QFREE
      COMMON BIF,BIP,BI,F,FK1,FK2,FK2P,FK3
      COMMON C(101),CF(101),CMP(101),QMF(101),QBP(101),QBF(101)
      COMMON XSP(101),XSF(101),XSM(101)
      DIMENSION XU(101),XSU(101),QSF(101),QSP(101),K1(4),K2(4),K3(4)
```

```
      REAL KF,KP,KB
      REAL K1,K2,K3
      DIMENSION CSTORE(400,3)
      TMIN=0.
      THETA =0.
      N=10
      IPLOT=0
      CALL READIN
      CALL CONSTS
      CALL SETINIT
      DO 5 KK=2,NZP1
      XSU(KK)=XSF(KK)
5     QSF(KK)=XSF(KK)**EQ(2)
      MULT=NIT/300+1
      IHNZ=NZ/2 + 1
      IZZ=TT*1440./720.
      WRITE(1) IZZ
      IPROF=IFIX(TT*1440./TFPINT) + 1
      PMULT=720./DT
      NMULT=IFIX(PMULT)
      ATERM=2. + FK2 + 2.*FK2P*(1.-FK3/(1.+FK3))
C*****************************************************************
C     COMMENCE ITERATIONS IN TIME
C*****************************************************************
C
      DO 100 ITIME=1,NIT
      IF((ITIME/MULT)*MULT.NE.ITIME) GO TO 99
      IPLOT=IPLOT+1
      CSTORE(IPLOT,1)=C(NZP1)
      CSTORE(IPLOT,2)=TMIN
      CSTORE(IPLOT,3)=C(IHNZ)


99    CONTINUE
      TMIN=TMIN+DT
      THETA=THETA+DTHETA
C*****************************************************************
C     COMMENCE ITERATIONS ALONG THE BED
C*****************************************************************
C
      DO 201 J=2,NZP1
      IF(C(J).GT.0.9999) GO TO 201
      BTERM=2.*OMP(J) + 2.*FK2P*OBP(J)/(1.+FK3)
      DO 1 JJ=1,4
      CTERM=-FK2*QSF(J)**2
      OMF(J)=(BTERM + SQRT(BTERM**2 - 4.*ATERM*CTERM))/2./ATERM
      OBF(J)=(FK3*(OMF(J) + OBP(J))/(1. + FK3)
      CF(J)=CF(J-1)/(1. + FK1) + FK1*YSF(J)/(1. + FK1)
      IF(EQ(2).EQ.1.) XSF(J)=-OMF(J)*BI+SQRT(OMF(J)**2*(1.+BI**2)
     1+2.*OMF(J)*BI*CF(J))
      IF(EQ(2).EQ.1.) GO TO 20                                    C
12    FXSU=XSF(J)**(2.*EQ(2))/BI+2.*OMF(J)*(XSF(J)-CF(J))-OMF(J)**2/BI
      FPXSU=2.*EQ(2)*XSF(J)**(2.*EQ(2)-1.)/BI+2.*OMF(J)
      XSH(J)=XSF(J)-FXSU/FPXSU
      IF(XSH(J).LT.0.0) GO TO 17
      XSF(J)=XSH(J)
      IF(ABS(FXSU/FPXSU/XSF(J)).GT.0.01) GO TO 12
      GO TO 20
17    XSF(J)=XSF(J)/10.
      GO TO 12
20     CONTINUE
      QSF(J)=XSF(J)**EQ(2)
      IF(ABS((XSF(J)-XSU(J))/XSF(J)).LT.0.01) GO TO 2
      XSU(J)=XSF(J)
1     CONTINUE
2      CONTINUE
201    IF(CF(J).LT.0.005) GO TO 204
204    CONTINUE
      DO 205 J=2,NZP1
      C(J)=CF(J)
      OMP(J)=OMF(J)
      OBP(J)=OBF(J)
```

```
C     CALCULATE XSF AT ENDPOINT OF NEXT TIME INTERVAL BASED ON LINEAR
C     EXTRAPOLATION OF PREVIOUS STEP.
      XSU(J)=2.*XSF(J)-XSP(J)
      XSP(J)=XSF(J)
205   XSF(J)=XSU(J)
      IF((ITIME/NMLLT)*NMULT.NE.ITIME) GO TO 98
      WRITE(1) C(NZP1),TMIN
 98   CONTINUE
      IF(ITIME.EQ.1) GO TO 501
      IF(INT(TMIN/TPRINT)*TPRINT.NE.TMIN) GO TO 100
 501  PRINT*,' TIME IN MINUTES = ',TMIN
      PRINT*,(C(I),I=1,NZP1)
      N=N+1
      DO 500 JJ=1,NZP1
      XXX=FLOAT(JJ)
      YYY=C(JJ)
      IF(YYY.GT.1.) YYY=1.
 500  CALL PLOTPT(XXX,YYY,N)
 100  CONTINUE
      CALL OUTPLT
      DO 600 I=1,IPLOT
      IF(CSTORE(I,1).GT.1.) CSTORE(I,1)=1.
 600  CALL PLOTPT(CSTORE(I,2),CSTORE(I,1),1)


      CALL OUTPLT
      DO 700 I=1,IPLOT
      IF(CSTORE(I,3).GT.1.) CSTORE(I,3)=1.
 700  CALL PLOTPT(CSTORE(I,2),CSTORE(I,3),1)
      CALL OUTPLT
      END FILE 1
      STOP
      END



      SUBROUTINE READIN
      COMMON CL,NZ,P,PHOB,PHOC,XCP,EO(2),KM,KB,KF,FRAC,C0,V
      COMMON DD,NIT,DZ,DTHETA,NZP1,VEL,TT,DT,XSA,EPS,TPRINT,DFREE
      COMMON PIF,ETP,BT,F,FK1,FK2,FK2P,FK3
      COMMON C(101),CF(101),CMP(101),QMF(101),QP(101),QBF(101)
      COMMON XSP(101),XSF(101),XSU(101)
      REAL KF,KM,KB
C*****************************************************************
C
C     ALL INPUT PARAMETERS ARE READ UNDER FREE FORMAT SPECIFICATION
C
C*****************************************************************
      READ(5,*)     CL,NZ
      READ(5,*)     R
      READ(5,*)     V,CP
      READ(5,*)     PHOB,PHOC
      READ(5,*)     KM,KB,FRAC
      READ(5,*)     DFREE
      READ(5,*)     C0
      READ(5,*)     (EO(I),I=1,2)
      READ(5,*)     TT,DT
      READ(5,*)     TPRINT
C     PRINT OUT VALUES WITH LABELS TO VERIFY INPUT DATA AND UNITS
      WRITE(6,1000)
      PRINT*,'CL    =',CL,' CMS COLUMN LENGTH'
      PRINT*,'NZ    =',NZ,' AXIAL INCREMENTS'
      PRINT*,'R     =',R,' CMS PARTICLE RADIUS'
      PRINT*,'V     =',V,' CM**3/SEC VOLUMETRIC FLOWRATE'
      PRINT*,'CP    =',CP,' CMS COLUMN RADIUS'
      PRINT*,'PHOB  =',PHOB,' GM/CM**3 PACKED BED DENSITY'
      PRINT*,'PHOC  =',PHOC,' GM/CM**3 APPARENT PARTICLE DENSITY'
      PRINT*,'KM    =',KM,' MACRO TRANSFER COEFF - CM/SEC'
      PRINT*,'KB    =',KB,' -SEC**(-1) BRANCH PORE M. T. RATE'
      PRINT*,'FRAC  =',FRAC,' PARTICLE PARTITIONING FRACTION'
      PRINT*,'C0    =',C0,' GM/CM**3 FEED CONCENTRATION'
      PRINT*,'EO(I) =',EO(1),EO(2),' EQUIL. COEFFS. Q=EO(1)*C**EO(2)'
      PRINT*,'DFREE =',DFREE,'FREE LIQUID DIFFUSIVITY CM**2/SEC'
      PRINT*,'TT,DT =',TT,DT,' RUN TIME IN DAYS, STEP TIME IN MIN.'
      PRINT*,'TPRINT = ',TPRINT,' MINUTES BETWEEN EACH PLOTTED PROFILE'
 1000 FORMAT(1H1,///,32H INPUT PARAMETERS ARE AS FOLLOWS ,//)
      RETURN
      END
```

```
      SUBROUTINE CONSTS
      COMMON CL,NZ,R,RHOB,RHOC,CO,EO(2),KM,KB,KF,FRAC,CO,V
      COMMON DO,NIT,DZ,DTHETA,NZP1,VEL,TT,DT,XSA,EPS,TPRINT,DFREE
      COMMON BIF,BIP,BI,F,FK1,FK2,FK2P,FK3
      COMMON C(101),CF(101),CMP(101),CMF(101),CBP(101),CBF(101)
      COMMON XSP(101),XSF(101),XSH(101)
      REAL KF,KM,KB
C*****************************************************************
C
C     CALCULATES ALL PARAMETER GROUP CONSTANTS
C     FILM TRANSFER COEFF. IS BASED ON CORRELATION OF WILSON AND
C     GEANKOPOLIS FOR LOW REYNOLDS NUMBER FLOW. WATER WITH DENSITY
C     1. GM/CM**3 AND VISCOSITY 0.01 POISE IS ASSUMED. FREE LIQUID
C     DIFFUSIVITY IS AN INPUT VARIABLE.
C
C*****************************************************************
      DO=EO(1)*CO**EO(2)
      NIT=INT(TT*24.*60./DT)
      XSA=3.142*CR*CR
      EPS=1.-RHOB/RHOC
      VEL=V/XSA/EPS
      RE=VEL*EPS*2.*R/0.01
      SC=0.01/DFREE
      SH=1.09*(RE*SC)**0.3333/EPS
      KF=SH*DFREE/2./R
      DTHETA=DT*60.*KM/R
      DZ=KM*CL/VEL/R/FLOAT(NZ)
      NZP1=NZ+1
      IF(FRAC.EQ.1.) KB=0.
      BIF=3.*KF/KM
      BIP=KB*R/KM
      FRCO/3./RHOC/DO
      BI=FR*BIF
      FK1=(1.-EPS)*BIF/EPS*DZ
      FK2=3.*DTHETA/FRAC
      FK2P=BIP*DTHETA/FRAC
      FK3=0.
      IF(FRAC.LT.1.) FK3=BIF*DTHETA/(1.-FRAC)
      PRINT*,'KF =',KF,' FILM TRANSFER COEFFICIENT CM/SEC'
      PRINT*,'DO,NIT,DZ,DTHETA,NZP1=',DO,NIT,DZ,DTHETA,NZP1
      PRINT*,'BIF,BIP,BI,F =',BIF,BIP,BI,F
      PRINT*,'EPS,VEL,XSA,RE,SC,SH =',EPS,VEL,XSA,RE,SC,SH
      PRINT*,'FK1,FK2,FK2P,FK3 =',FK1,FK2,FK2P,FK3
      RETURN
      END



      SUBROUTINE SETINIT
      COMMON CL,NZ,R,RHOB,RHOC,CO,EO(2),KM,KB,KF,FRAC,CO,V
      COMMON DO,NIT,DZ,DTHETA,NZP1,VEL,TT,DT,XSA,EPS,TPRINT,DFREE
      COMMON BIF,BIP,BI,F,FK1,FK2,FK2P,FK3
      COMMON C(101),CF(101),CMP(101),CMF(101),CBP(101),CBF(101)
      COMMON XSP(101),XSF(101),XSH(101)
      REAL KF,KM,KB
C*****************************************************************
C
C     SET ALL INITIAL VALUES
C
C*****************************************************************
      DO 10 J=1,NZP1
      CMF(J)=1.0E-10
      CMP(J)=CMF(J)
      CBF(J)=0.
      CBP(J)=CBF(J)
      XSF(J)=1.0E-10
      XSP(J)=XSF(J)
   10 CONTINUE
      C(1)=1.                S      CF(1)=1.
      DO 20 J=2,NZP1
      C(J)=C(J-1)/(1. + FK1)
   20 CF(J)=C(J)
      PRINT*,'INITIAL PROFILE =',(C(J),J=1,NZP1)
```

```
C       CALCULATE INITIAL CS VALUES
        DO 40 J=2,NZP1
 42     FX=XSP(J)**(3.*EO(2))/BI+2.*OMP(J)*(XSP(J)-C(J))-OMP(J)**2/BI
        FPX=2.*EO(2)*XSP(J)**(2.*EO(2)-1.)/BI+2.*OMP(J)
        CHECK=XSP(J)-FX/FPX
        IF(CHECK.LT.0.0) GO TO 50
        XSP(J)=CHECK
        GO TO 51
 50      XSP(J)=XSP(J)/10.
        GO TO 42
 51     IF(ABS(FX/FPX/CHECK).GT.0.01) GO TO 42
        XSF(J)=XSP(J)
 40     XSH(J)=XSP(J)
 41      CONTINUE
        PRINT*,'XSF  ',(XSF(J),J=1,NZP1)
        RETURN
        END
```

PART II - STUDIES OF THE APPLICATION OF MULTICOMPONENT FEEDSTREAMS TO ACTIVATED CARBON COLUMNS CONTAINING BACTERIA

CHAPTER 1

Introduction

In Part I of this study the adsorptive behaviour of selected single compounds was investigated. The results were shown to be well described by a proposed kinetic model which incorporated the effects of a very slow diffusion mechanism. This mechanism was further shown to be the cause of a characteristic long tail on the experimental breakthrough curves. Having proved the existence of this mechanism for single solutes, it was decided that the applicability of the model should be tested on influents which were typical of some actual applications of activated carbon in the environmental area.

In such systems, however, the modelling procedure is complicated by the fact that the feed streams may contain hundreds or even thousands of components, all present at similarly low concentrations. Furthermore, the individual components are not all identifiable by current analytical techniques. When faced with such complexity, the stream concentration can only be quantified using a lumped parameter such as total organic carbon (TOC), chemical oxygen demand (COD), or biochemical oxygen demand (BOD). Consequently a modelling study aimed at describing the performance of carbon columns operating on such feedstreams must also be based on a

lumped parameter, and must assume that the overall behaviour of the multitude of components can be described in terms of the properties of this parameter. Such an approach is unlikely to be able to describe the exact behaviour of an operating system, however the ability to describe even the gross behavioural characteristics would be of significant benefit in the understanding and design of adsorption systems. Current practice relies on expensive and time consuming pilot scale experiments which do not always give a clear understanding of the underlying mechanisms. This lack of knowledge of the processes responsible for the observed system performance can result in poor scaling up to full scale design.

An additional complication which arises when one attempts to model real adsorption systems is the presence of a viable bacterial population within the carbon filters. Activated carbon provides an excellent support surface for the growth of bacteria, and, as discussed in the following sections, bacterial activity has been noted in a wide variety of activated carbon applications. The presence of bacteria further increases the complexity of the adsorption modelling as the bacteria may degrade some or all of the components in the feedstream, and thus extend the life of the adsorber over that which would be obtained purely by adsorptive mechanisms. Typical breakthrough behaviour of a biological activated carbon column is shown in Figure 1-1. Such breakthrough curves have been interpreted as being due to two mechanisms; the initial breakthrough up to point 'a' being largely a result of adsorptive saturation whereas the removal after point 'a' is attributed to biological mechanisms. The breakthrough curve in Figure 1-1, however, bears a marked

resemblance to the breakthrough curves predicted by the branched pore kinetic model, and it appears possible that the continued removal after point 'a' may be due in whole or in part to continued adsorption as predicted by the slow removal mechanism.

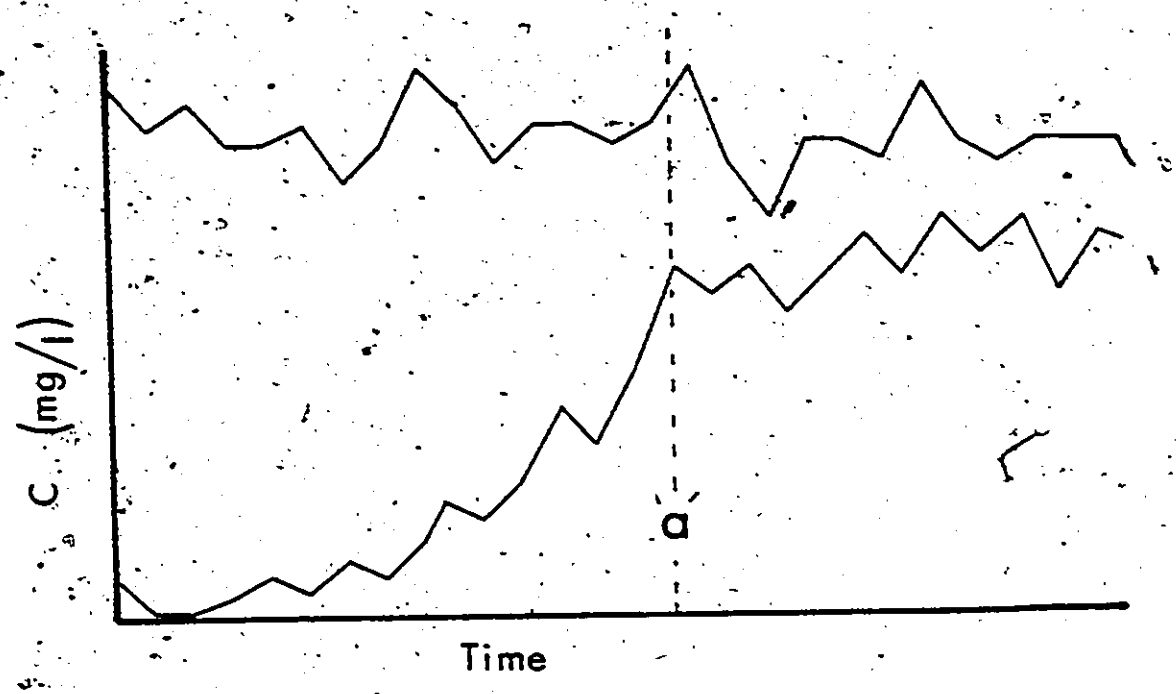

Figure 1-1. Typical Adsorption Column Breakthrough Curve.

In the present work the adsorptive behaviour of two complex feedstreams was investigated. By deliberate choice the feedstreams used were low in concentration and poorly degradable so that the influence of slow adsorption could be investigated most easily. It was proposed to compare the experimental breakthrough data with the predictions of the branched pore kinetic model and thereby attempt to differentiate between removal due to slow adsorption and removal due to biological degradation.

Each study is presented as a separate chapter; the first deals

with the adsorption of low level organics from tapwater. The water source is Lake Ontario and thus the majority of organics present are of natural origin. In the second study, a similarly low level biological effluent was generated by operating an activated sludge system on a single carbon source, the study was conducted to investigate the adsorptive behaviour of the residuals of conventional biological treatment. Such compounds are of interest in a water reuse system as they could potentially accumulate with repeated use of the water.

CHAPTER 2

Background and Literature Review

Since the range of feedstreams which can be applied to activated carbon adsorbers is very broad, it is necessary to define certain stream characteristics which are specifically of interest as it is beyond the scope of a single report to cover all possible applications. A simple division might be made on the basis of either high or low concentration and on the relative biodegradability of the stream. The streams chosen for investigation in the present study, low concentration and poorly degradable, can arise from each of the four main application areas of activated carbon adsorption.

2.1 Applications of Activated Carbon Adsorption

2.1.1 Physical Chemical Treatment

As a response to increasing competition for land usage, and also to obtain improved effluent quality over that provided by conventional biological treatment methods, much research was performed into physical chemical treatment methods in the late 1960's and early 1970's. In this scheme, the wastestream to be treated (normally raw sewage) was treated with chemical coagulants, then flocculated and settled to remove suspended matter and some adsorbed soluble organics. The stream was then treated by physical methods to remove the remaining organic contaminants and activated carbon was the primary adsorbent used. A

process diagram is shown in Figure 2-1. As has been shown in several studies (Weber et al., 1970; Directo and Chen, 1974; Maqsood and Benedek, 1977), biological activity within the carbon adsorbers was an inevitable consequence of this form of treatment. After an initial period during which adsorption was the primary removal mechanism, the rate of removal became constant and was attributed to biological activity. Peel and Benedek (1977) showed that the rate of removal during this phase was quite comparable amongst the various studies. Initially, bacterial activity was regarded as a drawback (Bishop et al.,1967) but was soon hailed as an economic benefit giving extended life to the carbon bed (Lawrence, 1970; Weber et al.,1973; Benedek, 1975). Several problems including excessive headloss due to biological growth within the bed, and generation of H_2S due to anaerobic conditions, were also noted. Because of these problems the whole rationale behind physical chemical treatment (PCT) needs to be reevaluated.

The carbon column feedstream in PCT systems is relatively low in suspended solids because of the prior chemical treatment but has a relatively high BOD/COD ratio and is thus well suited to biological treatment. Although the original concept of PCT was to have a non biological system which would be relatively insensitive to shock loads and intermittent operation, the development and acceptance of biological activity within the carbon beds made PCT just an alternative biological configuration. The carbon columns, after exhausting their initial adsorptive capacity, acted as submerged biological filters and the operational problems noted above can be regarded purely as limitations of submerged

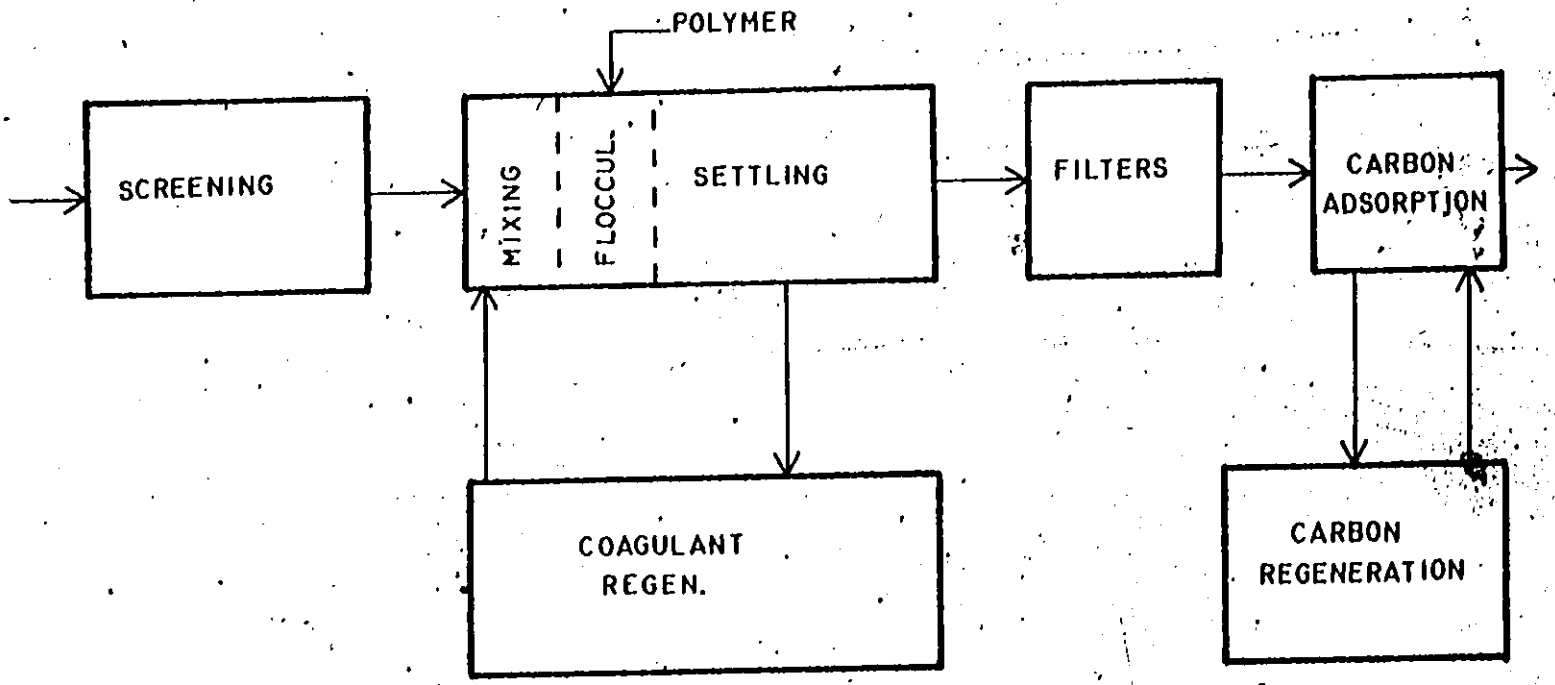

Figure 2-1. Schematic Flowchart of a Physical-Chemical Treatment Plant.

filters.

If both BOD and dissolved oxygen are available in the influent, rapid growth of bacteria within the bed must follow and because the bacteria fill the interstitial void spaces, the pressure losses across the filters increase rapidly. Weber et al., (1973) proposed the use of upflow expanded beds to overcome the problems of excessive pressure drop in packed beds.

Anaerobic activity and H_2S generation may occur in submerged filters whenever the oxygen demand due to substrate utilization and bacterial respiration exceeds that available in the influent. Once oxygen has been depleted alternative electron acceptors are utilized, and unless nitrate is deliberately added (Directo and Chen, 1974), H_2S production from the sulphate ion will normally result. Whereas conventional biological treatment schemes (activated sludge, trickling filter, rotating disc) provide a constant supply of oxygen, use of a submerged filter restricts oxygen to what can be dissolved in the influent stream. Consequently, optimal aerobic degradation is not achieved unless the influent BOD is less than the available dissolved oxygen. If the influent oxygen level is boosted by using pure oxygen, severe pressure drop problems ensue because of the increased bacterial growth (Directo and Chen, 1974). Thus the application of wastestreams which have a significant soluble BOD (>> 15 mg/l) to packed beds of activated carbon does not appear to be an operationally sound approach to the problem of soluble organics removal.

As shown by Weber et al., (1973), the use of an expanded bed

overcomes the problem of pressure drop while giving virtually the same removal as a packed bed. Expanded bed operation also allows for supplemental oxygen addition as two phase flow can be applied. In this application, however, activated carbon is not necessarily the best support medium as its low density, high cost, and relative fragility weigh against its use. There is no question that activated carbon gives an unmatched effluent quality while it acts as an adsorbent, but if it is proposed to run the activated carbon beds beyond the adsorptive capacity as is advocated in extended life usage, the available data indicates that sand or other non-activated media give equivalent removal. This point is discussed at length in section 2.2.

As a result of the above discussion, it was concluded that the application of easily degradable wastestreams to activated carbon adsorption columns in either flow mode is a poor process choice. A seemingly more appropriate choice would be passage through an inert media filter to remove the easily biodegradable components, followed by activated carbon filtration to remove the non biodegradable but adsorbable compounds. In this way the problems of excess growth and anaerobiosis within the carbon filter would be overcome and land area requirements would still be lower than for conventional biological processes. This configuration uses carbon as a post biological step and in domestic wastewater treatment typical feeds would have a COD of 20-40 mg/l, a TOC of 10-20 mg/l, and would have a relatively low BOD.

The above discussion concerns easily biodegradable wastes which exhibit a significant BOD_5. It has been proposed that activated carbon

can promote biological oxidation of low concentration organics by a so called 'enhancement' effect. If this effect does in fact occur, then differences in the long term removal of low level organics by activated and non-activated filters would be anticipated. This point is discussed in detail in a later section concerning biological mechanisms in carbon filters.

2.1.2 Tertiary Wastewater Treatment

Tertiary treatment of a wastewater by activated carbon means the upgrading of biological secondary treatment effluents by a subsequent adsorption step. Thus carbon functions as a post biological treatment process where easily biodegradable components have been removed upstream of the carbon adsorber. Several studies on such systems were conducted in the 1960's and 3 of the principal studies are reported by Joyce et al.(1966), Slechta and Culp (1967), and Parkhurst et al.(1967). More recently, studies using ozone to stimulate biological activity in the secondary effluent have been reported by Argo and Culp (1978).

In tertiary applications the influent stream, being already biologically degraded, does not promote rapid bacterial growths within the filters. However, the feedstream normally contains partially degraded or slowly degradable components and some suspended solids, principally bacteria carried over from the secondary treatment unit, and thus a bacterial population generally will develop within the activated carbon filters. Although the influent suspended solids level may cause periodic backwashing to be necessary due to filtration mechanisms, bacterial

growth within the bed is seldom such that it interferes with normal operation of the adsorbing carbon. Parkhurst et al.(1967) attributed about 15% of the COD removal to biological activity within their columns, and noted CO_2 production, dissolved oxygen removal and a drop in nitrate through the columns. If the nitrate were being converted to nitrogen it would indicate that some regions of the filter were anaerobic; unfortunately the authors did not give dissolved oxygen concentrations in the columns. Since the effluent was chlorinated upstream of the carbon columns, it was apparent that activated carbon removed the chlorine residual thus allowing the bacterial growth to develop. The ability to remove chlorine residuals appears to be limited, however, Argo and Culp (1978) reported that the 14 feet deep activated carbon beds at South Tahoe receive an influent chlorine residual of 10 to 20 mg/l and 1 to 2 mg/l remains in the effluent; thus they concluded that bacterial activity was unlikely in this plant.

In summary, tertiary treatment applications of activated carbon generally treat feedstreams having a relatively low level of organic contamination (TOC = 10-40 mg/l), and a low soluble BOD (SBOD). When biological growth is present, it is generally not sufficient to cause severe operating difficulties and it may contribute to organic removal within the filters. Since the waste is extensively biodegraded prior to application to the carbon filters the primary removal mechanism is expected to be by adsorption.

2.1.3 Drinking Water Supply

Activated carbon has historically been widely used by water supply utilities in North America for taste and odour control, often on

an intermittent basis to cope with specific short term problems. In this application, powdered activated carbon (PAC) is normally used as its use does not require additional capital expenditure, and the dosage can be adjusted to the treatment level desired.

In recent years, increasing concern has been given to the presence of anthropogenic materials in potable water sources. Of specific concern amongst these compounds are the halogenated organics which are also formed during chlorination of a potable water containing naturally occurring organic molecules. Since many of these materials are thought to be hazardous to humans, and some are known carcinogens (Cotruvo, 1979), regulations for the control of both trihalomethanes (THM) and total organic material (TOC or equivalent) have been proposed (USEPA, 1978). The principal mode of treatment in the proposed regulations was GAC filtration. Recent publications concerning the proposed regulations and the range of trace organics in potable water supplies include those of Cotruvo and Wu (1978), Snoeyink et al.(1977), McCreary and Snoeyink (1977), Love (1978), Cairo et al.(1978),(1979), Gaurino (1979). The description of the whole field of potable water treatment is beyond the scope of this report and only those aspects directly related to the work reported herein will be discussed.

Although the adsorptive behaviour of specific compounds such as THM's is of concern in operating a carbon filter, these identifiable compounds comprise only a small fraction of the total dissolved organic material and will not be studied further in this report. Rather, the object of this research is to describe the breakthrough of the bulk of the organic material, quantifiable only by a parameter such as TOC. If

the background TOC behaviour can be described, current work on modelling of a single component in the presence of these background organics (Frick et al. 1978) may enable the adsorptive behaviour of the single component to be described. As noted by DiGiano (1978) however, many uncertainties, some perhaps insurmountable, still exist in the area of multicomponent modelling.

In the area of potable water treatment, as in the previous description of tertiary treatment, the feedstream is generally low in total organic concentration (lower for potable water supply than AWT), and the organic materials are not easily biodegradable. Thus a similar situation exists wherein a relatively low level, biologically stable waste is fed to the carbon column. In both cases the principal mode of removal is by adsorption, however any biologically degradable materials in the feedstream may be removed by biological mechanisms. The adsorption beds in this application can be operated in packed bed mode, often as replacement media in gravity sand filters, because the biological growth, if present, does not cause excessive head loss or generate anaerobic conditions as long as the beds are backwashed at regular, and fortunately reasonably long, intervals.

Recently, a new area of potable water treatment, Biologically Active Carbon (BAC), has been proposed. This process began in Europe where ozone has been used for some time as a disinfectant and more recently as a biological stimulus. Some European treatment systems are summarized by Rice et al.(1977), Kühn et al.(1978), and DiGiano (1979), and some case histories are available in an EPA document on adsorption

(USEPA, 1976). Basically, the so called BAC process consists of ozonation followed by multimedia filtration and activated carbon adsorption. The ozonation step serves to break down some of the organic material into more readily degradable materials (Randtke and McCarty, 1979; Kühn et al.,1978; Guirguis et al.,1978; Stephenson et al.,1979), and at the same time greatly increases the oxygen content of the feedstream. Improved long term removal of organic material appears to be obtained as a consequence of increased biological activity within the multi media filter and activated carbon adsorber. The ozonation step increases the biodegradability, lowers the adsorptivity (Benedek, 1977), and oxygenates the carbon column feedstream, and as a result of these changes mutually interacting, much misunderstanding of the function of biological activity within the carbon adsorbers has arisen. Mechanisms have been proposed for the enhancement of biological activity within activated carbon columns, and for the in situ biological regeneration of the activated carbon capacity. In section 2.2 these mechanisms are discussed with respect to research findings to date. The discussions apply equally well to ozonated and non-ozonated cases as the main difference between the two is that the biological activity normally existing in an activated carbon adsorber may be enhanced by pre-ozonation.

2.1.4 Industrial.

It is difficult to give a general description of industrial application of activated carbon because of the vast range of industrial processes. Carbon may be used to remove specific toxic chemicals such as pesticides from a waste stream, or may be required to meet specific

effluent requirements with respect to COD and BOD. In some cases there may be rigid specifications on a particular component such as total phenols while control of the total quantity of organic carbon may not be necessary. Influent concentrations are typically high and thus bed service times are generally quite short. Because of the types of streams treated, and the highly variable nature of industrial waste streams, many industrial systems have failed to meet design criteria (Ford, 1977).

Some industrial feed streams may be quite biodegradable in which case activated carbon is used as a post biological polishing step, or powdered activated carbon may be added in the biological stage (Flynn, 1974, 1975). Generally the waste stream is toxic to bacteria at full strength, and direct application onto an activated carbon bed will not result in significant biological development during the adsorption step. Several authors however (Rodman and Shunney, 1971; Johnson, 1975; Sigurdson and Robinson, 1978) have proposed systems in which the carbon alternates between adsorption and 'biological regeneration' modes. In the adsorption mode the concentrated feed stream saturates the carbon capacity and a purified effluent is obtained. The saturated column is then taken off line and partially regenerated by pumping a biologically active oxygenated stream through the bed. The adsorbed materials slowly desorb from the carbon and are consumed by the bacteria. Since the concentration of substrate in this mode always remains low, the inhibitory effect of the high concentration in the initial feed stream is overcome. This method is only applicable to biodegradable components in the feed

stream, and therefore a biological treatment scheme should, in most cases, be capable of giving equivalent treatment at lower cost. Furthermore, in most wastewaters some nonbiodegradable materials will be present and the adsorptive capacity will eventually be exhausted by these components. The process will function predominantly as a solely biological treatment step after this time.

In the context of this report only those industrial applications where activated carbon is used as a post-biological polishing step will be discussed. In such an application the waste strength is generally low to intermediate and if the biological step is well designed, the waste will have a low biodegradability potential.

2.2 Biological Mechanisms in Activated Carbon Beds

2.2.1 Known Removal Mechanisms in Activated Carbon Filters

Before discussing the literature concerning proposed but as yet unproven biological mechanisms in carbon filters, it is worthwhile to review the removal mechanisms which could be expected, based on existing knowledge of adsorption and biological degradation. Peel and Benedek (1977) defined the following classes of compounds in the feed to a carbon adsorber:

(i) adsorbable and degradable,

(ii) adsorbable and non-degradable,

(iii) non-adsorbable and degradable,

(iv) non-adsorbable and non-degradable.

Type (iv) compounds will always pass directly to the effluent and need not be considered further. In a sterile filter, type (iii) compounds will

also pass to the effluent and type (i) and (ii) compounds will adsorb onto the carbon until the filter is saturated. If it is assumed that any filter coming on line will be almost sterile, then the conditions above will apply in the early stages of operation. As the run proceeds, however, bacterial numbers increase within the filter, and type (iii) compounds will be removed by biological action to an extent determined by the availability of oxygen, the substrate concentration, and the bacterial numbers. At the same time, some of the type (i) compounds entering the bed will also be removed by biological activity. With reference to Figure 2-2, if the wavefront of type (i) compounds had proceeded to position A before the beginning of the bacterial development, it would be expected to recede to a position B which would again depend on the substrate type, concentration, oxygen availability, and cell numbers. In the region between curves A and B the concentration of type (i) components in the liquid phase would decrease and therefore desorption of some material would be expected in order to maintain equilibrium. This phenomenon has been observed to occur with single substrates (Weber, 1977; Ying, 1978), although Benedek (1978) presented data to indicate that complete desorption is not achieved due either to irreversible adsorption or adsorption of non-degradable metabolites. Sigurdson and Robinson (1978) also found that only partial regeneration was possible by this mechanism.

If by the above mechanism certain sites are freed and become available for additional adsorption of type (ii) components, then in a sense a biological regeneration will have occurred. This regeneration

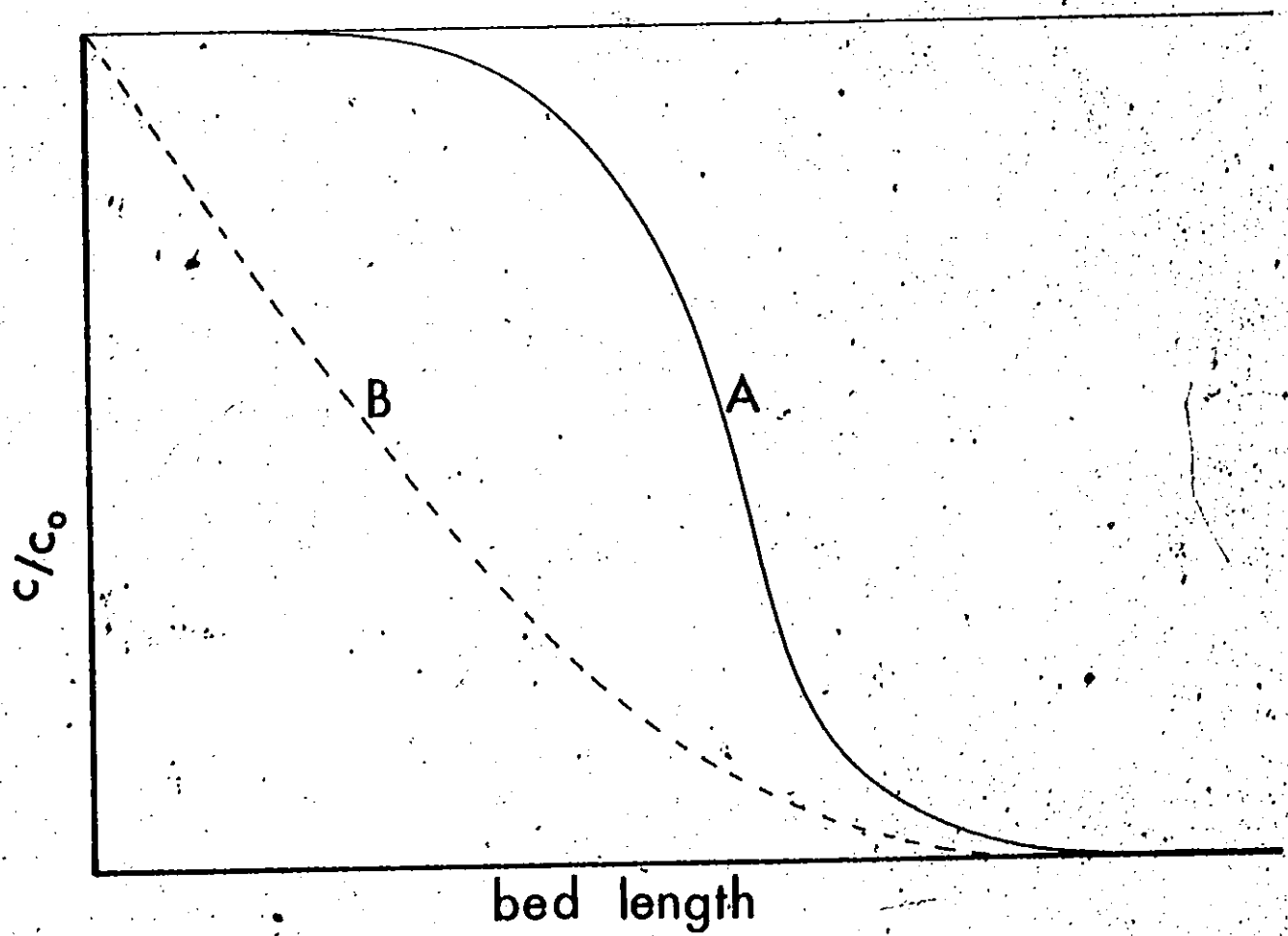

Figure 2-2. Adsorption Bed Concentration Profiles Before and After Bacterial Development.

however is only temporary, and once the bacterial levels reach steady state, biodegradable materials would be removed biologically and non biodegradable but adsorbable materials would be removed by the carbon until the adsorptive capacity is saturated. Thereafter, the only operative mechanisms would be biological, and the percentage removal should be similar to that of a sand filter having a sufficient residence time. In the above discussion competitive adsorption and displacement effects have been neglected, these mechanisms could be expected to occur and would further complicate the description.

2.2.2 Proposed Mechanisms of Bioenhancement and Bioregeneration

The theories of bioenhancement and bioregeneration rely on a common proposed mechanism and can therefore be discussed simultaneously. The possibility of biological enhancement was suggested by Weber et al. (1970) and subsequently elaborated by Kalinske (1972) and Besik (1973). These authors postulated that adsorption would result in the concentration of substrate, oxygen, and bacteria at the carbon surface, and would therefore lead to an acceleration of the biological degradation process. A similar claim was made by Eberhardt (1976) concerning biological regeneration when he likened bacteria in an activated carbon column to "cows grazing in a juicy and luscious meadow". According to the theory of biological regeneration, bacteria within activated carbon columns are continually degrading organic substrate which is adsorbed on the carbon, and thus constantly regenerate the adsorptive capacity.

Both of these theories rely on the ability of bacteria to utilize substrate directly from the carbon surface rather than from free solution

which is the normal method of metabolism. Since most of the adsorptive capacity of activated carbon is in pores too small for bacteria to penetrate, direct utilization requires that extracellular enzymes diffuse to the site of the adsorbed molecule, react, and that the reaction products diffuse back out to the bacteria at the external surface.

The discussions of biological enhancement by several authors have implied that the adsorption of molecules onto activated carbon results in an enriched environment adjacent to the carbon surface. As pointed out by Benedek (1978) in a review of biological activity in carbon beds, this is not the case and in fact just the opposite occurs. An example of this argument has been given by Weber (1978) and DiGiano (1979) who proposed that the adsorptive attraction between activated carbon and oxygen would increase the driving force through a biofilm surrounding the carbon particle and therefore stimulate biological growth. In fact, as indicated in Figure 2-3, adsorption onto the carbon particle actually lowers the oxygen concentration below that which would be obtained with an inert media, and can only serve to retard biogrowth. The oxygen concentration in the biofilm must be lower when the support medium exerts an oxygen demand as the driving force across the biofilm must increase to supply the additional oxygen. An increase in the driving force can only result in a lower average concentration within the film.

The argument concerning direct utilization of substrate from the adsorbed state is questionable as the following discussion concerning the steady state behaviour of a biologically active carbon particle shows.

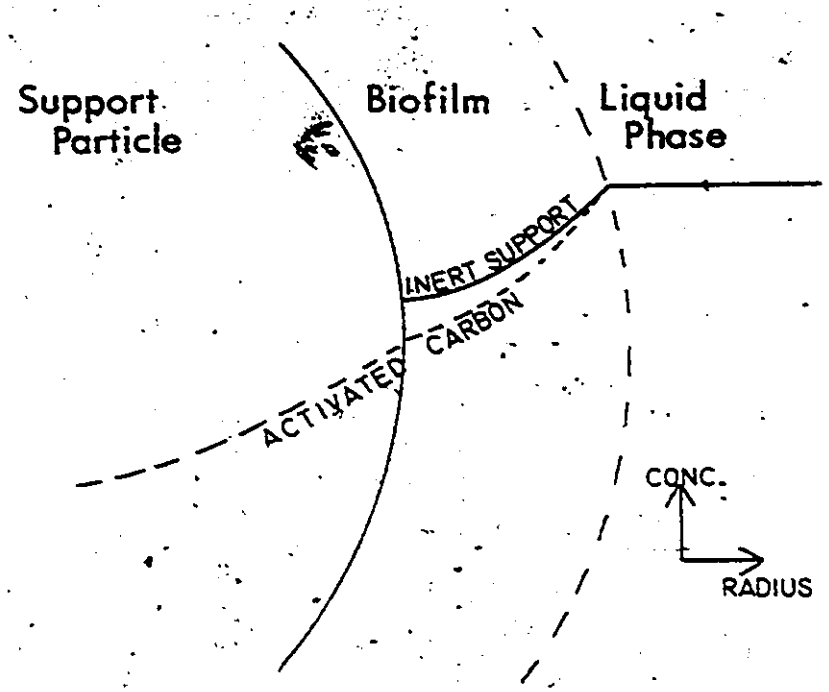

Figure 2-3. Dissolved Oxygen Profiles with Adsorbing and Inert Support Media.

For a molecule to adsorb onto the carbon surface it must first pass through a biological film or at least in close proximity to the bacteria on the external surface. If the bacteria have the ability to utilize this molecule as a substrate, it is reasonable to assume that the molecule will be utilized while still dissolved in the liquid phase rather than first passing through the film, adsorbing onto the carbon, and then being degraded by the bacteria. Taxonomy studies reported by Benedek (1978) showed that bacteria isolated from a biologically active carbon column were of similar type and distribution to those found in activated sludge plants. The mechanisms of substrate uptake could there-

fore be assumed to be the same in either case. Even if an initially high concentration of substrate on the carbon surface stimulated metabolism of that substrate, replacement of the consumed molecules must come from the bulk liquid, and again they could be expected to be utilized while in solution rather than first passing through an adsorbed state.

Thus although utilization of substrate while in the adsorbed state may be theoretically possible, there are grounds for considering this mechanism to be improbable. Since the mechanism can neither be directly verified or disproved at the present time, judgements as to its likelihood should be based on a rational analysis of the experimental evidence which is currently available. Only that evidence which cannot be explained by the conventional mechanisms discussed in section 2.2.1 should be regarded as supporting the concept of direct utilization from the adsorbed state.

2.2.3 Experimental Evidence concerning Biological Enhancement

A brief review of the literature concerning the enhancement of biological activity by solid surfaces such as activated carbon has been published by De Walle and Chian (1977b). The evidence presented was conflicting as some studies appeared to show increased biological removal rates upon addition of activated carbon whereas others did not. Many of these studies were carried out in combined PAC/activated sludge systems and as noted by Flynn et al.(1977), there are several problems which arise when interpreting the data from such systems. After allowing for these potential errors, Flynn found that the combined effect of the simultaneous processes of adsorption and biological degradation was

not greater than the sum of each separately. It was concluded that bacteria did not appear to be capable of utilizing substrate which was adsorbed on the carbon surface.

An additional permutation of the argument concerning biological enhancement is that which proposes that biodegradation of otherwise bio-refractory or poorly degradable organics may occur when in the presence of activated carbon. Eberhardt (1976) discussed previous work which suggested that the normally biologically resistant pentaerythritol (PE) could be degraded after 60 days when in contact with activated carbon. However, Ilic (1977) has shown that PE is biodegradable without activated carbon if given sufficient acclimation and thus the biodegradation discussed by Eberhardt cannot be attributed solely to the activated carbon presence. Activated carbon could in some instances cause the development of biological activity by lowering a previously toxic concentration of substrate to a level at which it becomes degradable. In this instance the biological degradation is not due to the activated per se, as the bioremoval could equally well be achieved with dilution water.

Eberhardt (1976) further proposed that biodegradation of very slowly degraded substances could occur in an activated carbon filter because the substrate adsorbed in the column is retained there for extended periods thus allowing sufficient time for bacterial acclimation. The same theory has also been supported by Sontheimer (1976), Flynn et al. (1977), Rice et al. (1977) and Weber (1978). While it is likely that substances defined as poorly degradable may be removed within an acti-

vated carbon filter for the reasons discussed below, it is more probably due to causes other than the long substrate residence time.

In order to utilize a given substrate, the bacteria and substrate must be in contact long enough for the bacteria to undergo necessary changes and develop enzyme systems. This time period is called the acclimation period. In the case of an activated carbon filter with a given component constantly in the feedstream, it is difficult to see why acclimation would not occur regardless of whether or not the component is adsorbed. In fact, acclimation may be delayed as initial adsorption would reduce the concentration of substrate near the bacteria, unless it is assumed that the bacteria utilize adsorbed substrate.

Substances defined as poorly degradable are generally classified as such on the basis of their removal in a conventional biological treatment system, such as activated sludge. The activated sludge system, however, has two potential disadvantages with respect to the removal of poorly degradable substances. Firstly, the sludge age in an activated sludge unit is limited to 5 to 10 days by the operational characteristics. Thus bacteria which grow more slowly than the sludge age cannot develop. Secondly, because the hydraulic characteristics of activated sludge units are somewhere between plug flow (PFTR) and completely mixed (CSTR) reactors, the return sludge is subjected to the full influent concentration, including all the most readily degradable materials, at the beginning of each cycle through the system. Such unsteady state conditions may disturb the ability of bacteria to acclimate to the poorly degradable substances.

In contrast, in a fixed bed with or without activated carbon, these circumstances do not occur. Since many of the bacteria are not removed during backwashing of the bed, the sludge age within a submerged filter can be equal to the operational life of the filter. Additionally, since the readily degradable materials are removed in the earlier stages of the filter, the only remaining substrates deep in the bed are the poorly degraded materials and thus bacteria are free to acclimate to these compounds under relatively steady state conditions.

The mechanism proposed by Eberhardt (1976) for the removal of these poorly degradable materials due to adsorption in activated carbon filters would only apply if:

(i) The substrates could be utilized directly from the carbon surface rather than from solution;

(ii) Growth of the bacteria is stimulated only by the presence of substrate on the carbon surface and not by substrate in the liquid phase.

Since neither possibility has yet been proven to occur, acceptance of this mechanism would require strong circumstantial evidence in its favour. In fact much of the available evidence is contrary to the proposed mechanism. In addition to the studies of Flynn et al.(1977) which were discussed earlier, two other studies have presented evidence which suggests that refractory materials do not become biodegradable within a carbon filter.

Van der Kooij (1976) measured die off rates of bacteria on activated and non-activated carbons drawn from columns which had been fed

with tap water for an extended period. He found virtually no differences in the half lives and therefore concluded that the bacteria were unable to degrade the adsorbed materials on the activated carbon particles. A similar result was reported by Klotz et al.(1976) who ran parallel sterile and non sterile activated carbon filters on the effluent from a sand filter in a drinking water plant. They noted very small differences in the organic removals in the sterile and non sterile filters over the 60 day experimental period suggesting that the bacteria were not able to utilize the organics in the feedstream.

Experimental evidence which would suggest that bacteria may be able to utilize adsorbed substrate has been used in support of the theory of biological regeneration and is discussed in the next section.

2.2.4 Experimental Evidence Concerning Biological Regeneration.

Much of the evidence supporting the theory of biological regeneration has been presented by Eberhardt et al.(1975) and Eberhardt (1976). Extensive studies at a potable water treatment plant in Bremen, Germany, were reported in these papers. By comparing the removal of dissolved organic carbon (DOC) to the production of inorganic carbon (CO_2), they proposed that various conditions within the carbon bed could be distinguished. At the end of a 3 year adsorption period they found that although DOC removal was only 0.5 mg/l, CO_2 production was 1.4 mg/l (as C). They attributed the difference to CO_2 produced during biological regeneration of the carbon surface as adsorbed molecules were degraded by the bacteria. The authors further noted that this excess CO_2 production paralleled a decrease in the activated carbon loading as

measured by dimethylformamide (DMF) extraction. A similar decrease in the carbon loading was reported by Fuchs and Kühn (1976) at one waterworks on the Lower Rhine but was not observed at other waterworks investigated. Because of the method of measuring the carbon loading (DMF extraction), these results may not be strictly correct. Quantitative desorption of all the organics found in natural waters has not yet been established (Fuchs and Kühn, 1976; unpublished work at McMaster), and the displacement of weakly by more strongly adsorbed molecules during the operation of a carbon filter may result in the desorption of a smaller fraction of the adsorbed organics at each successive extraction. The apparent carbon loading may thus decrease even though the true loading remains constant or continues to increase.

Additional evidence for the occurrence of biological regeneration during the Bremen study has been given by Eberhardt (1976) and was reviewed by DiGiano (1979). The reasons for proposing bioregeneration were:

(i) Oxygen consumption was higher in summer than in winter although nitrification, which accounts for significant oxygen usage, was present only during the winter;

(ii) Inorganic carbon production was much greater in summer than in winter;

(iii) A steady increase in CO_2 production was noted in a 1 year study following start up of a pilot filter. In one month of this study during the summer, CO_2 production was greater than DOC removal;

(iv) A recirculation study in which one column was put in a closed recycle loop for a period of two months showed a steady state production of CO_2 which was related to a bioregeneration rate.

In the interpretation of the above observations by Eberhardt (1976) and DiGiano (1979), one potentially significant factor has been overlooked. As noted by Eberhardt, conclusions can be drawn on the basis of CO_2 production only if conversion of DOC to CO_2 and adsorption are the sole mechanisms operative within the bed. Unfortunately, growth and/or adsorption of bacteria results in the accumulation of a significant number of bacteria within the bed. The production of CO_2 and the consumption of oxygen due to endogeneous respiration, as well as the release of metabolites by these bacteria, must also be considered in addition to the potential oxygen removal and CO_2 production due to assimilative mechanisms. The data reported by Eberhardt et al.(1975), indicates a 97% removal of colony forming bacteria from the influent during passage through the bed. It could be anticipated that much greater numbers of dead or inactive bacteria would also be present in the influent and would be adsorbed within the filter. As total cell numbers or total suspended solids removal data are not available, the relative contribution of suspended solids removal and endogeneous respiration to the oxygen consumption and CO_2 production cannot be estimated.

The Bremen observations reported above could all be explained by assuming endogeneous respiration was significant, and the results of the recirculation study support this hypothesis. The TOC concentration in the recycle stream rose initially, and did not fall to its

original level for some time. This observation is far more in accord with a theory of endogeneous respiration and cell death and lysis, rather than biological regeneration, for which the liquid phase concentration would be expected to decrease as adsorptive capacity was regenerated. One method of ensuring regeneration of adsorptive capacity is to withdraw carbon from the filter and measure an adsorption isotherm to determine the remaining capacity. This was done by Benedek (1977) who showed that there was no remaining capacity in the biologically active carbon column studied. The column had been in operation for an extended period prior to the sample withdrawal.

2.2.5. Comparison of Parallel Inert and Activated Carbon Filters.

One of the problems in determing the relative effects of adsorption and biodegradation in many experimental systems has been in differentiating between the two. Undoubtedly one of the most direct methods of comparison is the operation of parallel inert media and activated carbon columns under otherwise identical conditions. Once the adsorptive capacity of the activated carbon column is exhausted only biological removal should occur, and the behaviour of inert media (generally sand) and activated carbon filters should be identical. Complicating factors can arise however, and Benedek (1978) has given four reasons for apparent differences between the performance of activated carbon and sand filters:

(i) The adsorptive capacity of the activated carbon is not fully exhausted when comparisons are made. This possibility could be very important if the slow adsorption effects noted in part

I of this thesis are also found to occur with organics found in typical activated carbon applications;

(ii) There is a toxic component in the feedstream which is selectively removed in the carbon filter thus allowing biological growth to develop there. In drinking water treatment this factor is often important as prechlorination is widely used to prevent biological growth;

(iii) The external surface areas and thus available attachment sites for bacteria are not equal resulting in different total cell counts in the respective filters;

(iv) The bacteria on the carbon develop earlier due to adsorption of bacteria from the feedstream, and are better protected from shear and attrition during backwash because of the irregular surface.

If the known mechanisms of biological degradation and adsorption discussed in section 2.2.1 are assumed to occur, sand and activated carbon columns should give identical removals after the above factors are taken into account. Continued differences in the removals would be an indication of synergistic interactions between adsorption and biological degradation, and would lend support to the theories of biological enhancement and bioregeneration.

In the first studies to be discussed, the feedstreams were highly biodegradable and biological activity was generally quite profuse. Weber et al. (1973) fed a coagulated and filtered raw sewage to parallel activated carbon and inert media filters and concluded that activated carbon

was more effective. However, their data indicate approximately equal removals by the exhausted carbon and the non-activated media showing that the carbon was only more effective until its adsorptive capacity was saturated. Similar results can also be seen in the long term data of Johnson (1976).

Activated carbon column removals will always be better in the initial time period when the carbon's adsorptive capacity is being utilized. This is clearly demonstrated in Figure 2-4 in which TOC and specific substrate in the effluent from parallel non-activated and activated carbon columns are shown. Although instantaneous breakthrough occurs in the non-activated filter, the activated filter initially removes all the influent TOC by adsorption. As the capacity of the carbon

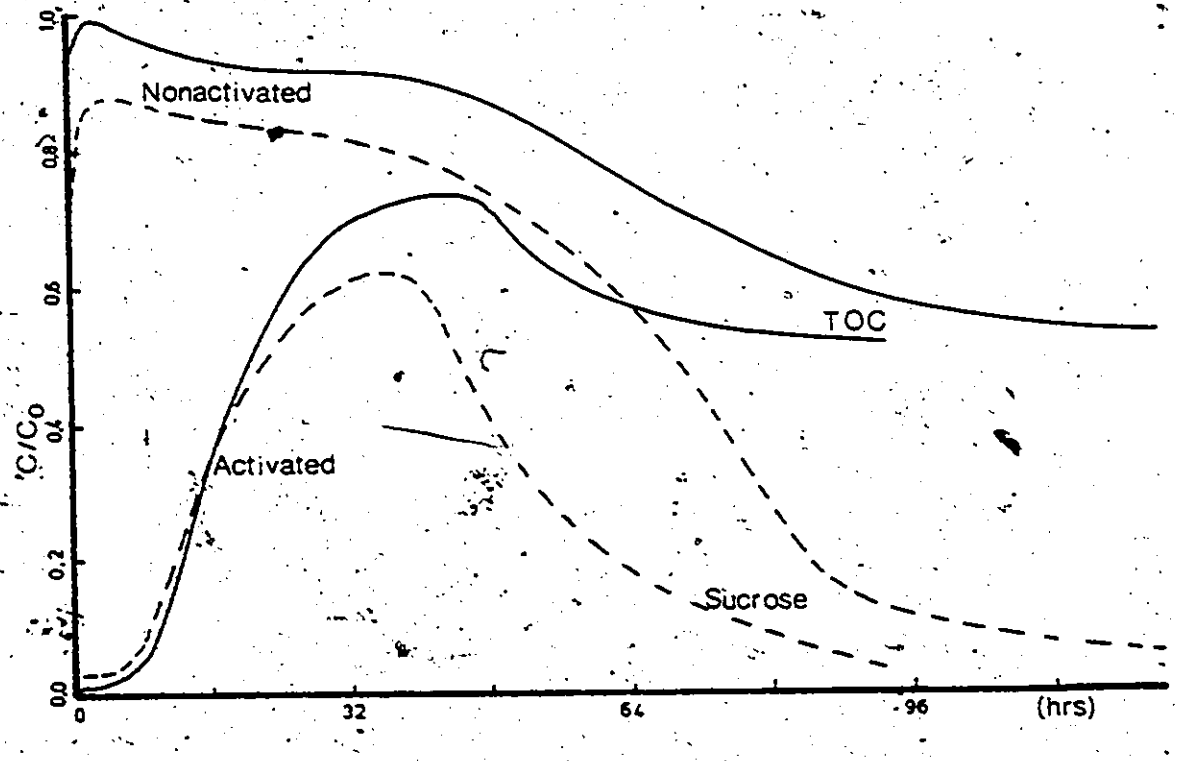

Figure 2-4. Comparison of Activated and Non-activated Carbon Column Effluents (after Weber (1977)).

becomes saturated the concentration in the effluent increases, while at the same time bacteria are growing in both the activated and non-activated carbon columns and removal due to biological degradation becomes significant. Near the end of the experiment the carbon's capacity is exhausted and the removal in both filters is identical, being wholly due to biological activity.

In a study designed to compare activated and non-activated carbon and sand filters, Lowry and Burkehead (1978) concluded that there were no significant differences, and that activated carbon offered no advantage over other media as a biological support. Young et al.(1975) and Jeris et al.(1977) have shown that good BOD and ammonia removal can be obtained in packed and fluidized sand filters. Jeris (1978) noted that "they have found that activated carbon is useful under appropriate conditions. However, it has been found that sand is usually the media of choice for both economic and other considerations."

Thus it can be concluded that at least for the easily biodegradable wastes used in the above studies, there is no conclusive evidence to support the concept of biological enhancement since activated carbon offers no advantage over an inert support once the adsorptive capacity of the carbon is exhausted. If such a mechanism does in fact exist, it would be expected to be most effective when adsorption columns are operated on low concentration and less degradable feedstreams such as in potable water application. Unfortunately there is little reliable data available for comparison of sand and activated filters in this area, and in many cases, prechlorination of the feedstream makes such comparison

impossible as activated carbon rapidly deactivates the chlorine residual whereas sand has no effect on it.

In the Bremen study reported earlier, parallel activated carbon and slow sand filters were operated for a three and a half year period. The results have been presented by Eberhardt et al.(1975) and DiGiano (1979) and are reproduced in Figure 2-5. The carbon column is seen to give a better quality effluent for approximately the first eighteen months after which time the removals in the sand and carbon filters are identical. DiGiano (1979) has suggested that because the contact time in the carbon columns was much less, it seemed to be more efficient than the sand column and therefore the equal removals may be evidence for

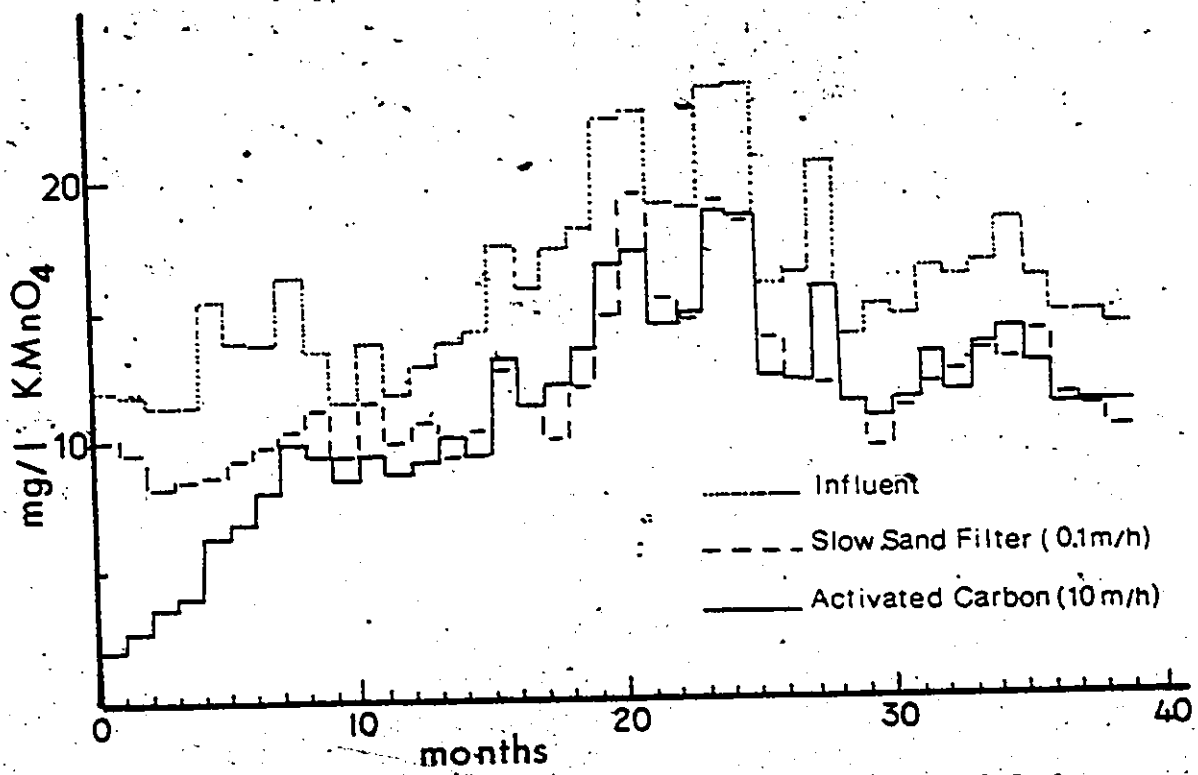

Figure 2-5. Comparison of $KMnO_4$ Removal by Sand and Activated Carbon (after Eberhardt et al. (1975))

biological enhancement. On the other hand, according to the mechanisms suggested in section 2.2.1, the data could equally well be interpreted as adsorptive removal in the carbon columns for eighteen months in parallel with biological removal of the biodegradable fraction of the influent in both columns. Without optimizing the contact times in both filters it is not possible to draw conclusions regarding the relative volumetric efficiencies of the support media. Some advantage in volumetric efficiency in the activated carbon column might be expected due to the higher external surface area of the irregularly shaped carbon particles.

Van der Kooij (1978) presented cell count data in sand, activated, and non-activated carbon filters fed with tapwater, and showed that the colony counts on the activated carbon were slightly higher than on the other media. He attributed this fact to the greater surface area in an activated carbon filter due to the irregular carbon particle shape and concluded that there was no evidence to suggest that the greater cell numbers in activated carbon filters should be attributed to the capacity of the carbon to adsorb dissolved organic material. This contention was further supported by experiments showing that bacteria on the activated and non-activated media withdrawn from the columns died at equal rates, and thus that the bacteria did not appear to be capable of utilizing the adsorbed organic molecules on the activated carbon.

The only other major study comparing parallel sand and activated carbon filters has been reported by Guirguis et al.(1978b). In this pilot scale study a chemically clarified and ozonated raw sewage was

passed through a multimedia filter then through three columns in parallel: a sand column, an activated carbon column, and an activated carbon column dosed with copper sulphate to hinder biological growth. Abundant biological growth and organic removal (BOD or COD) were found in the multimedia filter, a result which was not unexpected as the feedstream contained ample oxygen and a high BOD. After the multimedia filter, passage through the three filters in parallel showed:

(i) virtually no removal in the inert filter,

(ii) definite biological activity in the activated carbon filter as cumulative removal far exceeded the adsorptive capacity of the carbon,

(iii) significant removals in the copper dosed activated carbon filter and a small dissolved oxygen demand probably indicating some biological activity.

The fact that, when operated on the same feedstream, no removal was obtained in the inert filter whereas considerable biological growth was found in the activated carbon filter suggests the possibility of a bioregeneration mechanism. This possibility was proposed by the authors in an earlier paper (Guirguis et al.,1978a). Two alternative mechanisms may also offer an explanation of the observed behaviour:

(i) The dissolved oxygen level in the effluent of the multimedia filter was not reported however it could be assumed to be low as 25 mg/l of BOD was removed in this filter and this should exert a correspondingly large oxygen demand. After about five months operation when the carbon column was showing deteriorating

effluent quality, presumably because of adsorptive saturation, the influent to the carbon column had to be re-oxygenated to maintain performance. This would indicate that the oxygen level in the multimedia filter effluent was too low to sustain biological growth. Since reaerating the feed to the inert column is not mentioned, further removal may not have been obtained in this column because of a lack of dissolved oxygen. The influent to this column had a BOD of 25 mg/l and it is difficult to see why a bacterial culture would not develop in the filter if sufficient oxygen were present.

(ii) The other alternative is the possibility that some biologically toxic components were present in the feedstream. The Cleveland-Westerly plant described in this study receives substantial amounts of industrial waste which could exert an inhibitory effect on certain bacteria. If these compounds were adsorbed in the carbon filter, biological activity could proceed whereas their presence in the inert filter would limit biological growth.

2.2.6 Summary of Biological Mechanisms

The theories of biological enhancement and biological regeneration rely on the questionable ability of the bacteria to utilize substrate directly from the activated carbon surface. Since most of the adsorptive surface area of activated carbons is in pores too small for bacteria to penetrate, the mechanism requires that extracellular enzymes enter the carbon pore structure, react with molecules in the adsorbed state, and then that the products diffuse outwards to the bacteria on

the surface or in the large macropores. While this mechanism has been proposed, it has not been proven experimentally, and arguments for the existence of this mechanism are based on interpretation of operating data of pilot and full scale activated carbon columns.

The alternative explanation for the observed phenomena in biologically active activated carbon columns is the combined effects of adsorption onto the activated carbon and simultaneous biological degradation of organics from the liquid phase. If these combined mechanisms are responsible for the observed behaviour then the following should apply:

(i) After the adsorptive capacity of the activated carbon has been exhausted, equal removals should be obtained in sand and activated carbon beds provided that sufficient bacteria accumulate to accomplish the removal of biodegradable substrates, and no inhibitory substances which are selectively removed by the activated carbon are present.

(ii) If the feedstream does not exhibit a measurable BOD by respirometric or other methods, then no removal should be expected in a sand column and no removal beyond exhaustion of the adsorptive capacity should be expected in an activated carbon column unless, as discussed above, biologically inhibitory substances which are removed by the carbon are present.

(iii) Endogeneous dissolved oxygen demand and carbon dioxide production should be expected, irrespective of the removal of dissolved organic carbon, due to the presence of cell mass within the

biologically active carbon adsorber.

When interpreting experimental data, only that which is in disagreement with one or more of the above conditions should be regarded as potential evidence of biological regeneration or enhancement. In the discussion of the literature in the preceding sections it has been shown that most of the available data can be explained in terms of simple adsorption/biodegradation mechanisms, and that the studies which most strongly support the theories of biological regeneration and enhancement are open to alternative explanations of the data. Further, other studies have indicated that biological enhancement and regeneration does not in fact occur. Thus the evidence to date neither conclusively proves nor disproves either of the possible operating mechanisms however, since the data can generally be interpreted in terms of the simultaneous and parallel mechanisms of adsorption and biodegradation, there does not appear to be any justification for assuming that more complex or exotic mechanisms are at play.

There is no question that activated carbon provides a highly favourable biological support medium because of:

(i) Its ability to adsorb bacteria from solution (Klotz, et al., 1976),

(ii) Its ability to selectively adsorb or deactivate toxic components in the feed,

(iii) The protection given to bacteria from hydraulic shear and abrasion during backwash (Weber et al., 1978).

The combination of removal of biodegradable materials by biolo-

gical means, and removal of non-biodegradable materials by adsorption, allows for extended life of a biologically active carbon filter in comparison to a sterile filter. In addition, once the adsorptive capacity is reached and the filter operates in a steady-state by biological means only, the carbon may still have a higher volumetric efficiency than an inert filter because of higher cell counts. Its continued ability to adsorb toxic components by displacement of less strongly adsorbed molecules may also give the carbon bed an advantage over an equivalent non-activated bed in certain situations.

2.3 Biologically Active Filter Models

In recent years several models of biologically active packed and fluidized beds containing inert media have been presented. Other models have included the additional complication of simultaneous adsorption when activated carbon is used as the filter medium.

2.3.1 Inert Media Biological Filter Models

In either packed or fluidized mode, the bacteria are assumed to grow at the solid-liquid interface and result in the formation of a biological film surrounding the solid particles. The films are comprised of bacteria interspersed within a gelatinous polysaccharide matrix. The literature concerning the characteristics and kinetics of biological films is extensive, recent works in the area include those of Atkinson and Fowler (1974), Howell and Atkinson (1976), Williamson and McCarty (1976a, 1976b), Rittman and McCarty (1978), Famularo et al. (1978) and Mulcahy (1978).

A model of a biologically active filter must combine equations

describing local substrate uptake by the biological film with equations describing the changes in the liquid phase concentration as it passes through the filter. A complete description of the filter, since it is inherently an unsteady state process, requires the description of changes in porosity or bed expansion which are caused by growth of the biological films.

Jennings et al.(1975) modified the biolayer model of Williamson and McCarty (1976a) and developed a model describing the substrate uptake in a fluidized bed biological reactor (FBBR). External film resistance, diffusional resistance within the biological film, and bacterial reaction described by the Monod equation were included in the model. The absence of equations relating changes in the biological film thickness to substrate uptake limited the application of the model to pseudo-steady state operation when the film thickness remains essentially constant.

In a comprehensive model of an FBBR, Mulcahy (1978) developed hydrodynamic equations describing the changes in bed height and porosity with increasing bacterial mass, and solved these simultaneously with equations describing the rate of substrate uptake. The biological rate coefficients and yields for nitrate limited denitrification were calculated from experiments in a batch reactor. Using these coefficients and the calibrated hydrodynamic model, Mulcahy was able to describe the performance of experimental FBBR reasonably well.

Biological denitrification kinetics in a packed bed biological reactor (PBBR) were investigated by Harremoes (1976). As in the work of

Jennings (1975) with an FBBR, growth of bacteria and subsequent changes in porosity or pressure drop through the bed were neglected. Harremoes noted that the results of several PBBR studies of biological denitrification had indicated apparent half order reaction kinetics. He proposed a model in which biological reaction occurred on the walls of pores penetrating the biomass, and showed that a true zero order reaction in pores which substrate did not fully penetrate resulted in an apparent half order reaction. At lower concentrations the reaction became first order and was zero order at high substrate concentrations.

The effect of increasing biomass was incorporated into a model of a PBBR by Elmaleh et al.(1978). Equations were developed to describe extracellular storage of substrate by the bacteria as well as bacterial mass increase due to growth. In addition, changes in porosity, as well as oxygen and substrate uptake were described. When a highly degradable synthetic waste was fed to a bed of expanded clay particles, rapid blockage of the bed due to biomass accumulation was shown to occur. The model was fitted to the experimental data, and after calibration it appeared to be capable of describing the observed behaviour.

2.3.2 Biological Filter Models with Adsorptive Media

In an extension of an earlier model of Maqsood and Benedek (1977), Peel and Benedek (1977) presented a model for a PBBR containing activated carbon. The carbon particles were assumed to be surrounded by a biological film which presented an additional diffusional resistance to molecules adsorbing onto the carbon. A schematic diagram of the proposed model is shown in Figure 2-6. The concentration profile within the bio-

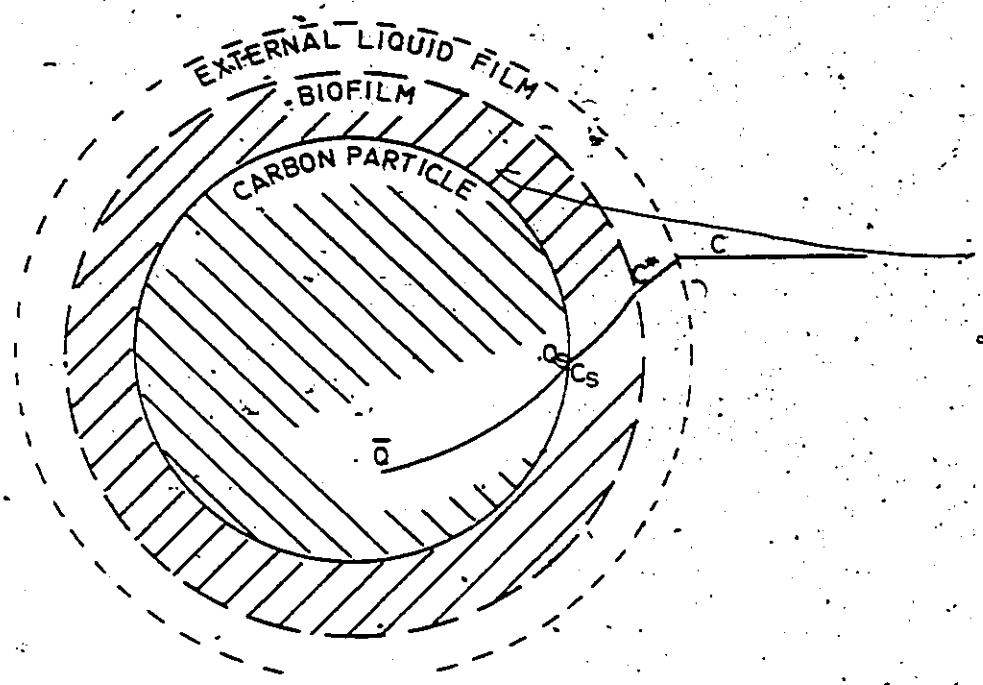

Figure 2-6. Schematic of Proposed Bioactive Adsorption Model of Peel and Benedek (1977).

logical film was calculated by assuming pseudo steady state operation and a zero order reaction; subsequent adsorption onto the carbon was described by the Glueckauf linear driving force equation. In addition, plug flow was assumed in the liquid phase. The model attempted to differentiate between components in the feedstream which were either adsorbable and degradable, or adsorbable and non-degradable, and treated the classifications separately. The model output was compared to data from physical chemical treatment systems and was shown to be reasonably able to describe the observed performance. However, the most significant parameter, that of biological reaction rate, had to be precalculated

from the data thus forcing the model agreement over much of the time span. The calculated reaction rates per unit of external surface area were shown to be comparable amongst the various studies thus giving an approximate guideline for the reaction rates which could be anticipated in other similar studies. It was proposed that experimental procedures for measuring the biological reaction rates be developed in subsequent work so that the model could be used as a predictive tool.

A somewhat similar model in many respects was proposed by Tien (1978) except that fluidized bed operation was assumed, and equations were included to describe the increase in biomass and subsequent expansion of the bed. In contrast to an earlier complex model of Andrews and Tien (1974), a mechanistic description of the respective transport processes and biological reaction rates was sought. Plug flow was assumed, the pseudo steady state assumption was invoked to calculate the biological film concentration profile, and the Glueckauf linear driving force was used to describe the adsorption rate. With the assumptions of first order biological reaction rate, a linear isotherm, and changes in biomass due only to growth, a set of equations describing the system performance was derived and solved by the method of characteristics. Tien also noted that a method for measurement of bacterial growth kinetics was under investigation but not yet fully developed, thus the model could not be used in a truly predictive capacity.

In addition to the works of Mulcahy (1978) and Tien (1978), Tsezos and Benedek (1979) have also proposed a method for calculating the biomass holdup in an FBBR, based on measurement of the bed height

expansion.

A different approach was taken by Ying (1978) in the modelling of packed and fluidized bed biological reactors. Ying noted that during the actual use of activated carbon columns, backwashing and air scouring are usually practiced at frequent intervals to remove excess biomass. He therefore proposed that a pseudo steady state thin film could be assumed to exist around the carbon particles and that the film would not appreciably retard the adsorption rate. By making this assumption the complications arising from modelling increasing film thickness and bed expansion can be avoided. In addition, the necessity of solving the diffusion equation within the biofilm is eliminated as the biological removal is assumed to occur at the concentration of the outer surface of the carbon particle. Ying assumed Monod kinetics for the biological reaction and a surface diffusion mechanism for adsorption and attempted to apply the model in a predictive mode to experimental data. As discussed in part I of this report the adsorption side of the study was unsuccessful as the adsorption parameters eventually had to be measured from actual column breakthrough data. The biological parameters were measured in batch experiments but because of considerable variation, the parameters used to describe the column behaviour were also calculated from preliminary bioactive column runs. Thus both the biological and adsorption parameters were calibrated from experimental column runs and the aim of developing a predictive model was not achieved.

In all of the modelling studies of biological-activated carbon filters reported above, relatively easily biodegradable substrates at

high concentrations were fed to the columns. The application of such feedstreams to activated carbon columns is questionable as it has been previously shown that these materials can be removed in beds containing inert media, and therefore that the adsorptive capacity of activated carbon is not necessary. Additionally, since activated carbon is more fragile than most inert media, biomass control techniques are not as effective in activated carbon columns. The applications where activated carbon has an obvious advantage are those where the waste is not easily degradable, and most of the influent contaminants must be removed by adsorption. In such situations the biological growth which does occur is not abundant, and a model such as that proposed by Ying (1978) which neglects the accumulation of biomass appears to be the most applicable. In this model the processes of biodegradation and adsorption occur simultaneously at the external surface of the carbon particle.

In the field of potable water treatment, Klotz et al.(1976), Van der Kooij (1976), and Cairo et al.(1979), have reported the results of scanning electron micrograms (SEM) of carbon particles withdrawn from operating filters. These SEM.s showed that the bacterial densities were low, and surface coverage was incomplete. Weber et al.(1978) reported SEM.s of carbon particles contacted with raw sewage and dilute humic acid for periods of 17 and 10 days respectively. In both cases the surface coverage by bacteria was incomplete, and did not suggest a significant diffusional resistance to the adsorbing molecules. Thus in some practical applications of activated carbon adsorption the observed results concur with Ying's hypothesis that diffusional resistance and

particle size expansion resulting from the presence of bacteria on the external carbon surface can be neglected.

2.4 Multicomponent and Bulk Parameter Modelling

In the majority of applications of activated carbon adsorption it is not possible to define the wastestream in terms of one, two, or even three components. In many cases, even when tens or hundreds of single compounds are identified, they still only comprise a small fraction of the total organic matter in the wastestream. In such situations the only way that the wastestream can be quantified or modelled is in terms of a lumped or gross parameter such as TOC. The use of a lumped parameter, however, imposes limitations on the ability of the model to describe the behaviour of adsorption beds.

As pointed out by DiGiano (1978) in a recent review of competitive adsorption, problems such as early breakthrough of poorly adsorbed components, and concentration of weakly adsorbed components in the effluent due to displacement effects within the filter, can occur when a complex feedstream is applied to an activated carbon column. It is not possible to predict these effects using a lumped parameter approach, and although it is theoretically possible to do so using multicomponent competitive adsorption models, DiGiano concluded that at the present time there are still uncertainties in the application of these models even to well defined binary systems. Therefore, a precise description of the adsorptive behaviour of a complex waste is presently impossible. DiGiano suggested that some degree of resolution may be obtainable by classifying the waste into groups of components exhibiting similar equi-

librium behaviour.

Some advances in the area of complex waste modelling have been made by Frick et al.(1978). In the reported study, the behaviour of a key component, p-nitrophenol (PNP), was observed in the presence of general background river water organics which were measured by a lumped parameter (UV absorbance or dissolved organic carbon (DOC)). This approach enables competitive effects between the key component of interest and the background organics to be estimated, and may eventually enable the behaviour of a specific component in a complex wastestream to be modelled. A case of particular interest at present in the potable water field is the behaviour of trihalomethanes in the presence of general background organics of which a large fraction are fulvic and humic acids. Predictive modelling would require the description of the adsorptive behaviour of both the key component and the background organics as measured by a lumped parameter, in addition to the competitive equilibrium effects.

The objective of the present study is the description of the adsorptive behaviour of the background organics as described by a bulk concentration parameter. While this approach cannot account for the differences in adsorption of the various components, nor the complex displacement and competitive adsorption effects, it is anticipated that because the concentration of any single component is much less than the gross concentration, the behaviour of single components may not be reflected in the overall behaviour of the system.

Very few activated carbon adsorption models using a gross para-

meter approach have been presented in the literature, and even fewer have attempted to verify the models against experimental data. Usinowicz (1972) conducted experiments to determine whether the Heister and Vermeulen kinetic model could be used to describe the adsorptive performance of synthetic complex wastes characterized by the chemical oxygen demand (COD) alone. He was able to predict the initial shape of the breakthrough curves reasonably well using kinetic constants determined from batch kinetic COD measurements but the later stages of the experimental breakthrough curves exhibited a strong tailing effect whereas the model predicted a more rapid approach to saturation. As discussed in part I of this report, this effect is more likely due to an inadequate kinetic model than to the use of a gross parameter. In addition, the single component breakthrough curves reported by Usinowicz showed a similar behaviour to that of the complex mixtures.

Modelling of waste treatment systems using a lumped parameter has also been proposed by Andrews and Tien (1974) and Tien (1978). In the latter paper, Tien noted the drawbacks of this type of approach but concluded that given the nature of most wastes which are to be treated, no alternative is possible. A similar conclusion was reached by Peel and Benedek (1977). These studies incorporated the effects of biological activity both in the models as well as in experimental data reported, and therefore it was not possible to separately assess the effectiveness of the lumped parameter adsorption modelling.

Thus although modelling using a lumped parameter should not be expected to give a precise description of the performance of an adsorp-

tion system, the results of Usinowicz (1972) indicate that reasonable predictions might be obtained. In the studies reported in the following chapter, the kinetic model developed in part I of this report is used to predict the performance of adsorption columns operated over extended periods using only a lumped parameter approach. Comparison of experimental data with the model predictions allows conclusions to be drawn regarding the effectiveness of this approach.

CHAPTER 3.

Experimental Materials and Methods

In the following chapters the results of two separate adsorption studies are reported. The first study, involving the adsorption of Hamilton, Ontario, tap water onto activated carbon, was conducted at McMaster University and is discussed in detail by Benedek and Bancsi (1977). In addition to the data contained in the report, separate isotherm experiments were conducted by the present author. Also, as the columns have been operated continually since the completion of the report in 1977, more long term breakthrough data is reported herein. In the second, the adsorption of biological residual materials onto packed beds of activated carbon was measured over an extended time period. The biological residual was generated by operating an activated sludge unit on a single carbon substrate (phenol), and isotherm and batch kinetic data were obtained for this material.

Since not all techniques or procedures were common to both of the studies, the experimental materials and methods are reported separately. Those techniques which were common are discussed in detail in the section on the bioresidual studies.

3.1 Tap Water Studies

The adsorption columns in this study were supplied directly with Hamilton tap water which is obtained from Lake Ontario and undergoes conventional treatment of prechlorination, alum clarification, sand filtra-

tion, and post chlorination. The water is generally of quite a high quality and has a typical TOC concentration of about 1.5 mg/l (based on A_{254nm}^{10cm}). The adsorbent used in the study was Filtrasorb F400, the same activated carbon as was used in the pure solute and bioresidual studies of the present work.

Details of the experimental study have been reported previously (Benedek and Bancsi, 1977) and are only summarized briefly herein.

3.1.1 Adsorption Systems

The columns were 5 cm i.d. PVC tubes with flow distributors at the inlet and each column contained 162.3 g of F400 giving a nominal bed-depth of 20 cm per column. A sand prefilter was used to remove suspended solids which were largely metal hydroxide flocs from the incoming water, thus preventing problems with excessive pressure losses across the carbon columns. Over the two year period of operation backwashing of the carbon columns was not found to be necessary. A flow diagram of the experimental system is shown in Figure 3-1. The system consisted of 3 activated carbon columns, one slow filter operating at 1.24 m/h (0.42 gpm/ft^2), and two rapid filters in series operating at 7.37 m/hr (2.5 gpm/ft^2). Influent and effluent samples were collected at regular intervals over a 2 year period and were filtered prior to UV absorbance measurement.

3.1.2 Analytical Techniques

Measurements of organic concentration were mostly made by UV absorbance (A_{254nm}^{10cm}) and converted to TOC data using a correlation developed at McMaster. In the last year of operation some measurements were by

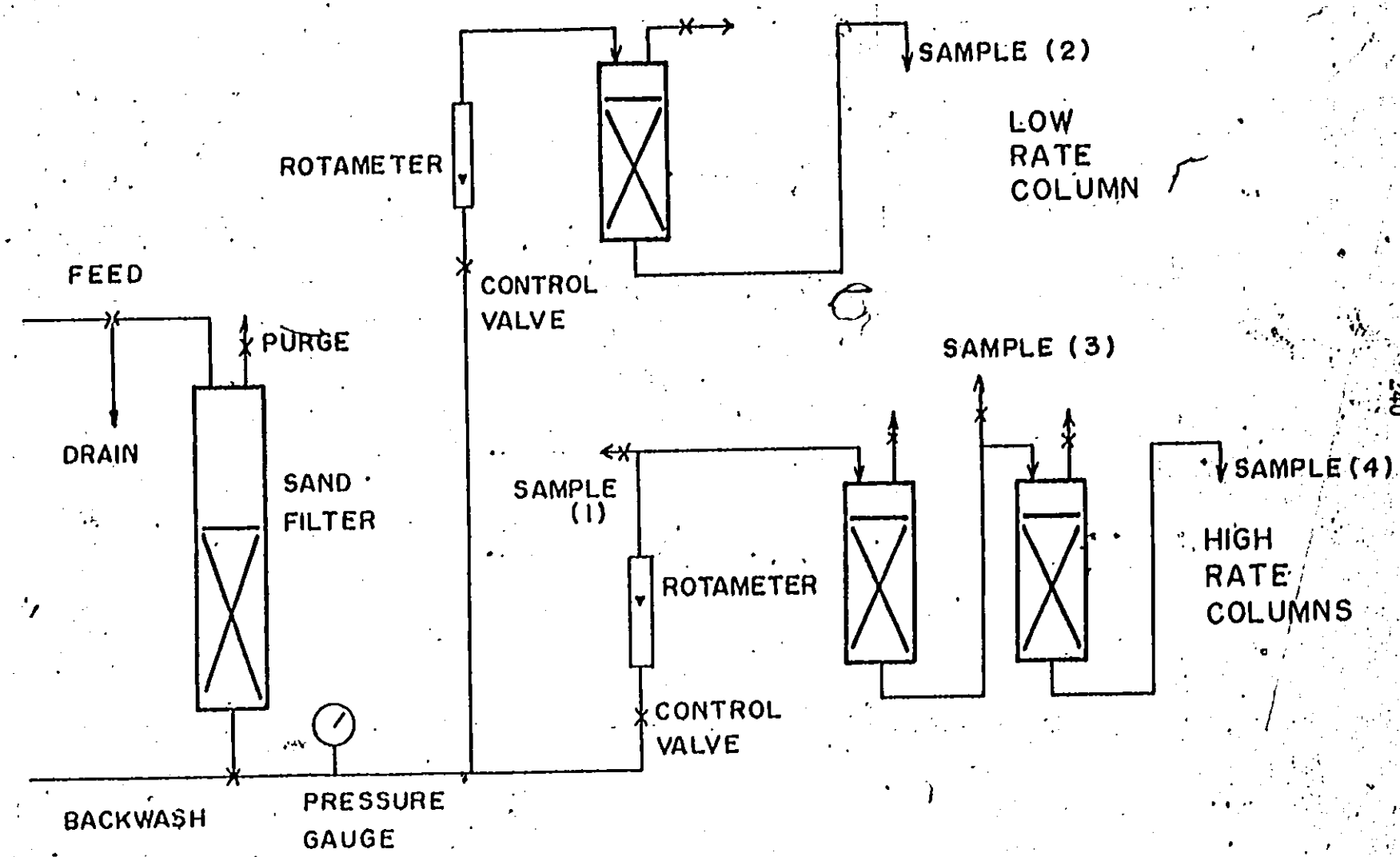

Figure 3-1. Schematic Diagram of Carbon Adsorption Pilot Plant, (after Benedek and Bancsi (1977)).

direct TOC analysis (see section 3.2.4). All samples were filtered through cellulose nitrate membrane filters with 0.2 μm pore size. The filters were soaked in distilled water overnight and rinsed with 200 ml of distilled water until no further TOC was leached from the filters. Ultrapure water was obtained by distilling previously distilled water from a permanganate solution.

3.1.3 Equilibrium Studies

As discussed further in section 3.2.5, the equilibrium isotherms in the reported study were suspect as large differences were found between GAC and PAC isotherms. To obtain an accurate isotherm, the same procedure as detailed later for the bioresidual studies was used for the tap water isotherms. Measured amounts of F400 were added to carefully cleaned 500 ml bottles. After adding 400 ml of tap water, the bottles were sealed and rotated for 14 days in a dark room. At this time the bottles were removed from the rotary apparatus and the liquid concentrations were measured by UV absorbance.

3.1.4 Batch Kinetic Studies

Adsorption kinetics were conducted by the multiple flask technique. A number of flasks each containing 120 mg of F400 and 250 ml of tap water were placed on an orbital shaker. Individual flasks were periodically withdrawn and the carbon immediately separated from the liquid phase by filtration. The filtrate was then analysed by UV absorbance.

3.2 Biological Residual Studies

The experimental system is shown in Figure 3-2. It consisted of

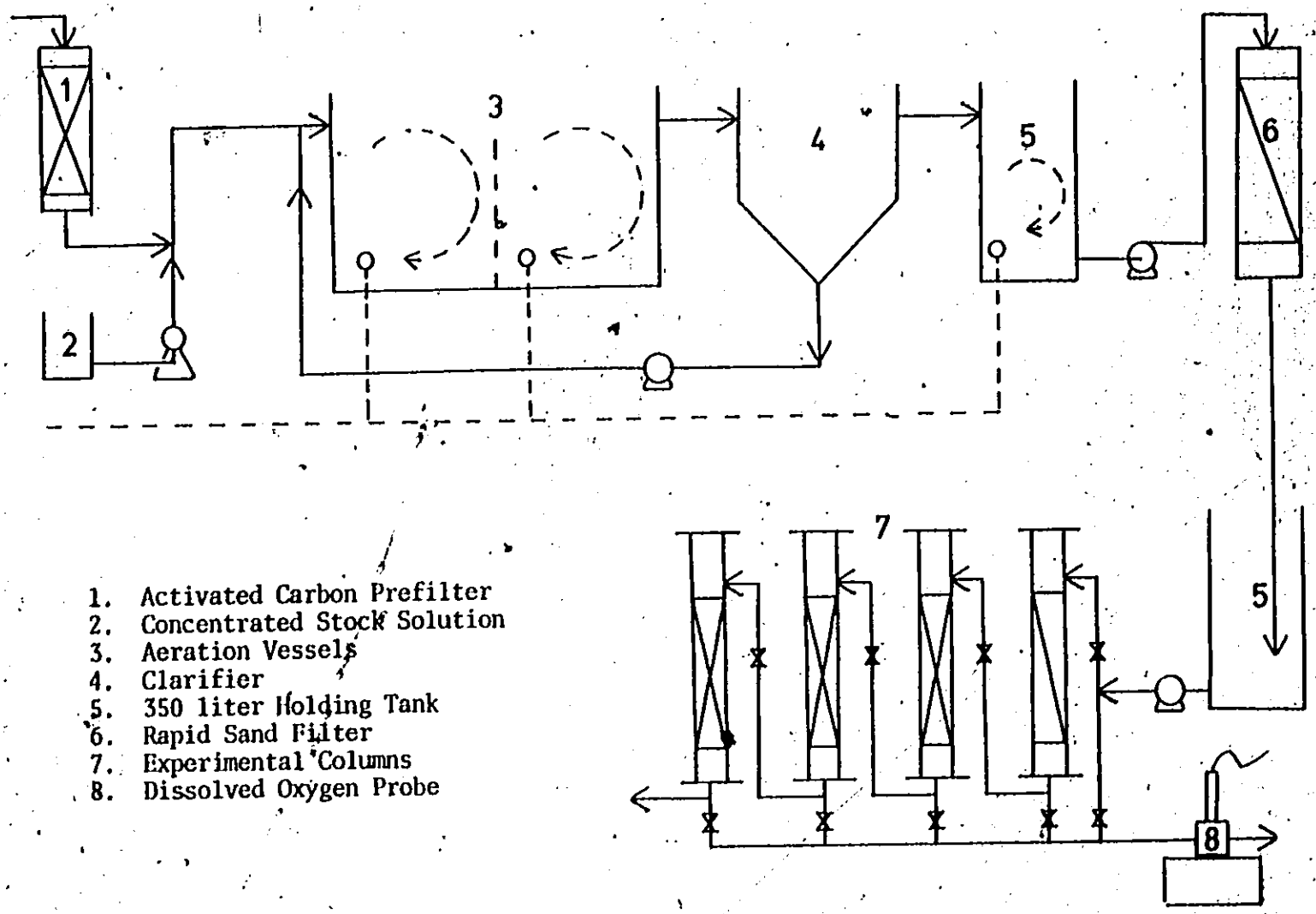

1. Activated Carbon Prefilter
2. Concentrated Stock Solution
3. Aeration Vessels
4. Clarifier
5. 350 liter Holding Tank
6. Rapid Sand Filter
7. Experimental Columns
8. Dissolved Oxygen Probe

Figure 3-2. Schematic Diagram of Bioresidual Generation and Adsorption System.

two parts, the bioresidual generating system, and the adsorption system. The bioresidual material was produced in an activated sludge unit which was followed by a secondary clarifier and an aerated 350 litre holding tank. From the holding tank the effluent was periodically pumped through a rapid sand filter to the feed tank of the adsorption system which consisted of several 2.8 cm diameter transparent acrylic columns in series.

3.2.1 Activated Sludge System

The aeration tank was of 10 litre total capacity and was divided into two equal sections by a baffle to give some plug flow character to the system, however, the flow pattern was not determined. The baffle was added to more closely approximate most full scale plants which are seldom perfectly mixed and have some degree of plug flow. An air diffuser in each section kept the sludge in constant suspension and each was adjusted to maintain the dissolved oxygen (DO) above 4 mg/l at the outlet.

A 5 litre glass cone with provision for sludge withdrawal and effluent overflow was used as a clarifier. Return sludge was pumped intermittently by connecting the sludge return pump to a timing device and sludge wasting was done manually by periodic withdrawal of mixed liquor after returning all the clarifier solids to the aeration tank.

In general, conditions in the activated sludge system were set at typical levels of municipal activated sludge plant operation. The conditions of operation are given in Table 3-1. Occasional problems with bulking filamentous sludge periodically interfered with the maintenance of these conditions.

Table 3-1 : Activated Sludge Operating Conditions

Substrate	Phenol
Feed concentration	110 mg/l
BOD : N*	100 : 5
Buffer system	0.001 M as K_2HPO_4
Flowrate	40 l/day
Hyd. detention time	6 h
Average sludge age	10 days
Average yield*	0.25 g VSS/g BOD
Aeration tank solids	2000 mg VSS/l
F/M	0.3 - 0.5 g BOD/day/g VSS
pH	6.9 - 7.2
D.O	> 4 mg/l

* Based on a theoretical phenol BOD of 2.38 g/g
Nitrogen added as $(NH_4)_2 SO_4$

The system was fed by inline mixing of a concentrated solution of phenol and nutrients with tap water. A diaphragm type metering pump supplied the concentrated stock solution, and the tap water was fed through a rotameter from a constant head tank. To remove potential interfering materials from the influent stream, the tap water was passed through a large activated carbon filter containing 5 kg of Filtrasorb F400 prior to being mixed with the feedstock. The residence time in the oversized filter was 3 h on an empty bed basis, ensuring that there were no kinetic limitations to adsorption. Periodic monitoring of the pre-filter effluent indicated a constant low level TOC throughout the duration of the experiment; thus ensuring no breakthrough of adsorbable components.

3.2.2 Effluent Collection

The overflow from the secondary clarifier led to an aerated 350 litre polyurethane tank. The effluent was allowed to accumulate in this tank over 7 day periods and was gently aerated to maintain a dissolved oxygen (DO) residual. Except at times of clarifier imbalance, the suspended solids level in the collection tank was less than 4 mg/l when measured with a 0.45 µm pore size fibreglass filter.

At the end of each 7 day period, the contents of the tank were pumped through a rapid sand filter at a rate of 8 m/hr (3 gpm/ft^2) to remove most of the remaining suspended solids. The filtrate was collected in another 350 litre tank which served as the adsorption system feed supply. The level of suspended solids in the filtrate was not closely monitored as it was always very low and at no time exceeded 1 mg/l.

The 7 day storage period was used to stabilize any undegraded substrate thus ensuring the feed to the carbon columns would not contain any easily biodegradable organics.

3.2.3 Adsorption System

A peristaltic pump was used to pass the residual material from the feed tank through a series of 2.8 cm diameter perspex columns at a rate of 30 l/day or 2 m/h (0.7 gpm/ft^2). The low flowrate was dictated by the amount of bioresidual material which could be produced in the activated sludge unit. Columns with smaller diameters were not used because of the increasing wall effects as the column diameter to particle

diameter ratio decreases below 30 (Schwartz and Smith, 1953). Four columns each 30 cm high were used, and the system generally consisted of a sand filter followed by 3 activated carbon filters. The masses of carbon in the filters were 14.6, 17.2 and 50 gms respectively, giving cumulative bed depths of 6.7, 14.6 and 31.3 cm.

In one part of the experiment, the sand filter was followed by a crushed coke filter and then by the activated carbon filters. The coke was obtained from Dominion Foundries and Steel Company in Hamilton, Ontario, and assayed as approximately 90% carbon. Both the sand and coke were sieved to 16 × 30 mesh so as to be comparable in size to the activated carbon. They were washed in hot 2N HCl then repeatedly rinsed in distilled, deionized water until no TOC increase in the wash water was observed. The quantities of sand and coke in the filters were chosen to give the same external surface areas as in the first two activated carbon filters.

Each filter was covered with aluminum foil to exclude light and thus prevent algal growth in the system. The feed tank and lines were similarly covered. Because biological solids built up in the sand and first and second activated carbon filters, periodical backwashing was performed when visual inspection revealed significant solids accumulation. The columns were first air scoured for 2 minutes to break up the filtered material, and were then backwashed with product water until a clear effluent was obtained.

The system was connected so that any stream could be routed

through a small stirred cell containing a dissolved oxygen probe. In this way direct inline measurements of the DO could be made without disturbing the system's operation or contaminating the sample with atmospheric oxygen.

3.2.4 Analytical Techniques

U.V. Absorbance and TOC : The use of A_{254nm}^{10cm} as an indirect measurement of the amount of organic contaminant in natural or potable water is quite widespread in Europe and was shown by Dobbs et al.(1972) to be reliable and accurate. In this work the absorbance was measured with a Bausch and Lomb Spectronic 21-UV-D spectrophotometer against an air reference blank set arbitrarily to 0.100 absorbance units. Previous work had indicated problems in obtaining high purity water of a consistent quality for a reliable water reference.

In previous studies at McMaster, a correlation between A_{254nm}^{10cm} and the TOC in natural waters had been developed (Benedek and Bancsi, 1977). This correlation was used as a basis for the present work and several additional sets of data were analyzed on a Dohrman Model DC-54 Low Level TOC instrument (Dohrman Instruments, Santa Clara, Cal.). One set of data was sent for TOC analysis to the Ontario Ministry of The Environment Laboratories in Toronto, Ontario, to provide an independent check.

The correlation between A_{254nm}^{10cm} and TOC for the phenolic residual material was found to be very similar to the correlation for natural waters suggesting that the components may be of the same general type. The data measured in the present study plus the previous correlation for

natural waters are shown in Figure 3-3 and indicate that the phenolic residual material in the present study can be adequately correlated to TOC measurements using the relationship developed for natural waters. As a consequence, all the A_{254nm}^{10cm} date in the present study were converted to TOC and have been reported as such in the remainder of the report. Since many of the data points in Figure 3-3 were obtained from simultaneous TOC and A_{254nm}^{10cm} measurements of the column concentration profiles, the UV absorbance proved to be an accurate indicator of the actual TOC removal through the columns.

Prior to all analyses, the samples were filtered through Gelman 0.45 μm membrane filters which had been thoroughly washed with 500 mls of distilled deionized water in 3 separate batches. The washing ensured that all leachable TOC was removed prior to sample filtration. In addition, the first 50 mls of filtrate were discarded.

NO_2 - NO_3 - NH_3 : Nitrogen analyses were not performed routinely, but nitrogen conversions within the columns were measured at different stages of the study, All the respective nitrogen component analyses were determined in a Technicon Auto Analyser (Technicon Corp., Tarrytown, N.Y.) using Technicon Method No.19-69W for NH_3-N and Method No.100-70W for NO_3-NO_2-N.

Dissolved Oxygen : A small stirred flow-through cell containing an oxygen probe connected to a YSI Model 54 Oxygen Meter was used to measure the DO concentrations. The system was calibrated by passing saturated water through the cell. Because contact with atmospheric oxygen was prevented, accurate measurements of DO could be obtained even at the low system flowrates encountered.

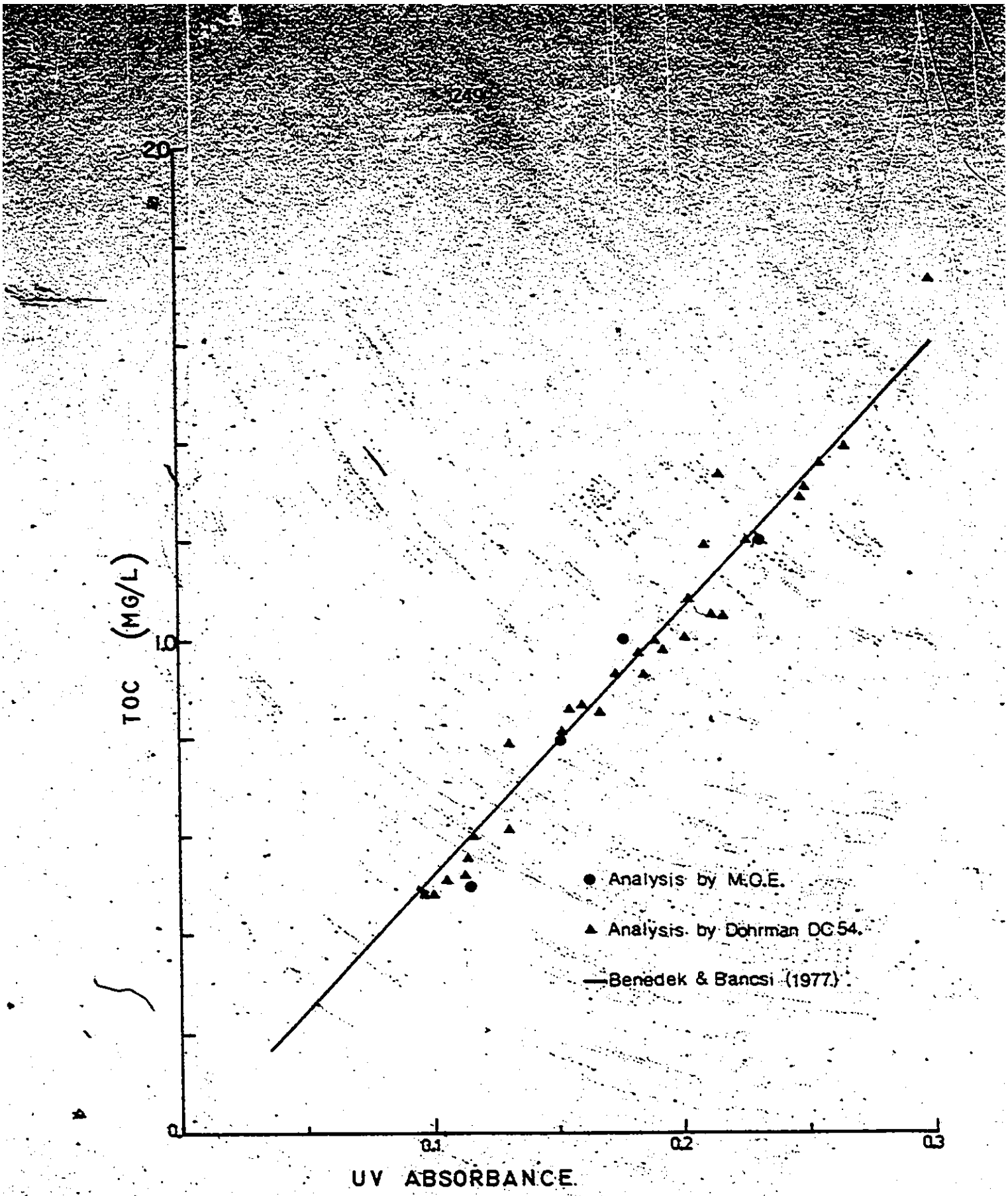

Figure 3-3. Correlation of TOC with UV Absorbance ($A^{10\ cm}_{254\ nm}$).

3.2.5 Equilibrium Studies

Experimental studies previously undertaken at McMaster University in which granular (GAC) and powered carbon (PAC) isotherms of natural waters were measured (Benedek & Bancsi, 1977), had shown large differences between GAC and PAC isotherms of the same water. GAC isotherms measured over 5-day periods generally showed about half the capacity of PAC isotherms measured over 24 h periods. The differences were attributed to either kinetic limitations in the GAC isotherms, or to a change in activated carbon properties upon crushing, and the former was considered more probable.

Based on the results of the pure solute equilibrium studies reported in part I of this thesis, the explanation regarding kinetic limitations appears very likely. Since it was shown that phenol and o-chlorophenol, which are both relatively small molecules, took about one month to reach equilibrium with GAC, the larger molecules in the bioresidual material and in natural waters could be expected to take much longer, perhaps even years to reach equilibrium. Because it is obviously not practical to measure isotherms over such extended periods, the only alternative is the use of PAC.

The equivalence of GAC and PAC isotherms where small molecules are adsorbed was demonstrated in part I of this report. The possibility exists that PAC and GAC isotherms may differ when very large molecules are adsorbed if the molecules attach at the outer surface of the adsorbent rather than entering the pore structure. Because a given mass of PAC has a greater external surface than the same mass of GAC, greater

adsorption onto PAC might be expected. This possibility is discussed further in Appendix IIA of this report where it is shown, based on experimental data of adsorption of large molecules, that differences in adsorption due to attachment to the external surface do not appear to be significant.

The experimental isotherms in the present study were therefore measured with PAC, and a 14 day contact period was allowed. The use of PAC to measure natural organic isotherms is common practice in European studies (Frick et al. 1978) where the validity of its use has not been questioned. In the present study, quantities of PAC were added to 500 ml bottles and then 400 ml of the bioresidual containing water were added. The bottles were then sealed and rotated end over end for the chosen contact period after which samples were filtered through washed 0.45 um Gelman membrane filters prior to analysis by UV absorbance. A check for equilibrium attainment was made four days prior to isotherm termination, the changes in concentrations in the bottles over the 4-day period were small, and within the error of the experimental measurement.

Although biological degradation in the isotherm bottles was considered unlikely because of the stability of the waste, the bottles and seals were thoroughly cleaned with chromic acid prior to use, and the bioresidual water was filtered through a 0.1 um membrane filter to remove any bacteria carried over from the activated sludge unit. Furthermore, no change in concentration was observed in the blanks which did not contain activated carbon.

3.2.6 Batch Kinetic Studies

To prevent contamination of the low level organics in the adsorbate solution, the batch kinetic equipment was constructed of stainless steel and glass only. A 4 litre glass beaker with stainless steel baffles attached to the walls was used, and, as the kinetics were measured over an extended period (10 days), the carbon was contained in stainless steel baskets on a stainless steel impeller. The system, shown in Figure 3-4 was thoroughly cleaned with chromic acid prior to use and heavy gauge aluminum foil was used to preclude light and minimize exchange with the atmosphere. To measure the kinetic parameters the system was filled

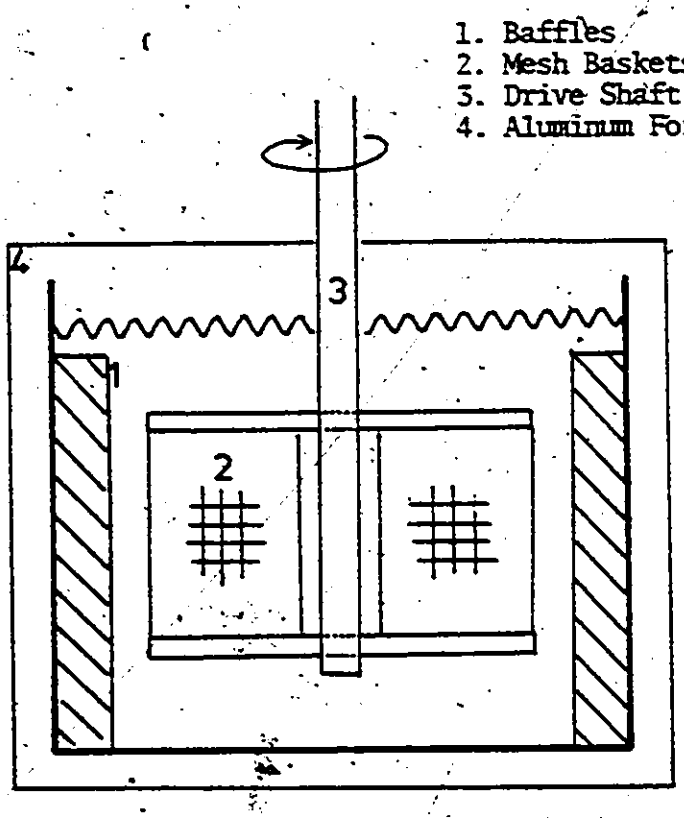

Figure 3-4 : Batch Kinetic Apparatus for Bioresidual Studies

with 2.0 litre of the bioresidual containing water which had been filtered through a 0.1 μm Gelman membrane filter to remove any bacteria remaining after the rapid sand filtration. The basket impeller containing a measured quantity of carbon was then lowered into the solution and rotation commenced at 100 rpm. Measurements of UV absorbance were taken at 5 minute intervals initially to determine the film transfer coefficient, then at ever increasing intervals until the experiment was terminated. Because the samples were returned to the system after UV measurement there was no cumulative error due to sampling losses.

3.2.7 Recirculation Studies

To further investigate the mechanisms involved in removal of TOC within the adsorption columns, recirculation studies were undertaken on the columns after they had been in service for several months. A column was isolated from the adsorption system and connected in a closed loop to a reservoir containing 1 litre of the bioresidual feed. An air diffuser supplied with ultrapure bottled air which was saturated with distilled water was used to mix the reservoir and maintain a DO level. During the experiment a peristaltic pump was used to circulate the reservoir contents through the column and back to the reservoir and at intervals samples were withdrawn for UV absorbance measurement.

CHAPTER 4

ADSORPTION STUDIES WITH TAP WATER

The removal of organic contaminants from potable water supplies by activated carbon is widely practised in Europe and in certain critical areas in North America. The tap water in the present study was chosen as it contains organics which are representative of those naturally occurring in lakes and rivers.

4.1 Equilibrium Isotherm

The effluent from a large activated carbon prefilter treating tap water for the bioresidual study, as well as equilibrium determinations using large quantities of activated carbon, indicated that a fraction of the organics in tap water were non-adsorbable. The level remained quite constant over the period of the study at 0.36 mg/l TOC. Since this material passes directly to the effluent in an adsorption column and has no effect on the behaviour of the adsorbable material, it was subsequently subtracted from all equilibrium and kinetic data so that only the adsorbable TOC is reported. When predicting the column effluent profiles, this fraction of non-adsorbable TOC was added to the adsorbable TOC to give the total effluent concentration.

The equilibrium isotherm determined ofter 14 days contact with PAC is shown in Figure 4-1. After subtracting the non-adsorbable fraction the isotherm relationship appeared to be quite linear, and to pass

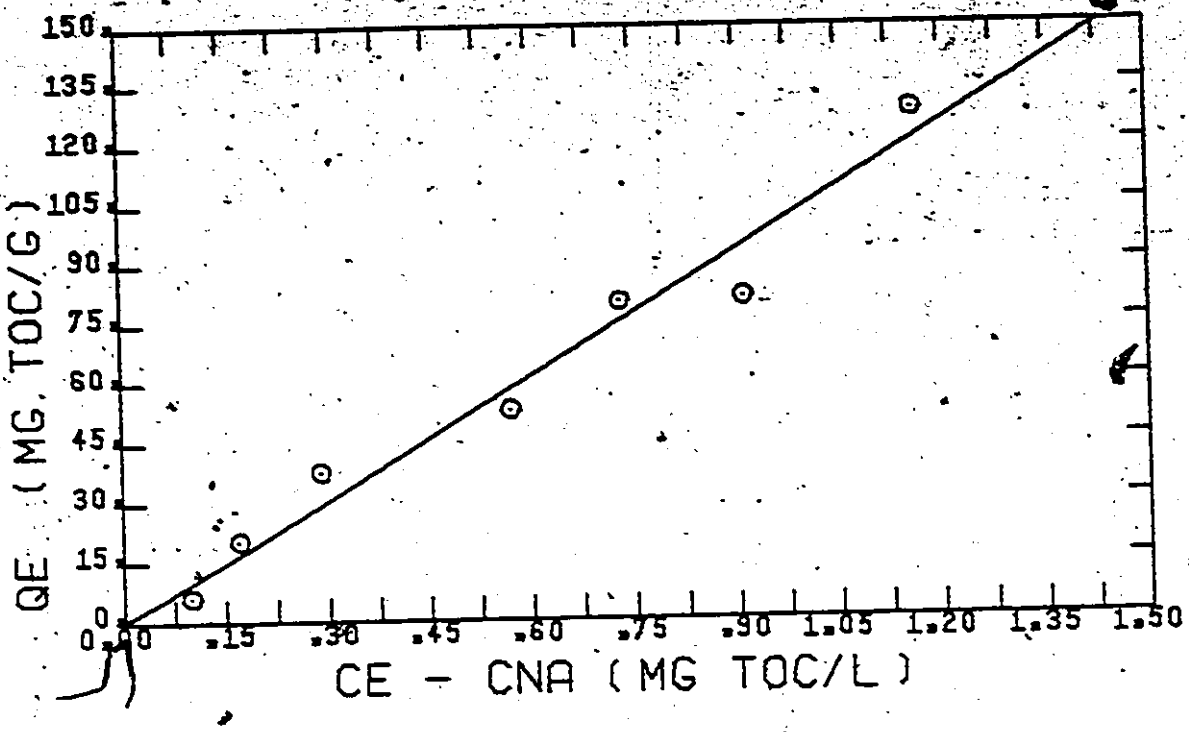

Figure 4-1. Isotherm of Hamilton Tap Water Organics.

through the origin.

The data were fitted to a Freundlich equation using a non-linear least squares procedure which yielded the equation

$$q_e = 103.6\ C_e^{1.02} \qquad (4.1)$$

where q_e = mg TOC/g carbon; and C_e = mg TOC/l. Since the exponent was not significantly different from unity at the 95% confidence level, a linear isotherm was assumed in solving the kinetic model, thus reducing the amount of computation required for a solution.

The measured isotherm indicates significantly greater adsorptive capacity than was reported in the original study (Benedek and Bancsi,

1977). The difference is probably due to the increased contact time allowed between the tap water and PAC in the present study, and indicates that a 24 h contact time between PAC and low level tap water organics may be insufficient to achieve equilibrium. However, since the isotherms were conducted on different samples of tap water, the possibility that the nature of the organic substances had changed cannot be precluded. When compared to isotherms published in the literature for the adsorption of OSW and humic acids onto activated carbon, the tap water isotherm of the present study falls somewhere in the middle of the range. The isotherms are presented in Table 4-1 in descending order of adsorptive capacity as measured at 1 mg/l TOC.

4.2 Batch Kinetic Studies

The batch kinetic data and the best fit predictions of the branched pore adsorption model presented in part I of this report are shown in Figure 4-2. The simplified form of the model incorporating the quadratic driving force (QDF) assumption was used in conjunction with a linear isotherm and the model is seen to give an excellent description of the data over the 20 day experimental period. The low value of f = 0.2 indicates that most of the adsorptive capacity is in the slowly diffusing region in contrast to the results reported in part I for phenolics, where f was approximately 0.7 and most of the adsorptive capacity was in the more rapidly diffusing region. The difference is attributed to the different sizes of the adsorbing molecules, while the molecular weights of the tap water organics are unknown, the average molecular weight and thus molecular size would be significantly greater than for phenol.

Isotherm $q_e = M C_e^n$		Organic Source	Activated Carbon	Reference
M	n			
350	1.9	Rhine River	LEV 693	Fokken and Kurz (1979)
210	1.1	Rhine River	ROW 08S	" "
137	0.75	Biological residual	F400	Present Study
120	0.97	Rhine River	LSS	Fokken and Kurz (1979)
112	0.47	Rhine River	-	Frick et al. (1978) *
103.6	1.02	Hamilton tap water	F400	Present study
60	2.1	Rhine River	Norit	Holzel and Sontheimer (1979) *
27.1	0.55	Commercial humic acid	F400	Snoeyink et al.(1977) *
22.8	0.91	Soil humic acid	F400	" " "

* Graphical data reported only. Coefficients calculated from plotted data.

Table 4-1. Adsorption Isotherms of Organics Present in Potable Water Supplies

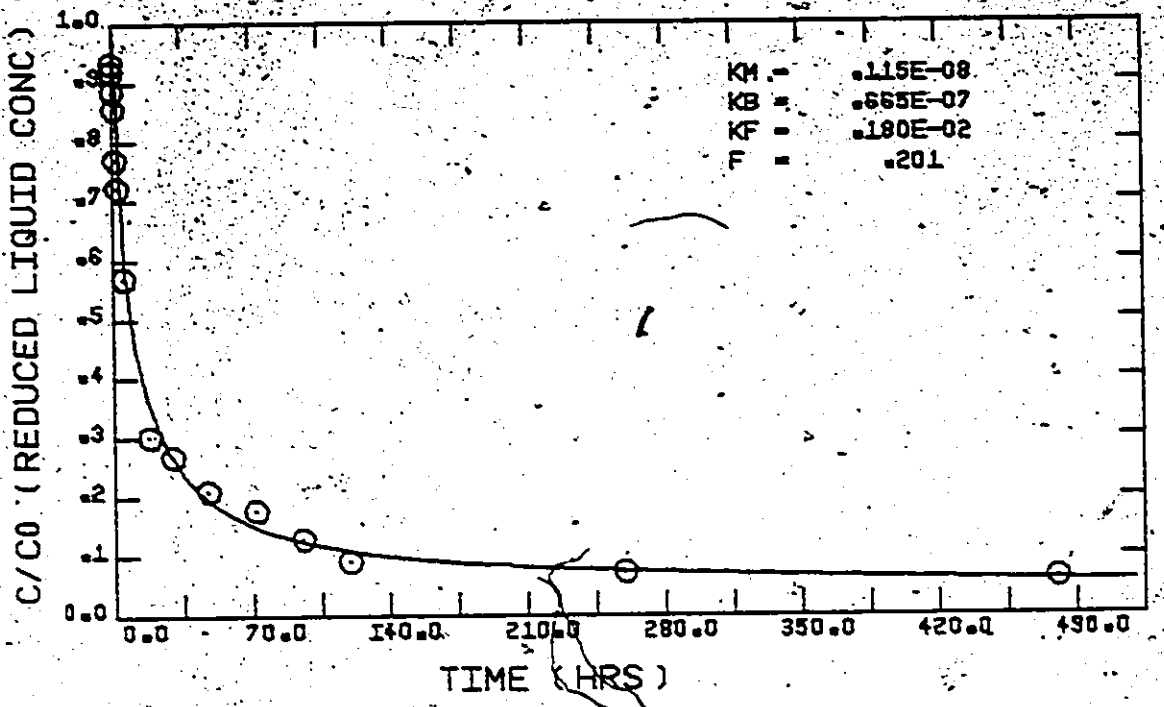

Figure 4-2. Tap Water Batch Kinetic Data - Branched Pore Model.

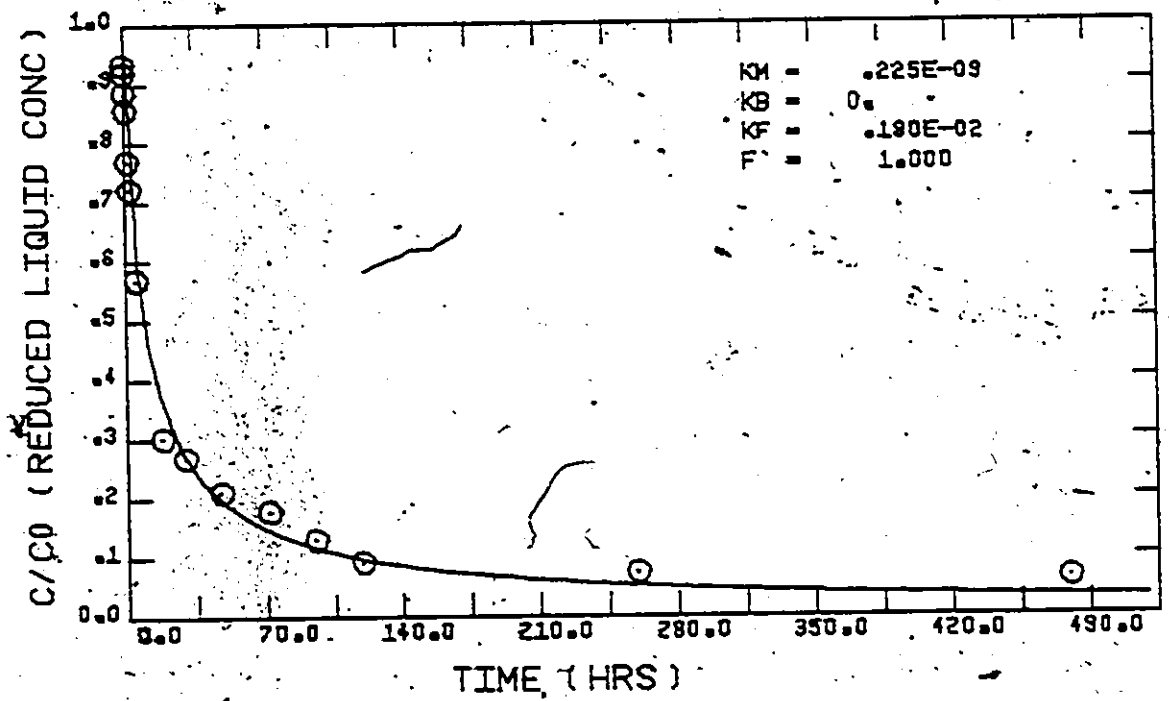

Figure 4-3. Tap Water Batch Kinetic Data - Single Parameter Model.

Thus, whereas phenol molecules are smaller than the majority of the adsorbing pores, the organics in tap-water appear to be of a comparable size and therefore diffusion within the carbon particle is much reduced. The very low transport rates within the carbon particle support the earlier contention that slow adsorption may be a significant removal mechanism even after prolonged operation of a carbon filter.

Since the low value of f calculated by the branched pore model indicated that most of the adsorption occurred in the slowly adsorbing region, the possibility that the data could be fitted by a single rate parameter model was investigated. When the fraction 'f' in the branched pore model is set equal to unity, the standard surface diffusion model results, in this case with the quadratic driving force approximation to describe the diffusion mechanism. The result of fitting the single parameter model to the batch kinetic data is shown in Figure 4-3 which indicates that the single parameter model describes the data reasonably well except in the long term where it over-predicts uptake. The total sum of squares of the residuals for the single parameter case was 7.1×10^{-3} compared to 5.0×10^{-3} when using the branched pore model.

Because of the choice of model, the intraparticle rate transfer coefficient (k_m) cannot be directly compared to surface diffusion coefficients (D_s) reported in the literature for similar organics. However, the ratio k_m:D_s for pure phenolic compounds is available from the results of part I of this study and is approximately 45:1. If the same ratio is assumed to hold for the organics in natural waters, the surface-diffusion coefficient corresponding to the value of k_m in Figure 4-3 is 0.5 $\times 10^{-11}$ cm^2/sec. Holzel and Sontheimer (1979) have reported values of

2.6 - 6.1 x 10^{-11} cm^2/sec for the adsorption of Rhine River water onto activated carbon (Norit Row 0.8), and are thus in reasonable agreement with the results of the present work. Exact correspondence should not be expected because the water source, activated carbon, and the experimental techniques were different from those of the present study.

4.3 Prediction of Column Performance and Comparison to Experimental Data

Since both the single parameter and 3-parameter models were able to describe the batch kinetic data, the use of both models was investigated in predicting the breakthrough behaviour of the experimental columns. The columns were operated at 2 different flow rates, one column at 1.24 m/h and 2 columns in series at 7.37 m/h. The columns are designated as 20 cm slow, 20 cm rapid, and 40 cm rapid, respectively.

Aside from the experimental isotherm and batch kinetic parameters, the only additional information required to predict the behaviour of the columns was the external film mass transfer coefficient. As in part I of this study a correlation presented by Wilson and Geankoplis (1966) for low Reynolds number flows was used, and the free liquid diffusion coefficient of the organics was assumed to be 1.0 x 10^{-6} cm^2/sec (Holzel and Sontheimer, 1979).

Although the model is easily adapted to handle a variable influent concentration, the tap water in this study had a relatively constant TOC which averaged 1.522 mg/l. A constant level influent was therefore assumed and the breakthrough curves of the adsorbable fraction of the influent are plotted in reduced form. The ability of the model to describe the adsorptive behaviour of the columns is more clearly

seen when data are presented in this manner and no information was lost as the actual predictions of column behaviour with or without a constant feed concentration were quite similar.

4.3.1 20 cm Rapid Column

The predicted and experimental breakthrough and cumulative profiles are shown in Figures 4-4 and 4-5 for the 3 parameter branched pore model. The uptake beyond about 50 days of operation was well predicted, but the model calculated a more rapid breakthrough than was measured experimentally. The difference is most clearly seen in Figure 4-5 which shows that the predicted and experimental curves diverge in the initial breakthrough period but are almost superimposable thereafter. When the single parameter model was used to predict the experimental behaviour, relatively poor correspondence was obtained as is indicated in Figures 4-6 and 4-7. The predicted effluent concentrations are consistently higher than those observed experimentally and are a result of the inherent constraints in the single parameter model. As shown in Figure 4-3, although the single parameter model gives a good description of the initial batch kinetic uptake data, it predicts a more rapid approach to equilibrium than the long term data would indicate. Thus when used to predict column performance the model tends to calculate a more rapid approach to saturation than is achieved in practice. Consequently its use was discontinued in favour of the branched pore model which gave a better description of the adsorption kinetic behaviour.

4.3.2 40 cm Rapid Column

The same characteristics noted for the 20 cm rapid columns were

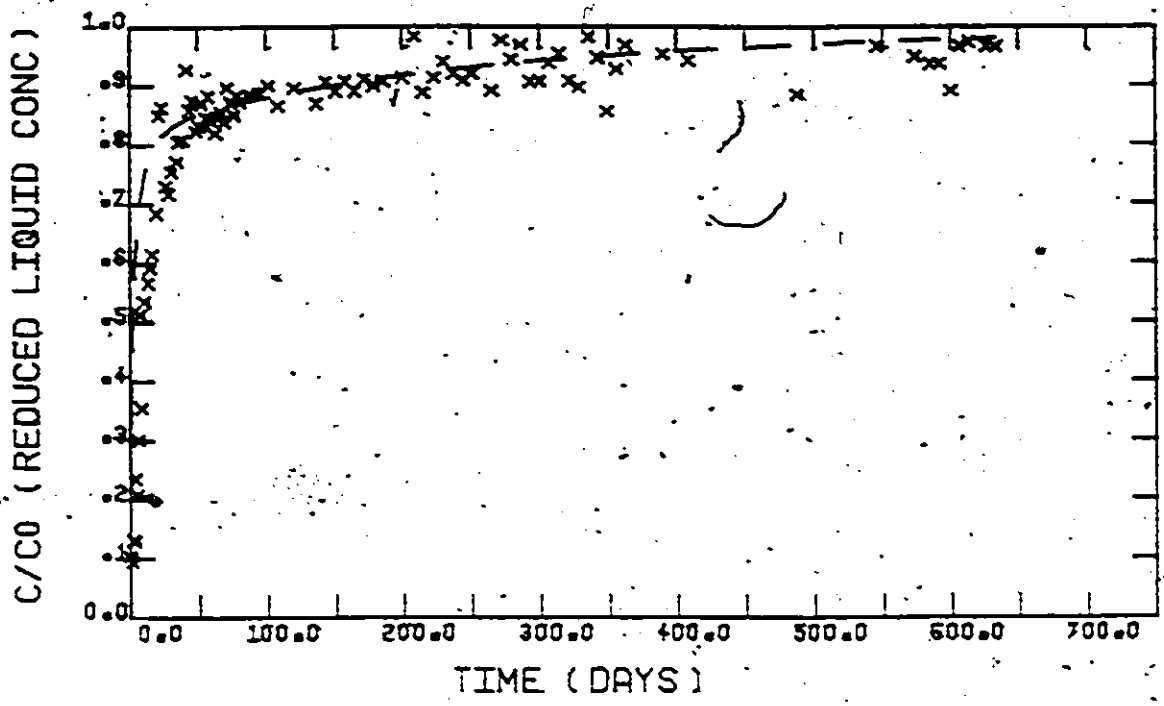

Figure 4-4. Breakthrough Curve - 20 cm Rapid Column
(x - experimental data, --- 3-parameter model prediction).

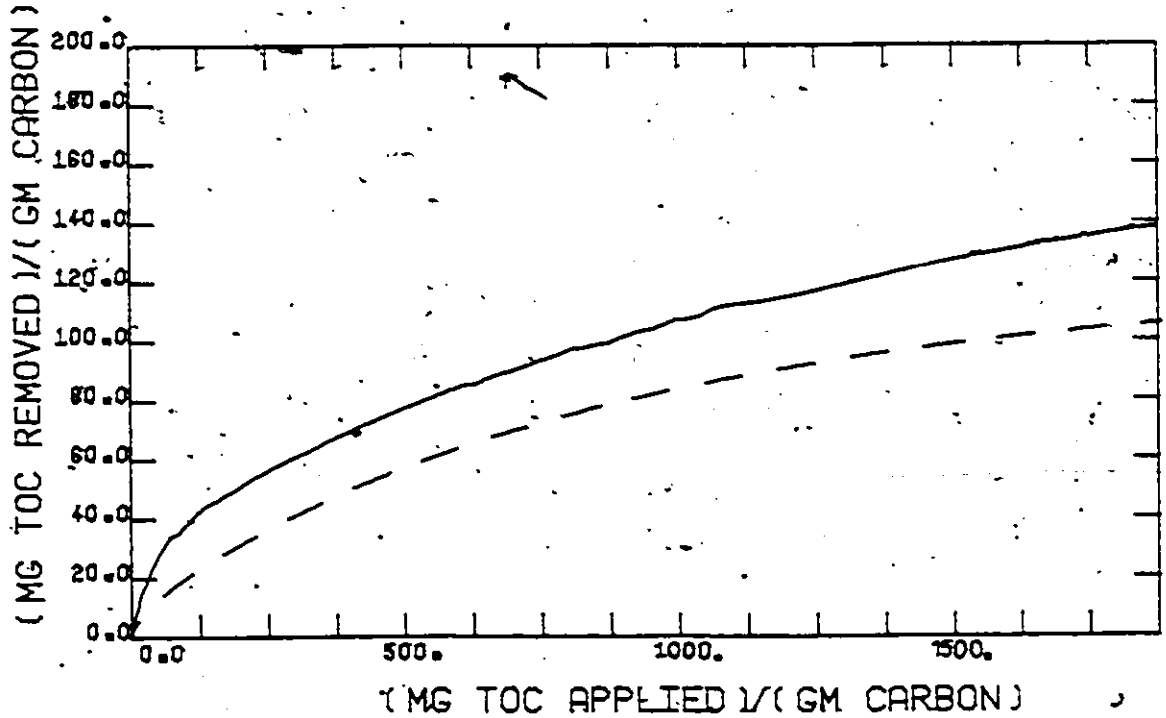

Figure 4-5. Cumulative Uptake Profiles - 20 cm Rapid Column
(– experimental data, --- 3-parameter model prediction)

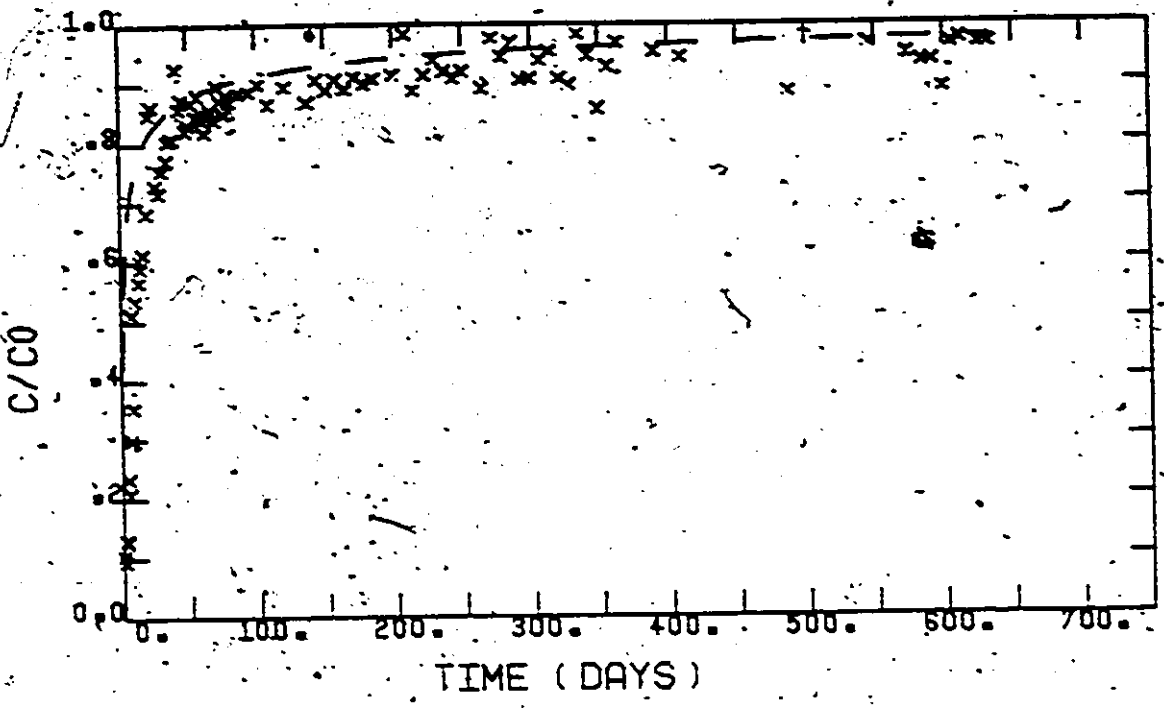

Figure 4-6. Breakthrough Curve - 20 cm Rapid Column.
(x - experimental data, --- single parameter model prediction).

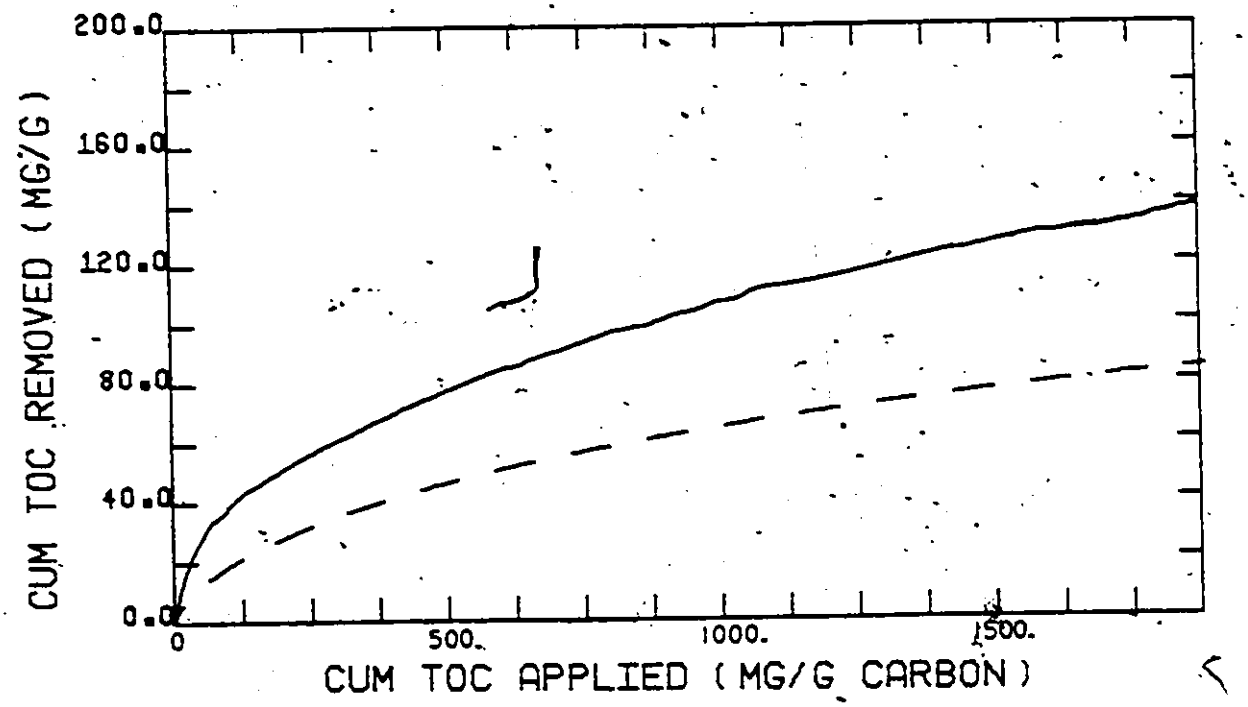

Figure 4-7. Cumulative Uptake Profile - 20 cm Rapid Column..
(— experimental data, --- single parameter model prediction).

also found with the 40 cm rapid columns. Figures 4-8 and 4-9 show the experimental and predicted data for the 3-parameter branched pore model. Again the initial breakthrough data is not well predicted as the cumulative uptake curves in Figure 4-9 diverge in the initial operating region. The divergence is less than was observed with the 20 cm columns however, and over the remainder of the operating period extremely good correspondence between the experimental and predicted profiles was found.

4.3.3 20 cm Slow Column

In contrast to the results with the rapid columns, the model prediction shown in Figures 4-10 and 4-11 for the slow column under predicts rather than over predicts the initial breakthrough region. The cause of this behaviour is presently unknown but may be related to the use of TOC as a lumped parameter to describe the adsorption of a complex mixture of components. As with the predictions for the rapid columns, the model describes the long term uptake data well and indicates the importance of the slow diffusion mechanism in the long term behaviour of activated carbon filters.

4.4 Discussion of Results

In general, prediction of column performance using the branched pore model was quite good, especially in the extended tail of the breakthrough curves. The model did not describe the initial breakthrough region well, a failing which is attributed to the use of a single lumped parameter (TOC) to describe the behaviour of a multitude of different compounds. As was noted in Chapter 2, the use of a lumped parameter could not be expected to lead to a precise description of adsorptive be-

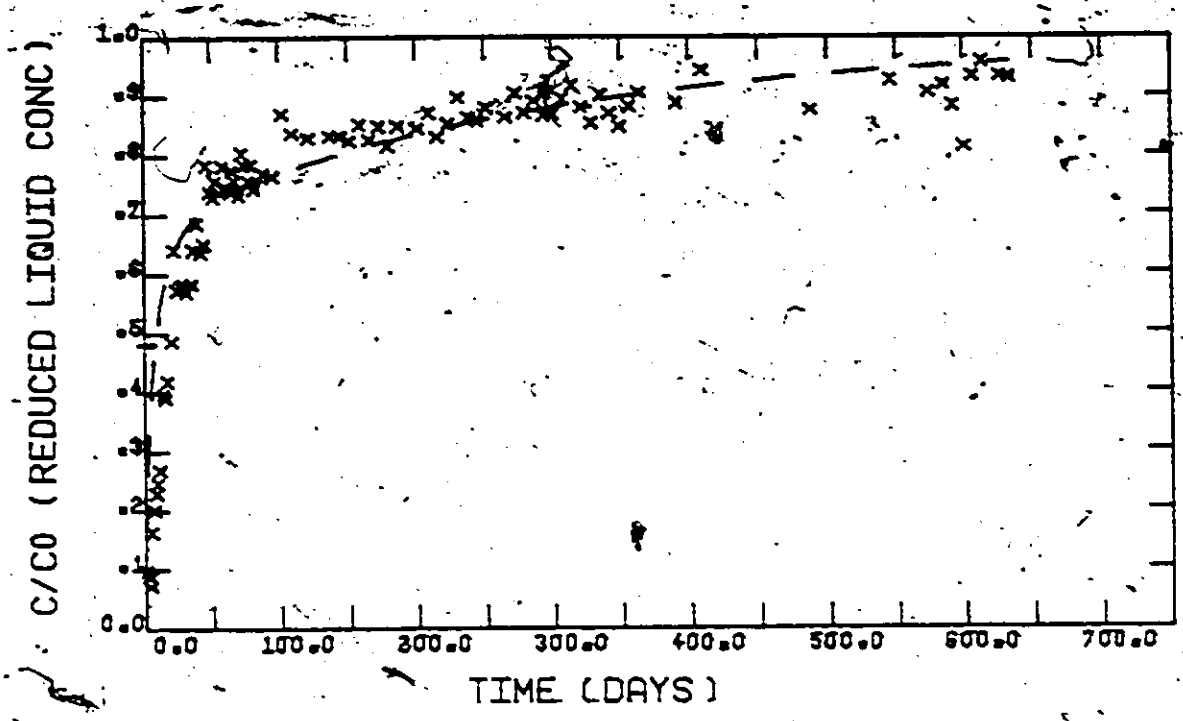

Figure 4-8. Breakthrough Curve - 40 cm Rapid Column.
(x - experimental data, --- 3-parameter model prediction).

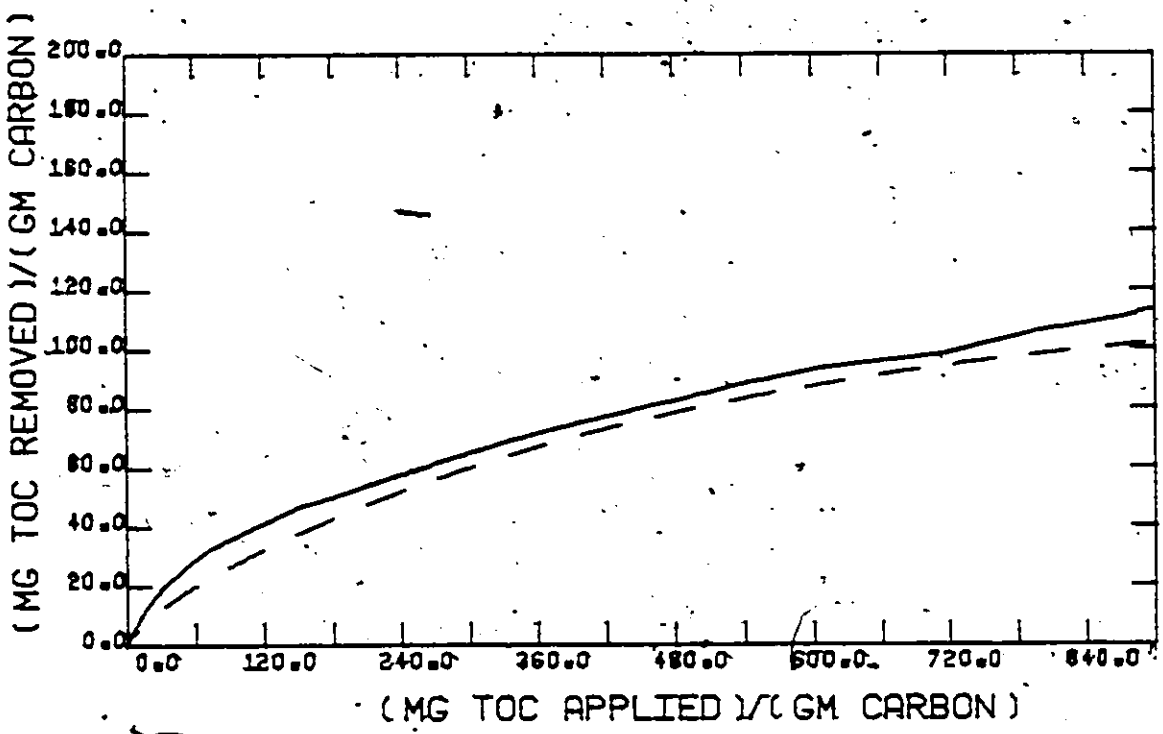

Figure 4-9. Cumulative Uptake Profile - 40 cm Rapid Column.
(—— experimental data, --- 3-parameter model prediction).

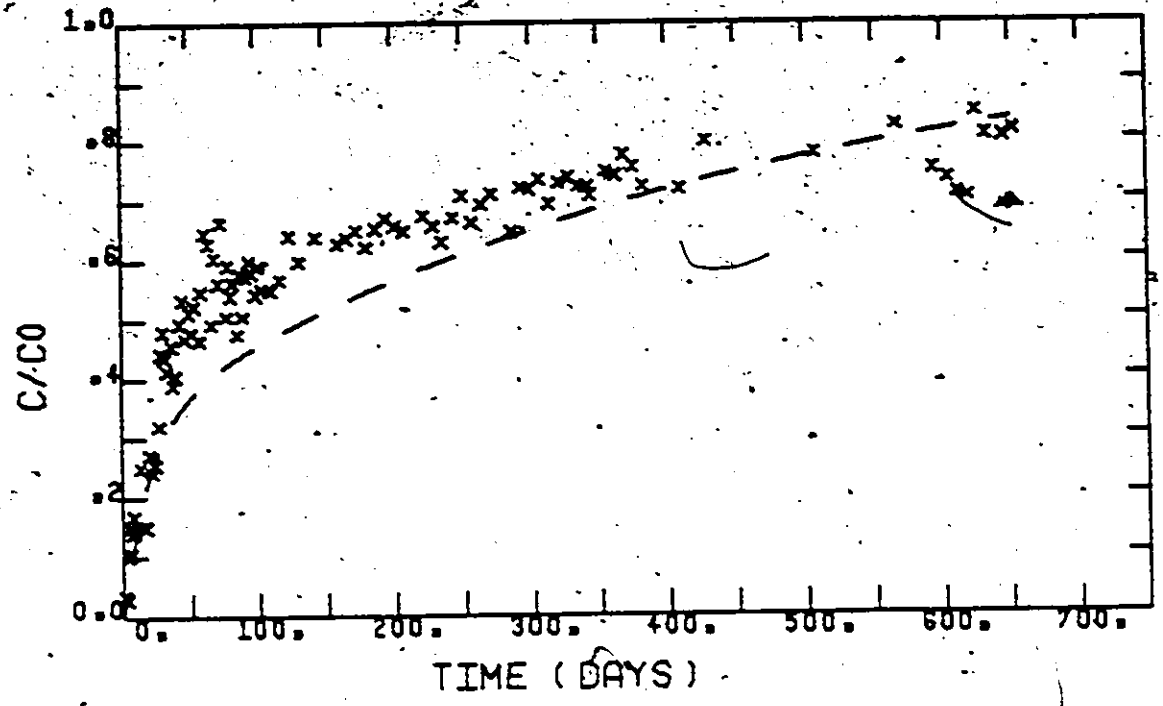

Figure 4-10. Breakthrough Curve - 20 cm Slow Column.
(x - experimental data, --- 3-parameter model prediction).

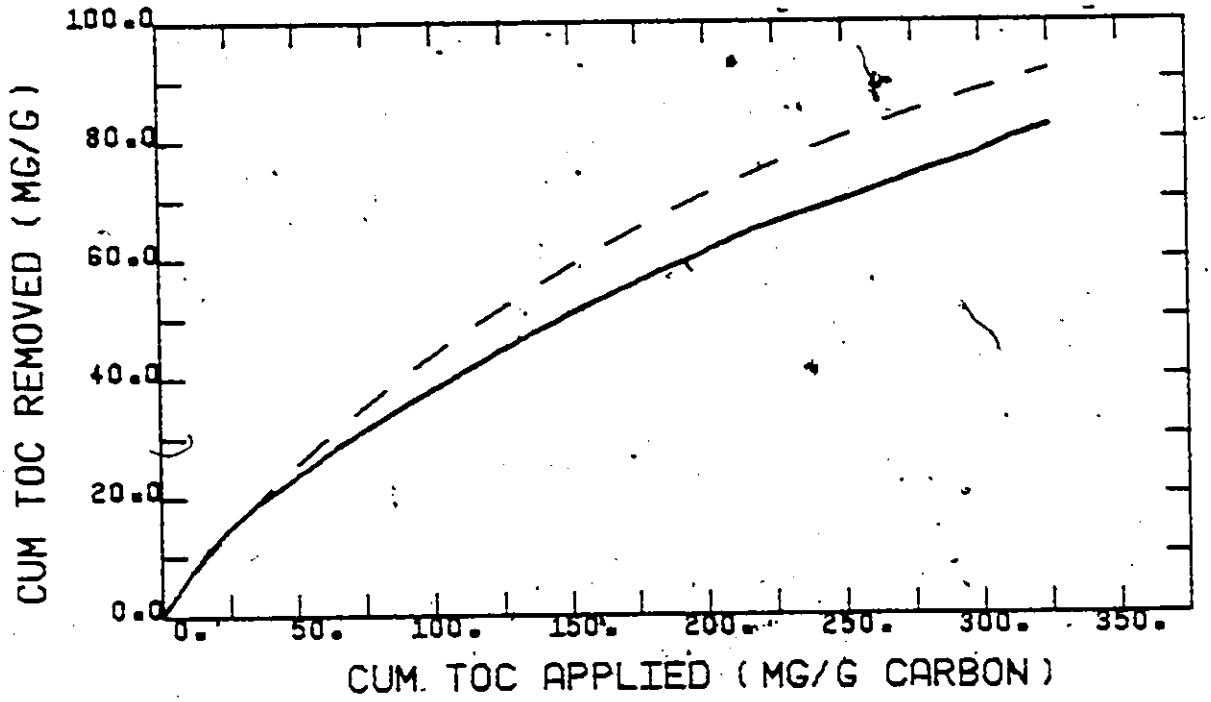

Figure 4-11. Cumulative Uptake Profile - 20 cm Slow Column.
(—— experimental data, --- 3-parameter model prediction).

haviour. Nevertheless, the results shown above indicate that at least for the organics in tap water, such an approach enables a surprisingly good prediction of the bulk of the breakthrough curve. The organics in tap water show the same type of behaviour as was observed in part I with pure components, a rapid partial breakthrough followed by an extended period of slow adsorption which gives the characteristic tail to the breakthrough curve.

This tail has important ramifications in the analysis of data when biological activity is thought to be a possible removal mechanism. The results above show that for the tap water in this study, the small amount of uptake occurring after two years of operation is explained by adsorption kinetics, and is apparently not due to biological mechanisms as might be anticipated on initial inspection of the data. The cumulative uptake curve can be used to check the following criteria for differentiating between adsorptive and biological mechanisms.

(i) If the cumulative adsorption capacity significantly exceeds that suggested by the isotherm, then biological activity may be presumed to be an active removal mechanism. However, since higher loadings than predicted by the isotherm may be achieved in columnar operation due to successive displacement of less strongly adsorbed compounds, removal capacities in the region of, or only slightly greater than the isotherm prediction may be due to either biological or adsorptive removal.

(ii) If only adsorptive mechanisms are responsible for removal, a slow but steady decline in the rate of removal should be observed.

Biological removal mechanisms, on the other hand, should give a constant rate of removal once the bacterial growth is fully developed. On the cumulative uptake curve these characteristics are represented by a curve and a straight line respectively, as the slope of the cumulative curve is equal to the instantaneous percentage removal.

Although the tap water breakthrough profiles in Figures 4-4 and 4-10 show the type of behaviour described in Figure 1-1, which is typical of biologically active carbon columns, reference to the cumulative uptake figures shows that the experimental data plots exhibit a marked curvature throughout the data collection period. This curvature is indicative of an adsorptive removal mechanism and implies that the curve will eventually become horizontal, at which point the column is saturated and no further uptake will occur. The absence of significant biological removal in these columns is strongly supported by the correspondence between the experimental data and the predictions of the adsorption kinetic model. Additionally, given the highly stable nature of the tap water and the extensive residence time available for biological removal at its source, the absence of biologically degradable materials in the carbon column influent is not unexpected. Based on previous experiences reported in the literature, the presence of bacteria in the columns would be expected but was not experimentally verified in this study. The presence and effect of bacteria within activated carbon filters are discussed in detail in the following chapter.

Although modelling using a lumped parameter approach has been

shown to have some limitations with respect to the initial breakthrough region, the ability of the kinetic model to describe the bulk of the breakthrough curve was very good, especially considering the time period involved. The fact that continued removal after an extended period of operation can be explained purely by adsorption mechanisms has great significance in the interpretation of operating data, as removal which has hitherto been regarded as due to biological mechanisms may in fact be purely adsorptive in some cases. This point is discussed in more detail in the following chapters.

CHAPTER 5

ADSORPTION STUDIES WITH BIORESIDUAL ORGANICS

In the previous chapter the adsorptive properties of naturally occurring organic materials in a potable water supply were studied. Many potable water supplies are also subject to organic contamination due to discharges from industrial sources, sewers, and municipal treatment plants, and the study reported in this chapter was undertaken to investigate the adsorptive properties of organic materials generated during biological treatment of wastewaters.

5.1 Bioresidual Organics

Whenever organic carbon substrates are biologically degraded some TOC remains in solution even after the original substrate is no longer detectable. This residual TOC is assumed to be generated by the bacteria during metabolism of the substrate and it appears to be biorefractory as the TOC does not fall to zero even when extended contact periods are allowed.

These metabolic by-products or bioresidual materials are of interest as they are generated in any biological treatment system, and will build up in a receiving body unless removed by physical methods. This chapter deals with the adsorptive properties of these bioresidual organics which in the present case were generated by biologically degrading the pure compound phenol in an activated sludge system.

5.1.1 Literature Review

The production of bioresidual organics was extensively studied by Chudoba et al. (1968, 1969). These authors measured the residual COD of a number of compounds after extensive biological degradation and found it to lie between 0.5 and 1.0% of the influent COD. Grady and Williams (1975) suggested that a portion of the original substrate is returned to the medium in a non-biodegradable form but the nature of these compounds was not specified.

De Walle and Chian (1974) stated that carbon in the effluent of an activated sludge plant is mostly refractory or inert material that the bacteria are not able to degrade. They suggested that its constituents are primarily polymerized waste products of the bacteria as well as cell fragments and inert material from lysed cells. Many of these materials were associated with humic substances having molecular weights ranging from several hundreds to tens of thousands. De Walle and Chian reviewed the literature concerning biological effluent composition and molecular weight distributions, and found that from 20-50% of the organic matter in secondary effluents consists of high molecular weight compounds which are thought to be humic in nature. Because the influents to these systems also consisted of a wide range of different compounds, it was not possible to determine what fraction of the effluent was generated by the bacteria and what fraction was unchanged from the influent. In the experimental work a solid refuse leachate was biologically treated in batch aeration vessels and molecular weight determinations of the mixed liquor were made at intervals during the biodegradation. Two

main molecular weight (MW) fractions were found, a 1000-5000 MW fraction which was assumed to be fulvic acid and a >50,000 MW fraction which was assumed to consist of humic acids. The experimental results showed an increase in the high MW fraction after removal of the readily available carbon source and it was proposed that this material was refractory in nature. The results of the study were only tentative, however, as both molecular weight fractions were also present in the influent and were adsorbed by the bacteria. Subsequent release of these adsorbed materials back into solution could not be differentiated from the proposed production.

Adsorption of a secondary effluent produced by an activated sludge plant operating on raw sewage was reported by Kim et al.(1976). The sludge age was varied, and the changes in the adsorptivity of the effluent were noted. The principal relationship investigated was that between the operating characteristics of the system and the concentration of non-adsorbable organics in the effluent; the concentration of non-adsorbable organics was found to decrease as the sludge age was increased. Molecular weight fractionation of the effluents showed that the high molecular weight fraction was adsorbed by activated carbon but the fraction less than a nominal 500 MW was not well adsorbed. The non-adsorbable low molecular weight organics were assumed to be highly soluble in water and therefore highly polar. The results were in agreement with earlier findings of Tofflemire et al.(1973) who had found a non-adsorbable non-degradable fraction with a molecular weight of about 180 at the outlet of a carbon column treating a secondary effluent. Manka et al.(1974) found that a relatively large amount of the substan

ces in secondary effluents that were characterized as fulvic acids had a molecular weight less than 500.

The composition of the residual organics cannot therefore be ascribed to a particular group of compounds. The studies above suggest that the organics may be largely composed of fulvic and humic acids, but may also contain proteins, carbohydrates, and other metabolic by-products and cellular fragments. Both humic and fulvic acids are polar (Schnitzer and Khan, 1972), but because of their high molecular weights they are expected to be relatively well adsorbed by activated carbon unless physically excluded from the pores due to their size. There is some evidence to suggest that a part of the low molecular weight highly polar fraction of the fulvic acids may not be adsorbable on activated carbon.

5.1.2 Experimental Bioresidual Generation

The influent to the activated sludge unit consisted of tap water supplemented with phenol and nutrient salts. The tap water had previously been passed through a large activated carbon prefilter and because of the 3 h residence time in this filter, the steady 0.36 mg/l. TOC in the filter effluent was assumed to be non-adsorbable and non-biodegradable. Since the only carbon substrate added to the activated sludge unit was analytical grade phenol, all TOC in the activated sludge plant effluent in excess of 0.36 mg/l was therefore a result of the microbial metabolism of phenol. It was assumed that the TOC in the influent tap water would pass unchanged through the activated sludge unit.

The experiment lasted for 220 days during which time the acti-

vated sludge unit was operated at or near the conditions given in Table 3-1. During this period the influent TOC was 85 mg/l and the effluent TOC averaged 1.2 mg/l indicating a high degree of biological purification. After accounting for the non-adsorbable TOC in the influent tap water, the TOC produced by microbial degradation constituted 1% of the influent TOC due to phenol and therefore supported the findings of Chudoba et al. (1968,1969). The absence of phenol in the effluent was confirmed by UV analysis as indicated in Figure 5-1 where UV scans of the effluent and a 100:1 dilution of the influent are shown. The characteristic absorption peak of phenol can be seen in the influent but not in the effluent, indicating that only very low concentrations of phenol, if any, were present.

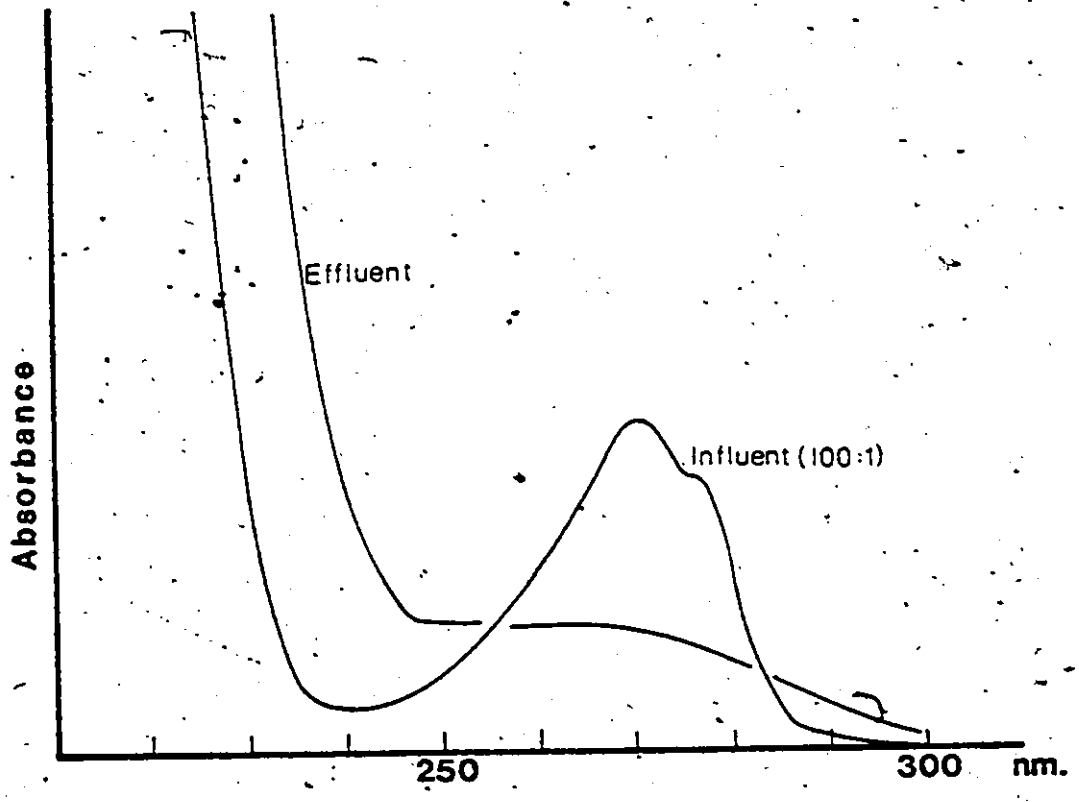

Figure 5-1. UV Spectra of Activated Sludge Influent and Effluent.

The activated sludge effluent was normally very stable and the TOC in the collection tank at the end of 7 days storage was equal to the average clarifier effluent during the collection period whenever the activated sludge unit was operating well. Occasional upsets of the activated sludge unit caused increased effluent concentrations but the additional holding time in the collection tank was sufficient to stabilize the waste and lower the concentrations.

After rapid sand filtration the residual organics were stored in another large holding tank which acted as a feed reservoir for the activated carbon adsorption system. Generally the feed tank was filled every 7 days and a constant TOC between recharges gave further evidence that the residual organics were quite stable. The organic material used in the isotherm and kinetic studies was withdrawn from this tank and filtered through 0.2 μm Gelman membrane filters prior to use.

5.2 Equilibrium Isotherm

Two isotherms were conducted on the bioresidual material and the results plus the fitted Freundlich isotherm are shown in Figure 5-2. The calculated isotherm is:

$$q_e = 137.5\, C_e^{0.75} \qquad (5.1)$$

As with the tap water isotherms reported in the previous chapter, the non-adsorbable fraction of the TOC was subtracted from the equilibrium concentration when determining the isotherm. The non-adsorbable TOC determined by isotherm and column experiments averaged 0.49 mg/l and was quite constant throughout the study. This quantity represented an increase of 0.13 mg/l over the non-adsorbable TOC in the activated sludge

influent. If, as discussed previously, this refractory influent TOC is assumed to pass without change to the outlet, the non-adsorbable TOC increase in the effluent represents 0.15% of the total influent TOC, and constitutes 15% of the bioresidual material produced in the activated sludge unit. It is interesting to note that the fraction of TOC which is non-adsorbable is similar to that found in untreated water from Lake Ontario where the proportions are approximately 0.4:2.5 mg/l TOC or 16%.

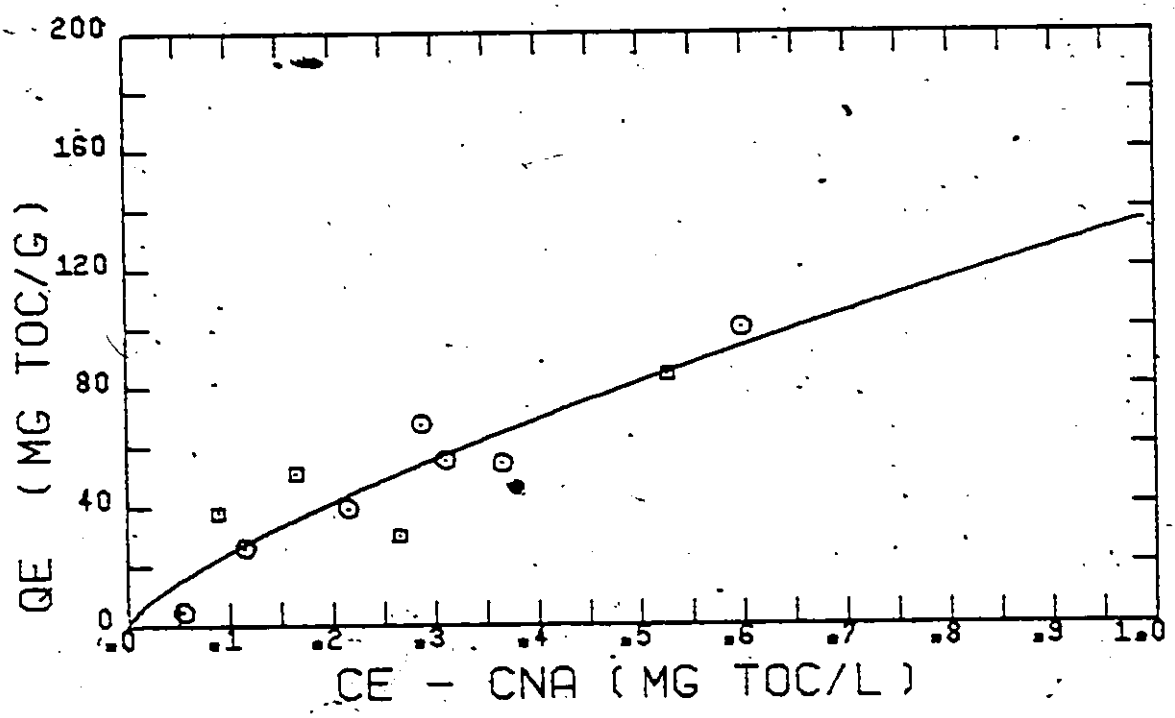

Figure S-2. Bioresidual Isotherm

(⊙ - Isotherm A, UV Absorbance; ⊡ - Isotherm B, Direct TOC Measurement)

5.3 Batch Kinetic Studies

A batch kinetic experiment was conducted with the bioresidual material according to the procedures outlined in Chapter 3. The experiment was carried out over an 8 day period and the data plus the fitted branch pore model parameters are shown in Figure 5-3. The plotted data are for the adsorbable fraction only, the non-adsorbable fraction (0.49 mg/l) being subtracted from all readings prior to analysis.

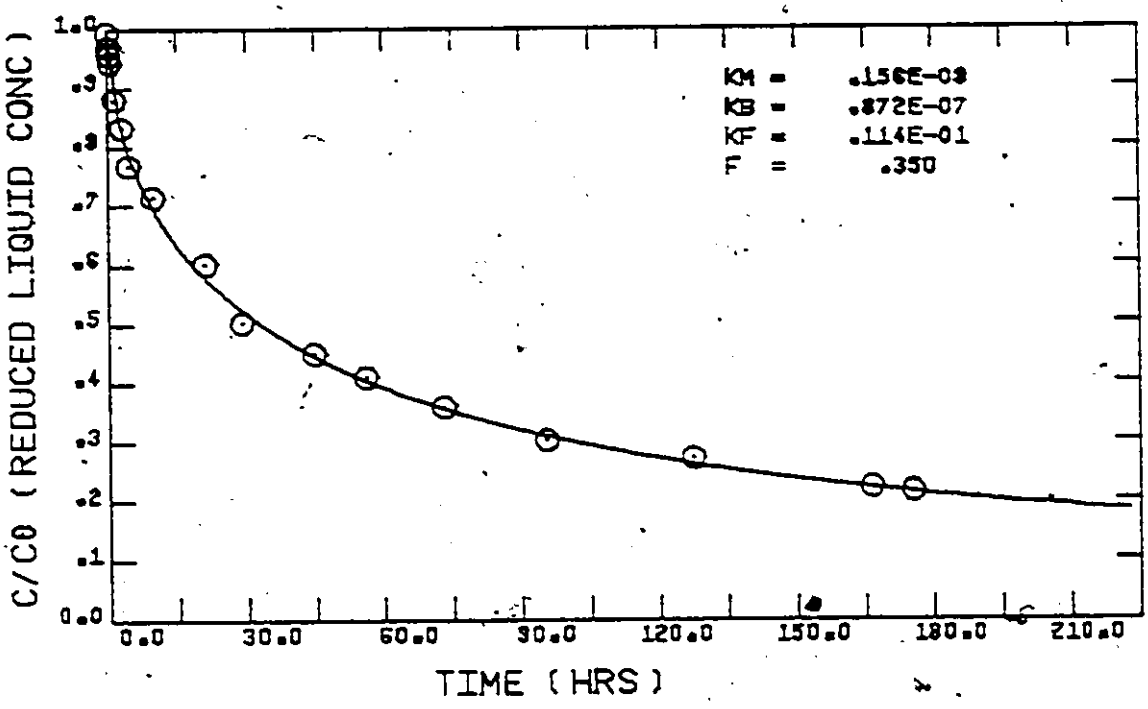

Figure 5-3. Bioresidual Batch Kinetic Experiment.

The model parameters are in each case larger than those determined in the previous chapter for tap water, suggesting that the components of the bioresidual material are smaller and diffuse more rapidly than the organic molecules in the tap water which was obtained from Lake Ontario. Rebhun and Manka (1974) presented data showing that the major part of the humic substances in Lake water are over 10,000 MW whereas the major part in secondary effluents are from 1,000 to 5,000 MW and thus the results of the present study indirectly support their findings.

Since the amount of adsorption in both the micro- and macropore regions was quite significant, and also because it was shown in the previous chapter that the branched pore 3-parameter model gave better predictions of column performance than did the single parameter surface diffusion model, only the branched pore model was used to analyse the bioresidual data.

Aside from evaluating the kinetic model parameters, the batch kinetic experiment was also used to estimate the free liquid diffusion coefficient of the bioresidual TOC. The experiment was repeated under identical conditions but with phenol as the adsorbate instead of the bioresidual material and the initial slope was again used to calculate k_f. Since

$$k_f \propto D_\ell^{2/3} \qquad (5.2)$$

in either a packed bed or free suspension (Wilson and Geankoplis, 1966; Letterman et al., 1974), the free liquid diffusion coefficient for the bioresidual TOC can be calculated from

$$\mathcal{D}_\ell^{TOC} = \mathcal{D}_\ell^{Phe}\left[\frac{k_f^{TOC}}{k_f^{Phe}}\right]^{3/2} \qquad (5.3)$$

For the experiment with phenol k_f was measured to be 1.83×10^{-2} cm/sec and $\mathcal{D}_\ell^{Phe}$ is approximately 9.0×10^{-6} cm^2/sec. Therefore, using equation (5.3), $\mathcal{D}_\ell^{TOC}$ was calculated to be 4.4×10^{-6} cm^2/sec. This value is higher than diffusivities reported by Holzel and Sontheimer (1979) for raw river waters and comparable to values reported for ozonated and filtered waters. As with the intraparticle diffusion parameters noted above, the magnitude of the free liquid diffusion coefficient suggests that the molecules are smaller than those found in natural waters.

5.4 Prediction of Column Performance and Comparison to Experimental Data

The branched pore adsorption model was used to predict the performance of the experimental columns using the equilibrium and kinetic data measured in sections 5-2 and 5-3. The experimental period extended for over 200 days and the predicted and experimental breakthrough curves at bed depths of 6.7, 14.5 and 37.3 cm are shown in Figures 5-4, 5-5 and 5-6. Because of the variation in the feed TOC, the model was run with the actual feed concentrations rather than with the overall average as was done in the tap water study. The predicted effluent profiles therefore reflect the dynamic changes in the influent concentration.

In general the model gives quite good predictions of the column

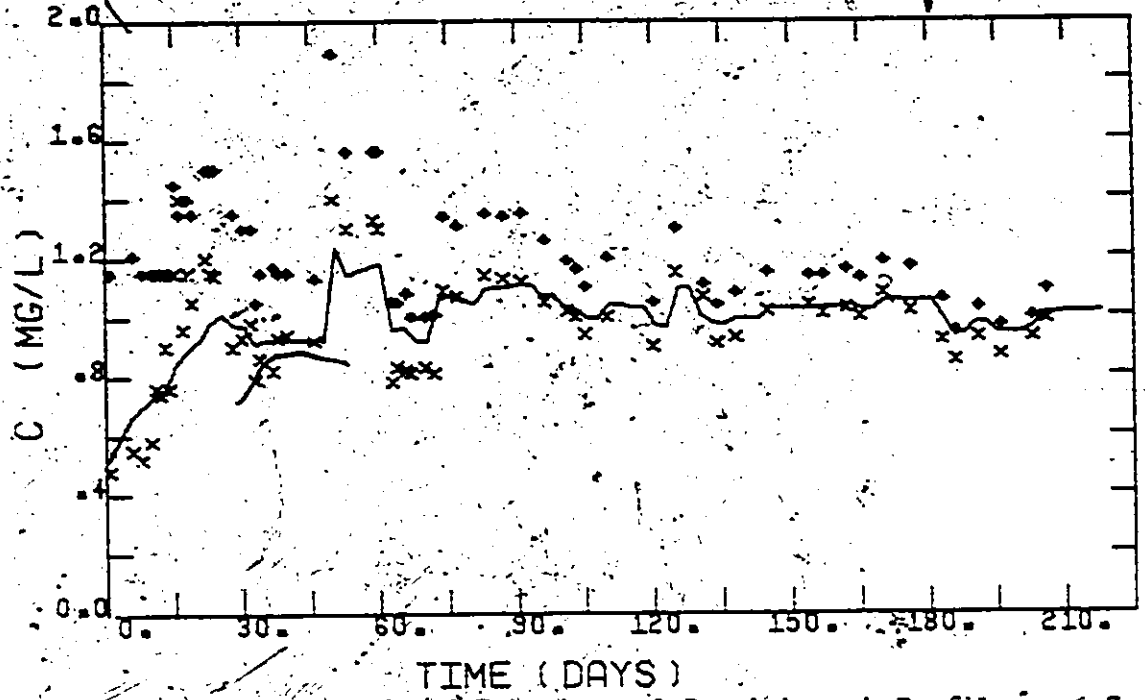

Figure 5-4. Predicted and Experimental Breakthrough Profiles - 6.7 cm
(* - feed, x - effluent, —— model prediction)

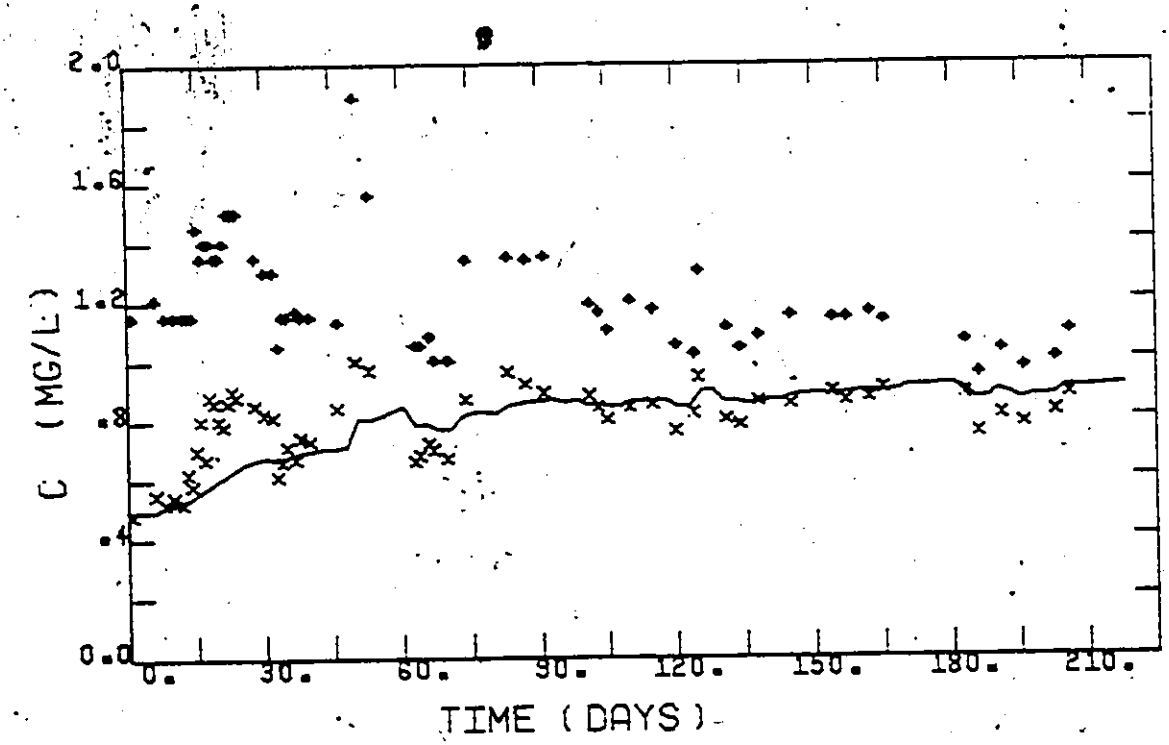

Figure 5-5. Predicted and Experimental Breakthrough Profiles - 14.6 cm
(* - feed, x - effluent, —— model prediction)

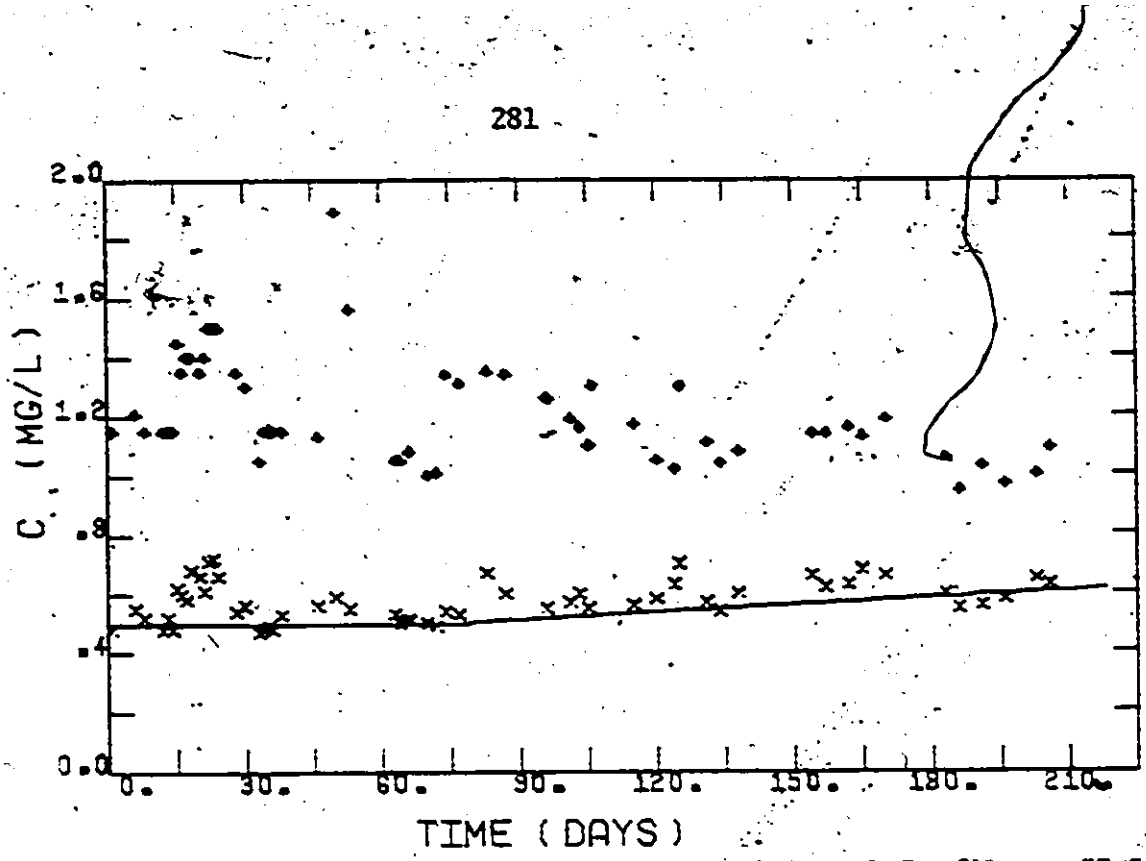

Figure 5-6. Predicted and Experimental Breakthrough Profiles - 37.3 cm (* - feed, X - effluent, —— model prediction)

effluent although it does not fully reflect the dynamic range of the experimental data. The predictions are restricted by the fact that although the concentration of non-adsorbable material in the feed did vary during the experiment, as shown by the effluent data at the full column length (Figure 5-6), the model assumed that it remained constant. This limitation is clearly seen in the data between 15 and 30 days during which time the effluent profile in Figure 5-6 shows higher levels which are presumably due to the breakthrough of non-adsorbable material. The model, however, is unaware of the change in concentration of non-adsorbable TOC in the feed, and consequently under predicts the effluent concentration at all 3 column lengths during this period.

Considering the time scale involved and the inherent limitations of a lumped parameter modelling approach, the ability of the model to describe the experimental data is really quite remarkable. The model appears to be able to describe the adsorptive behaviour of bioresidual organics as well as it was able to describe the adsorption of tap water organics in the previous chapter. The cumulative uptake curves in Figures 5-7, 5-8 and 5-9 show good correspondence between that observed experimentally, and that predicted by the model.

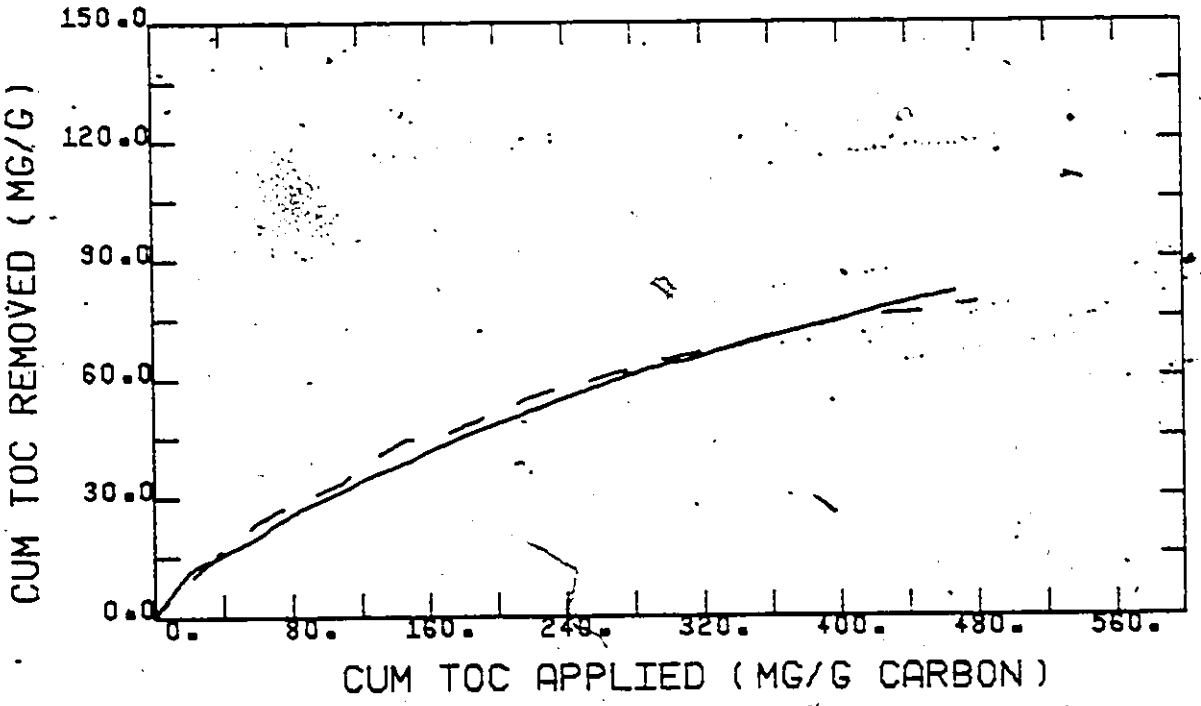

Figure 5-7. Cumulative Uptake Curves - 6.7 cm
(—— experimental, --- predicted)

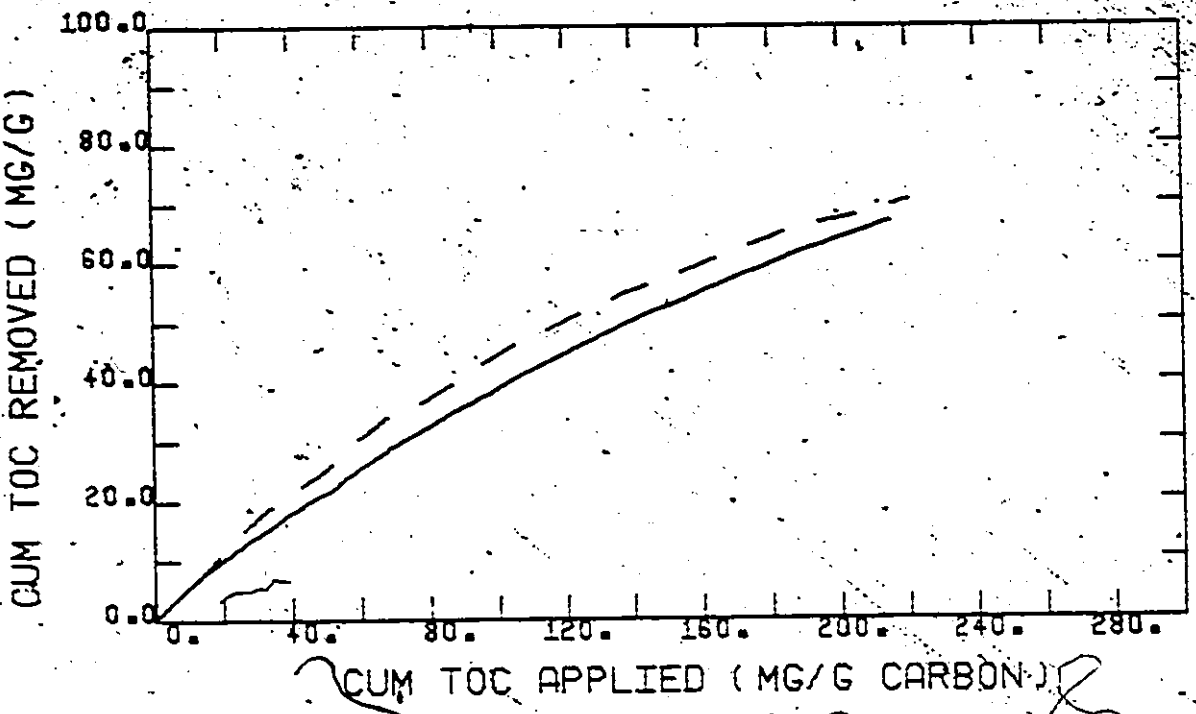

Figure 5-8. Cumulative Uptake Curves - 14.5 cm
(—— experimental, --- predicted)

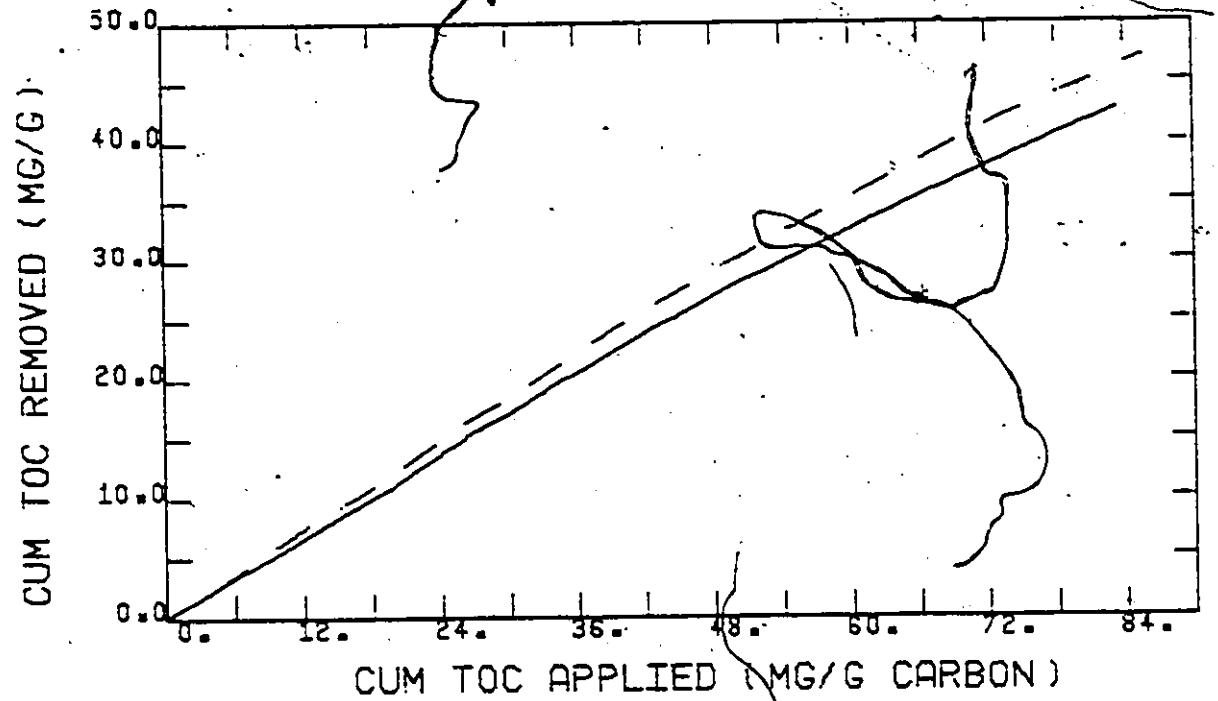

Figure 5-9. Cumulative Uptake Curves - 37.3 cm
(—— experimental, --- predicted)

All the cumulative plots of the experimental data show a pronounced curvature which, as discussed in the previous chapter, is indicative of adsorptive and not of biological mechanisms. As with the tap water study, the fact that the adsorption model is capable of describing the long term uptake data, and also because the feed to the carbon columns was believed to be relatively non degradable, the results of the modelling study strongly indicate that biological removal mechanisms were not active within the adsorption columns even though large numbers of bacteria were present. In order to further test this contention, several aspects of the operation of the carbon columns were investigated.

5.5 Aspects of Biological Activity in Carbon Columns.

5.5.1 Dissolved Oxygen Uptake

Immediately after the columns were brought into service a DO demand was observed across each column and was proportional to the masses of carbon. This DO demand was assumed to be chemical and not biochemical in nature as identical specific uptake rates were measured in all columns although neither adsorbable TOC nor bacteria had presumably penetrated beyond the first column at this stage. The oxygen uptake rate during this period was 0.43 μ mole O_2/hr/g. This rate is comparable to data previously reported by Prober et al.(1975) who showed that after a brief rapid uptake period, activated carbon exhibited a small but only slowly decreasing oxygen demand over an extended period. Prober further showed that only about 5% of the adsorbed oxygen could subsequently be desorbed from the carbon, indicating that much of the DO uptake was due to chemical and not physical adsorption.

After the start up period the oxygen demand across the 1st and 2nd carbon columns began to increase and simultaneously a build up of a whitish-grey mass of bacteria in the upper sections of these downflow columns was observed. When the bacterial masses in these columns became quite visible, they were taken off line and backwashed resulting in a simultaneous decrease in the DO demand. Backwashing was required approximately once every 2 weeks. The 3rd carbon column showed no visible build up of bacteria and was backwashed approximately once every 50 days.

The relationship between DO demand and levels of bacteria in the columns indicated that the bacterial masses were viable and were either actively assimilating substrate or endogeneously respiring. The chemical oxygen demand was neglected after the initial start up period as it was always much less than the measured oxygen demands. It accounted for only about 0.1 mg/l in the first two columns even shortly after start up.

5.5.2 Nitrification

The source of nitrogen in the feed to the activated sludge unit was ammonium sulphate and as a relatively long sludge age was maintained, the effluent was generally well nitrified although nitrogen as NH_3 was occasionally noted in the adsorption system feed tank. A comprehensive study of nitrification was not conducted but on the occasions when nitrogen profiles in the columns were measured, residual NH_3 in the feedstream was completely converted to NO_2-NO_3 in the first 3 columns with the majority of the removal occurring in the 1st carbon column. Large

DO demands correlated approximately with significant NH_3 removal, and the ratio approximated the theoretical 4.4 mg O_2/mg NH_4. One set of data is shown in Figure 5-10.

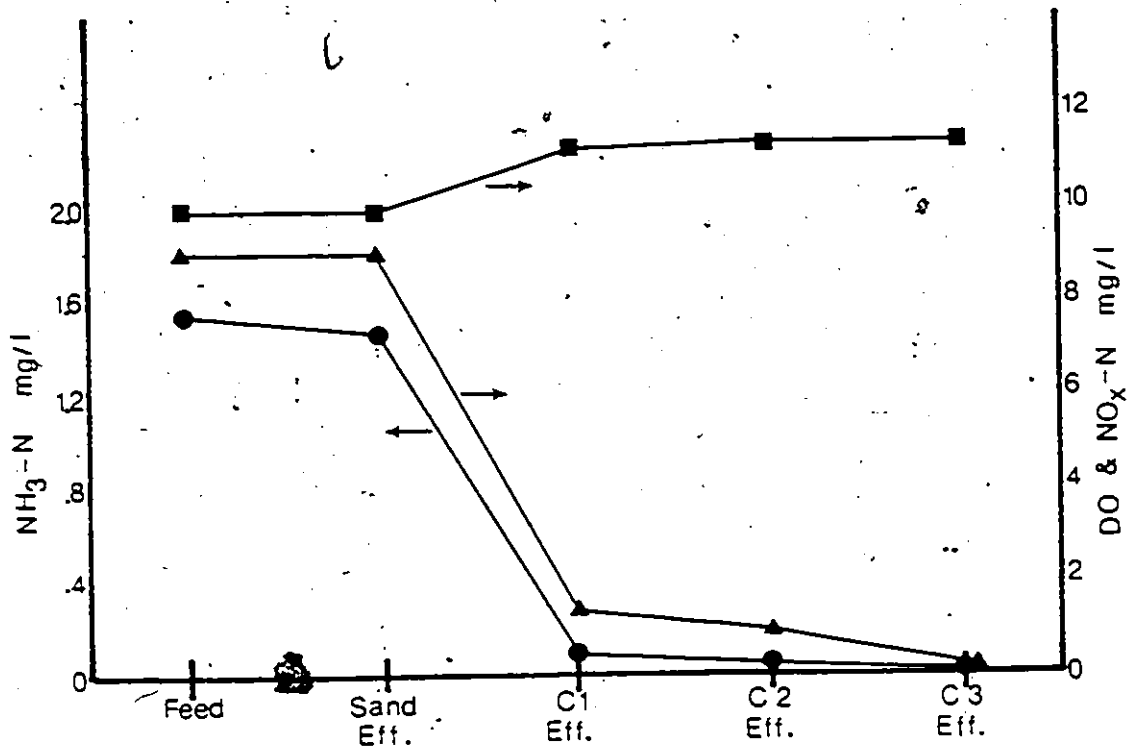

Figure 5-10. Profiles of N and O_2 in Adsorption Columns - 16.10.78
(● - NH_3, ▲ - DO, ■ - NO_x)

Since the nitrifying bacteria (Nitrobacter and Nitrosomas) are autotrophic and therefore do not require an organic carbon source, the presence of these active organisms within the columns should have no bearing on discussions regarding biological TOC removal. Significant nitrification can, however, explain large DO demands which were occasionally observed in the system and it also indicates that at least some

of the bacteria in the columns were viable.

5.5.3 Backwash and Scanning Electron Microscope (SEM) Studies.

Inspection of the columns prior to backwash indicated that the bacteria appeared to fill the interstices of the bed rather than visibly coating the carbon particles. This observation was more suggestive of filtration mechanisms than of biological growth as experience would suggest that the bacteria would be physically attached to the support media if actively growing in the filter.

The backwash water was collected and the sludge was flocculant and settled well. Microscopic examination of the sludge revealed that the majority of the bacteria were cocci, whereas most of the biomass in the activated sludge unit was filamentous. It was assumed that the large and interwoven masses of filamentous organisms were largely removed in the rapid sand filter while small dispersed bacteria passed through this filter and were subsequently removed in the experimental columns. The microscopic examination also revealed large numbers of motile protozoan species as well as rotifers and nematodes: tests for identification and speciation were not undertaken. The presence of these predatory organisms indicated that bacteria were being utilized as a food source inside the columns.

At the termination of the experiment the carbon columns were thoroughly air scoured and backwashed, and quantities of carbon were withdrawn from each column and prepared for Scanning Electron Microscopy. Samples were fixed in 2% glutaraldehyde in a 0.1 M Na Cacodylate solution for 24 h at pH 7.3 and 4°C. They were then post-fixed in a 1%

buffered OsO_4 solution for 2 h at 4°C before being dehydrated with graded ethanol (50, 70, 90, 2x100%). A Bomar SPC 900 EX critical point drier (Bomar Instrument Co., Tacoma, Wa.) was used for drying the samples from CO_2, and the particles were then coated with gold in a Polaron Cool Sputter Coater E5100 (Polaron Instrument Co., Hertfordshire, England). A Phillips PSE501 Scanning Electron Microscope operated at 15 kV was used for observing the specimens. Some particles were fractured prior to shadowing to examine the interior surfaces.

Figure 5-11 shows a single carbon particle at low magnification. Many filamentous strands are evident and these were assumed to be fungal or bacterial and to be carried over from the filamentous biomass in the activated sludge unit. Figure 5-12 is at a similarly low magnification and shows the interior surface of a fractured particle as well as the exterior surface which again is covered with filamentous organisms. At low magnification there is no evidence of biological presence in the interior of the carbon particle and a close-up of the fractured edge in Figure 5-13 further suggests that bacteria are restricted to the external surface of the particle. Pores of about 10u in diameter are evident in this picture and there is no indication of bacteria inhabiting the pores. In Figure 5-14 a virgin carbon surface is shown for comparison to the fractured surface in Figure 5-13. The surfaces appear to be quite similar although the fractured surface shows several pores whereas the virgin external surface is heavily fissured.

The external surface in Figure 5-13 shows a covering of biological debris which is depicted in more detail in Figures 5-15 and 5-16.

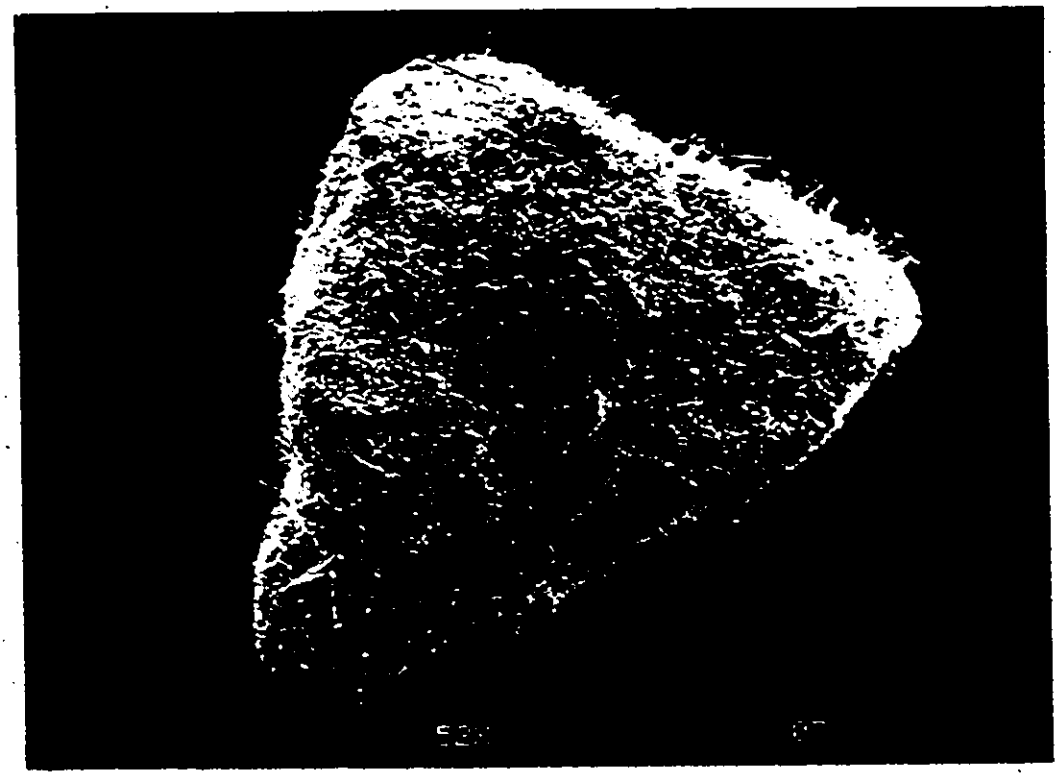

Figure 5-11

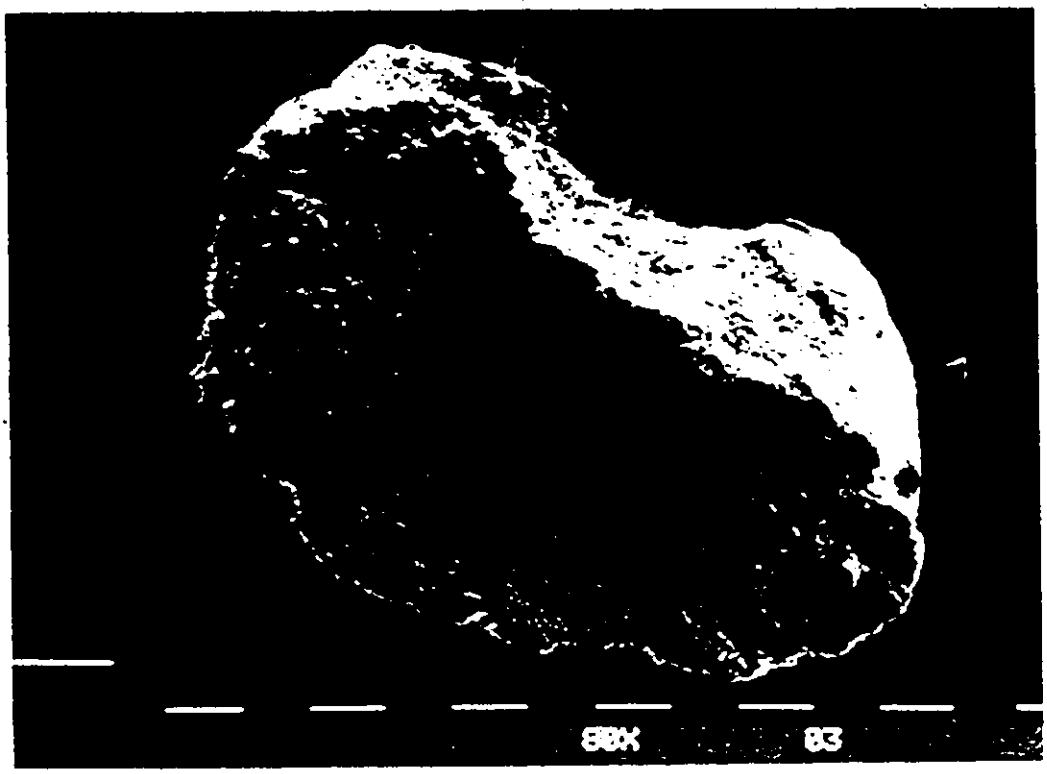

Figure 5-12

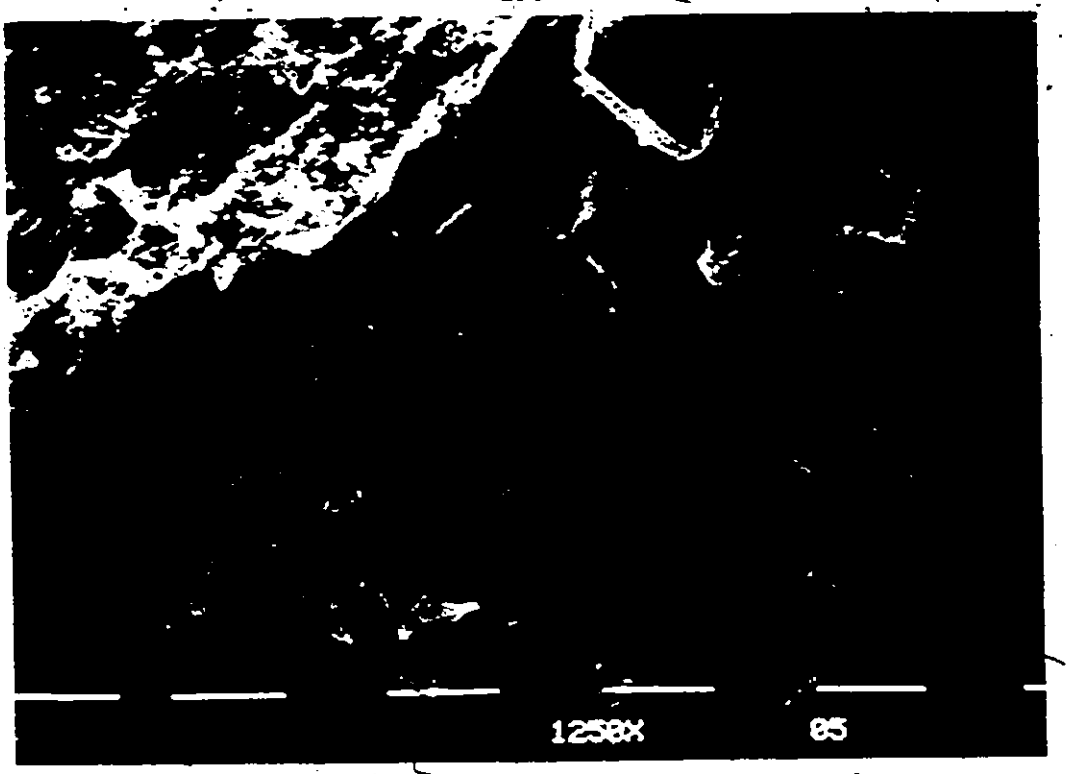

Figure 5-13

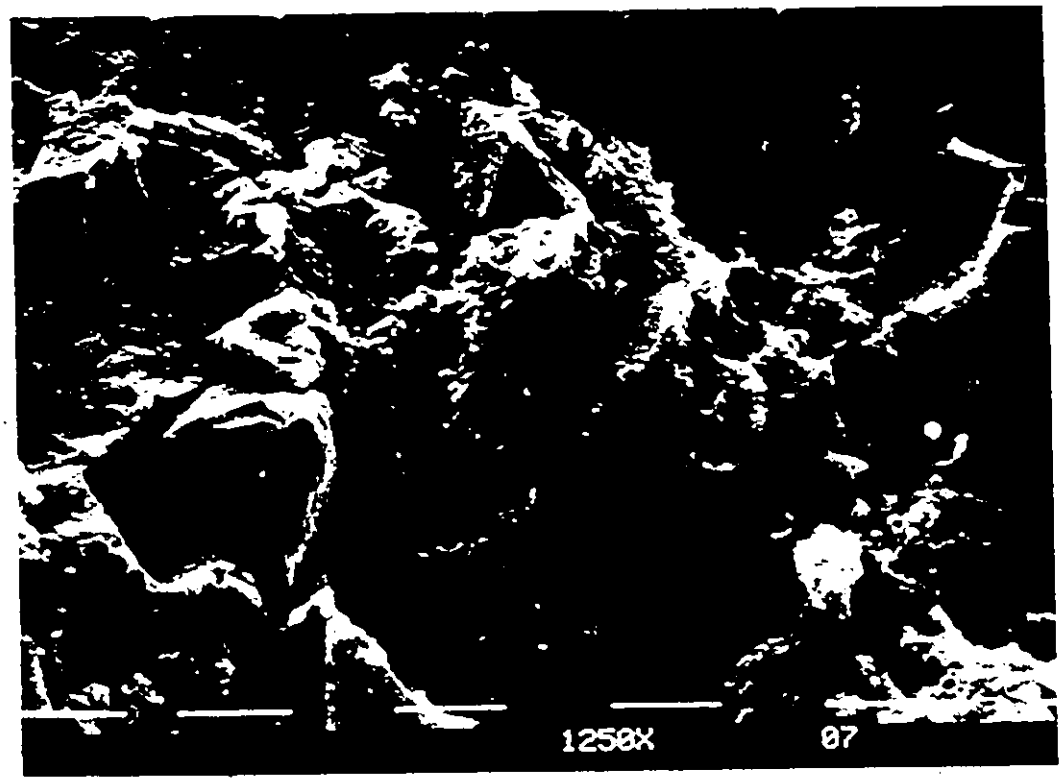

Figure 5-14

Figure 5-15

Figure 5-16

Figure 5-15 shows several of the filaments which are approximately 1.3μ in diameter and numerous spheres about 1μ in diameter are evident and are assumed to be bacteria. A funnel shaped protozoan about 1μ in diameter and 6μ long is also seen in the centre of the figure. A close-up of one of the funnel-like protozoans is shown in Figure 5-16 in which some of the carbon surface is also evident. This figure plus other micrographs which are not presented, clearly indicates that although the bacteria and biological debris cover much of the external surface, the coverage is not complete and the biomass does not appear to offer a significant resistance to diffusion of the adsorbing molecules. Distinct colonies of bacteria are not apparent and it is not possible on the basis of these micrographs to determine whether the bacteria were adsorbed from the liquid phase or have grown in situ.

5.5.4 Alternative Media Studies

A sand column was placed before the activated carbon filters and remained there throughout the course of the study except for a one month period when a coke filter was used in its place. Solids accumulated in the sand filter and it required backwashing at about the same frequency as the first carbon column. Occasional DO profiles were measured across the sand column and indicated that the uptake was zero initially and increased to an average of 0.7 mg/l, a level which was reasonably constant throughout the remainder of the study. Thus it appeared that a bacterial population was quickly established in the sand filter and microscopic examination of the backwash sludge showed it was similar to that obtained from the 1st and 2nd carbon columns.

A very significant result of this study was that even though the sand column appeared to contain an active microbial population, at no time was there any removal of UV adsorbing TOC. Analysis by UV absorbance is a very sensitive technique and the influent and effluent from the sand column gave identical readings. As was shown in the previous sections the UV absorbing organics were rapidly removed in the carbon filters and the rates of removal could be explained purely on the basis of adsorption kinetics. The results of the sand/carbon study further support the contention that these UV absorbing materials are non-biodegradable and the only removal mechanism was by adsorption. Since the carbon and sand filter biota appeared to be similar in all aspects other than TOC removal, if biological removal of TOC were to occur in the carbon filters it is reasonable to assume that at least some removal, no matter how little, would be observed in the sand filter. In fact, removal was not observed at all and thus the data strongly suggest that these organic materials are in fact biorefractory. The data for DO and TOC uptake across the sand filter are presented in Appendix B at the end of this part of the thesis.

Although the majority of concentration measurements were made by UV absorbance and conversion to TOC via the correlation reported in Chapter 3, occasional TOC profiles were measured by direct TOC analysis. In the carbon columns the removals of direct TOC and UV absorbance TOC corresponded very closely indicating that all of the TOC removal was UV absorbing material. Direct TOC measurements across the sand filter generally indicated very small or insignificant removals but some TOC removal

was noted on two occasions, as detailed in Appendix B. This TOC change was assumed to be due to the assimilation of small quantities of biodegradable and seemingly non UV-absorbing organics from the feedstream. Because the UV-TOC changes corresponded very closely to the direct TOC changes in the carbon columns, it appeared that these biodegradable materials, when present, were completely utilized in the bioactive sand filter.

To investigate whether the media surface had an effect on the removal of TOC, a coke filter was substituted for the sand filter during one month of the study. The coke had an insignificant total surface area compared to activated carbon but it was felt that if the observed removals were biological and due to the presence of an irregularly shaped surface which was predominantly carbonaceous, some removal might be observed in the coke filter. The coke filter functioned similarly to the sand filter and again UV-TOC changes were not observed across this column. Direct TOC measurements indicated very small increases in TOC suggesting leaching of organics from the coke or the release of metabolites by the bacteria in the column. As with the sand column, a DO demand was observed across the coke bed.

5.5.5 Recirculation Studies

In the recirculation studies a column was taken off line and connected in a closed loop to a 1 litre reservoir. The reservoir was gently aerated with ultrapure air to replace oxygen used on passage through the bed and to mix the reservoir contents. A peristaltic pump circulated the water through the columns at the same rate that the ad-

sorption column experiments were conducted and samples were periodically withdrawn from the reservoir for UV-TOC analysis.

The results of a study with the 1st and 2nd carbon columns are shown in Figure 5-17. Also shown are the effluent concentrations of the two columns immediately prior to starting the recirculation experiments, at the time the experiments were conducted the columns had been in operation for 200 days. The curves for both columns show a rapid initial drop followed by a plateau region where little if any change was apparent. While the results are inconclusive with regard to discriminating between adsorptive and biological uptake, the following observations can be made:

(i) The initial rate of uptake was much greater in column 2 than in column 1, although both columns had similar masses of carbon. If the removal was principally biological, equal uptake rates would be expected whereas if the uptake was principally adsorptive, the less saturated column 2 could be expected to adsorb more rapidly than column 1.

(ii) The plateau regions for both columns were below the effluent concentration from column 2 when operated in the normal adsorption mode, and the levels of the plateau regions were different. If the removal was primarily biological, both columns should remove the degradable organics and should attain the same plateau concentrations. Additionally, the rate of uptake should not change significantly until the degradable organics are completely utilized. On the other hand, if the removal were due to adsorption, the concentration in the liquid phase would fall until desorption and re-equilibration effects began to play a part. The beha-

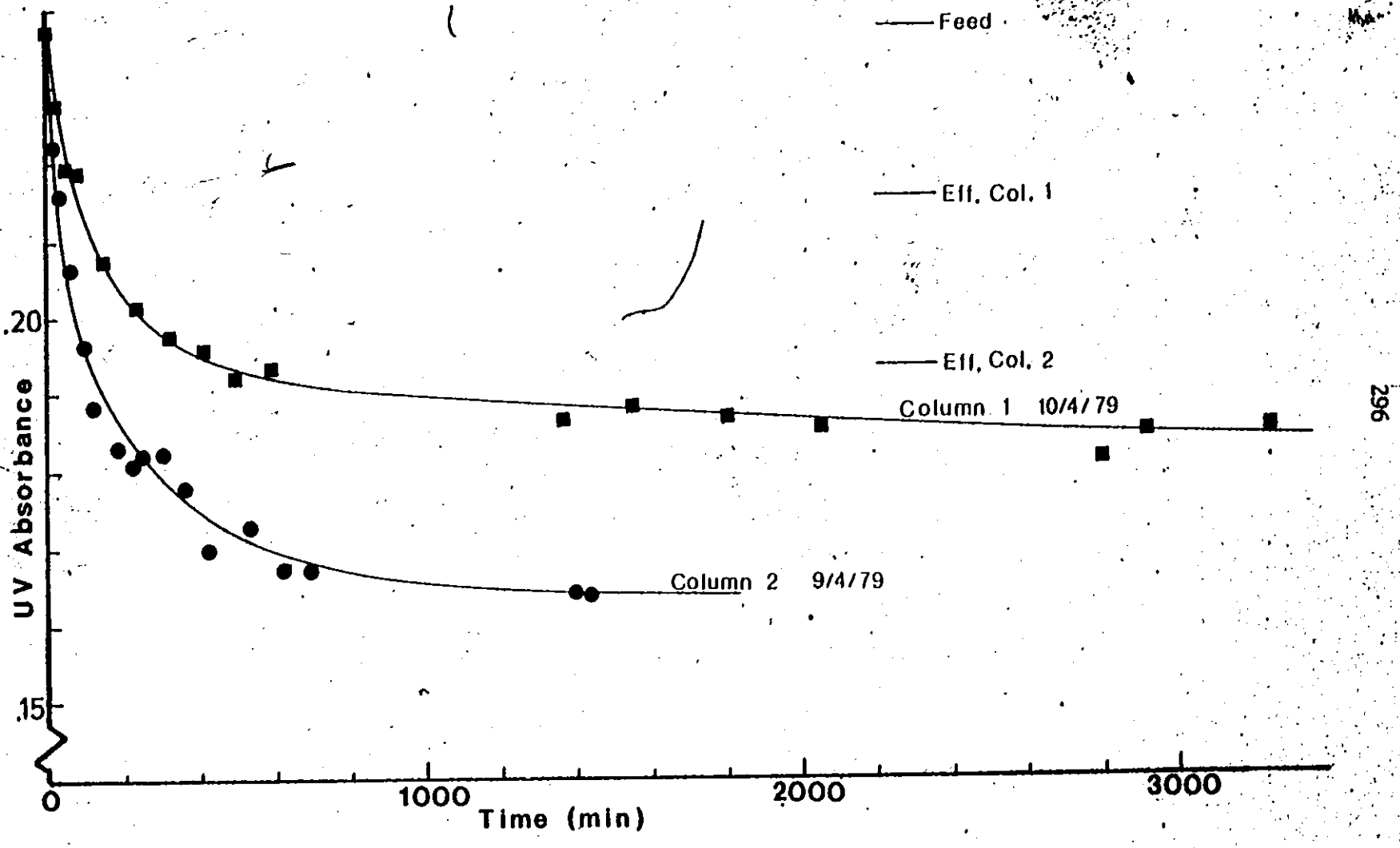

Figure 5-17. Results of Recirculation Studies on Carbon Columns No.1 and 2.

viour of the system under these conditions cannot be predicted because of the complexity and unknown nature of the desorption kinetics, but it might be anticipated that the behaviour would be somewhat akin to that observed in Figure 5-17 where the first column being more heavily loaded would begin to equilibrate or desorb at higher concentrations than the less heavily loaded second column.

5.6 Discussion of Results

While none of the individual studies in the previous section conclusively prove that biological removal of TOC did not occur within the activated carbon columns, the combined weight of all the separate observations does strongly support this contention. The studies on the columns therefore agree with the results of the modelling work which showed that the observed removals could be explained solely on the basis of adsorptive mechanisms.

Thus the overall results suggest a description of the column operation in which a feedstream containing bacteria and extensively biologically degraded dissolved organic material is purified by adsorptive and filtration mechanisms. The constituents of the soluble TOC are biorefractory and pass through the sand filter unchanged. These materials are subsequently adsorbed by the activated carbon particles except for a non-adsorbable fraction which passes directly through the entire system. Because the molecules are quite large, consisting partly of fulvic and humic materials, the diffusion rates within the carbon particle are very small resulting in the system taking many months or even years to reach

equilibrium.

At the same time that the soluble organics are being adsorbed by the activated carbon, bacteria accumulate in the beds both by adsorption onto the outer surface of the carbon particles and by filtration. These bacteria are viable as evidenced by the dissolved oxygen uptake and nitrification within the columns. The columns also support a large population of predatory organisms which utilize bacteria as a food source.

Although biological activity and adsorption occur simultaneously within the columns there is no evidence to suggest that the two processes are linked; and all the observed data are consistent with the two phenomena being completely independent of each other.

CHAPTER 6

PRACTICAL IMPLICATIONS OF THE SLOW-DIFFUSION MECHANISM TO ADSORPTION BED DESIGN.

6.1 Introduction

In the previous two chapters the ability of the branched pore adsorption model to describe the adsorptive behaviour of two complex feedstreams has been demonstrated. The branched pore model incorporates the effect of very slow diffusion in small pores, and this phenomenon was shown to be very significant in the adsorption of these complex organic materials. Aside from describing the performance of experimental adsorption columns, it is of interest to use the model to investigate the implications that the slow diffusion mechanism might have on the design of adsorption systems.

In this chapter the behaviour of two systems are examined; surface water and a refinery wastewater. The surface water parameters were measured in chapter 4, and measurement of the refinery wastewater parameters is discussed in the following section. These two systems represent opposite ends of the concentration spectrum in terms of biorefractory effluents, and the practical implications to adsorption bed design that are valid to both systems are likely to be valid for most biorefractory wastewaters, e.g. domestic secondary effluent (TOC = 15 mg/l).

6.2 Refinery Wastewater Parameter Estimation

This waste stream had a TOC of approximately 70 mg/l and was biologically stable, having been previously ozonated (60 mg/l absorbed O_3), and then biologically degraded in a respirometer until oxygen uptake ceased. The isotherm and batch kinetic data are shown in Figures 6-1 and 6-2, three sets of data being used to calculate the isotherm as three different doses of ozone (0, 60, 120 mg/l O_3 absorbed) had been used prior to the extended biological degradation. Quite a lot of scatter was observed in the data but no distinct differences between the three sets of data were apparent. Powdered activated carbon was used in the isotherm and the Freundlich equation fitted to the combined data was

$$q_e = 3.71\, c_e^{1.08} \qquad (6.1)$$

Using equation (6.1) in the branched pore model, the batch kinetic data were regressed and the fitted parameters k_m, k_b and f are shown in Figure 6-2. As before, the external film transfer coefficient (k_f) was calculated from the initial uptake rate. The parameters k_m and k_b lie between the values for the pure phenolic compounds determined in part I of this study and the values of the purely biological residual materials or surface water organics determined in the previous two chapters. This result was anticipated since the refinery wastewater is likely to consist of components from both of the above categories as well as numerous biorefractory organics of intermediate molecular weight emanating from the refining process. The low value of the 'f' parameter indicates that for this relatively high strength waste the amount of adsorp-

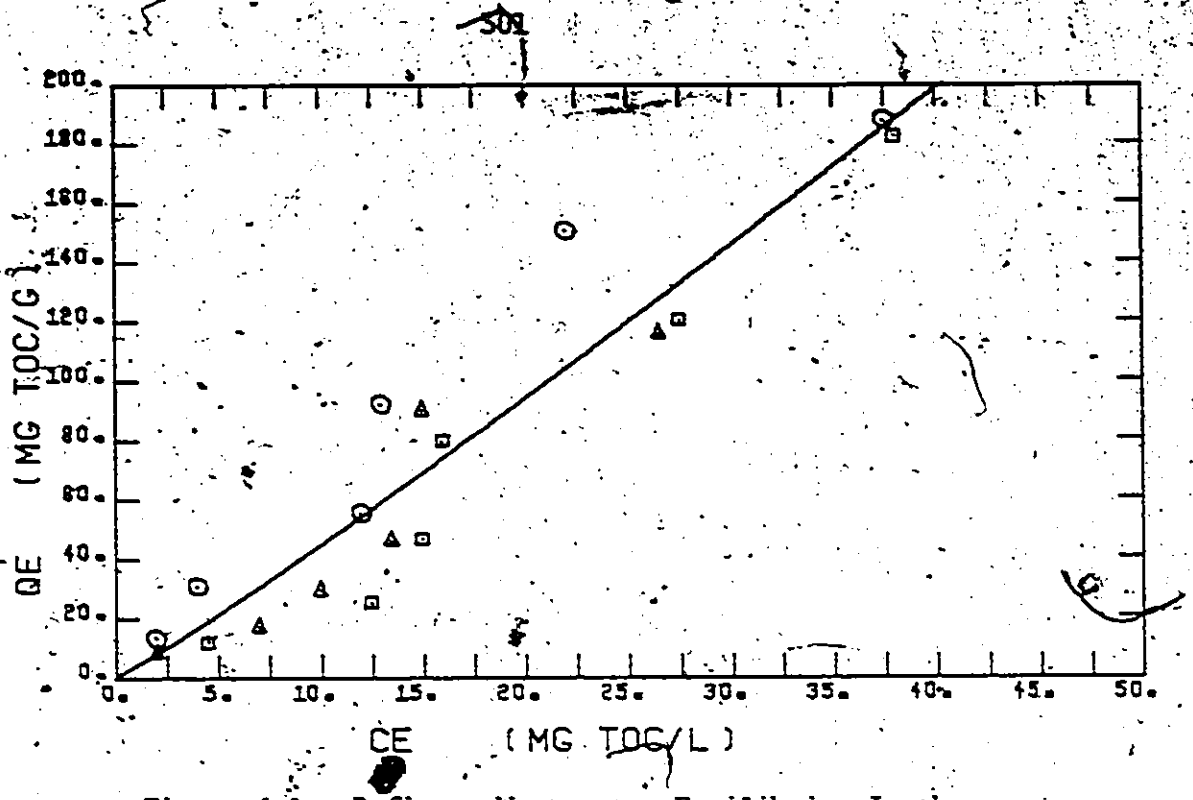

Figure 6-1. Refinery Wastewater Equilibrium Isotherms
(⊙ - 0 mg/l O_3, ⊡ - 60 mg/l O_3, △ -120 mg/l O_3)

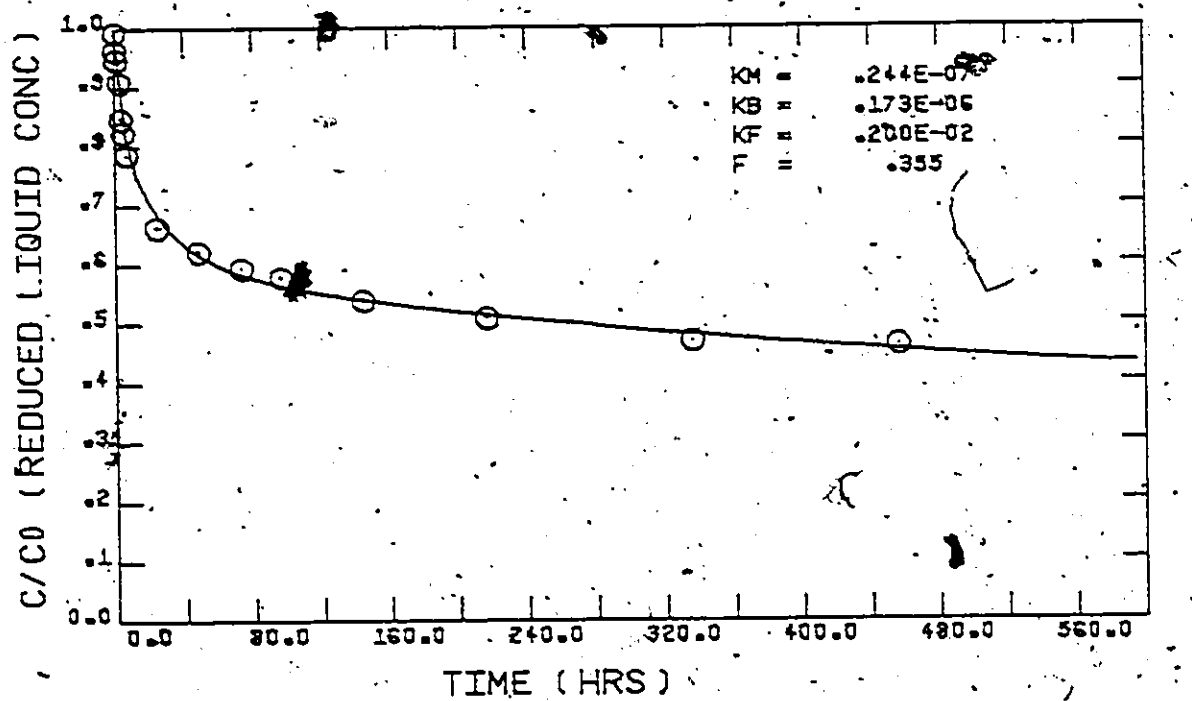

Figure 6-2. Refinery Wastewater Batch Kinetic Experiment
(⊙ - experimental data, — regressed model prediction)
(W = 0.4204 gm, V = 1.0 ℓ, c_o = 65 mg/ℓ)

tion occurring in the slow diffusion region is quite significant.

6.3 Adsorption Column Performance as Predicted by the Branched Pore Model.

6.3.1 Variation of Hydraulic Loading at Constant Contact Time

Two sets of simulations were carried out in which the hydraulic loading rate was varied while the empty bed contact time (EBCT) was held constant. The kinetic parameters for tap water and the refinery wastewater were used, and the respective influent concentrations were assumed to be 2.5 and 100 mg/l TOC.

In Figure 6-3 breakthrough profiles for tapwater at hydraulic loadings (V) of 0.1, 0.5, 1.0 and 5.0 m/h are shown. The EBCT in each case was 24 minutes which at 1.0 m/h corresponds to a bed depth of 40 cm. The curves show improved removal with increasing flowrate which is due to the decreasing external film resistance at the higher velocities. A free liquid diffusion coefficient of 1.0×10^{-6} cm^2/sec was assumed for these organics (Holzel and Sontheimer, 1979).

The corresponding curves for the refinery wastewater are shown in Figure 6-4 and indicate the same pattern of response although less pronounced. The liquid phase concentration is higher than in the tap water case and a free liquid diffusion coefficient of 3.0×10^{-6} cm^2/sec was assumed, both factors contributing to a reduction of the influence of the external film resistance.

Both studies suggest that at a given contact time the use of a bed with a high aspect ratio, i.e. height to diameter, will give impro-

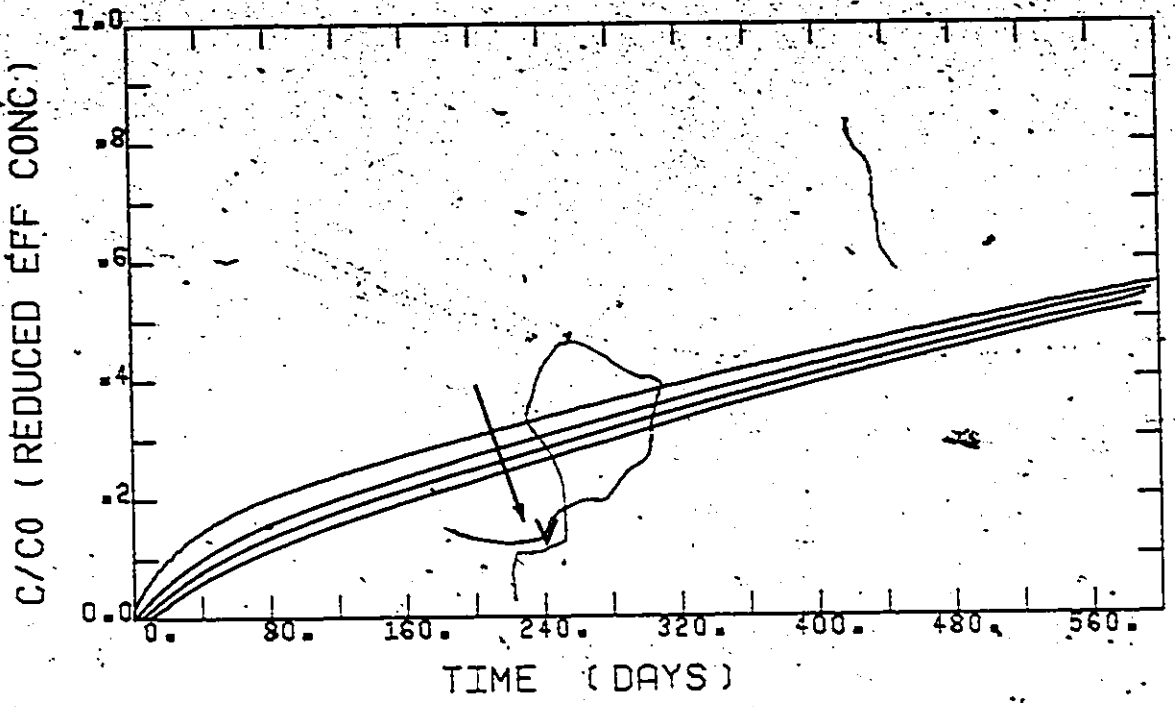

Figure 6-3. Effect of Varying Flowrate at Constant Contact Time - Tapwater (V = 0.1, 0.5, 1.0, 5.0 m/h, Contact Time = 24 min.)

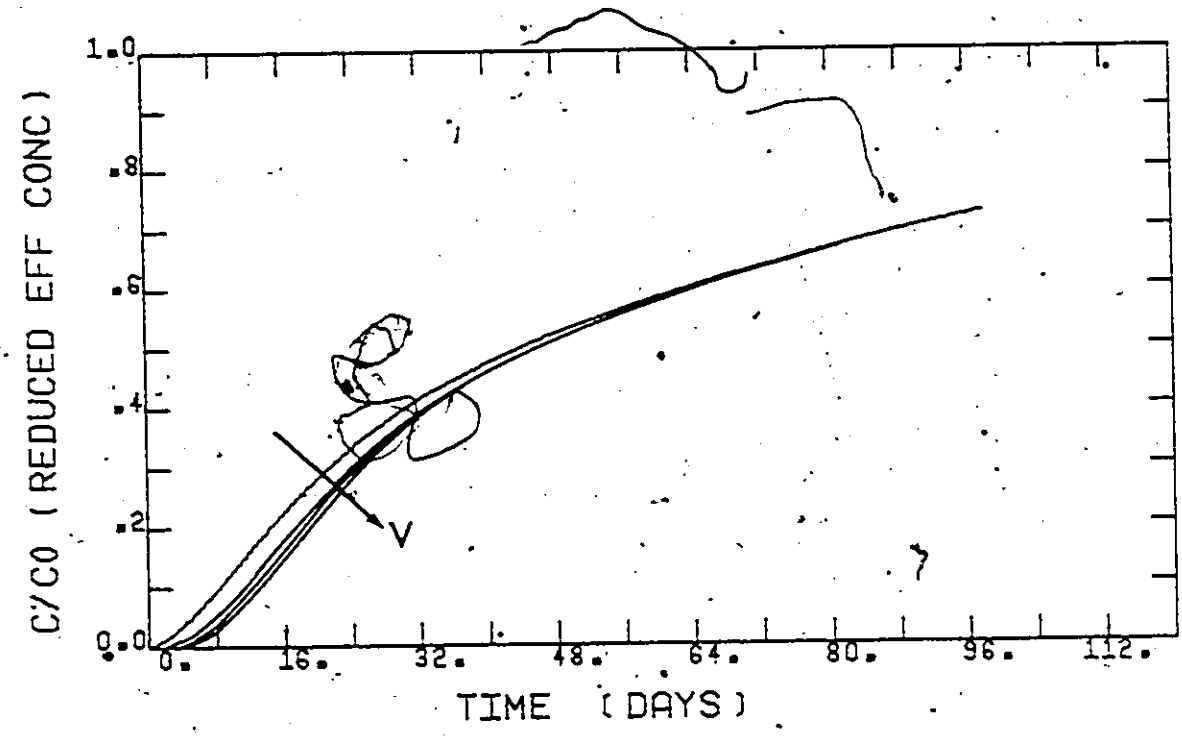

Figure 6-4. Effect of Varying Flowrate at Constant Contact Time - Refinery Wastewater (V = 0.1, 0.5, 1.0, 5.0 m/h, Contact Time = 48 min).

ved removals. However, the increase is not large, and may not compensate for the increased pressure drop across the columns at higher flow rates.

6.3.2 Variation of Contact Time

The variation of contact time was investigated for both tap water organics and the refinery wastewater, and the results are presented in two alternative forms.

In Figure 6-5 cumulative uptake curves for tap water are plotted at EBCT's of 4.8, 24, 48 and 240 minutes, and the amount of TOC removed at a given applied TOC is seen to keep increasing even to very long contact times. The slopes of these curves represent the % removal of influent TOC, and at 240 minutes contact time complete removal of the influent is obtained up to about half of the predicted maximum loading of 0.258 kg TOC/kg of carbon.

The same data plotted as carbon usage per unit volume of wastewater versus contact time is shown in Figure 6-6. This plot is analogous to the operating line diagram introduced by Erskine and Schuliger (1971). In the present case the amount of carbon required to treat a unit volume of influent is plotted against contact time for 10, 20 and 50% breakthrough of TOC. The plotted data shows that the criterion chosen to ascertain breakthrough is crucial to the selection of the contact time. A severe specification such as 10% breakthrough of adsorbable components requires very long contact times to approach maximum utilization of the carbon (zero slope), whereas at 50% breakthrough the

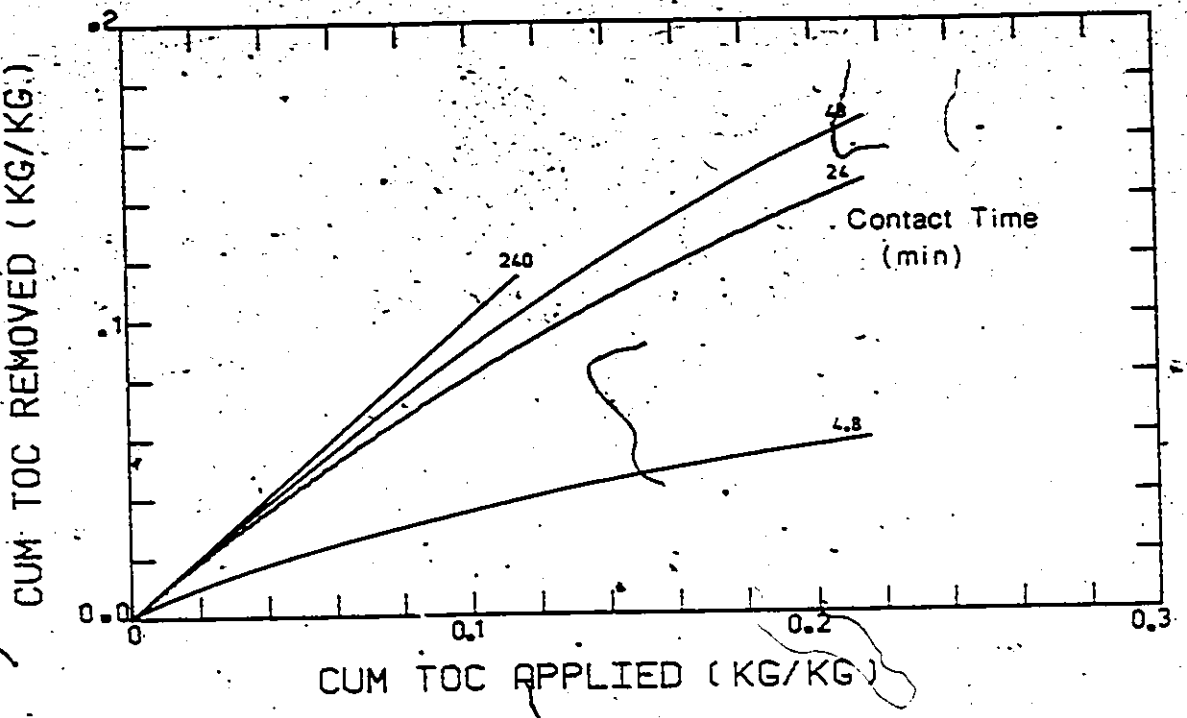

Figure 6-5. Variation of Contact Time as Cumulative Uptake Curves - Tapwater

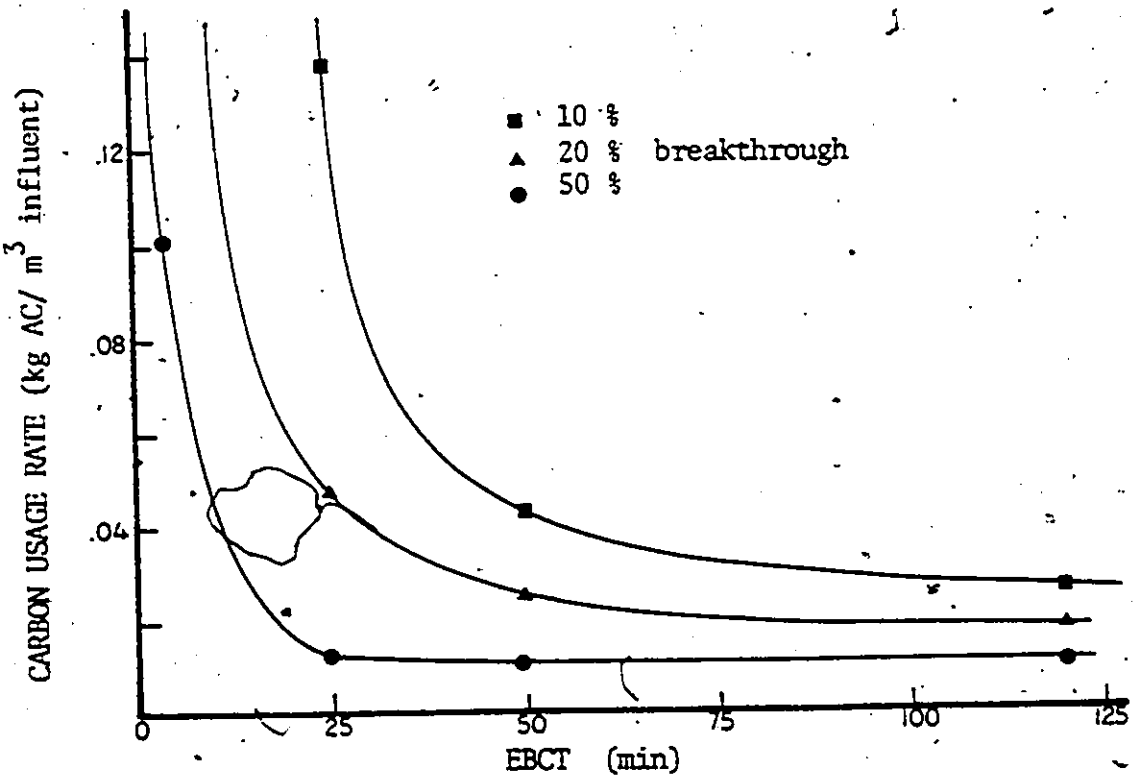

Figure 6-6. Operating Line Diagram - Tapwater

optimal carbon usage rate is approached at much lower contact times. For example, doubling the contact time from 30 to 60 minutes results in a 60% reduction in the carbon usage rate if 10% breakthrough is specified, but causes virtually no change in the usage rate at 50% breakthrough. Naturally, the size of a proposed installation would also depend on the initial capital costs which rise with increasing contact time. The very long contact times suggested in Figure 6-6 may not be practical as 120 minutes contact time at 5 m/h surface loading would require a 10 m deep bed.

The situation with the refinery wastewater is similar, the cumulative uptake curves being shown in Figure 6-7 and the operating line plot shown in Figure 6-8. Longer contact times have been allowed because of the greater influent concentration and also because smaller daily flows are usually found with industrial wastes and thus longer contact times are more practical. The seemingly very high equilibrium loading implied in Figure 6-7 (0.536 kg TOC/kg) is a consequence of assuming an influent concentration of 100 mg/l in conjunction with the isotherm shown in Figure 6-1. At this concentration the isotherm is extrapolated considerably beyond the measured range, and the calculated maximum loading may be optimistic. Regardless of the true loading, however, the conclusions reached concerning the effects of contact time are quite valid.

The curves in Figure 6-7 show similar behaviour to those in Figure 6-5 but at the higher influent concentration longer contact times are required to approach the maximum removal rate. The same situation

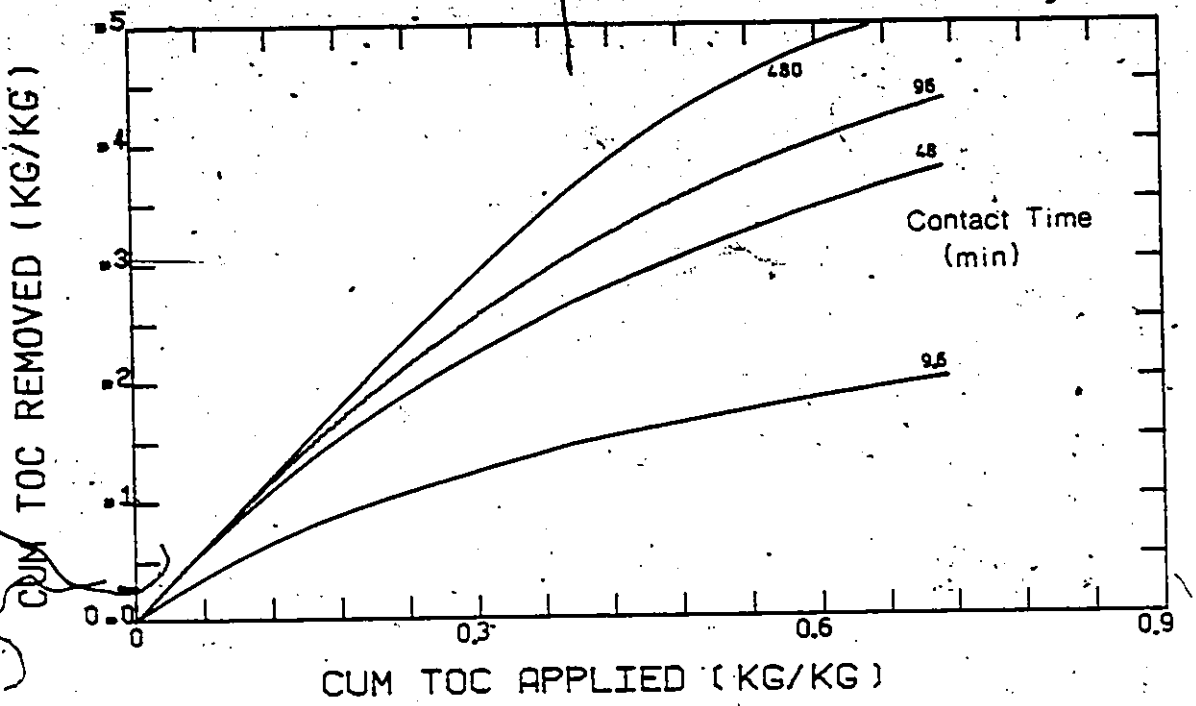

Figure 6-7. Variation of Contact Time as Cumulative Uptake Curves - Refinery Wastewater

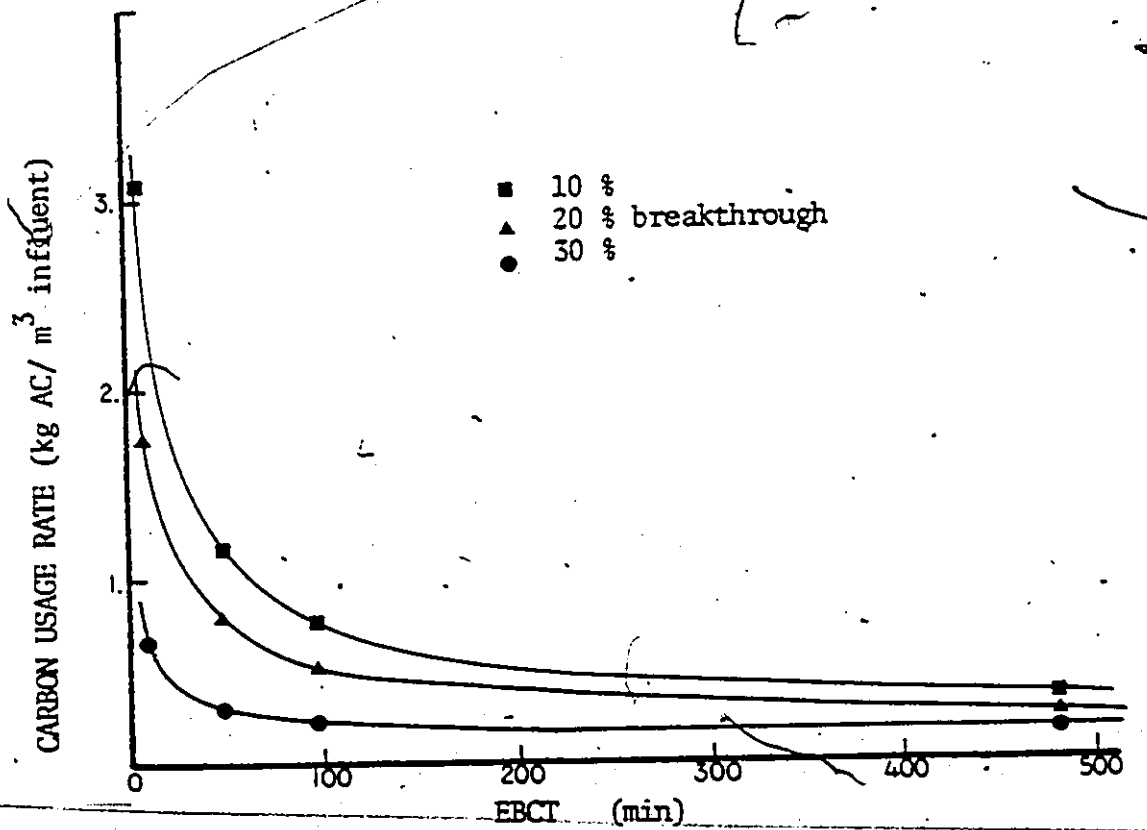

Figure 6-8. Operating Line Diagram - Refinery Wastewater

is shown in Figure 6-8 where at 10% breakthrough, a large reduction in the carbon usage rate can still be obtained by increasing the contact times beyond 2 hours, which is extremely long compared to current practice.

6.4 Discussion of Results

The very long contact times required to obtain maximum utilization of the carbon's adsorption capacity are a direct consequence of the slow diffusion phenomenon. The length of the breakthrough zone is considerably increased over that which would be obtained with more rapidly diffusing adsorbates, and leakage from the columns due to kinetic limitations occurs long before adsorptive saturation is approached.

Because of the slow adsorption kinetics, a bed which removes only a small fraction of the influent and might be thought to be exhausted may yet be far from saturation. An example is the curve in Figure 6-5 for a contact time of 24 minutes. At a cumulative applied loading of 0.2 kg TOC/kg, the percentage removal in this bed is only 40% and yet the bed is only about 50% saturated (maximum loading = 0.258 kg TOC/kg), and it would continue to remove organics for an extended period if left in service. At a surface loading of 5 m/h this contact time corresponds to a bed depth of 2 m.

Thus the means of maximizing the carbon usage rate is to have the carbon in service for as long a period as possible so that it can reach saturation, and the only way this long service can be obtained in conjunction with a satisfactory effluent quality is by the use of

a long contact time, achieved through the use of either a long bed, or a low surface loading rate.

Support for the model's predictions can be found in the data of Schalekamp(1976). A slow filter at a waterworks on the Lake of Constance, Switzerland, was fitted with a 5 cm layer of activated carbon and the carbon loading was measured at yearly intervals by DMF (dimethylformamide) extraction. The data is reproduced in Figure 6-9 which shows that the loading on the carbon increased year by year at a slowly decreasing rate, exactly as would be predicted by the slow diffusion mechanism in the branched pore model. To obtain maximum use of this carbon's adsorptive capacity the filter should clearly be left in service for a period far in excess of 3 years. The amount of COD removed by the carbon filter was almost constant during the 3 years of the study and some biological activity was anticipated, however, the contribution of adsorption to the total removal was not calculated.

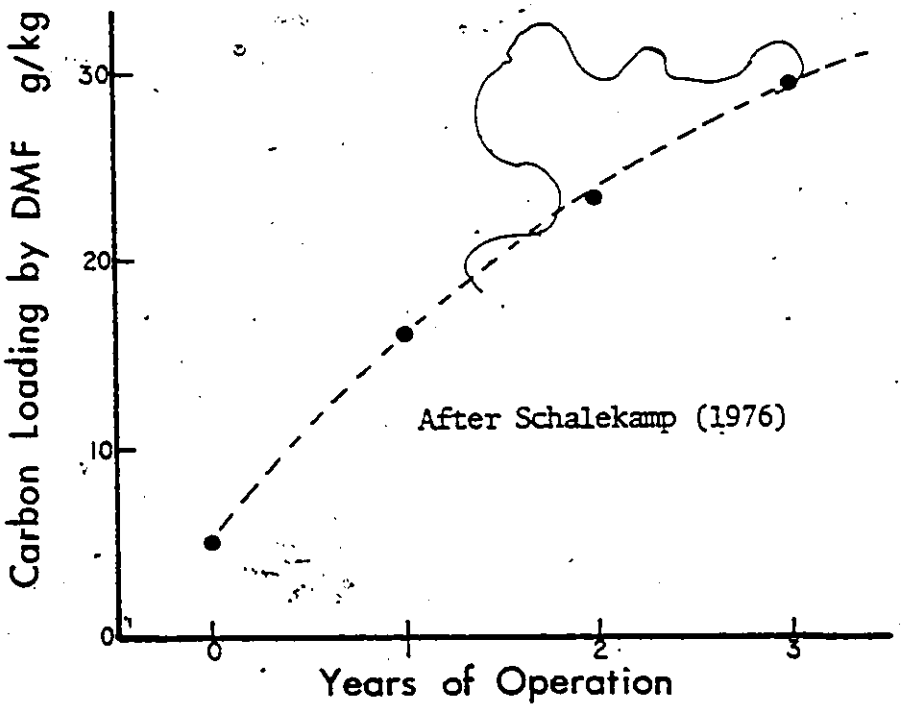

Figure 6-9. Activated Carbon Loadings as a Function of Time

CHAPTER 7

CONCLUSIONS AND RECOMMENDATIONS FOR FURTHER RESEARCH

7.1 Conclusions

1. Analysis of the adsorptive behaviour of complex mixtures of low level organics from two different feedstreams; the first tap water from Lake Ontario; and the second a bioresidual material generated by degrading phenol in an activated sludge plant, indicates the following:

(i) The use of TOC as a lumped parameter to describe the combined adsorptive behaviour of all the various molecules in the feedstream is generally successful for modelling column breakthrough patterns;

(ii) Application of the branched pore kinetic model developed in part I of this study to batch kinetic data of these complex organic mixtures indicates that about 70% of the total capacity is associated with the slow diffusion region of the carbon particle. The measured intraparticle diffusion parameters are much less than those found with pure phenolic compounds, and the carbon's adsorptive capacity is utilized at a very low rate which continues for an extended period of time.

(iii) With no prior knowledge of the behaviour of adsorption columns operating on these feedstreams, the model was used to predict the performance of experimental columns using only the parameters

determined in the batch kinetic and isotherm experiments. Over the major part of the breakthrough curves which span two years of operation in the case of tap water, the model gives a very good description of the actual behaviour, and indicates the importance of the slow adsorptive uptake over extended periods. The initial region of rapid breakthrough is not as accurately predicted which may be a result of the use of a lumped parameter to describe the concentration of a wide range of different organic molecules.

2. The long term uptake of a small amount of organic material, which results from the very slow diffusion within the carbon particle, has important ramifications in the interpretation of operating data from experimental and full scale adsorption systems. When such systems continue to exhibit a removal capacity after an extended period of operation, biological degradation of the organics has been suggested to be the cause and some as yet unproven mechanisms have been proposed to account for this removal. The present study indicates that in many cases the observed removals may be solely due to adsorptive mechanisms which continue to occur for extended periods, and further, that there is no reason to assume that biological activity is any different in an activated carbon column from that occurring in any other biological contacting mode.

4. An analysis of carbon column operation using the branched pore model indicates that maximum utilization of the activated carbon's capacity requires contact times far in excess of those currently in use. In addition, the contact times necessary for maximum use of the adsorptive

capacity are a strong function of the criterion chosen to determine breakthrough. These conclusions apply equally well for the low level bioresidual and tap water organics as they do for a higher strength refinery wastewater stream for which the kinetic parameters were also measured.

7.2 Recommendations for Future Research

1. Since the contact times necessary to obtain a minimal carbon usage rate may not be practical from either a land usage or economic standpoint, methods of increasing the adsorptive rate of uptake onto the activated carbon should be investigated. This objective might be achieved by using smaller carbon granules or using carbons with different pore size distributions.

2. Experiments using carbon columns operated at a range of contact times of up to four hours should be undertaken to verify the conclusions of the model concerning optimal contact time. Such experiments would require several years of operating data before conclusions could be reached if low level organics were to be used, and therefore higher strength wastes such as the refinery effluent used in part of this study would be more suitable.

3. Further research should be undertaken to better describe the initial breakthrough zone, and analysis of the breakthrough organics, perhaps by molecular weight fractionation, would indicate if the breakthrough was due to a particular component or group of components in the influent.

BIBLIOGRAPHY

Andrews, G.F. and Tien, C. "The Inter-reaction of Bacterial Growth, Adsorption, and Filtration in Carbon Columns Treating Liquid Wastes," Pres. 67th Ann. Mtg. AIChE, Washington D.C. (1974).

Argo, D.G. and Culp, R.L. "Ozone and Biological Activated Carbon," Pres. Div. Environ. Chem., Amer. Chem. Soc., Miami, Florida (1978).

Atkinson, B. and Fowler, H.W. "The Significance of Microbial Film in Fermenters," Advances in Biochem. Eng., 3, 221 (1974).

Benedek, A., "The Effect of O_3 on Activated Carbon Adsorption - A Mechanistic Analysis of Water Treatment Data," Pres. IOI Symp. on Advanced Ozone Technol., Int. Ozone Inst. Inc., Toronto (1977).

Benedek, A. "Simultaneous Biodegradation and Activated Carbon Adsorption - A Mechanistic Look," Pres. Div. Environ. Chem., Amer. Chem. Soc., Miami, Florida (1978).

Benedek, A. "The Role of Biological Activity in Activated Carbon Adsorbers," Pres. 30th Ann. Purdue Indus. Waste Conf. (1975).

Benedek, A. and Bancsi, J.J. "A Study of the Removal of Synthetic Organics from Drinking Water by Activated Carbon," Health & Welfare Canada, 77-EHD-17 (1977).

Besik, F. "High Rate Adsorption & Biological Oxidation of Domestic Sewage," Water & Sewage Works, 120, 68 (1973).

Bishop, D.F. et al., "Studies on Activated Carbon Treatment," Jl. Water Poll. Contr. Fed., 39 (2), 188 (1967).

Cairo, P.R. et al., "Development of Criteria for the Design of Full Scale Carbon Adsorption Systems," Pres. A.W.W.A. Water Qual. Technol. Conf., Louisville, Kentucky (1978).

Cairo, P.R., McElaney, J. and Suffet, I.H. "Design & Operational Experiences with Activated Carbon Adsorbers: Treatment of Delaware River Water," Pres. Practical Applications of Adsorption Techniques in Drinking Water, Reston, Virginia (1979).

Chen, W., "The Effect of Surface Curvature on the Adsorption Capability of Porous Adsorbents." Ph.D. Thesis, University of South Carolina (1970).

Chudoba, J., Prasil, M. and Emmerova, H. "Residual Organic Matter in Activated Sludge Process Effluents. III. Degradation of Amino Acids and Phenols under Continuous Conditions," Technology of Water, Scientific Papers of the Institute of Chemical Technology, Prague F 13, 45 (1968).

Chudoba, J., Cervenka, J. and Zima, M. "Residual Organic Matter in Activated Sludge Process Effluents, IV. Treatment of Municipal Sewage," Technology of Water, Scientific Papers of the Institute of Chemical Technology, Prague F 15, 5 (1969).

Cotruvo, J.A. "Control of Organic Chemical Contaminants in Drinking Water - Background, Development and Rationale," Pres. EPA Joint Conf. NATO/CCMS, Reston, Virginia (1979).

Cotruvo, J.A. and Wu, C. "EPA's Views on the Use of Activated Carbon to Remove Trace Organic Chemicals from Drinking Water," Pres. Div. Environ. Chem., Amer. Chem. Soc., Miami, Florida (1978).

Dedrick, R.L. and Beckmann, R.B. "Kinetics of Adsorption by Activated Carbon from Dilute Aqueous Solution," Chem.Eng. Prog. Symp. Series, 63 (No. 74), 68 (1967).

De Walle, F.B. and Chian, E.S. "Kinetics of Formation of Humic Substances in Activated Sludge Systems and Their Effect on Flocculation," Biotech. Bioeng. 16, 739 (1974).

De Walle, F.B. and Chian, E.S. "Biological Regeneration of Powdered Activated Carbon Added to Activated Sludge Units," Water Research, 11 (5), 439 (1977b).

DiGiano, F.A. "Mathematical Models of Competitive Adsorption: Successes, Failures, and Future Implications," Proceedings Int. Water Conf., Eng. Soc. West Pa., 39, 209-18 (1978).

DiGiano, F.A. "Influence of Microbial Activity on the Performance of Granular Activated Carbon," Pres. A.W.W.A. Preconf. Seminar on Organics, San Francisco, California (1979).

Directo, L.S. and Chen, C.L. "Pilot Plant Study of Physical Chemical Treatment," Pres. 47th Ann. Water Poll. Contr. Fed. Conf., Denver, Colorado (1974).

Dobbs, R.A., Wise, R.H. and Dean, R.B. "The Use of Ultraviolet Absorbance for Monitoring the Total Organic Carbon Content of Water and Wastewater," Water Research, 6, 1173 (1972).

Eberhardt, N. "Experience with the Use of Biologically Effective Activated Carbon," in Translation of Reports on Special Problems of Water Technology, vol.9 - Adsorption, EPA-600/9-76-030 December, 331 (1976).

Eberhardt, M., Madsen, S. and Sontheimer, H. "Research on the Use of Biologically Active Activated Carbon Filters for Drinking Water," Das Gas-und Wasserfach, 116 (6), 245 (1975).

Elmaleh, S., Labaquère, H. and Ben Aim, R. "Biological Filtration Through a Packed Column," Water Research, 12, 41 (1978).

Erskine, D.B. and Schuliger, W.G. "A Graphical Method to Determine the Performance of Activated Carbon Processes for Liquids," Pres. AIChE Meeting, Cincinnati, May (1971).

Famularo, J., Mueller, J.A. and Mulligan, T. "Application of Mass Transfer to Rotating Biological Contactors," Jl. Water Poll. Contr. Fed., 50 (4), 653 (1978).

Flynn, B.P. "The Determination of Bacterial Kinetics in a Powdered Activated Carbon Reactor," Pres. 29th Ann. Purdue Indus. Waste Conf. (1974).

Flynn, B.P. "A Model for the Powdered Activated Carbon-Activated Sludge Treatment System," Pres. 30th Ann. Purdue Indus. Waste Conf. (1975).

Flynn, B.P., Robertaccio, F.L. and Barry, L.T. "Truth or Consequences: Biological Fouling and Other Considerations in the Powdered Activated Carbon-Activated Sludge System," Pres. 32nd Ann. Purdue Indus. Waste Conf. (1977).

Fokken, B. and Kurz, R. "Removal of Purgeable Organic Chlorine Compounds by Activated Carbon Adsorption," Pres. EPA Joint Conf. NATO/CCMS, Reston, Virginia (1979).

Ford, D.L. "Putting Activated Carbon in Perspective to 1983 Guidelines," Indus. Water Eng., May/June, 20 (1977).

Frick, B., Bartz, R., Sontheimer, H. and DiGiano, F.A. "Predicting Competitive Adsorption Effects in Granular Activated Carbon Filters," Pres. Div. Environ. Chem., Amer. Chem. Soc., Miami, Florida (1978).

Fuchs, F. and Kühn, W. "The Use of Activated Carbon to Analyse Natural Waters with Regard to their Behaviour in Waterworks Filters," in Translation of Reports on Special Problems in Water Technology, vol.9 - Adsorption, EPA-600/9-76-030 December, 182 (1976).

Gaurino, C.F. "A Local Utility Manager's Approach to Implementation of Regulations," Pres. EPA-PTI Seminars, January, Philadelphia, Pennsylvania (1979).

Grady, C.P. and Williams, D.R. "The Effects of Influent Substrate Concentration on the Kinetics of Natural Microbial Populations in Continuous Culture," Water Research, 9, 171 (1975).

Guirguis, W., Cooper, T., Harris, J. and Ungar, A. "Improved Performance of Activated Carbon by Preozonation, Jl. Water Poll. Contr. Fed., 50 (2), 308 (1978a).

Guirguis, W.A., Prober, R. and Slough, J.W. "Effects of Ozone Pretreatment and Bacterial Growth on Activated Carbon Treatment," Pres. Div. Environ. Chem., Amer. Chem. Soc., Miami, Florida (1978b).

Harremoes, P., "The Significance of Pore Diffusion to Filter Denitrification," Jl. Water Poll. Contr. Fed., 48(2), 377 (1976).

Hölzel, G. and Sontheimer, H. "Laboratory Activated Carbon Test Methods," Pres. EPA Joint Conf. NATO/CCMS, Reston, Virginia (1979).

Howell, J.A. and Atkinson, B. "Influence of Oxygen and Substrate Concentration on the Ideal Film Thickness and the Maximum Overall Substrate Uptake Rate in Microbial Film Fermenters," Biotech. Bioeng., 18, 15 (1976).

Ilić, P., "Degradation of Persistent Materials in a Fixed Bed Reactor Using Nitrate as the Electron Acceptor," Institut Für Wasserversorgung, WO 220/1, Darmstadt (1977).

Jennings, P.A., Snoeyink, V.A. and Chian, E.S. "Theoretical Model for Submerged Biological Filter," Pres. 1st Chem. Congress of North America, Mexico City (1975).

Jeris, J.S., Author's Response to a Discussion by W.J. Weber, Jl. Water Poll. Contr. Fed., 50 (4), 784 (1978).

Jeris, J.S., Owens, R.W., Hickey, R. and Flood, F. "Biological Fluidized Bed Treatment for BOD and Nitrogen Removal," Jl. Water Poll. Contr. Fed., 49, 816 (1977).

Johnson, R.L., "Biological Regeneration of Activated Carbon in Advanced Wastewater Treatment," Fritz. Eng. Lab Report No. 3882, Office of Research, LeHigh Univ. (1975).

Joyce, R.S., Allen, J.B. and Sukenik, V.A. "Treatment of Municipal Wastewater by Packed Activated Carbon Beds," Jl. Water Poll. Contr. Fed., 38(5), 813 (1966).

Kalinske, A.A., "Enhancement of Biological Oxidation of Organic Wastes Using Activated Carbon in Microbial Suspensions," Water and Sewage Works, June, 62 (1972).

Kim, B.R., Snoeyink, V.L. and Saunders, F.M. "Carbon Adsorption of Organic Compounds from Activated Sludge Process Effluents as a Function of Cell Residence Time," ASCE, Jl.Envir. Eng. Div., 102(EE1), 55 (1976).

Klotz, M., Werner, P. and Schweisfurth, R. "Investigations Concerning the Microbiology of Activated Carbon Filters," in Translation of Reports on Special Problems of Water Technology, vol.9 - Adsorption, EPA-600/9-76-030 December, 312 (1976).

Kühn, W., Sontheimer, H., Steiglitz, L., Maier, D. and Kurz, R. "The Use of Ozone and Chlorine in Water Utilities in the Federal Republic of Germany," Jl. Amer. Water Works Assoc., 70, 326 (1978).

Lawrence, A.W., "Granular Activated Carbon Treatment of Primary and Chemically Treated Effluents," in Reuse Recycle Wastes, Proc. 3rd Ann. N.East Region Antipollut. Conf., 65-80 (1970).

Letterman, R.D., Quon, J.E. and Gemmel, R.S. "Film Transport Coefficients in Agitated Suspensions of Activated Carbon," Jl. Water Poll. Contr. Fed., 40, 2537 (1974).

Love, O.T. and Symons, J.M. "Operation Aspects of Granular Activated Carbon Adsorption Treatment," Water Supply Research Div., Municipal Environment Research Laboratory, EPA, July (1978).

Lowry, J.D. and Burkehead, C.E. "The Role of Adsorption in Biologically Extended Activated Carbon Columns," Proc. 51st Ann. Conf. Water Poll. Contr. Fed., Anaheim, California (1978).

McCreary, J.J. and Snoeyink, V.L. "Granular Activated Carbon in Water Treatment," Jl. Amer. Water Works Assoc., 69 (8), 437 (1977).

Manka, J., Rebhun, M., Mandelbaum, A. and Bortinger, A. "Characterization of Organics in Secondary Effluents," Envir. Sci. and Technol., 8(12), 1017 (1974).

Maqsood, R. and Benedek, A. "The Effect of Low Temperature on Organic Removal and Denitrification in Activated Carbon Columns," Jl. Water Poll. Contr. Fed., 49, 2107 (1977).

Martin, R.J. and Al-Bahrani, K.S. "Adsorption Studies Using Gas-Liquid Chromatography - II. Competitive Adsorption," Water Research, 11, 991 (1977).

Mulcahy, L.T., Mathematical Model of the Fluidized Bed Biofilm Reactor, Ph.D. Thesis, University of Massachusetts (1978).

Parkhurst, J.D., Dryden, F.D., McDermott, G.N. and English, J. "Pomona Activated Carbon Pilot Plant," Jl. Water Poll. Contr. Fed., 39, R70 (1967).

Peel, R.G. and Benedek, A. "The Modelling of Activated Carbon Adsorbers in the Presence of Bio-oxidation," Water - 1976, AIChE Symp. Series 166, 25 (1977).

Prober, R., Pyeha, J.J. and Kidon, W.E. "Interaction of Activated Carbon with Dissolved Oxygen," AIChE Jl., 21(6), 1200 (1975).

Randtke, S.J. and McCarty, P.L. "Removal of Soluble Secondary Effluent Organics," ASCE, Jl. Environ, Eng. Div., 105 (EE4), 727 (1979).

Razzaghi, M. "The Competitive Adsorption of Carbohydrates, Proteins, and Ligninsulphonates on Activated Carbon," M.Eng. Thesis, McMaster University, (1976).

Rebhun, M. and Narkis, N. "Physico - Chemical Treatment of Raw Wastewater," Pres. 7th Int. Conf. on Water Poll. Research, Paris (1974).

Rice, R.G., Miller, G.W., Robson, C.M. and Kuhn, W. "Biological Activated Carbon," Pres. IOI Symp. on Advanced Ozone Technol., Int. Ozone Inst. Inc., Toronto (1977).

Rittman, B.E. and McCarty, P.L. "Variable-Order Model of Bacterial-Film Kinetics," ASCE, Jl. Eng. Div., 104 (EE5), 889 (1978).

Rodman, C.A. and Shumney, E.L. "Bio-Regenerated Activated Carbon Treatment of Textile Dye Wastewater," Water Poll. Contr. Research Series, EPA, PB-203 599 (1971).

Schalekamp, M. "Use of Activated Carbon in the Treatment of Lake Water," in Translation of Reports on Special Problems of Water Technology, vol.9 - Adsorption, EPA-600/9-76-030 December, 128 (1976).

Schnitzer, M. and Khan, S.U. Humic Substances in the Environment, Marcel Dekker Inc., New York (1972).

Schwartz, C.E. and Smith, J.M. "Flow Distribution in Packed Bed," Ind. & Eng. Chem., 45, 1209 (1953).

Sigurdson, S.P. and Robinson, C.W. "Substrate Inhibited Microbiological Regeneration of Activated Carbon," Can. Jl. Chem. Eng., 56(6), 330 (1978).

Slechta, A.F. and Culp, G.L. "Water Reclamation Studies at the South Tahoe Public Utility District," Jl. Water Poll. Contr. Fed., 39 (5), 787 (1967).

Snoeyink, V.L., McCreary, J.J. and Murin, C.J. "Activated Carbon Adsorption of Trace Organics," Environ. Prot. Technol. Series, EPA 600/2-77-223 (1977).

Sontheimer, H. "Considerations on the Optimization of Activated Carbon Use in Waterworks," in Translation of Reports on Special Problems of Water Technology, vol.9 - Adsorption, EPA-600/9-76-030 December, 208 (1976).

Stephenson, P., Benedek, A., Malaiyandi, M. and Lancaster, E.A. "The Effect of Ozone on the Biological Degradation and Activated Carbon Adsorption of Natural and Synthetic Organics in Water. Part I. Ozonation and Biodegradation," Paper pres. IOA Houston Meeting, Nov. (1979).

Tien, C., "Bacterial Growth and Adsorption in Granular Activated Carbon Columns," Pres. Div. Environ. Chem., Amer. Chem. Soc., Miami, Florida (1978).

Toffiemire, T.J., Hetling, L.J. and Schuster, W.W. "Activated Carbon Adsorption and Polishing of Strong Wastewaters," Jl. Water Poll. Contr. Fed., 45(10), 2166 (1973).

Tsezos, M. and Benedek, A. "A Method for Calculation of Biofilm Volume in Fluidized Bed Biological Reactors," in press, Water Research (1979).

USEPA, Translation of Reports on Special Problems of Water Technology, vol.9 - Adsorption, EPA-600/9-76-030, December (1976).

USEPA, "Interim Primary Drinking Water Regulations, : Control of Organic Chemical Contaminants in Drinking Water," Federal Register, 43 (No.28), 5756-5780 (Feb.9, 1978).

Usinowicz, P., Mathematical Simulation and Prediction of Adsorber Performance for Complex Waste Mixtures, Ph.D. Thesis, University of Michigan (1972).

Van der Kooij, D. "Some Investigations into the Presence and Behaviour of Bacteria in Activated Carbon Filters," in Translation of Reports on Special Problems of Water Technology, vol.9 - Adsorption, EPA-600/9-76-030 December, 348 (1976)

Van der Kooij, D. "Processes During Biological Oxidation in Filters," Pres. Conf. on Oxidation Techniques in Drinking Water Treatment, Karlsruhe (1978).

Weber, W.J. "Integrated Biological and Physico-Chemical Treatment for Reclamation of Wastewater," Indus. Water Eng., 14(7), 20 (1977).

Weber, W.J. Discussion of a paper by Jeris et al.(1977), Water Poll. Contr. Fed., 50(4), 781 (1978).

Weber, W.J., Friedman, L.D. and Bloom, R. "Biologically-Extended Physicochemical Treatment," Proc. 6th Conf. of the Inter. Assoc. Water Poll. Res., Pergamon Press, Oxford, U.K. (1973).

Weber, W.J., Hopkins, C.B. and Bloom, R. "Physicochemical Treatment of Wastewater," Jl. Water Poll. Contr. Fed., 42(1), 83 (1970).

Weber, W.J., Pirbazari, M. and Melson, G.L. "Biological Growth on Activated Carbon: An Investigation by Scanning Electron Microscopy," Environmental Sci. & Technol., 12(7), 817 (1978).

Williamson, K. and McCarty, P.L. "A Model of Substrate Utilization by Bacterial Films," Jl. Water Poll. Contr. Fed., 48(1), 9 (1976a).

Williamson, K. and McCarty, P.L. "Verification Studies of the Biofilm Model for Bacterial Substrate Utilization," Jl. Water Poll. Contr. Fed., 48(2), 281 (1976b).

Wilson, E.J. and Geankoplis, C.J. "Liquid Mass Transfer at Very Low Reynolds Numbers in Packed Beds," Ind. & Eng. Chem. Fund., 5 (1), 9 (1966).

Ying, W. Investigation and Modeling of Bio-Physicochemical Processes in Activated Carbon Columns, Ph.D. Thesis, University of Michigan (1978).

Young, J.C., Baumann, E.R. and Wall, D.J. "Packed-Bed Reactors for Secondary Effluent BOD and Ammonia Removal," Jl. Water Poll. Contr. Fed., 47(1), 46 (1975).

APPENDIX A

The Likelihood of Significant Adsorption on the External Surface of Activated Carbon Granules.

Powdered carbon (PAC) was used in the present study to measure low low level isotherms as has previously been done by Frick et al.(1978). Previous work has shown that for phenolic compounds, granular carbon (GAC) and PAC isotherms are identical (Dedrick and Beckman, 1967; Martin and Al-Bahrani, 1978; Part I of this report). For the organics found in potable water sources, many of which are high molecular weight fulvic and humic acids, it was thought that differences might be observed in the isotherm capacities if the molecules adsorbed by single or multi point attachment to the outer surface of the carbon particle rather than entering the pore structure. If such external attachment were to occur, higher capacities would be measured with PAC because of the higher external surface area of the smaller particles. Because of the extremely slow diffusion rates, measurement of GAC isotherms on these materials is not possible and thus a direct comparison of the isotherms cannot be made.

There is some evidence to suggest that external attachment of large molecules, if it does occur, is negligible. Razzaghi (1976) investigated the adsorption of a number of carbohydrates (dextrans) and lignin sulphonates onto various types of activated carbons, all in powdered form. She found that the adsorptive capacities for these large

molecules correlated quite well with the pore volume available in pores 3 to 6 times the molecular radius (Chen, 1970). The extent of adsorption varied over a wide range depending on the carbon type, whereas if external surface adsorption were the main mechanism, all carbons of similar size should have similar adsorptive capacities.

The materials used were;

	MW	rÅ	
Dextran T70	70,000	60-90	$q_e = 16.5\ C_e^{0.19}$
Dextran T2000	2,000,000	250-500	$q_e = 5.7\ C_e^{0.29}$
Lignin Sulphonate	35,000		$q_e = 4.2\ C_e^{0.17}$

Although the results of the above study are not conclusive, they suggest that external surface attachment is probably an insignificant mechanism and consequently it was assumed in the present study that PAC and GAC isotherms will be identical regardless of the type of organics encountered.

APPENDIX B

TOC and DO Data in Sand and Coke Columns

Date	Inf TOC	Sand/Coke Eff TOC	Inf DO	S/C Eff DO	Carbon 1 Eff DO	Carbon 2 Eff DO	Carbon 3 Eff DO
Start sand 9-10-78							
10-10-	1.05	1.05	10.0	10.0	2.5	0.8	0.6
11-10-	1.05	1.05	7.3	7.3	0.2	0.2	0.1
12-10-	1.04	1.08	6.4	6.4	0.3	0.3	0.3
13-10-	1.00	1.00	8.2	8.0	0.3	0.3	0.2
16-10-	1.00	1.00	9.0	9.0	1.4	0.9	0.1
18-10-	1.03	1.01	8.0	7.4	4.5	3.9	3.2
*18-10-	1.09	1.02					
20-10-	1.34	1.35	7.9	7.2	5.4	4.6	3.9
23-10-	1.31	1.31	7.4	6.8	5.1	4.1	3.1
*23-10-	1.54	1.33					
27-10-	1.26	1.25	8.2	7.7	6.8	6.0	5.4
31-10-	1.35	1.35	6.0	5.4	2.4	2.2	1.7
*31-10-	1.37	1.32					
8-11-	1.35	1.35	6.3	6.0	4.9	4.3	3.5
23-11-	1.09	1.10	4.9	4.1	3.2	2.5	1.3
Start Coke 7-12-78	1.02	1.02					
*16-12-	1.11	1.14					
27-12-	1.08	1.09	7.4	6.6	5.6	5.0	4.2
2-1-79	1.15	1.15	6.1	5.5	4.3	3.6	2.6
* 2-1-	1.10	1.18					
Start Sand 6-1-79							
9-1-	1.14	1.22	-	5.7	4.7	4.1	2.8
10-1-	1.14	1.14	-	5.7	5.2	4.5	3.5
17-1-	1.16	1.16					
22-1-	1.13	1.13					
6-3-	0.97	0.97					

* TOC by Dohrman DC-54 Low Level TOC Analyzer.
All other TOC measurements via UV absorbance correlation.